Investigating the homing and healing properties of adipose-derived mesenchymal stromal cells using a model of wound repair

THESIS

Submitted in fulfilment of the requirements for the degree

Doctor of Philosophy (Medical Immunology)

By

KARLIEN KALLMEYER

10552082

In the Faculty of Health Sciences

Department of Immunology

University of Pretoria

2019

Supervisor:

Prof. M.S. Pepper (University of Pretoria)

Co-supervisors:

Prof. B. Pittet-Cuénod and Dr. A. Modarressi (University of Geneva, Faculty of Medicine)

Prof J-C. Martinou (University of Geneva, Faculty of Science)

UNIVERSITÉ DE GENÈVE
Département de Chirurgie
Service de chirurgie plastique,
reconstructive et esthétique

FACULTÉ DES MÉDECINE
Professeure B. Pittet-Cuénod
Directrice de thèse

Département de Biologie

FACULTÉ DE SCIENCES
Professeur J-C. Martinou
Co-directeur de thèse

UNIVERSITÉ DE PRETORIA
Département d'immunologie

FACULTÉ DES SCIENCES DE LA SANTÉ
Professeur M.S. Pepper
Co-directeur de thèse

Investigating the homing and healing properties of adipose-derived mesenchymal stromal cells using a model of wound repair

THÈSE

Présentée à la faculté des sciences de l'Université de Genève

Pour obtenir le grade de Docteur ès sciences, mention biologie

En cotutelle avec l'Université de Pretoria, Afrique de Sud

par

KARLIEN KALLMEYER

de

Howick (Afrique du sud)

Thèse n° 5389

Genève

2019

IMPRIMATUR (UNIVERSITY OF GENEVA)

UNIVERSITÉ DE GENÈVE

FACULTÉ DES SCIENCES

DOCTORAT ÈS SCIENCES, MENTION BIOLOGIE

Thèse de Madame Karlien KALLMEYER

En cotutelle avec la University of Pretoria, South Africa

intitulée :

«Investigating the Homing and Healing Properties of Adipose-derived Mesenchymal Stromal Cells Using a Model of Wound Repair»

La Faculté des sciences, sur le préavis de Madame B. PITTET-CUENOD, professeure ordinaire et directrice de thèse (Faculté de médecine, Département de chirurgie), Monsieur J.-C. MARTINOU, professeur ordinaire et codirecteur de thèse (Département de biologie cellulaire), Monsieur M. PEPPER, professeur et codirecteur de thèse (Université de Pretoria, Afrique du Sud), Monsieur G. MAGALON, professeur émérite (Chirurgie plastique et reconstructive, Université Aix-Marseille, Marseille, France) autorise l'impression de la présente thèse, sans exprimer d'opinion sur les propositions qui y sont énoncées.

Genève, le 9 septembre 2019

Thèse - 5389 -

Le Doyen

N.B. - La thèse doit porter la déclaration précédente et remplir les conditions énumérées dans les "Informations relatives aux thèses de doctorat à l'Université de Genève".

This thesis led to a single publication:

Kallmeyer, K, André-Lévigne, D, Baquié, M, *et al.* Fate of systemically and locally administered adipose-derived mesenchymal stromal cells and their effect on wound healing. *STEM CELLS Translational Medicine*. 2019; 1– 1

DECLARATION OF ORIGINALITY

UNIVERSITY OF PRETORIA

DECLARATION OF ORIGINALITY

This document must be signed and submitted with every essay, report,

project, assignment, dissertation and / or thesis.

Full names of student:......KARLIEN KALLMEYER..

Student number:........10552082...

Declaration

1.   I understand what plagiarism is and am aware of the University's policy in this regard.

2.   I declare that this ...PhD THESIS............... (eg essay, report, project,
     assignment, dissertation, thesis, etc) is my own original work. Where other people's
     work has been used (either from a printed source, Internet or any other source), this
     has been properly acknowledged and referenced in accordance with departmental
     requirements.

3.   I have not used work previously produced by another student or any other person to
     hand in as my own.

4.   I have not allowed, and will not allow, anyone to copy my work with the intention of
     passing it off as his or her own work.

SIGNATURE OF STUDENT:..

SIGNATURE OF SUPERVISOR:..

SUMMARY

Adult mesenchymal stromal cells show promise therapeutically due to their multipotent differentiation capacity, immunomodulatory properties, paracrine signalling and ability to migrate to sites of injury. The potential use of adipose-derived stromal cells (ASCs) as a cellular therapy for treating delayed healing, non-healing and chronic wounds, their optimal route of administration, bio-distribution and fate needs to be investigated. Therefore, this study aimed first to establish the location and survival of systemically and locally administered ASCs during wound repair under physiological conditions (model 1) and second, the effect of locally administered ASCs during wound repair under pathological conditions of hyperglycaemia and ischemia (model 2). A dual tracking approach was used to follow firefly luciferase (Fluc) and green fluorescent protein (GFP) expressing ASCs by bioluminescence imaging (BLI) and histological analysis.

The immuno-phenotype and differentiation capacity of rat ASCs transduced to express Fluc and GFP were assessed before the cells were used in the wound repair models. In model 1, full-thickness bilateral wounds were created on the dorsal aspect of the hind paws in healthy rats and two treatment modes were assessed: a single dose of 2×10^6 ASCs or NaCl administered systemically into the tail vein or 2×10^5 ASCs injected locally around each wound. Animals were followed by digital photography, BLI and sacrificed for histological analysis. In model 2, ischemia was induced unilaterally by resection of the femoral artery in hyperglycaemic rats before full-thickness bilateral wounds were created and 2×10^5 ASCs or NaCl administered locally around each non-ischemic and ischemic wound. Animals were followed by digital photography and sacrificed for histology and immunohistochemistry (IHC). Haematoxylin/eosin (H/E) staining as well as Masson's trichrome staining and IHC for alpha-smooth muscle actin (αSMA), ionised calcium binding adaptor molecule 1 (Iba1) and GFP were performed on sample sections. Wound closure time and the contraction/epithelialisation ratio were assessed in both models.

Transduced ASCs maintained their immuno-phenotype and differentiation capacity. Under physiological conditions, systemically administered ASCs were filtered out in the lungs, whereas locally administered ASCs survived at the injection site and migrated into the wound bed. Wound closure was accelerated by 5 and 7 days with systemic and local ASC treatment

respectively compared to control animals, and this was the result of increased epithelialisation. Under pathological conditions, locally administered ASCs significantly enhanced wound closure in non-ischemic and ischemic wounds by 9 days compared to control wounds. Semi-quantitative analysis revealed that ASC treatment led to enhanced cellularity in the wound. No changes in collagen deposition, vascularisation (as determined by αSMA staining) or macrophage infiltration were observed between ASC treated and control groups. However, αSMA staining was detected earlier and remained higher at wound closure in the former without enhancing wound closure by contraction.

Despite the limited systemic homing capacity of ASCs, wound healing was improved. Locally injected ASCs migrated from the wound edge into the wound bed where they promoted wound repair. Under pathological conditions, ASCs enhanced wound closure. A significant increase in wound cellularity was observed, possibly through a mechanism of paracrine signalling that recruited more immune regulating and tissue repair cells into the granulation tissue. Administration of ASCs for delayed healing wounds show promise as a cellular treatment for enhancing wound repair.

Key words: Adipose-derived mesenchymal stromal cells (ASCs), *in vivo* imaging, bioluminescence imaging (BLI), green fluorescent protein (GFP), firefly luciferase (Fluc), re-epithelialisation, contraction, wound healing, wound repair, homing

RÉSUMÉ

Les cellules stromales mésenchymateuses adultes sont prometteuses du point de vue thérapeutique en raison de leur capacité de différenciation multipotente, de leurs propriétés immunomodulatrices, de leur signalisation paracrine et de leur capacité à migrer vers les sites de la lésion. Le potentiel d'utilisation des cellules stromales dérivées du tissu adipeux (ASC) en tant que thérapie cellulaire pour traiter les cicatrices à cicatrisation retardée, les cicatrices non cicatrisées et les plaies chroniques, ainsi que leur modalité optimale d'administration doivent être enquêté. Cette étude a donc comme but d'évaluer 1) la distribution et la survie des ASCs injectées par voie systémique ou administrées localement, dans le contexte de cicatrisation des plaies dans des conditions physiologiques (modèle 1), et 2) l'effet des ASCs administrées localement sur la cicatrisation des plaies dans des conditions pathologiques d'hyperglycémie et d'ischémie (modèle 2).

Afin de suivre le parcours des ASCs, une approche de double marquage cellulaire a été utilisée par transduction génétique via l'expression de bioluminescence (BLI) et de la protéine fluorescente verte (GFP). L'immunophénotypage et la capacité de différenciation des ASCs transduites ont été évalués avant que celles-ci ne soient utilisées dans les modèles de cicatrisation. Dans le modèle 1, des plaies pleine épaisseur ont été créées sur la face dorsale des deux pattes arrières des rats sains et deux prises en charge différentes sont évaluées: l'injection systémique dans la veine de la queue de 2×10^6 de ASCs ou de NaCl, ou l'injection locale autour de chacune des plaies de 2×10^5 de ASCs. Les animaux ont été suivis par photographie numérique et BLI, puis sacrifiés pour l'analyse histologique. Dans le modèle 2, des rats hyperglycémiques ont été utilisés et la condition d'ischémie a été créée artificiellement via la résection de l'une des artères fémorales. Les mêmes plaies sur la face dorsale des deux pattes arrière ont ensuite été créées, suivi de l'injection locale autour des plaies ischémiques et/ou non-ischémiques de 2×10^5 de ASCs ou de NaCl. Les animaux ont été suivis par photographie numérique, puis sacrifiés pour l'analyse histologique et immunohistochimique (IHC), avec les colorations d'hématoxyline/éosine (H/E) et de trichrome de Masson, ainsi que le marquage de l'actine alpha du muscle lisse (αSMA), du ionise calcium binding adaptaur molécule 1 (Iba1) et du GFP. Le temps de fermeture des plaies et le ratio contraction/épithélialisation ont été évalués dans les deux modèles.

Nos résultats montrent que les ASCs transduites ont pu maintenir leur immunophénotypage et leur capacité de différenciation par rapport aux ASCs non-induites. Dans des conditions physiologiques, les ASCs injectées par voie systémique ont rapidement été séquestrées dans les poumons, tandis que les ASCs administrées localement sont restées au point d'injection et ont migré dans le lit de la plaie. Le temps de fermeture des plaies traitées par ASCs a été réduit de 5 et 7 jours, que la voie d'administration soit par voie systémique ou locale par rapport aux animaux témoins, grâce à une épithélialisation plus importante. Dans les conditions pathologiques, les ASCs administrées localement ont considérablement amélioré le temps de fermeture des plaies ischémiques et non ischémiques de 9 jours par rapport aux plaies témoins. Les analyses semi-quantitatives des coupes histologiques ont révélé que le traitement par ASCs a induit une augmentation de la cellularité des plaies par rapport aux plaies non traitées, sans modifier le dépôt de collagène, la vascularisation (quantifiée par l'immunomarquage de αSMA), ou l'infiltration de macrophages. Cependant, l'expression αSMA a été détectée plus précocement dans les plaies traitées, et est demeurée plus importante à la fermeture de celles-ci, sans toutefois augmenter la contraction.

Malgré la capacité limitée de migration vers la plaie des ASCs injectées par voie systémique, celles-ci ont amélioré le processus de cicatrisation. De leur côté, les ASCs injectées localement au pourtour des plaies ont pu migrer dans le lit des plaies et favoriser leur fermeture. Dans des conditions pathologiques, le traitement par ASCs injectées localement a également amélioré la fermeture des plaies. Nous avons observé une augmentation significative de la cellularité des plaies suite à l'administration d'ASCs, probablement secondaire à la signalisation paracrine permettant le recrutement d'un nombre plus important de cellules de régulation immunitaire et de réparation dans le tissu de granulation. Nous avons donc conclu que l'administration d'ASCs constitue un traitement cellulaire prometteur dans la prise en charge des plaies à cicatrisation retardée et nécessiterait des investigations supplémentaires.

TABLE OF CONTENTS

LIST OF ABBREVIATIONS

(c)DNA: (complementary) deoxyribonucleic acid

(m)RNA: (messenger) ribonucleic acid

18s: 18S ribosomal RNA

ACTB: beta-actin

Adipor2: adiponectin receptor 2

AEC: aminoethyl carbazole

Ang-1: angiopoietin 1

APC: allophycocyanin

ARS: alizarin red S

ASC(s): adipose-derived stromal cell(s)

ATP: adenosine triphosphate

bFGF: basic fibroblast growth factor

BLI: bioluminescence imaging

BMC(s): bone marrow mononuclear cell(s)

BM-MSC(s): bone marrow-derived MSC(s)

BSA: bovine serum albumin

BSD: blasticidine

C/EBPα or β: CCAAT/enhancer-binding protein alpha or beta

CD: cluster of differentiation

CGM: complete growth medium

CO_2: carbon dioxide

Cq: quantitation cycle

d7: day 7

DAPI: 4',6-diamidino-2-phenylindole

DC: dendritic cell

DMEM: Dulbecco's Modified Eagle's Medium

DMSO: dimethyl sulphoxide

DPC: dermal papilla cells/stem cells

DSC: dermal sheath cells

ECM: extracellular matrix

EDTA:	ethylenediaminetetraacetic acid
EGF:	epidermal growth factor
EPC:	endothelial progenitor cell
ESC:	embryonic stem cell
FABP4:	fatty acid binding protein 4
FBS:	foetal bovine serum
FFPE:	formaldehyde fixed paraffin embedded
FGF:	fibroblast growth factor
Fluc:	firefly luciferase
GAPDH:	glyceraldehyde 3-phosphate dehydrogenase
GFP:	green fluorescence protein
GvHD:	graft versus host disease
H/E:	haematoxylin/eosin
h:	hour(s)
HBOT:	hyperbaric oxygen therapy
HBS:	HEPES buffered saline
HBSS:	Hanks' Balanced Salt Solution
HFSC:	hair follicle stem cell
HGF:	hepatocyte growth factor
HRP:	horse radish peroxidase
HSC(s):	haematopoietic stem cell(s)
IA:	intra-arterial
Iba1:	ionised binding adaptor molecule 1
IBMX:	3-isobutyl-methylxanthine
ICAM:	intercellular cell adhesion molecule
ICM:	inner cell mass
IFATS:	International Federation for Adipose Therapeutics and Science
IFNγ:	interferon gamma
IGF:	insulin growth factor
IgG:	immunoglobulin G
IHC:	immunohistochemistry
IL:	interleukin

IM:	intramuscular
IP:	intraperitoneal
iPSC(s):	induced pluripotent stem cell(s)
ISCT:	International Society for Cellular Therapy
IV:	intravenous
KGF:	keratinocyte growth factor
KLF:	krüppel-like factor 2
LFA-1:	lymphocyte function-associated antigen 1
MDH1:	malate dehydrogenase 1
MMP:	matrix metalloproteinase
MOI:	multiplicity of infection
MRI:	magnetic resonance imaging
MSC(s):	mesenchymal stem/stromal cell(s)
MWM:	molecular weight marker
NaCl:	sodium chloride
NADPH:	nicotinamide adenine dinucleotide phosphate
NK:	natural killer cell
NTC:	non-template control
OCT4:	octamer binding transcription factor 4
ORO:	oil red O
ORS:	outer root sheath
P:	passage
PBS:	phosphate buffered saline$
PC7:	phycoerythrin cyanin 7
PDGF:	platelet derived growth factor
PE:	phycoerythrin
Pen/strep:	penicillin-streptomycin
PET/CT:	positron emission tomography/computed tomography
PPARγ:	peroxisome proliferator-activated receptor gamma
PSGL-1:	P-selectin glycoprotein-1
ROI:	region of interest
ROS:	reactive oxygen species

RT:	room temperature
RT-qPCR:	reverse transcriptase quantitative polymerase chain reaction
SC:	subcutaneous
SD:	standard deviation
SDF-1:	stromal derived factor-1
SOX2:	sex determining region Y box-containing gene 2
SPIO:	supermagnetic iron oxide
STZ:	streptozotocin
SVF:	stromal vascular fraction
TGFβ:	transforming growth factor beta
Tm:	melting temperature
TNFα/β:	tumour necrosis factor alpha/beta
UBC:	ubiquitin C
UC:	umbilical cord
UCB:	umbilical cord blood
UV:	ultraviolet light
v/v:	volume/volume
VCAM:	vascular cell adhesion molecule
VEGF:	vascular endothelial growth factor
VLA-1:	very late antigen 1
WC:	wound closure
YWHAZ:	tyrosine 3-monooxygenase/tryptophan 5-monooxygenase activation protein zeta
αSMA:	alpha smooth muscle actin

ACKNOWLEDGEMENTS

"For I know the plans I have for you" declares the Lord, *"plans to prosper you and not to harm you, plans to give you hope and a future"* Jeremiah 29:11 (NIV)

On a personal note:

Praise to my Father in Heaven. Every path I have chosen to take has been through Your guidance. I stand here today by Your grace, and with Your love I was able to overcome the obstacles that came my way.

I would like to thank my parents, Pieter and Mariza, for all your love, support and motivating words. No words can describe the love and gratitude I have for you. I appreciate all the sacrifices you have made to get me here. Thank you to my family and friends for supporting me in all my endeavours, keeping me motivated when things were not going well and bringing some sanity to my otherwise stressful life.

On a professional note:

I would like to thank the following funders:

I would like to thank all the rats who were sacrificed for my scientific research.

Finally, thank you to my supervisors, Michael Pepper, Brigitte Pittet-Cuénod and Ali Modarressi.

Michael, thank you for believing in me, pushing me out of my comfort zone and allowing me to pursue this PhD internationally.

Brigitte, thank you for making a place for me in your research laboratory and sharing another world, surgery, with me. Your passion for your work has been an inspiration to me.

Ali, thank you for your personal supervision and for being there to discuss the project and share scientific ideas.

LIST OF TABLES

LIST OF FIGURES

CHAPTER 1. INTRODUCTION

1.1 PHYSIOLOGY OF SKIN WOUND HEALING

1.1.1 <u>Structure of skin</u>

Skin is the largest organ in the body. It functions as a protective barrier against outside factors while maintaining homeostasis of the human body. It is comprised of three layers, namely the epidermis, dermis and the hypodermis (Figure 1.1A).[1, 2] The epidermis is composed of various layers of organised keratinocytes to form a stratified epithelium (Figure 1.1B).[2] The different layers, or strata, described from deep to superficial are (i) the basal layer, referred to as stratum *basale*, which is the deepest layer containing proliferating keratinocytes and inter-follicular keratinocyte stem cells; (ii) the stratum *spinosum*, which is found above the basal layer and consists of several layers of polyhedral keratinocytes; (iii) the stratum *granulosum* which has a granular appearance from the presence of kerato-hyalin granules that contain proteins crosslinked with keratin filaments; and the outer layer, (iv) the stratum *corneum*, which is made up of 15 to 20 layers of cornified (dead) cells devoid of nuclei and cytoplasmic organelles, and is responsible for making the skin hydrophobic. Thick skin, found on the palms of the hands and the soles of the feet, contain a fifth layer located between the stratum corneum and the stratum granulosum, called the stratum *lucidum*. The dermis is made up of densely packed connective tissue that houses hair follicles (Figure 1.1C), sebaceous and sweat glands, nerves, and blood vessels. The hypodermis is formed from loose connective and fatty tissues. In the dermis, the hair follicle complex (known as the pilosebaceous unit in humans) is comprised of the hair follicle, sebaceous and apocrine glands. However, in humans, the pilosebaceous unit is devoid of apocrine glands. The dermal papilla cells (DPCs) found at the base of the hair follicle modulate hair follicle cycling, whereas the dermal sheath cells (DSCs) have been implicated in replacing the dermis in response to injury.[3, 4] This will be further discussed under section 1.5.2.1 "Endogenous stem cells in the hair follicle". Humans are tight skinned, unlike other mammals, such as mice, rats and rabbits, which are loose skinned animals. The panniculus carnosus in loose skinned animals is a thin layer of striated muscle beneath a relatively thin adipose layer making the skin

independent from deeper muscles, thereby allowing for large skin movements.[5] It plays an important role in wound healing by facilitating wound contraction.

1.1.2 <u>Cutaneous wounds</u>

A cutaneous wound is defined as a disruption in the normal anatomical organisation of skin resulting in reduced function.[6] Wounds can be classified into three categories based on their location, depth and degree of tissue loss.[7] Superficial wounds occur where damage affects the epidermis; partial-thickness wounds involves damage to the epidermis and a portion of the dermis; and in full-thickness wounds where the dermis has been destroyed and in severe cases includes damage to subcutaneous fat tissue and bones.[2, 7] Healing takes place by repair, which involves restoring the injured tissue in order to re-establish tissue architecture and function.[8] Repair includes two different processes, namely regeneration and replacement.[9] Healing by regeneration aims to rebuild damaged tissues to their normal state so that tissue morphology and functionality are completely restored. Replacement, on the other hand, repairs severely damaged tissues by filling the wound with connective tissue, forming a scar where the tissue used to be.

Superficial and partial-thickness wounds heal by repair through epithelialisation to reconstitute damaged epithelium, whereas full-thickness wounds heal by replacement which requires formation of granulation tissue to fill the void of the wound and in so doing provides a scaffold for epithelialisation to occur on. Depending on how wounds progress through the normal healing process, they can further be categorised as acute and chronic wounds.[7, 10] Acute wounds occur either from surgical intervention or following a traumatic accident, and include abrasions, superficial burns, and partial-thickness wounds presenting with significant loss of tissue.[10] Chronic wounds result when the wound is unable to proceed through the normal phases of wound healing in an orderly and timely manner for repair and for structural and functional integrity to be regained.[11] Chronic wounds are identified as wounds that do not proceed to heal within three months. The chronic state is further exacerbated by various factors and is associated with senescence, ischemia and bacterial colonisation. In contrast to an acute wound, the chronic
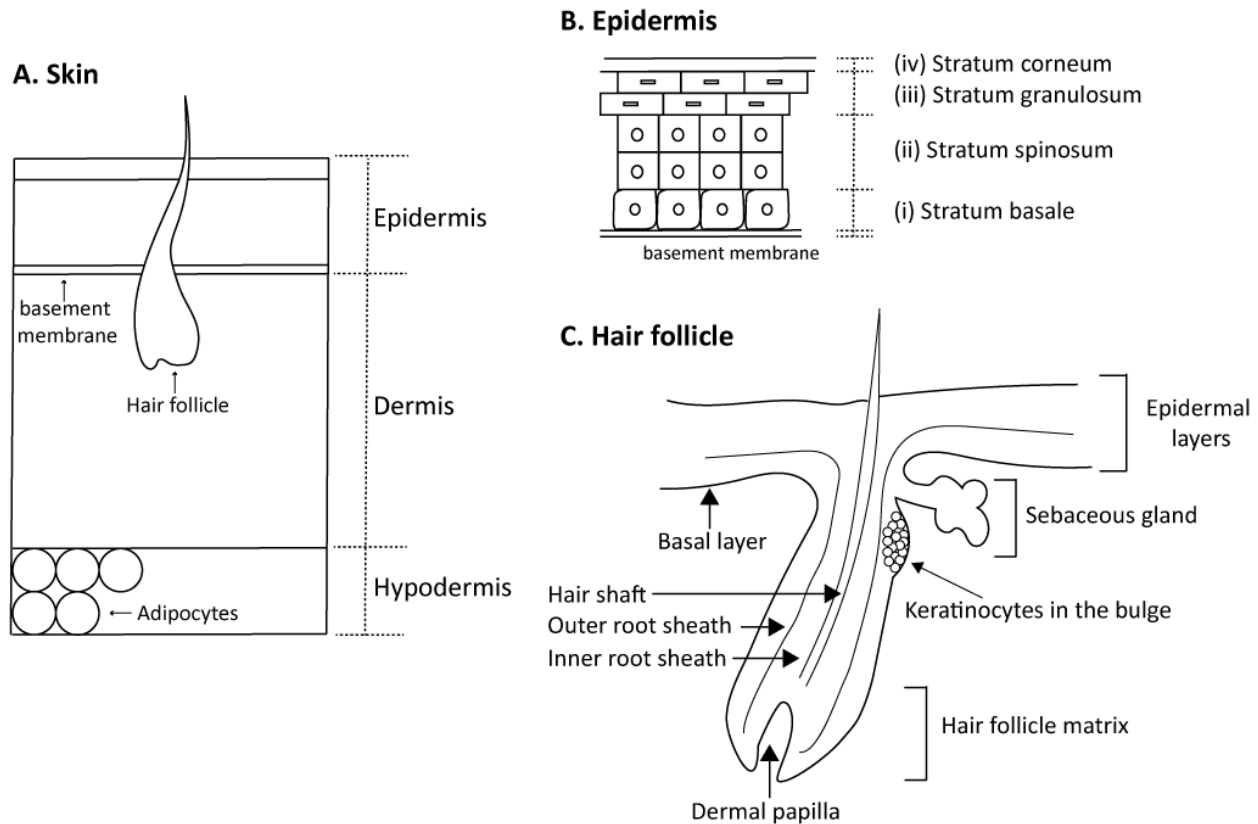
Figure 1.1 A diagrammatic representation of skin histology.
(A) The skin is composed of 3 layers, the epidermis, dermis and the hypodermis. (B) The epidermis can further be divided into 4 layers from deep to superficial: (i) stratum basale, (ii) stratum spinosum, (iii) stratum granulosum, and (vi) stratum corneum. (C) The hair follicle found in the dermis is a source of stem cells that can be found in the dermal papilla and dermal sheath cells. Figure adapted from Rittié *et al*., 2016 and Alonso and Fuchs, 2003.[2, 12]

wound is characterised by persistent inflammation as well as impaired extracellular matrix (ECM) synthesis and neo-vascularisation.[7, 13] All cutaneous wounds have the potential to become chronic if there is an underlying cause leading to the chronic state. Common underlying causes include vascular insufficiency, diabetes mellitus, compromised immunity, malnutrition, advanced age and other comorbidities that contribute to poor wound healing.[11]

1.1.3 Phases of wound healing

Wound healing is a complex process that involves the interaction of soluble mediators, ECM components and a variety of infiltrating and resident cells.[14] It is commonly described as four

overlapping phases: haemostasis, inflammation, proliferation, and tissue remodelling and maturation (Figure 1.2).[2]

1.1.3.1 Phase of haemostasis

Injury to the vasculature caused by trauma initiates molecular and cellular responses to facilitate vasoconstriction, platelet aggregation and fibrin deposition to prevent excessive bleeding, and provisionally protects the wound from the external environment through the formation of a clot.[15] The clot is composed of platelets, blood cells and fibrin.[16] Platelets become activated and respond by releasing growth factors (e.g. platelet-derived growth factor (PDGF)) and cytokines (e.g. transforming growth factors (TGFs)) that in turn attract inflammatory cells (such as monocytes/macrophages, lymphocytes) and fibroblasts.[17, 18] Fibrin participates in the formation of a meshwork, stabilising platelets, and allowing fibronectin, released by resident fibroblasts and epithelial cells, to bind to this meshwork. This fibrin-fibronectin matrix acts as a provisional matrix in the wound for cell attachment and migration during the repair process.[16]

1.1.3.2 Inflammatory phase

Shortly after haemostasis, there is an increase in vascular permeability and chemotactic agents are released that recruit neutrophils, monocytes/macrophages and lymphocytes into the wound.[2, 7, 10, 19, 20] Neutrophils dominate the first 48 hours (48h) to clean the wound site of bacteria, cell debris and damaged tissue.[21] Monocytes penetrate after the number of neutrophils decreases. Monocytes differentiate into pro-inflammatory macrophages that further phagocytose and digest tissue debris and expended neutrophils. Furthermore, macrophages secrete collagenases and elastases to break down damaged tissue, and release growth factors and cytokines that promote tissue proliferation and cell migration.[22, 23] T-lymphocytes are attracted to the injured site where they secrete lymphokines to promote fibroblast proliferation.[7, 24, 25] The transition from inflammation to proliferation requires a shift from a pro-inflammatory to an anti-inflammatory phenotype. As a key player in this transition, the macrophage shifts from a pro-inflammatory phenotype (M1) to a reparative phenotype (M2) in

response to specific cues such as interleukin-4 (IL-4) and 10, where they (M2 macrophages) now secrete anti-inflammatory mediators and growth factors.[22, 26-28]
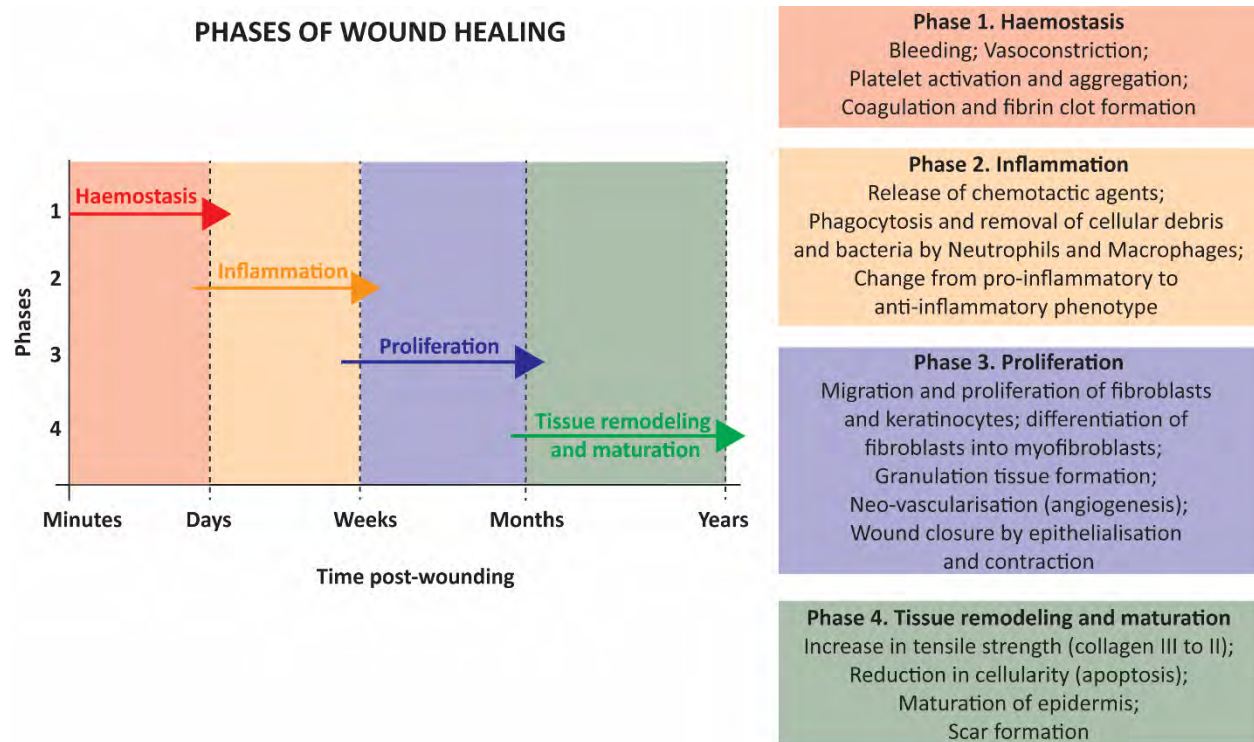
Figure 1.2 Phases of wound healing.
The wound healing process is described as four overlapping phases: phase of haemostasis, inflammatory phase, proliferative phase and phase of tissue remodelling and maturation.

1.1.3.3 Proliferative phase

Three days post wounding, the proliferative phase is initiated to restore the damaged epidermis and dermis. It is characterised by migration and proliferation of fibroblasts and keratinocytes, migration of epidermal cells, synthetisation of ECM and formation of granulation tissue, ultimately resulting in coverage of the wound surface and restoration of the vascular network.[2]

1.1.3.3.1   Granulation tissue formation

A substrate is required for epithelialisation to occur in full-thickness wounds where the basement membrane has been destroyed.[2] New fibroblasts colonise the provisional ECM laid down during

the inflammatory phase. They produce proteases to degrade the existing matrix and start to deposit collagen and cellular fibronectin to form granulation tissue.[29, 30]

1.1.3.3.2 Neo-vascularisation: angiogenesis and vasculogenesis

To supply the wound with the necessary nutrients and oxygen required for wound repair, restoration of the vascular network is required. The process of angiogenesis is initiated by growth factors, such as vascular endothelial growth factor (VEGF), PDGF and basic fibroblast growth factor (bFGF), that activate endothelial cells from existing vessels to sprout and form new blood vessels.[31] Another process, vasculogenesis, also contributes to forming blood vessels from recruited bone marrow-derived endothelial progenitor cells (EPCs).[32]

1.1.3.3.3 Wound epithelialisation

Epithelialisation requires new cells to replace the keratinocytes that were lost. At the wound edge, the marginal epidermis expands to contribute to generating a new epidermis. Epidermal keratinocytes become activated and migrate out of the marginal epidermis, building the new epidermis by successive implantation of cells to advance the epidermal tongue, eventually covering the wound with a new epithelium once the margins meet.[2, 30] To supply the high demand in cells required to cover the wound, keratinocytes resident at the basal layer of the wound edge and epithelial cells from nearby hair follicle complexes start proliferating and migrating.[12]

1.1.3.3.4 Wound contraction

As the ECM composition changes, mechanical stimuli and TGF-beta (TGFβ) expression prompt fibroblasts to mature and differentiate into myofibroblasts. Myofibroblasts can be identified by the expression of alpha-smooth muscle actin (αSMA) and have contractile activity which promotes wound contraction.[33, 34] Contraction can be described as the movement of the wound margin toward the centre of the wound to reduce the size of the wound bed without tissue regeneration.[2] Insufficient wound contraction can lead to non-healing wounds whereas excessive wound contraction can lead to scarring.[35]

1.1.3.4 Remodelling and maturation

During the remodelling phase, all the previously activated processes are switched off to allow normalisation of epidermal thickness, cellular content, ECM composition and blood vessel count to mimic as closely as possible the pre-wound state of the dermis. A transition occurs from collagen III to collagen I, which has a higher tensile strength and takes longer to be deposited.[29] Overall remodelling and maturation, which can take months to years, lead to an avascular and acellular environment, referred to as the scar tissue.

1.2   PATHOPHYSIOLOGY OF CHRONIC WOUNDS

The pathophysiology of chronic wounds is not fully understood. Progress has been hampered due to the heterogeneity of chronic wounds, difficulty in performing clinical trials, a lack of appropriate animal models as well as the complexity of the wound repair process. The treatment of ischemic wounds, particularly of the lower limb, remains a significant clinical challenge. Pre-disposing factors such as diabetes mellitus, ischemia and age impair the healing process. Diabetes mellitus is the leading cause of impaired wound healing, and minor wounds in diabetics often develop into chronic, non-healing wounds/ulcers that are pre-disposed to infection. Severe infections can lead to gangrene and ultimately amputation. Commonly, chronic wounds present with excessive inflammation, persistent infection and impaired responses by repair cells (dermal and epidermal cells) (Figure 1.3).[19]

1.2.1 <u>Effect of diabetes on wound repair</u>

In diabetes, inflammatory cytokines and chemokines are elevated post-wounding for extended periods, keeping the wound in a chronic inflammatory state.[36] Superficial wound fluid from non-healing wounds of diabetic patients presented with up-regulated levels of IL-1β, IL-6, IL-8, and down-regulation of PDGF, VEGF, epidermal growth factor (EGF) and bFGF.[37] In diabetic mice, prolonged expression of CCL2 and CXCL2 was correlated with elevated neutrophils and macrophages, who further up-regulated the expression of inflammatory cytokines IL-1β and TNF-alpha (TNFα).[38] Cellular processes affected by diabetes include abnormal keratinocyte and fibroblast migration, proliferation, and enhanced apoptosis, abnormal macrophage polarisation

(increased pro-inflammatory M1 macrophages and decreased anti-inflammatory M2 macrophages), impaired recruitment of mesenchymal stromal/stem cells (MSCs) and EPCs, and decreased vascularisation.[39] Figure 1.3 illustrates the differences found between normal and chronic wounds. Macrophages isolated from the wounds of diabetic mice and patients showed impairment in efferocytosis which is associated with a higher burden of apoptotic cells as well as increased expression of pro-inflammatory and decreased expression of anti-inflammatory cytokines.[40] Fibroblasts from chronic wounds of patients with and without diabetes have a lower mitogenic response to PDGF, insulin growth factor (IGF), bFGF and EGF.[41] Isolated diabetic mouse fibroblasts have reduced cellular migration, increased matrix metalloproteinases-9 (MMP-9) production and reduced VEGF production.[42] Keratinocytes from chronic ulcers of patients with diabetes have impaired migratory potential.[43] Furthermore, hyperglycaemia leads to matrix glycation and increase in MMP production, both of which ultimately lead to impaired ECM formation and maturation in the wound.[19, 44-46]

1.2.2 <u>Effect of ischemia on wound repair</u>

Arteriosclerosis and microvascular disease put diabetic patients at a higher risk of developing chronic wounds of the feet in part due to reduced blood flow to the lower limbs. Reduced blood flow can result in insufficient oxygen delivery, reduced supply of nutrients and an inability to maintain tissue homeostasis, leading to cell and/or tissue death.[47] Cells use oxygen during aerobic metabolism to fuel cellular processes during wound repair, increasing the demand for oxygen.[48] Disruption of the skin and vasculature upon injury increases the consumption of oxygen, leading to acute hypoxia. Hypoxia is initially favoured for wound repair by enhancing the migration and proliferation of endothelial cells and fibroblasts and other key wound repair components, such as inflammatory cell chemotaxis and keratinocyte migration.[49] However, during normal wound repair, oxygen recovery occurs through vasodilation, and neo-vascularisation. Neo-vascularisation, the formation of new blood vessels, occurs by angiogenesis and vasculogenesis.[31, 50] Angiogenesis occurs when endothelial cells from pre-existing blood vessels sprout, migrate and proliferate to form new blood vessels, whereas vasculogenesis is the *de novo* synthesis of blood vessels from differentiating progenitor cells, such as EPCs that are

recruited from the bone marrow. Chronic wound environments have an imbalance between the supply and demand of oxygen for healing tissue.[47] If oxygen levels cannot be restored, chronic hypoxia results which is deleterious and inhibits wound repair. Redox signalling and production of reactive oxygen species (ROS) are initiated by hypoxia in a process that relies on the activation of the nicotinamide adenine dinucleotide phosphate (NADPH) oxidase family of enzymes.[51] Increased ROS signalling provides phagocytotic immune cells with disinfecting capabilities and mediates signalling to initiate cell proliferation, migration and differentiation. However, excessive ROS production contributes to a hypoxic environment that will cause cell death.[47, 52] Thus, the inability to shift away from the initial acute hypoxic environment through a lack of oxygen supply will cause impaired redox signalling during the healing process.

1.3   APPROACHES TO TREATING CUTANEOUS WOUNDS

Wounds are managed by performing an initial assessment to determine the type of wound, the state of the wound and the approach needed for treatment. Three main approaches are taken to treat cutaneous wounds: primary, secondary and tertiary intention healing.[2] Primary intention is used when there is no or little tissue loss. The wound is closed within 8h post creation using aseptic techniques to suture the area or by using synthetic adhesive materials. An example is uninfected incised surgical wounds, where wounds are closed immediately post operatively. Secondary intention allows the repair process to restore wounds with extensive tissue loss where the wound edges cannot be brought together. Overall such healing takes longer to repair, results in greater scarring as well an increased chance of infection. Tertiary intention, also referred to as delayed primary intention, is when a wound is deliberately left open, for reasons such as infection, need for debridement, or lack of vascularisation, and then closed or sutured later.

To assist with the implementation of the concept of preparing the wound bed to encourage endogenous healing, the concept of TIME was introduced in 2002.[53, 54] This concept summarises four main components that are used for wound bed preparation, namely *tissue* management, control of *infection* and *inflammation*, identifying *moisture* imbalance and evaluation of whether advancement of the epithelial *edge* of the wound is impaired. This helps with the identification
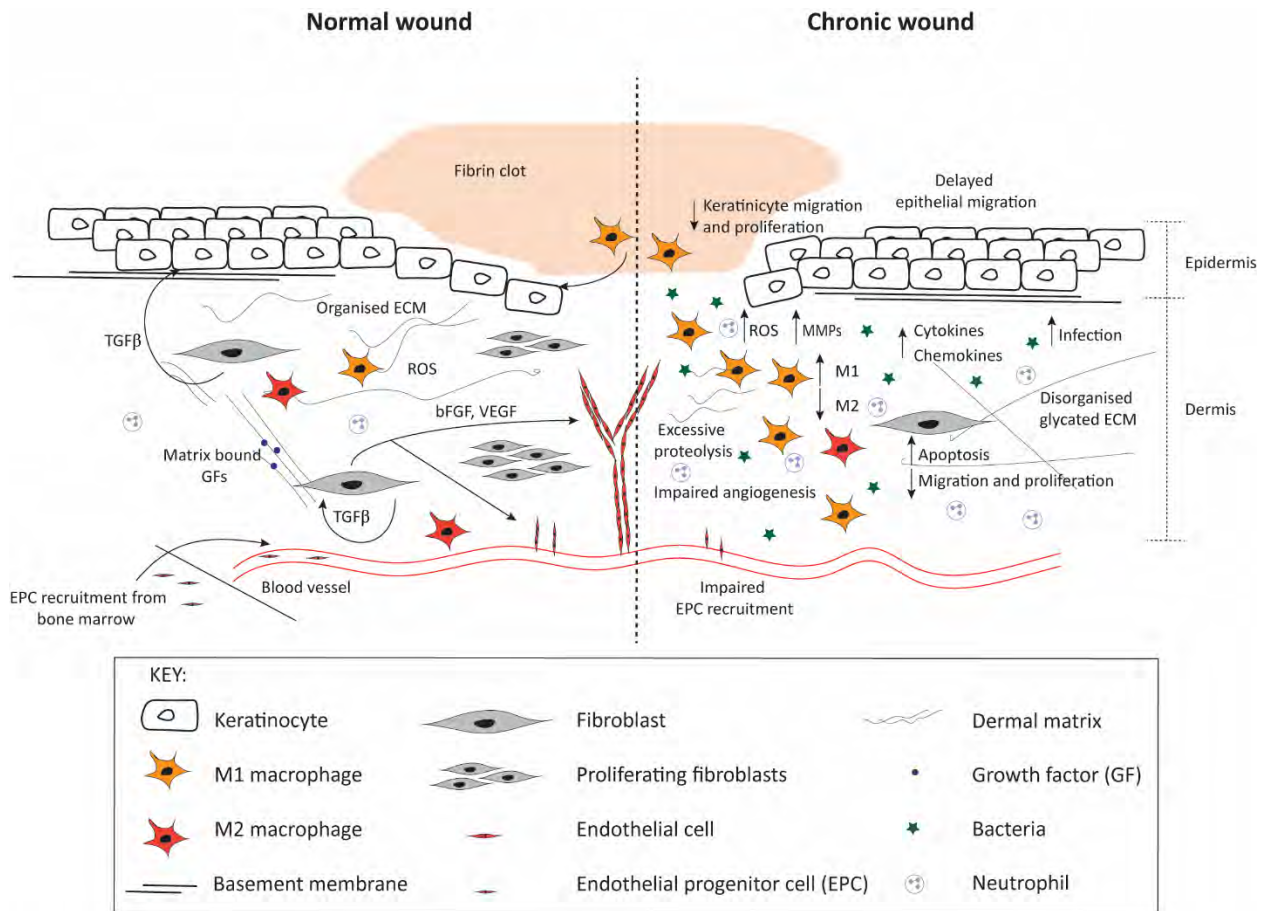
Figure 1.3 Normal and chronic wound healing.

The microenvironment of a normal wound bed (left) is characterised by the presence of growth factors, cytokines and chemokines, responsive epidermal and dermal cells (keratinocytes and fibroblasts), and a well organised extracellular matrix (ECM). The angiogenic response proceeds in a timely manner via sprouting of existing blood vessels and through the recruitment of endothelial progenitor cells (EPCs). Acute wounds also have low bacterial burden. Chronic wounds (right) have a high incidence of bacteria which leads to an excessive and persistent inflammatory response. High levels of matrix metalloproteinases (MMPs), reactive oxygen species (ROS) and proteases are secreted by macrophages (M1) which fail to convert to an anti-inflammatory phenotype (M2) leading to proteolysis, degradation of growth factors and ECM. Epidermal and dermal cells (keratinocytes, fibroblasts) present with delayed migration, proliferation and differentiation. Impaired angiogenesis prevents the supply of oxygen and nutrients required for cellular metabolism. All these factors exacerbate the delay in wound repair found in chronic wounds. Figure adapted from Demidova-Rice *et al.*, 2012 and Xu *et al.*, 2013.[19, 39]

of barriers to healing and the implementation of a plan of care to remove these barriers and in so doing, promote wound healing. Evaluation of the "T" will determine if the wound tissue is necrotic or deficient. Debridement is the process implemented to remove the necrotic tissue. Common debridement approaches are surgical, autolytic, enzymatic, bio and mechanical debridement.[55] The "I" will determine whether the wound is infected and shows elevated levels of inflammation. This will be followed by treatment with anti-microbials, anti-inflammatories and protease inhibitors. Superficial wounds are often treated with topical anti-microbial agents, whereas deep or systemic infections are treated with systemic antibiotics. The "M" refers to the moisture content of the wound. A dry wound will slow epithelial cell migration and can be corrected by applying moisture balancing dressings. Excessive moisture will cause maceration of the wound margin and increased proliferation of bacteria and can be controlled by negative pressure treatments. The "E" tries to identify why the wound edge is not advancing and whether this is due to non-migrating keratinocytes, non-responsive wound cells, abnormal ECM or protease activity. This component requires re-assessment of the underlying cause and then the use of corrective therapies: surgical approaches such as debridement, secondary wound closure, use of skin grafts or flaps, or conservative approaches using biological agents or other therapies to help with the healing process. Traditional wound management, which has been extensively reviewed by Zeng and colleagues, includes the use of skin grafts (such as split-thickness skin grafts or full-thickness skin grafts) as autografts, allografts or xenografts, and wound dressings (such as gauze, human amniotic membrane, polysaccharide-based dressings, hydrocolloid dressings, foam dressings and transparent film dressings).[56] Other potential wound management options that still require further testing and are not yet widely accepted or used is the use of engineered skin substitutes, hyperbaric oxygen therapy (HBOT), the use of growth factors and cytokines, and stem cell therapy. The role of stem cell therapy, particularly the use of MSCs will be discussed in the next section.

1.4   STEM CELLS

Multicellular organisms can regenerate damaged tissue through cycles of apoptosis and tissue regeneration. Stem and progenitor cells have been proposed to be involved during these

processes as they may be recruited to sites of inflammation in response to signalling events initiated as a result of tissue damage.[57, 58] However, tracking endogenous stem and progenitor migration from their specific niche *in vivo* is hampered by the lack of a single identifiable marker and appropriate *in vivo* models. Upon arrival, stem and progenitor cells proliferate and differentiate to eventually replace the damaged tissues, and/or exert paracrine effects in response to specific environmental stimuli. Stem cells are the body's natural reservoir of unspecialised cells with the capacity to self-renew and differentiate into specialised cell types to replenish depleted and/or replace damaged tissues. Four major groups of stem cells have been defined: embryonic stem cells (ESCs), foetal stem cells, induced pluripotent stem cells (iPSCs) and adult stem cells. Embryonic stem cells are found during development in the inner cell mass (ICM) of the blastocyst before it is implanted. They are pluripotent in nature and have the ability to generate any cell type of the body.[59] However, the use of ESCs is associated with ethical concerns as their isolation involves the destruction of a human embryo.[60] Foetal stem cells are derived from neonatal tissues such as the amniotic fluid, Wharton's jelly, placenta, and amniotic membrane, and portray characteristics between embryonic and adult stem cells.[61] The potency of these different populations of stem cells is still being investigated. Induced pluripotent stem cells are not naturally found, but instead are engineered from adult differentiated somatic cells.[62] Induced pluripotent stem cells are adult cells that have been re-programmed to an embryonic-like state by introduction of genes for the transcription factors, octamer-binding transcription factor4 (*OCT4)*, sex determining region Y box-containing gene 2 (*SOX2*), proto-oncogene *c-MYC* and tumour suppressor Krüppel-like factor 2 (*KLF2*). This technology allows stem cell research to move away from embryo destruction while opening doors to a new era of personalised medicine whereby patient-specific iPSCs could be used in drug screening and for generating *in vitro* models of human diseases.[60] All adult tissues contain a population of resident committed progenitor/stem cells.[63] Adult stem cells are multipotent as they can only give rise to cells from a single germ layer (endoderm, ectoderm or mesoderm). Overall, they play a role in tissue maintenance and repair of the specific niche they reside in.[64] Adult stem cells can further be classified as either haematopoietic or non-haematopoietic. Haematopoietic stem cells (HSCs) were the first tissue-specific stem cells to be studied and are involved in constituting the blood

system through regulating haematopoiesis. They were discovered when systemic transplantation of bone marrow cells from healthy adult mice protected recipients from a lethal dose of irradiation.[65] Umbilical cord blood (UCB) was recognised as another source of HSCs in the late 1980's.[66-68] It has become common to store UCB either privately, as a donor-specific source, or publicly, as an allogeneic source for later use.[69] Haematopoietic stem cell transplantation is well established for the treatment of a variety of malignant and non-malignant diseases affecting the haematopoietic system. Soon after the discovery of HSCs, the existence of non-haematopoietic bone marrow multipotent precursor cells was identified.[70] These cells are now known as MSCs. Although MSCs were originally isolated from bone marrow more than 40 years ago,[70] they reside in virtually all post-natal human tissues and organs.[71]

1.5   MESENCHYMAL STEM CELLS

Mesenchymal stromal/stem cells are easily available and can be isolated from various tissues. *In vitro,* they display high proliferative properties and maintain their undifferentiated multipotent state.[72] Clinically, MSCs show repair potential, both as immune system modulators and as a source of new tissue following cell engraftment. Adult MSCs show promise therapeutically, firstly due to their differentiation capacity into cells required for wound repair, and secondly for their ability to activate endogenous progenitor cells through paracrine signalling.[73] Mesenchymal stromal/stem cells may improve wound repair as they have been shown to preferentially home to ischemic myocardium and facilitate tissue repair.[74] Another study using an excisional splint wound model in diabetic mice showed that significant wound repair was initiated by grafted human bone marrow-derived MSCs (BM-MSCs) through paracrine signalling.[58] Mesenchymal stromal/stem cell therapy is not yet considered a routine form of clinical treatment. Potential clinical applications of MSCs include tissue engineering, tissue repair, treating autoimmune diseases, treating inflammation, cartilage and bone injury, and graft-versus-host (GvHD) disease, to name a few. However, the outstanding challenges preventing clinical use of MSCs are a lack of clinical data to support their safety, a lack in understanding of their biology following *in vivo* transplantation, and a lack in understanding the mechanisms of MSC recruitment and homing to sites of inflammation. Although MSCs have demonstrated significant potential for clinical use, a

barrier for effective implementation of MSC therapy is the inability to target these cells to tissues of interest with high efficiency and engraftment.[75]

1.5.1 <u>Nomenclature: stem or stromal cells?</u>

Growing interest in MSCs has led to inconsistencies regarding their nomenclature. The acronym MSC is currently used to refer to both mesenchymal stem- and stromal cells. To clarify the terminology, the International Society for Cellular Therapy (ISCT) proposed that fibroblast-like plastic adherent cells, regardless of tissue origin, be named multipotent mesenchymal stromal cells, while reserving the term mesenchymal stem cell for a subset of these cells that clearly demonstrate stem cell activity.[76, 77] However, it is left up to the scientist to clearly state which nomenclature is being referred to in order to avoid confusion. The designation "mesenchymal stromal cells" will be used in this study. The International Federation for Adipose Therapeutics and Science (IFATS) has proposed the use of the term "adipose-derived (mesenchymal) stromal cells" (ASCs) to identify the plastic-adherent, multipotent cell population isolated specifically from adipose tissue.[78] This study will use the acronym ASC to describe MSCs isolated from adipose tissue. Mesenchymal stromal cells isolated from bone marrow will be referred to as BM-MSCs. The term MSC will be used to refer to stromal cells, irrespective of their tissue of origin. Stromal cells are classified as MSCs *in vitro* if they meet certain criteria. The ISCT have proposed minimal criteria to define human MSCs: (1) they need to be plastic adherent in culture; (2) display a specific immuno-phenotype, with ≥95% of the MSC population positive for CD105, CD73 and CD90 and ≤2% lacking the expression for CD45, CD34, CD14 or CD11b, CD79α or CD19 and HLA-DR; and (3) show multilineage differentiation capacity into adipocytes, osteoblasts and chondroblasts.[79] In 2013, IFATS and ISCT made a joint statement to define stromal cells specifically from adipose tissue.[78] They proposed the use of multi-colour flow cytometry analysis to confirm the phenotype of ASCs along with qualitative and quantitative evaluation of differentiation capacity. They define ASCs as being positive for the surface markers CD90, CD73, CD29, CD105/CD13 and CD44 and negative for CD45 and CD31. Furthermore, they suggested that by including CD36 and CD106, MSCs from bone marrow and adipose tissue can be distinguished as BM-MSCs are positive for CD106 and negative for CD36, whereas ASCs are negative for CD106

and positive for CD36. Overall, they suggest that at least two positive and two negative surface markers should be evaluated in the same analysis along with a viability stain during phenotypic characterisation of MSCs.

1.5.2 The role of MSCs during wound repair

Mesenchymal stromal cells are believed to migrate to damaged tissue in a process called homing.[80] Homing has been described as the passive or active "arrest of circulating MSCs within the vasculature of a tissue followed by trans-migration across the endothelium".[75] When the skin is injured, MSCs from the surrounding tissue or mobilised out of the bone marrow niche are attracted to the wound site by cytokines and/or chemokines that are up-regulated under conditions of inflammation.[81, 82] More specifically, *in vitro*, MSCs respond to ILs, TNFα and interferon gamma (IFNγ) that are elevated during the inflammatory reaction.[83] Mobilised MSCs play a role in the complex events of inflammation, proliferation, contraction and maturation/remodelling that are necessary for efficient reconstitution of the cutaneous barrier.[81, 84] They can respond and modulate their function when exposed to cells and biochemical factors that are characteristic of an injured environment by (i) regulating the local cellular environment; (ii) promoting angiogenesis; and by (iii) differentiating into keratinocytes and fibroblasts.[84, 85]

1.5.2.1 Endogenous stem cells in the hair follicle

Resident in the epidermis of hair bearing areas, there is the interfollicular epidermis, and in the dermis hair follicles and sebaceous glands (Figure 1.1C). New hair follicles are not made postnatally, but throughout life, the lower part of existing hair follicles regenerates to produce new hair. To maintain homeostasis, the interfollicular epidermis, hair follicles and sebaceous glands can self-renew by using their reservoirs of multipotent stem cells.[12, 86] Observations that hair bearing areas tend to heal faster than areas that lack hair follicles[87, 88] have led investigators to try and understand the relationship between hair follicles and the epidermis. Two main stem cell populations can be found in hair follicles, namely hair follicle stem cells (HFSCs) and DPCs.[89] Hair follicle stem cells are located in the outer root sheath (ORS) within the area known as the

bulge. These cells are also referred to as DSCs. They are responsible for regeneration of epidermal cells and the structure of hair follicles and sebaceous glands. Dermal papilla stem cells play a role in inducing and regulating hair growth and the formation of new hair follicles. The cycling of hair is well described in various reviews and will not be discussed here.[12, 86, 89, 90]

Studies using genetic lineage analysis and transplantation have demonstrated that under physiological conditions, hair follicles do not maintain homeostasis of the epidermis.[91-93] Epidermal stem cells from the basal layer of the epidermis may not be sufficient to promote tissue repair after full-thickness wounds where extensive skin damage has occurred to both the epidermis and dermis.[94] Under such conditions, a study by Ito and colleagues reported that wounding resulted in activation of epithelial cells in the hair follicle.[92] Cells from the bulge were recruited into the epidermis and migrated into the centre of the wound. In the wound, although they acquired an epidermal phenotype, most of these cells were not maintained in the newly formed epidermis. It was further proposed that bulge cells responded as "short-lived transient amplifying cells".[92] Another study showed that hair follicles are involved in the initiation of rapid epithelialisation, but when absent, are not required to achieve complete wound closure.[95] Taken together, it appears that stem cells from hair follicles may contribute to wound repair by acting as supportive cells during the process.

1.5.2.2 Involvement of MSCs during the phases of wound healing

During the late inflammatory phase, MSCs display a strong anti-inflammatory response by decreasing secretion of pro-inflammatory cytokines (TNFα and IFNγ) while also increasing the production of prostaglandin E2 to regulate inflammatory cytokines.[83, 85] Mesenchymal stromal cells regulate the function of leukocytes that have invaded injured tissue. They inhibit the proliferation and activation of effector T cells, natural killer (NK) cells, dendritic cells (DCs), and macrophages, by promoting the recruitment, activation and proliferation of regulatory T-cells.[96, 97] In response to their interaction with T-cells in a pro-inflammatory environment, MSCs up-regulate the expression of inducible nitric oxide synthase to scavenge ROS.[84] Reactive oxygen species secreted by neutrophils are highly cytotoxic compounds used to achieve sterility in the

wound after injury, but also intensify collagen deposition.[98] Prolonged exposure to ROS during wound healing can lead to enhanced fibrogenesis and the accumulation of fibrotic tissue.[99] In the proliferative phase, the antimicrobial activity of MSCs combats infection. This is a significant advantage in reducing excess inflammation in the wounds. The mechanism is based on the secretion of LL-37, a peptide which has a wide variety of antimicrobial properties.[100, 101] Mesenchymal stromal cells express TGFα, TGFβ, hepatocyte growth factor (HGF), EGF, bFGF and IGF-1 to increase fibroblast, epithelial and endothelial cell division. The secretion of VEGF, IGF-1, and EGF also initiates vascularisation.[102] Furthermore, *in vitro* studies has revealed that growth factors secreted by MSCs promote proliferation, migration, and differentiation of microvascular endothelial cells, thereby assisting with angiogenesis.[103-105] It is believed that resident MSCs may also assume a phenotype resembling dermal fibroblasts, myofibroblasts, and keratinocytes as this trans-differentiation has been shown *in vitro.*[106, 107] Several reports suggest that MSCs differentiate into epidermal keratinocytes, endothelial cells and pericytes *in vivo.*[106, 108] While other investigators have reported no evidence of MSC differentiation.[109] Through the secretion of cytokines and growth factors with anti-fibrotic properties, such as HGF, MSCs also help to reduce scar formation.[84]

1.5.3 <u>Recruitment of MSCs during inflammation</u>

A study investigating the engraftment of systemically administered human BM-MSCs to sites of inflammation provided evidence of MSC homing to injured sites.[110] Bone marrow-MSCs homed to the lungs, liver and spleen of healthy and injured mice, as well to sites of injury in mice (cutaneous needle stick, surgical incision wound and xenogeneic and syngeneic tumours). In a study of type 2 diabetes, mice treated with CM-Dil-labelled umbilical cord-MSCs (UC-MSCs) showed homing to the lungs, liver and spleen, and some homing to pancreatic islets.[111] The homed UC-MSCs exerted anti-diabetic effects, alleviated dyslipidaemia and improved liver function. In addition, an increase in M2 macrophages was detected in the islets, liver, fat and muscle tissue. Although the homing of leukocytes to sites of inflammation has been well studied, [112-114] the mechanism of MSC homing to sites of injury or ischemia is still poorly understood.[57, 75] Data describing the exact positioning of MSCs post infusion is still needed, making it difficult to

determine whether the cells arrest within the vasculature or undergo trans-endothelial migration.[75] A better understanding of homing mechanisms will be crucial to enable enhancement of cell engraftment during tissue regeneration.

1.5.3.1 Leukocyte homing: key players involved in leukocyte recruitment

Leukocyte trafficking involves three main elements: adhesion molecules (selectins), integrins and chemoattractants (including chemokines and cytokines).[115] The selectin family consists of three adhesion molecules, L-selectin (expressed on leukocytes), E-selectin and P-selectin (expressed on stimulated endothelial cells). Selectins bind sialyl-Lewis-X-like carbohydrate ligands presented by sialomucin-like surface molecules such as P-selectin-glycoprotein ligand-1 (PSGL-1).[57, 115] E-selectin also binds CD44.[116] Integrins are glycosylated heterodimeric proteins expressed on the cell surface. They mediate the adhesion of cells to ECM proteins and to other cells.[57] The most relevant integrins involved in leukocyte migration are $\alpha4\beta1$ (VLA-4) and $\beta2$ integrins (LFA-1), that bind to vascular cell adhesion molecule-1 (VCAM-1) and intercellular cell adhesion molecule-1 (ICAM-1) respectively. Chemoattractants include cytokines and chemokines.[57] Cytokines are small proteins released by various cells in the body in response to an activating stimulus. They induce responses through binding to specific receptors. Examples include IL, TNF and IFN. Growth factors such as VEGF, EGF, and IGF amongst others form part the cytokine group. Chemokines are small proteins that induce directed chemotaxis in nearby responsive cells. They guide cells to sites of infection. These consist of CC chemokines that bind to CC chemokine receptors such as CCR1 to 9, and CXC chemokines that bind to CXC receptors such CXCR1 to 6.[117] Proteases also play a crucial role, especially to facilitate trans-migration through the basement membrane. They consist of a large family of MMPs.[57] Leukocytes respond to activation signals and inflammation-induced cues through alterations in their trafficking molecules resulting in a co-ordinated sequence of adhesive and signalling events. The leukocyte adhesion cascade involves three main steps: (1) selectin-mediated tethering and rolling; (2) chemokine-triggered activation and integrin-mediated adhesion; and (3) endothelial trans-migration.[112] Injured/inflamed tissue activate endothelial cell receptors on the endothelium of blood vessels in response to inflammatory mediators such as TNFα. Circulating leukocytes then become loosely captured

through the interaction of their cell surface markers to the vascular wall. As the cells slow down, they roll over the endothelium, bringing their surface markers in close contact for firm attachment to occur. Intraluminal crawling using adhesion molecules direct leukocytes to a place where they can overcome the endothelial barrier, basement membrane and pericyte sheath to complete endothelial trans-migration.

1.5.3.2 Current understanding of MSC recruitment

The mobilisation and migration of MSCs has been proposed to be directed by cytokines and/or chemokines that are up-regulated under conditions of inflammation, released into circulation, and stimulate MSCs to down-regulate the adhesion molecules that keep them in their niche.[118] The chemokine receptors CCR1, CCR4, CCR7, CXCR5, and CCR10 are expressed on MSCs and may be involved in their homing.[119, 120] Stromal derived factor-1 (SDF-1) and its receptor CXCR4 are crucial for bone marrow retention, mobilisation, and homing of HSCs.[121, 122] *In vitro* work has shown that MSC migration is regulated by SDF-1/CXCR4 and HGF/c-Met complexes.[123] In a hepatic ischemia-reperfusion injury model, hypoxia pre-conditioned human BM-MSCs were injected systemically via the tail vein in mice. The elevated levels of SDF-1 in the injured liver attracted the CXCR4 expressing MSCs to the liver.[124] There is evidence, reviewed in Karp and Teo., 2009, that infused MSCs home in response to inflammation or injury.[75] It is unclear whether MSCs actively home to tissues using leukocyte-like cell-adhesion and trans-migration mechanisms or whether they become passively entrapped in small-diameter blood vessels. It is suggested that specific MSC-endothelium interactions regulate trans-migration as integrin blocking and knockout studies have reported reduced engraftment and homing of MSCs.[125, 126] However, further studies are required under conditions of inflammation to test this hypothesis.[75, 112] *In vitro* studies attempting to elucidate the mechanism of MSC extravasation was reviewed in Nitzsche *et al*., 2017 and noted that MSCs can either become actively or passively arrested in capillaries due to their large size. Passive arrest has been identified by altered local blood flow, but it remains unknown whether passive arrest triggers MSC extravasation. Another difference is that diapedesis was recorded to take two to three times longer compared to leukocytes.[127]

1.5.4 Impairment of MSCs in chronic wounds/diabetic patients

Diabetic patients are often faced with impaired wound healing. They suffer frequently from diabetic ulcers which is a leading cause of leg amputation. Diabetes has detrimental effects on endogenous MSCs. Mesenchymal stromal cells derived from diabetic rat adipose tissue and bone marrow show reduced proliferation, differentiation and migration potential *in vitro*.[128, 129] Normal wound healing is initiated by the integration of multiple intercellular signals, such as cytokines and chemokines, released by keratinocytes, fibroblasts, endothelial cells, macrophages, platelets, and other immune cells. In diabetes, inflammatory cytokines and chemokines are elevated, leading to a state of chronic inflammation. Diabetes affects cellular processes leading to abnormal keratinocyte and fibroblast migration, proliferation, and enhanced apoptosis; increased pro-inflammatory macrophages and decreased anti-inflammatory macrophages; impaired recruitment of endogenous stem/progenitor cells (such as MSCs and EPCs), and decreased vascularisation.[39] During wound healing, impaired MSCs fail to reduce acute inflammation, regulate the expression of growth factors, and promote the proliferation of fibroblasts and basal keratinocytes. Macrophages in the wound site are important for driving wound inflammation following injury. They clear dead cells and debris within the wound, and produce a range of cytokines, growth and angiogenic factors that drive fibroblast proliferation and angiogenesis.[130] Depletion of macrophages results in impaired clearance of damaged tissue and provisional matrix, further delaying wound healing.[131] Mesenchymal stromal cells and macrophages have been implicated for their ability to produce nitric oxide.[84] Inhibition of wound nitric oxide synthesis has been shown to lower wound collagen accumulation, suggesting that nitric oxide is critical for wound collagen accumulation and mechanical strength.[132] Having impaired MSCs and macrophages will result in reduced nitric oxide production and subsequently impede normal wound healing. Wound healing also requires the transition of basal and suprabasal keratinocytes from an inactive phenotype to a migratory and hyperproliferative phenotype. Keratinocytes express key chemotactic cytokines that stimulate the recruitment of leukocytes, monocytes, neutrophils and macrophages. Impaired keratinocytes or lack thereof will delay the process of epithelialisation. Fibroblasts primarily produce proteins such as collagen and fibronectin to facilitate ECM formation. Specialised fibroblasts called

myofibroblasts contribute to wound healing by producing ECM and their ability to contract help to bring the edges of a wound together. Reduced formation of myofibroblasts will contribute to impaired wound contraction and possibly delayed wound closure.[133] Angiogenesis is a complex cascade of cellular, humoral, and molecular events whereby growth factors bind to their receptors on endothelial cells of existing vessels. Stimulated endothelial cells react by proliferating and migrating into the wounded tissue to form small cylindrical canals which mature into new vessels.[31] Impaired endothelial cells will impede angiogenesis and will contribute to wounds not healing. Reactive oxygen species are thought to interact with several pathways which affect MSC differentiation. Elevated levels of ROS, defined as oxidative stress, lead to arrest of the MSC cell cycle and apoptosis. Tight regulation of ROS levels is therefore critical to direct MSC terminal differentiation. The precise source, localisation, level and exact species of ROS implicated in MSC differentiation is still undetermined.[134] High levels of ROS are found in injured tissue and may be a leading cause of impaired differentiation of MSCs into fibroblasts, keratinocytes and endothelial cells needed for wound repair. Under conditions where local endogenous MSCs are impaired, their exogenous administration (either autologous or allogeneic) could overcome these problems. In situations where local resident MSCs are impaired, such as in wounds, the use of autologous MSCs from alternative depots, such as from adipose tissue and bone marrow, would be appropriate. Whereas in situations where the problem is associated to a genetic disorder or disease that affects all the body`s cells, the use of allogeneic MSCs would be more appropriate. The immunomodulatory effects of MSCs allows them to evade the immune system and overcome problems such as immune rejection, facilitating the clinical use of allogeneic MSCs.[135, 136] These "fresh" MSCs will be able to influence the wound's ability to progress beyond the inflammatory phase and not regress to a chronic wound state by directly attenuating the inflammatory response and reprogramming the resident immune and wound repair cells to favour tissue regeneration.[84, 85]

1.5.5 MSC pro-regenerative properties

Over the years there has been a paradigm shift regarding the mechanism of how exogenously administered MSCs are therapeutically effective. Initially MSCs were believed to migrate to the

injured site where they engraft long-term and differentiate into tissue cells to replace damaged cells. It is now believed that MSC pro-regenerative properties can be attributed rather to their immunomodulatory effects[137, 138] and paracrine signalling[139, 140]. Administered MSCs play a role in controlling tissue inflammation at the injured site. In response to released inflammatory factors by immune cells and inflamed tissues, such as IFNγ and TGFα, MSCs adopt an immunoregulatory phenotype, increase anti-inflammatory factors, and modulate the function of innate immune cells.[141, 142] Through the release of various growth factors, MSCs down-regulate ongoing inflammation and restore tissue homeostasis. The different growth factors released by MSCs has previously been reviewed by Ma and colleagues, and include EGF, fibroblast growth factor (FGF), PDGF, TGFβ, VEGF, HGF, IGF-1, angiopoietin 1 (Ang-1), keratinocyte growth factor (KFG) and SDF-1 amongst others.[137] These growth factors promote fibroblasts, endothelial cells and tissue progenitor cells to initiate tissue repair. Depletion of adenosine triphosphate (ATP) from the surrounding environment and its conversion to adenosine by MSCs further modulate the function of immune cells.[143-145] Taken together, MSCs seem to act as trophic mediators who can modulate the function of immune cells and tissue resident progenitor cells through the secretion of growth factors, angiogenic factors, immune regulating factors and through their secretome (by releasing extracellular vesicles).[142] A novel hypothesis proposes that the immunomodulation by MSCs is indirect and is triggered through phagocytosis of MSCs by monocytic cells.[146] The engulfment of apoptotic MSCs by phagocytic cells (such as monocytes) lead them to adopt an immunoregulatory phenotype. These "immune primed" cells then travel into the circulation and migrate to distant tissue sites where they can exert immunoregulatory effects.

1.5.6 <u>MSC therapy</u>

A limitation to the effective use of MSCs in wound therapy is the method of delivering the cells. Systemically administered MSCs are an attractive option for regenerative medicine as *in vivo* animal studies and clinical studies have shown the ability of MSCs to migrate to and accumulate at sites of injury and inflammation where they contribute to the repair and/or replacement of damaged tissue.[73] However, in most cases, only low amounts of administered MSCs engrafted at

the injured sites. The engraftment of MSCs into damaged tissues via migration to enhance tissue repair/regeneration is a crucial process for clinical efficacy. The site and route of administration will most likely affect the trafficking of MSCs to injured tissue. The optimal route of administration specifically in wound repair is a matter of further investigation. Therapeutic applications are based on exogenous administration of MSCs by local or systemic administration.

Engraftment efficiency of administered MSCs at the site of injury is still a concern. Studies have suggested that engraftment efficiency is directly influenced by the delivery site, mode, and time of delivery, along with the number of MSCs delivered.[75] Another consideration is that since MSCs exist in hypoxic conditions *in vivo*, it may be important to consider the level of oxygen used during *in vitro* culturing to maintain their stem cell properties.[147] Self-renewal and multipotency are the key characteristics of stem cells that permit them to maintain growth, homeostasis and repair tissues. Hypoxic conditions has been shown to decrease the differentiation capacity of MSCs compared to normoxic conditions, supporting the notion that low oxygen tension promotes MSCs to stay undifferentiated.[148] Data reviewed in Haque *et al.*, suggests that hypoxia will improve growth kinetics, genetic stability, and expression of chemokine receptors during *in vitro* expansion of MSCs leading to increased efficiency of MSC-based therapies that require cells to be cultured prior to administration.[149]

Clinical studies using MSCs to enhance wound healing have shown promising results.[85] In a study on chronic diabetic foot ulcers, following injection of BM-MSCs into the edges of the wounds, improved dermal thickness and decreased size of the ulcers were observed.[150] Various methods of administration have been used, from topical suspensions with or without appropriate carriers/scaffolds to intramuscular (IM) injections using BM-MSCs. In a study conducted by Lu *et al.*, systemic administration of MSCs were clinically beneficial.[151] Briefly, one limb of the patient was injected IM with cultured autologous BM-MSCs or fresh bone marrow mononuclear cells (BMCs). Compared to control groups (receiving only saline injections), patients who received either MSC or BMC injections showed improvement in pain-free walking and increased ulcer healing rates. A clinical trial conducted in 2008 treated chronic wounds from 20 patients with

autologous BM-MSCs cultured on a collagen sponge.[152] Complete wound closure was recorded for 90% of the wounds. In a randomised control study conducted in 2009 on 24 patients with a history of diabetes and non-healing leg ulcers, treatment with autologous BM-MSCs showed a significant increase in healing compared to the control group.[153] Although these studies show promising results, further studies are needed to determine the best source of the MSCs, the benefit of MSCs alone or within a matrix, the timing and frequency of MSC administration, and the number of cells to administer.

Most studies on the efficacy of MSCs in wound repair are done using BM-MSCs. However, plastic surgeons have been using autologous fat grafting for more than a century and have modified techniques for harvesting and administering fat to maintain the viability of MSCs within the lipoaspirate.[154, 155] Adipose tissue can be extracted as solid adipose tissue or by liposuction, which is a less invasive and safer procedure than bone biopsies. A promising and cost-effective source of autologous MSCs is subcutaneous adipose tissue.[156] Adipose-derived stromal cells are considered an appropriate cell population because of their availability, ease of harvest as solid adipose tissue or by liposuction, high cell yield, and ability to be expanded in culture for clinical use.

1.6   PROJECT AIMS AND OBJECTIVES

This PhD study aimed to investigate the homing and healing properties of ASCs using a model of wound repair. To achieve this, a three-step approach was taken:

1.6.1 <u>Step 1. Chapter 2: The isolation, transduction and characterisation of primary rat ASCs</u>

Setup the techniques to (i) isolate and characterise ASCs from rat subcutaneous inguinal adipose tissue and (ii) label ASCs to enable *in vivo* tracking.

1.6.2 Step 2. Chapter 3: The fate of systemically and locally administered ASCs and their effect on wound repair under physiological conditions

Use a wound repair model under physiological conditions (Figure 1.4) to investigate the fate of ASCs administered *in vivo* in normoglycaemic animals with non-ischemic wounds by examining two different modes of ASC administration; systemic versus local. Also, to track administered ASCs by live cell imaging using bioluminescence imaging (BLI) and post mortem in tissue sections by immuno-histological analysis to detect green fluorescent protein (GFP) positive ASCs.

1.6.3 Step 3. Chapter 4: The effect of ASCs on wound repair under pathological conditions

Use a wound repair model under pathological conditions (Figure 1.5) to investigate the effect of ASCs on wound healing in hyperglycaemic animals with ischemic wounds by examining the effect of locally administered ASCs. Also, assess wound repair by looking at the expression of alpha-smooth muscle actin (αSMA) and ionised calcium binding adaptor molecule 1 (Iba1) by immunohistochemistry (IHC), and histological staining for Masson's trichrome within the wound and haematoxylin/eosin (H/E) staining.
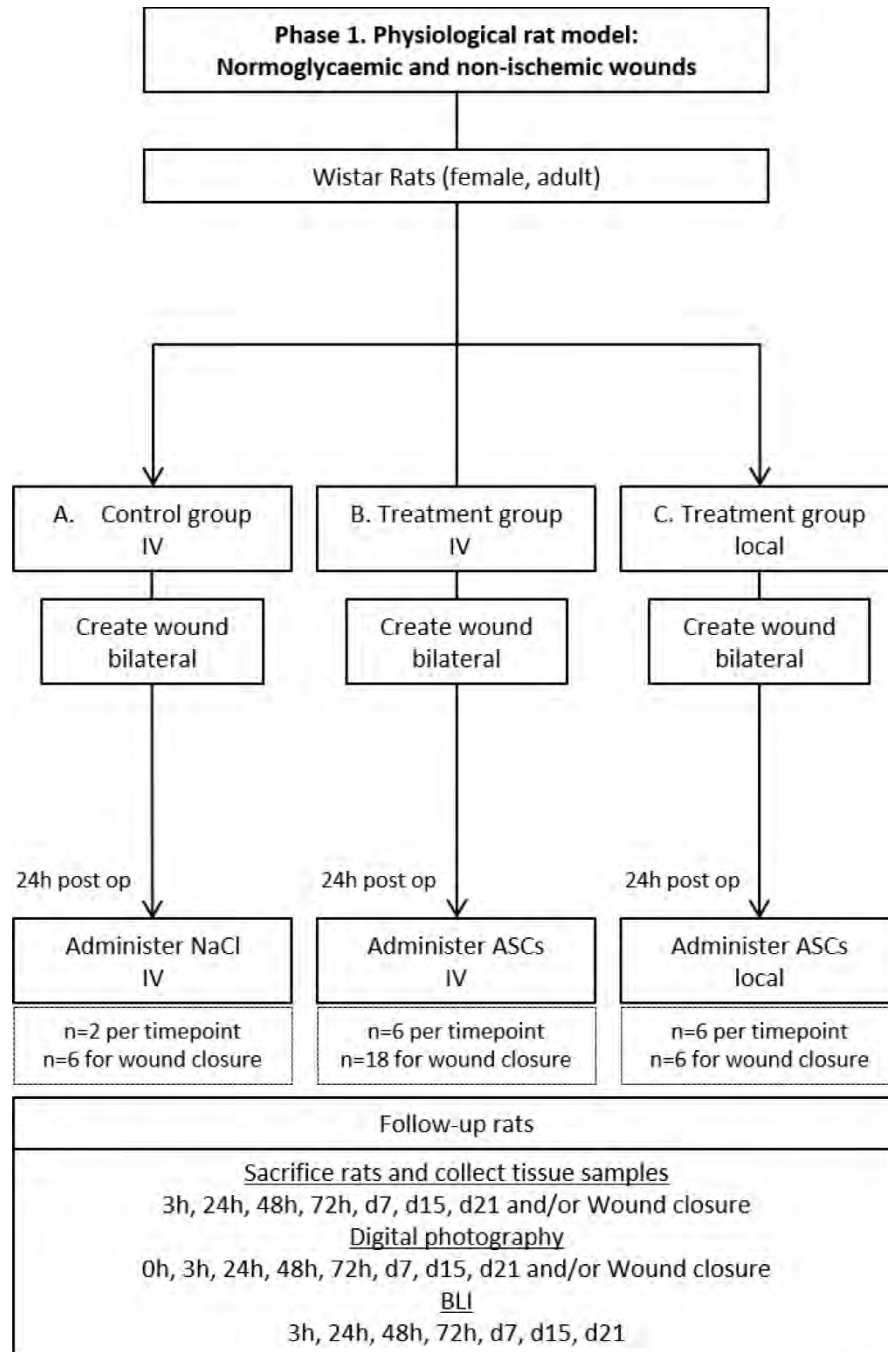
Figure 1.4 Experimental design for the physiological rat model.
The effect of locally and systemically administered ASCs was investigated in normoglycaemic animals with non-ischemic wounds.
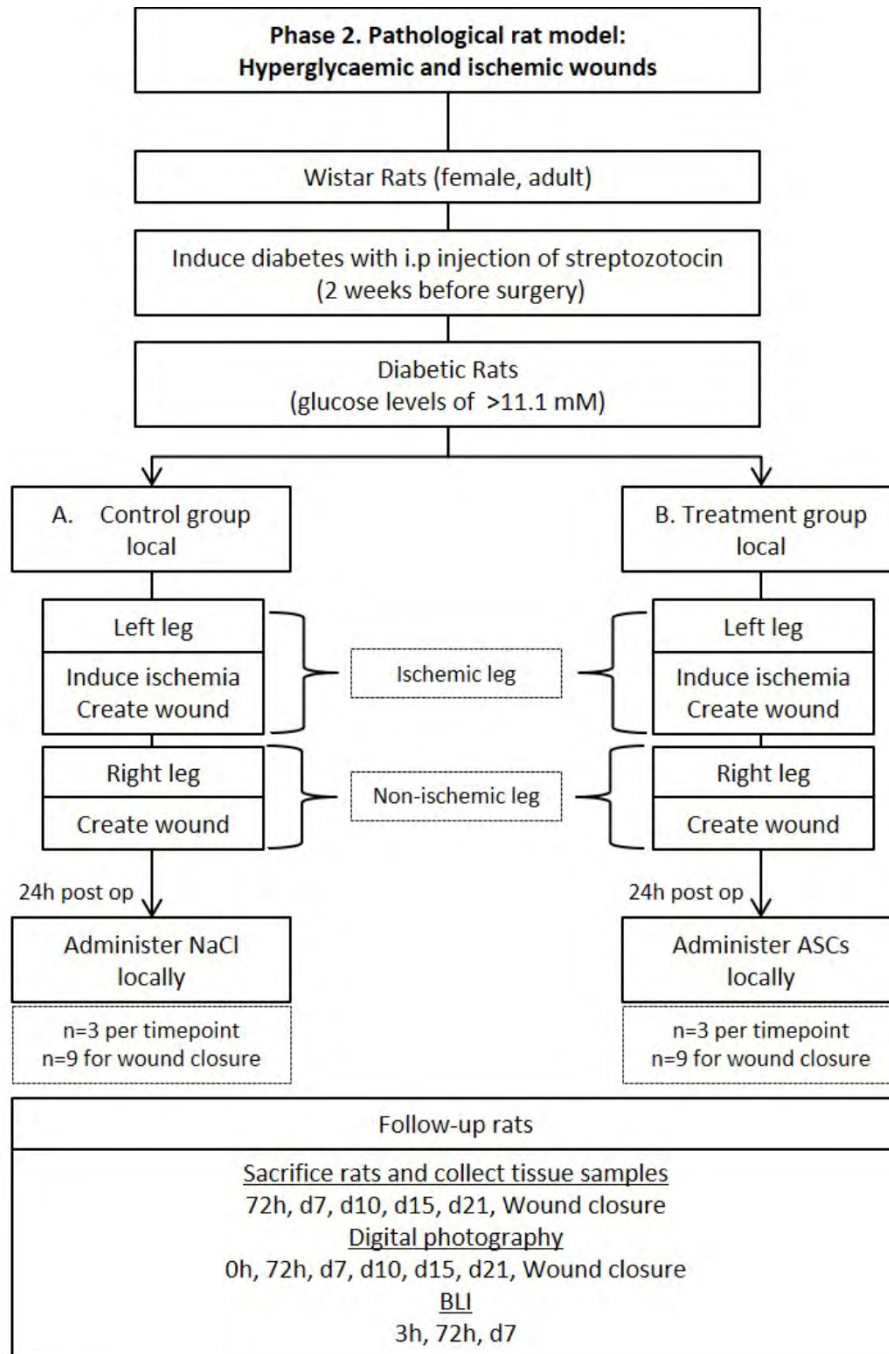
Figure 1.5 Experimental design for the pathological rat model.
The effect of locally administered ASCs was investigated in hyperglycaemic animals with ischemic and non-ischemic wounds.

CHAPTER 2. THE ISOLATION, TRANSDUCTION AND CHARACTERISATION OF PRIMARY RAT ASCs

2.1   INTRODUCTION

Mesenchymal stromal cells are a heterogeneous population containing a subset of multipotent adult stem cells that reside in virtually all post-natal human tissues and organs.[71, 79, 157] They have the ability to self-renew and differentiate into tissues of the mesodermal lineage.[156, 158] Although MSCs were originally isolated from bone marrow more than 40 years ago,[70] a source used with increasing frequency is subcutaneous adipose tissue.

Liposuction is a popular surgical procedure with large volumes of adipose tissue being routinely discarded as waste. Utilising this waste product as a potential source of stem/stromal cells could yield large numbers of cells with therapeutic potential. In 2001, stem/stromal cells were identified and characterised in lipoaspirate, leading to the recognition that adipose tissue may provide an alternative source of MSCs to bone marrow.[159] Mesenchymal stromal cells isolated from bone marrow and adipose tissue share biological characteristics; however differences in their phenotype, differentiation potential, gene expression profile and immunomodulatory activity have been noted.[160-162] Generally, MSCs from adipose tissue are considered to be a potentially useful cell population because of their availability, ease of harvest, high cell yield, and ability to be expanded in culture for clinical use. The International Federation for Adipose Therapeutics and Science has proposed the use of the term "adipose-derived mesenchymal stromal cells" (ASCs) to identify the plastic-adherent, multipotent cell population isolated specifically from adipose tissue.[78]

Functional assays using cultured progenitor cells are commonly used to characterise ASCs *in vitro*. Currently no single surface marker has been identified as being unique to ASCs. Thus, they are characterised based on morphological characteristics, *in vitro* differentiation capacity and surface antigen expression.[79] According to a joint statement by IFATS and ISCT, ASCs are phenotypically characterised according to their positive expression for CD105/CD13, CD73, CD90, CD44 and

CD29 and negative expression for CD45, and CD31 surface antigens.[78] Defining the location of ASCs post administration is complicated by the lack of a single identifying marker. *In vitro* ASCs are characterised by the co-expression of a panel of surface markers.[78] Studying the bio-distribution of administered ASCs *in vivo* is still a challenge. Methods for cell labelling and tracking, appropriate animal models, as well as the relevance for human use are aspects that still need to be analysed.[163] Various methods of labelling ASCs for *in vivo* tracking after infusion have been proposed in the literature, such as the use of superparamagnetic iron oxide (SPIO) labelling for magnetic resonance imaging (MRI) and the use of Zirconium[89] for positron emission tomography/computed tomography (PET/CT). However, molecular imaging offers the opportunity to track cells in intact organisms, for which a promising method for cell tracking in small animal models is BLI.[164-166] Luminescence is generated by the conversion of chemical energy into visible light produced when cells modified to express reporter enzymes, such as firefly luciferase (Fluc), react with their specific bioluminescent substrate, D-luciferin, after which the luminescence can be imaged as deep as several centimetres within tissue.[164] Combinational tracking approaches alongside BLI that also include the use of the genetic marker, GFP will enable not only live imaging, but also more precise location of cells post mortem in tissues that have been processed for IHC.

Prior to assessing the benefit of ASCs in *in vivo* models of wound healing, an appropriate tracking system needs to be established to follow administered cells. In this chapter, the techniques used to isolate, characterise and label ASCs are described. Rat isogenic ASCs will be used and transduced to express both Fluc and GFP to enable *in vivo* imaging and post mortem identification by histological analysis of tissues.

2.2   MATERIALS AND METHODS

All animal experiments were approved by the local veterinary authority in Geneva (Direction general de la santé de Genève, refer to Appendix 6 for approval letters). The techniques used to isolate, expand, characterise and label MSCs derived from rat subcutaneous inguinal adipose tissue *in vitro*, hereafter referred to as ASCs, are described below.

2.2.1 <u>Isolation and culture of primary rat ASCs</u>

For all *in vivo* experiments, fresh rat isogenic ASCs were used. Female Wistar rats (≥ 10 weeks old, ≥ 250 g, n=14, Janvier labs, Le Genest-Saint-Isle, France) were sacrificed by injecting 150 mg/kg sodium pentobarbital intraperitoneal (IP) (Esconarkon AD US. VET., Streuli Pharma, Uznach) followed by excision of the inguinal subcutaneous adipose tissue. The stromal vascular fraction (SVF) containing ASCs was isolated as previously described (Figure 2.1).[167-169] Briefly, the tissue sample was diced and digested at 37°C for 30 min in 0.075% (w/v) collagenase Type I (GIBCO, Grand Island, NY, USA) dissolved in Hanks' Balanced Salt Solution (HBSS, BioWhittaker, Lonza, Basel, Switzerland) containing 1.5% bovine serum albumin (BSA, Sigma Life Science, Merck, Darmstadt, Germany), with agitation. Following digestion, the sample was centrifuged (5 min, 426 x *g*) to obtain the SVF. The SVF was washed with phosphate buffered saline (PBS) supplemented with 2% penicillin (10 000 units/ml)-streptomycin (10 000 µg/ml) (pen/strep) (GIBCO by Life Technologies™, Grand Island, NY, USA), centrifuged (5 min, 426 x *g*) and the cell pellet re-suspended in high glucose Dulbecco's Modified Eagle's Medium (DMEM 1X + GlutaMAX™, 4.5 g/l glucose) supplemented with 20% foetal bovine serum (FBS) and 1% pen/strep. The SVF was filtered through a 100 µm cell strainer (BD biosciences, MA, USA) before being plated into a 75 cm^2 flask (NUNC™, Kamstrupvej, Denmark) overnight at 37°C, 5% CO_2 in high glucose DMEM supplemented with 20% FBS and 1% pen/strep. After 24h, non-adherent cells were removed, and the medium changed to complete growth medium (CGM) containing high glucose DMEM supplemented with 10% FBS and 1% pen/step. The isolated cells were maintained at 37°C and 5% CO_2 in CGM. At 80% confluence, the cells were trypsinised by the addition of 0.05% trypsin-ethylenediaminetetraacetic acid 1X (trypsin-EDTA 1X, GIBCO by Life Technologies™, Grand Island, NY, USA) for 5 min at 37°C. Cells were counted using the trypan blue dye exclusion assay[170] and re-plated as passage 1 (P1) cells at a density of 5 x 10^3 cells/cm^2 or used for further experiments.
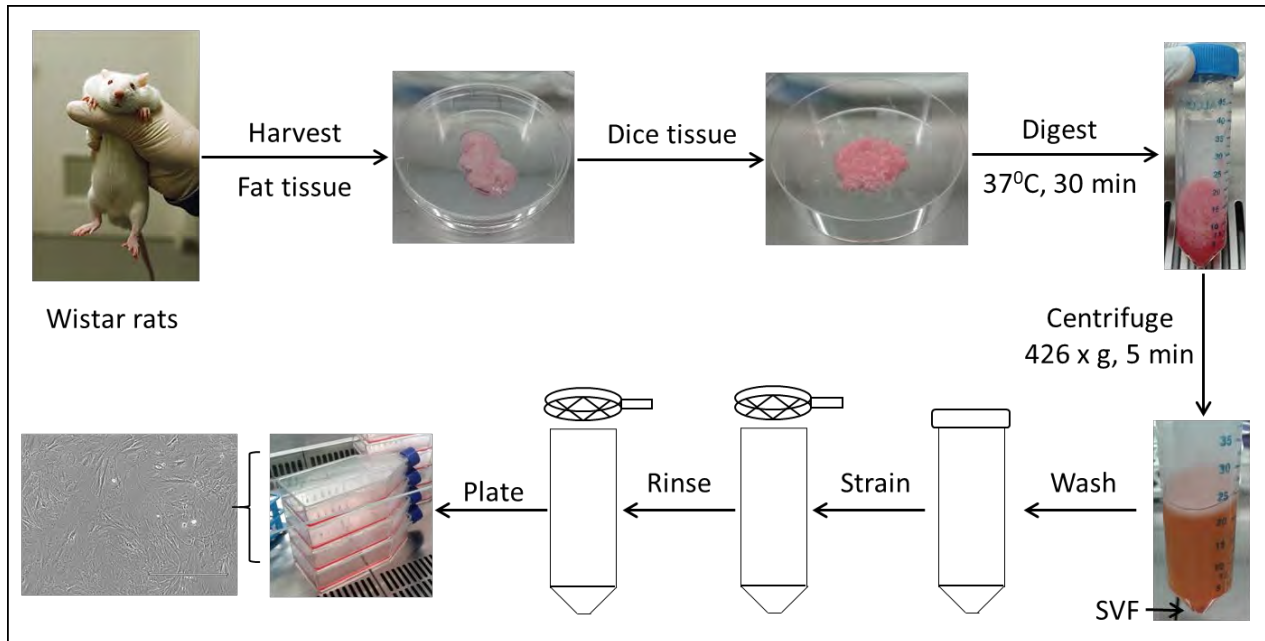
Figure 2.1 The isolation of rat ASCs.

Inguinal subcutaneous adipose tissue was harvested from female Wistar rats and the tissue digested to obtain the stromal vascular fraction (SVF) containing ASCs. The pellet was plated, and the adherent cells allowed to proliferate.

2.2.2 Lentivector production

A dual lentivector expressing the gene for both Fluc and GFP, pCWX-UBI-Fluc-PGK-GFP, was produced and used to transduce the ASCs. The cell lines, 293 and 293T cells are commonly used for vector production. The presence of the SV40 T-antigen in 293T cells makes this cell line more efficient for vector production.[171] The 293T cells were selected as the producer cell line due to their increased cell growth and transfection efficiencies compared to 293 cells. To determine lentivector titres, the target cell must be readily permissive to all the steps from viral entry, to integration of the vector genetic cargo. Although HeLa cells are commonly used in laboratories, they have an unstable morphology and karyotype. Instead HT-1080 cells are preferred as they are stable cells, of human origin and give titres identical to HeLa cells.[172]

2.2.2.1 Transfection of 293T cells

Lentivectors were produced by transient transfection of the plasmid set (envelope plasmid, packaging plasmid and transfer vector) into 293T cells (ATCC, VA, USA) by the calcium phosphate

method as previously described.[172] Briefly, in the morning of day 0 (d0), 293T cells were seeded at 1.5 to 2.5 x 10^6 cells in a 10 cm culture dish with 10 ml of CGM. In the evening of the same day the deoxyribonucleic acid (DNA) mix containing the envelope plasmid, packaging plasmid and transfer vector (see Table 2.1) was prepared and adjusted to 250 µl with buffered water. HEPES-buffered saline 2X (HBS, 500 µl) precipitation buffer was added to the DNA mix. The water-DNA-HBS mix was added dropwise on 250 µl $CaCl_2$ (0.5 M) with mixing. The precipitate was left to develop for up to 30 min and then 1 ml was added dropwise on the 293T cell monolayer with gentle shaking and the culture dish incubated overnight (37°C, 5% CO_2). The following morning (d1), the culture medium was removed and discarded before being replaced with fresh 10 ml of CGM. On d2, the supernatant was harvested (stored at +4°C) and replaced with 10 ml CGM. On d3, the supernatant was harvested, pooled with the d2 supernatant, centrifuged (2500 rpm, 10 min, +4°C) and filtered through a 0.45 µM filter before being transferred to tubes and stored at -80°C.

$CaCl_2$ 0.5 M (4X) was prepared by mixing 18.4 g of $CaCl_2.2H_2O$ (MW 147, SigmaUltra C5080) with 2.5 ml of Hepes 1 M pH 7.3 (Gibco-BRL, Ref 15630-056) and adjusted to 250 ml with H_2O (milliQ 18.2 Mohm grade). The solution was filtered (0.22 µm) and stored at -70°C in 25 ml aliquots. HBS (2X) was prepared by mixing 8.18 g (0.28 M final) of NaCl (MW 58.44, FLUKA Ultra 71376), 6g (0.05M final) of HEPES (MW 238.3, SigmaUltra H7523) and 0.107 g of anhydrous Na_2HPO_4 (MW 141, SigmaUltra S7907) in a total of 400 ml of H_2O (milliQ 18.2 Mohm grade). The solution was adjusted to pH 7.15, filtered (0.22 µm) and stored at -70°C in 50 ml aliquots. Buffered water was prepared by adding 250 µl of HEPES 1 M pH 7.3 (GIBCO-BRL, Ref 15630-056) to 24.75 ml of H_2O (milliQ 18.2 Mohm grade).

2.2.2.2 Transduction of HT1080 cells to determine lentivector concentration

Using a 6-well culture plate, 50 000 HT1080 cells (ATCC, VA, USA) were plated per well into 3 wells in ATCC-formulated Eagle's Minimum Essential Medium (ATCC, VA, USA) supplemented with 10% FBS. After 24h, 5 µl, 50 µl and 500 µl of the pooled supernatants containing the lentivector was added to each well to transduce the cells and incubated at 37°C in 5% CO_2. After

5 days, the wells were trypsinised with 0.25% trypsin-EDTA. The cell suspension was fixed with 4% paraformaldehyde and transferred to flow tubes and run on the BD Accuri C6 (Becton Dickinson, NJ, US) flow cytometer to determine the percentage of cells that were positive for GFP (Figure 2.2). The lentivector titre was calculated with the following calculation using the 5 µl well:

$$\text{X TU/ml} = \frac{\text{X \% (\% of GFP positive cells)} \times 100\,000 \text{ cells (approximation of cell number)}}{0.005 \text{ ml}}$$

Note: Only dilutions yielding 1 to 20% of GFP-positive cells were considered for titre calculations.

Table 2.1 DNA mix for transfection of 293T cells

Mix	Name of plasmid	Concentration	Amount needed per dish
Envelope plasmid	pCAG-VSVG	1 µg/µl	4 µl
Packaging plasmid	psPAX2	1 µg/µl	8 µl
Transfer vector	Positive control pCWX-UBI-Fluc-PGK-GFP	1 µg/µl	8 µl
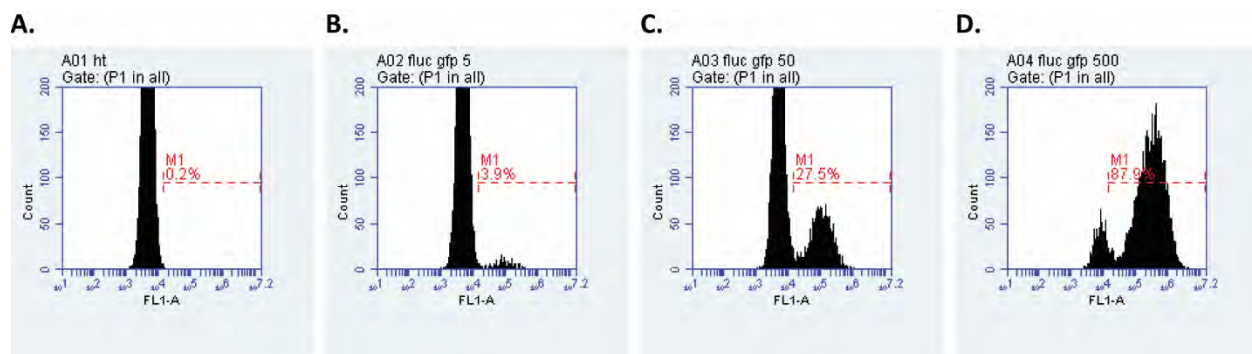
Figure 2.2 A representative flow cytometric analysis of HT1080 cells used for titrating the Fluc-GFP coding lentivector.
The percentage of green fluorescent protein (GFP) expressing cells was measured when transduced with (A) no lentivector (control), (B) 5 µl, (C) 50 µl and (D) 500 µl of the lentivector stock.

2.2.3 Transduction of ASCs

Adipose-derived stromal cells were transduced with a dual lentivector pCWX-UBI-Fluc-PGK-GFP expressing Fluc and GFP. To determine the amount of lentivector needed to transduce greater

than 70% of the cells, a multiplicity of infection (MOI) of 0, 2, 5, and 10 was tested (n=4). A MOI of 10 was selected and used for all further experiments. Adipose-derived stromal cells at P1 or P2 were plated at 5 x 10^3 cells/cm^2 and allowed to adhere for 24h. Lentivectors were added to the ASCs and cultures left for 72h before replacing the medium. At 80% confluence, the cells were trypsinised and prepared for flow cytometric analysis (n=6) as described below to determine whether they maintained their immuno-phenotype as well as the percentage of ASCs expressing GFP. To determine whether the cells also expressed the gene for Fluc, 1 x 10^5 cells were plated in opaque flat bottom 96 well plates (Thermo Fisher Scientific, MA, US) in triplicate (n=4) and allowed to adhere for 24h before being imaged. Prior to imaging on the Xenogen IVIS® spectrum *in vivo* imaging system (PerkinElmer, MA, US), XenoLight™ D-luciferin potassium salt (PerkinElmer, MA, US) at 150 µg/ml (prepared in CGM) was added to the cells. A photographic image of the plate followed by a luminescent image was recorded. For quantification, the intensity of the luminescent signal in each well was recorded as total flux (average photons per second, p/sec).[173] Images were analysed using Living Image® 4.3.1 software (PerkinElmer, MA, US).

2.2.4 Characterisation of ASCs

Prior to using transduced ASCs in the *in vivo* model, the stromal cells were evaluated to determine whether they still adhered to the minimal criteria set out by IFATS and ISCT.[78, 79] In particular, whether they maintained an MSC phenotype as well as the ability to differentiate into adipogenic and osteogenic lineages. For phenotypic characterisation of ASCs, a minimum of two positive and two negative surface markers should be used in the same analysis. Furthermore, IFATS and ISCT suggest that multicolour flow cytometry analysis should be performed to show that the ASCs express the surface markers co-currently. Due to the lack of rat specific antibodies conjugated to fluorochromes that can be used for multicolour flow cytometry analysis, for this study a minimum of two positive and two negative surface markers were evaluated. The expression of CD90 and CD29, both strongly positive MSC surface markers suggested by IFATS and ISCT along with lack of expression for CD45, a hematopoietic cell marker and CD31, and endothelial cell marker, were evaluated. The expression of GFP, to detect transduced ASCs, as well as a viability stain were also

included, making this a combined six-colour analysis. Both adipogenesis and osteogenesis was assessed by histological analysis, whereas end-point gene expression was only assessed for adipogenesis. The evaluation of adipogenesis genes was already set up in the lab, thus this analysis was included as an extra quality check of the adipogenic differentiation capacity of rat ASCs. However, the lab had not previously investigated osteogenesis at the gene level and seeing as this was not set up and not necessary for the main experiments it was not evaluated.

2.2.4.1 Immuno-phenotypic assessment by flow cytometry

To analyse surface marker expression profiles of the isolated ASCs (n=6), flow cytometric analysis was performed using fluorochrome-conjugated anti-mouse/rat monoclonal antibodies.

2.2.4.1.1   Sample preparation

Immuno-phenotyping was performed on cells before the start of each experiment. The monoclonal antibodies that were used are summarised in Table 2.2. For each sample, a 100 µl cell aliquot containing at least 1×10^5 viable cells was incubated for 15 min at 37°C in the dark after simultaneous addition of the four monoclonal antibodies (CD29, CD45, CD90, and CD31) in a single tube. Following incubation, cells were washed thrice with PBS supplemented with 2% FBS, re-suspended in PBS, and then analysed for antigen expression. A single tube containing unstained cells as well as a tube stained with the isotype controls were prepared on each experimental day for every sample to verify protocol settings and to serve as a negative control.

Table 2.2 Monoclonal antibodies used for immuno-phenotyping of ASCs

Marker	Antibody	Volume used (µl)	Supplier
CD29	Armenian hamster anti-mouse/rat CD29 APC	1.25	eBioscience, ThermoFisher Scientific, MA, USA
	Armenian hamster anti-mouse/rat IgG Isotype Control APC		
CD45	Mouse anti-rat CD45 APC-eFluor®780	2	
	Mouse anti-rat IgG1 K Isotype Control APC-eFluor®780		
CD90	Mouse anti-mouse/rat CD90.1 PC7	1	
	Mouse anti-mouse/rat IgG2a K Isotype Control PC7		
CD31	Mouse anti-rat CD31 PE	3	BD Biosciences, CA, USA
	Mouse anti-rat IgG1, κ Isotype Control PE		

Key: APC= allophycocyanin; PE= phycoerythrin; IgG= Immunoglobulin G; PC7= PE-Cyanine 7

2.2.4.1.2 Flow cytometry setup, data acquisition and analysis

The same analysis strategy was followed for all samples. Cells were gated on forward scatter (proportional to cell size) and side scatter (proportional to cell granularity and structural complexity) to exclude debris and cell aggregates (Figure 2.3A). The analysis protocol was comprised of both two-parameter (Figure 2.3B-K) and one-parameter (Figure 2.3L-P) plots. A minimum of 5000 events per sample was analysed during data acquisition. Data was acquired on a Gallios (10 colour, 3 laser) flow cytometer (Beckman Coulter, CA, USA). Unstained cells were analysed prior to the labelled samples and the regions set accordingly. To determine the percentage of transduced cells, GFP fluorescence was measured either separately or together with the other surface markers. The viability stain 4',6-diamidino-2-phenylindole (Dapi 5 µl, Beckman Coulter, CA, USA) was also included to ensure that only living cells were measured. Cell analysis was gated for viable cells using the one-parameter and dot plot for DAPI (Figure 2.3Q and R). Another dot plot was included to distinguish between GFP negative and positive cell populations (Figure 2.3S). Data analysis was performed using Kaluza Flow Cytometry analysis software 1.3 (Beckman Coulter, CA, USA).

The six-colour protocol was set-up using single antibody staining's, combinational staining's, unstained and isotypic controls to set the correct voltages. VersaComp Antibody Capture Beads

(Beckman Coulter, CA, USA) were also run to set up the correct compensation between different fluorochromes. The gating strategy used can be seen in Figure 2.3 and 2.4. Instrument voltage settings were set so that the unstained and isotypic control populations were visible in the first decade (L-, Figure 2.4A and C-G) and lower left quadrant (L--, Figure 2.4B and C-G). The APC-eFluor fluorochrome gave some compensation issues leading to the negative peak sitting more into the second decade in the one-parameter plots (Figure 2.3P, 2.4F) and showed more flattened and comet shaped cell populations in the two-parameter plots (Figure 2.3E, H, J and K). However, this fluorochrome could not be replaced and was used alongside the other fluorochrome conjugated antibodies. To determine the percentage of cells expressing the combinational phenotypic markers, CD29+, CD31-, CD45- and CD90+, tree plots were used to summarise the data from the one-parameter plots (Figure 2.5). The branches categorise the populations based on whether they are negative or positive for a specific phenotypic marker.
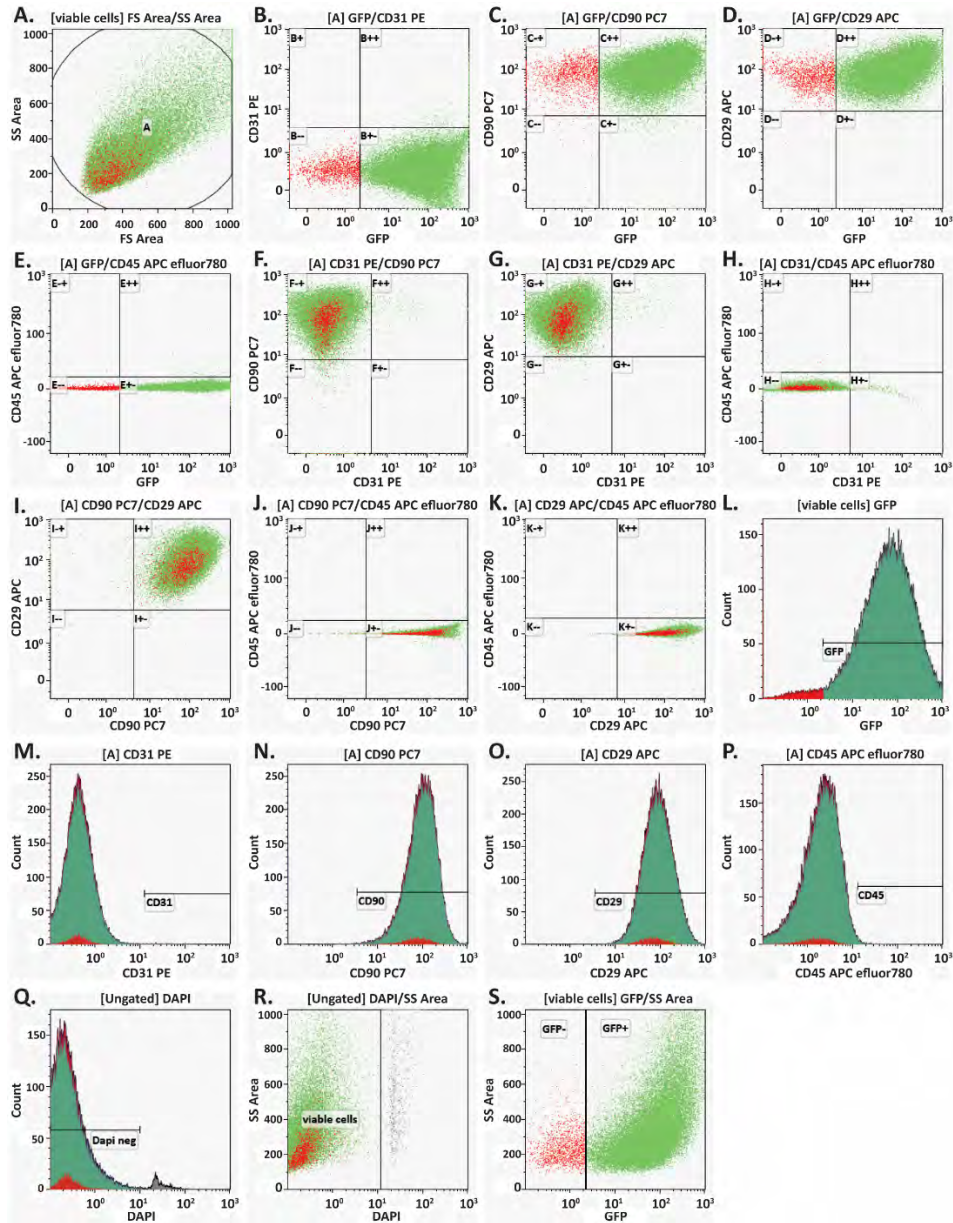
Figure 2.3 Analysis strategy used for determining the phenotypic profile of transduced ASCs.
Flow cytometric analysis of sample A120116-01 at passage 2 transduced to express Fluc and GFP showing positive expression for CD90 and CD29 and lack of expression for CD31 and CD45. (A) Dot plot showing the cell population, A, which is gated for viable cells. (B-K) Two-parameter plots. (L-Q) One-parameter plots. Plots (B-P) were gated for the cell population, A. (R) Dot plot showing the viable cells that are negative for DAPI. (S) Dot plot showing the cells that are either negative or positive for GFP.
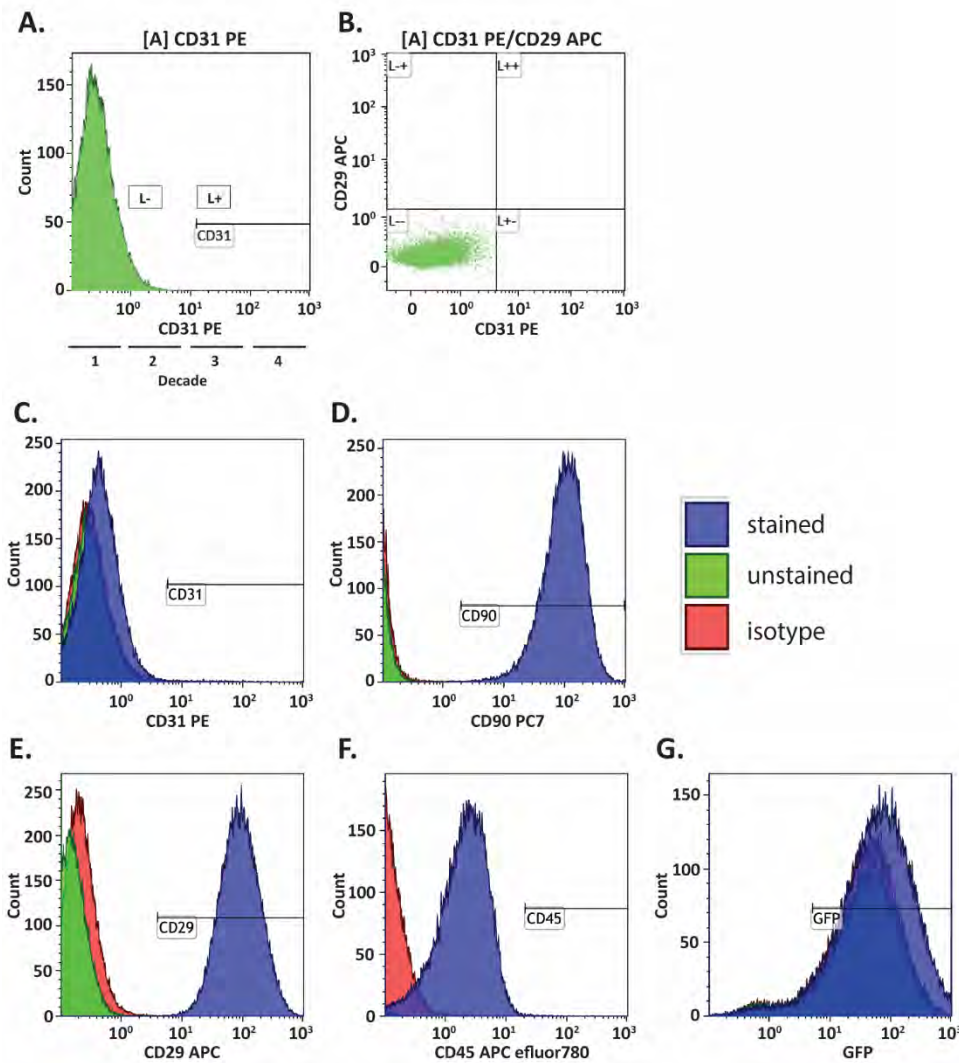
Figure 2.4. Flow cytometry plots.

(A) One-parameter plot: the first and second decade represent the negative population and decades three to four represent the positive population. Here unstained cells are shown and are negative for CD31. (B) Two-parameter plot: shows four distinct populations, L--, L-+, L+- and L++. Here the unstained cells are negative for CD29 and CD31. (C-G) Overlays of one-parameter plots depicting the differences between unstained, isotype controls and stained cells.
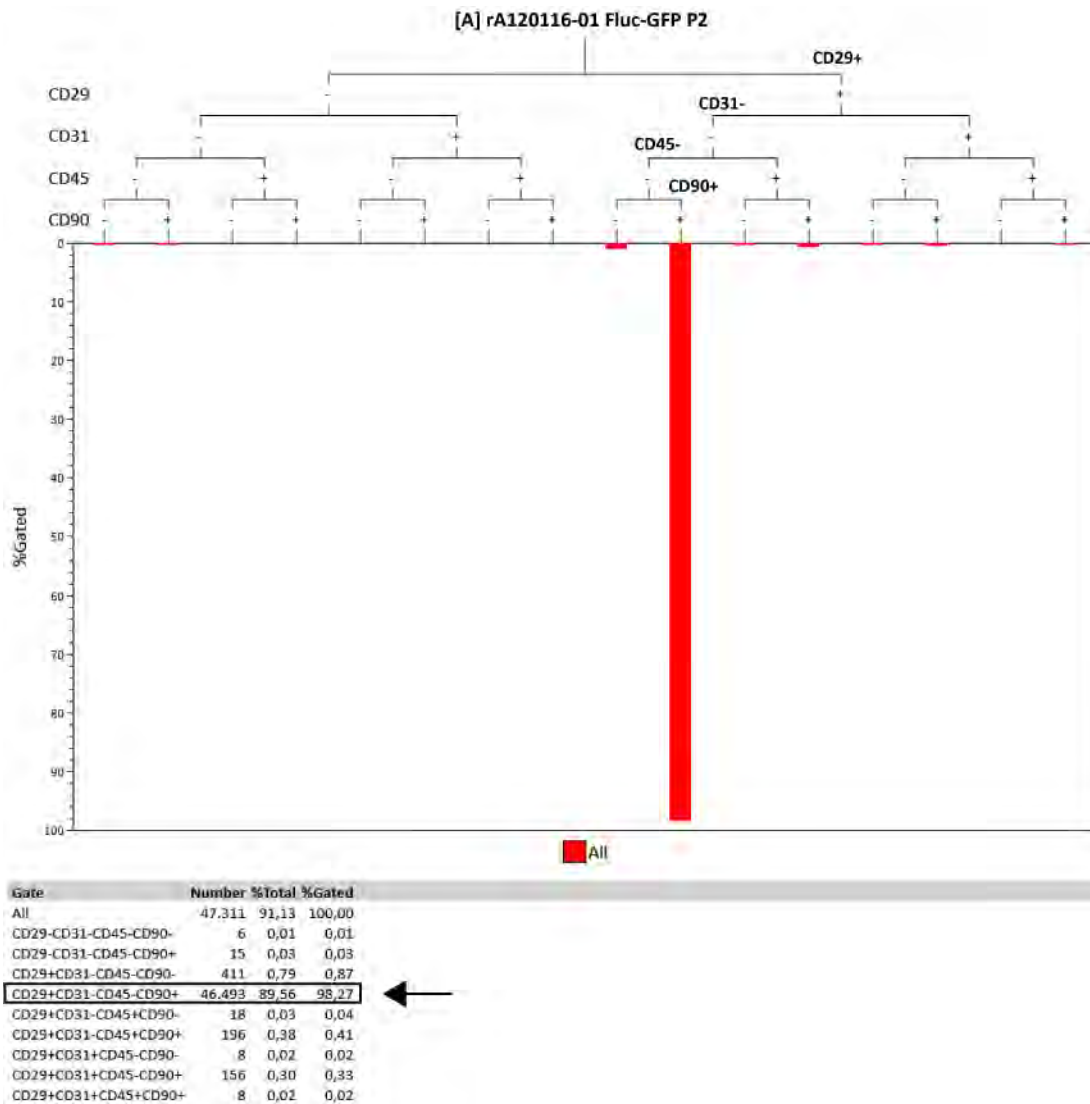
Figure 2.5 Tree plot generated for determining the combined phenotypic profile of the ASC population. Flow cytometric analysis of sample rA120116-01 at passage 2 transduced to express Fluc and GFP. The plot is gated for GFP positive ASCs and show that 98.27% of the transduced ASCs express an MSC phenotype being CD29+, CD31-, CD45- and CD90+.

2.2.4.2 *In vitro* differentiation capacity of ASCs

To confirm the differentiation capacity of non-transduced and transduced ASCs, they were induced to differentiate along adipogenic and osteogenic lineages using specific induction media. Cell cultures were trypsinised, counted, phenotypically characterised and re-plated into 75 cm^2 flasks for reverse transcriptase quantitative polymerase chain reaction (RT-qPCR) analysis and 24-well µ-plates (iBidi, Martinsried, Germany) for histological analysis at 5 x 10^3 cells/cm^2. Adipogenic-inducing differentiation medium consisted of DMEM supplemented with 10% FBS, 1% pen/strep, 0.1 µM dexamethasone, 0.5 mM 3-isobutyl-methylxanthine (IBMX), 56 µM indomethacin and 10 µM insulin (human recombinant Zinc, GIBCO by Life Technologies™, NY, USA). Osteogenic-inducing differentiation medium consisted of DMEM supplemented with 10% FBS, 1% pen/strep, 10 nM dexamethasone, 50 µM ascorbate-2-phosphate and 10 mM β-glycerophosphate. Stock solutions of dexamethasone and indomethacin were prepared in ethanol, whereas IBMX stock solutions were prepared in dimethyl sulphoxide (DMSO). Non-induced control cells were maintained in CGM. The cultures, both induced and non-induced, were maintained for 14 (for histological analysis) and 21 days (for RT-qPCR) in adipogenic-inducing differentiation medium and for 21 days in osteogenic-inducing differentiation medium. Cells were fixed for 60 min using 4% (v/v) formaldehyde solution and stored at 4°C in PBS until used for histological staining or until ribonucleic acid (RNA) was extracted from fresh cells for RT-qPCR. The accumulation of lipid droplets was detected by staining the cells with a 0.3% oil red O (ORO) working solution for 10 min at RT. Mineralisation was detected by staining the cells with 2% alizarin red S (ARS, pH 4.1) for 10 min at RT. Cells exposed to differentiation medium as well as control cells were stained. Images were acquired using an Eclipse Ts2-FL inverted microscope fitted with a DS-Fi3 camera and DS-L4 control unit (Nikon corporation, Tokyo, Japan). Dexamethasone, IBMX, indomethacin, ascorbate-2-phosphate, β-glycerophosphate, DMSO, formaldehyde solution, ORO and ARS were all from Sigma-Aldrich Chemie, Steinheim, Germany.

2.2.4.3 Adipogenic differentiation assessment by RT-qPCR

To confirm expression of adipogenic differentiation marker genes in transduced and non-transduced ASCs (n=2) after 21 days in adipogenic-inducing medium, messenger RNA (mRNA)

levels for four target (*Adipor2, FABP4, C/EBPα, PPARγ*) and three reference (*18s, GAPDH, ACTB*) genes was measured by RT-qPCR. Total RNA was extracted from differentiated and undifferentiated ASCs plated in 75 cm^2 flasks using the RNeasy Minikit (Qiagen, Hilden, Germany). Messenger RNA was reverse transcribed to complementary DNA (cDNA) with the SensiFast cDNA synthesis kit (Bioline, London, England) using 1 µg RNA. For RT-qPCR, LightCycler 480 SYBR Green I Master Mix (Roche, Basel, Switzerland) was used. Reactions for PCR were performed in triplicate in a final volume of 10 µl. Primer and cDNA concentrations were adjusted to 500 nM and 20 ng/µl respectively. Primer mix for the reference genes from the geNORM kit (Primerdesign Ltd, Southampton, UK) was adjusted to 300 nM. Quantitative PCR was performed in 96-well plates on a LightCycler 480 II instrument (Roche, Basel, Switzerland) using the following cycling conditions: activation at 94°C for 3 min and 45 cycles of amplification at 94°C for 30 sec, 60°C for 30 sec, 72°C for 30 sec. After amplification, a melt curve was performed at 95°C for 30 sec, 40°C for 30 sec, and ramped at 0.1°C/sec. Primers (IDT, Coralville, IA, USA) and their target sequences are shown in Table 2.3. For selecting reference genes (internal controls), a six gene rat geNORM reference gene selection kit (*18s, MDHI, YWHAZ, UBC, GAPDH, ACTB*) was used. geNORM analysis using the analysis software qbase+ version 3.1 was used to select the appropriate number of reference genes, as well as the most stable reference genes for the experiment. The reference genes *18s, GAPDH* and *ACTB* were selected. For both non-induced and induced samples, either from transduced or non-transduced cultures, each reaction was performed in triplicate (technical replicates), and the standard deviation (SD) of the quantification cycle (Cq) values was determined. As samples were not always run on a single plate, for each plate, samples were first normalised to a calibrator sample on the plate to obtain a calibrator normalised value. This normalised value was then normalised to the reference genes. Normalisation factors and fold changes were calculated using the geNORM method.[174] For extra information refer to the MIQE guidelines in Appendix 1.

Table 2.3 Target gene primers and sequences in 5' to 3' direction

Target Gene		Forward	Reverse
Fatty acid binding protein 4	*FABP4*	CAGGAAAGTGAAGAGCATC	TTGTCACCATCTCGTCTC
Adiponectin receptor 2	*Adipor2*	CTCTGGTATTGCTCTTCTG	CCACTGAGAGACGATAATG
Peroxisome proliferator-activated receptor gamma	*PPARγ*	TCAGAGGGACAAGGATTCA	GCCAAGTCACTGTCATCTAA
CCAAT/enhancer-binding protein alpha	*C/EBPα*	AGAGGGACTGGAGTTATG	GGTGGTTTAGCATAGACG

Primers were designed and assessed on IDT website (see MIQE guidelines, Appendix 1)

2.2.4.4 Mycoplasma testing of ASCs

All ASC samples were routinely tested for mycoplasma contamination before and after transduction by PCR. Only mycoplasma negative samples were used. Refer to Appendix 2 for a detailed protocol on how to test for mycoplasma contamination in cells and cell medium.

2.2.5 <u>Preliminary experiment: Tracking Fluc positive ASCs *in vivo*</u>

At the start of the project, before the dual lentivector was prepared, a single lentivector expressing Fluc (pCWX-UBI-Fluc-PGK-bsd) was available. Isolated ASCs were transduced with a MOI of 5 and treated with 5 µg/ml blasticidine (bsd) to select for the transduced cells. A preliminary *in vivo* experiment was performed where Fluc expressing ASCs (at P10) were injected systemically in healthy female Wistar rats (n=4, mean weight 290 g). A total of 2 x 10^6 Fluc expressing ASCs were injected systemically via the tail vein into each animal. Animals were imaged by BLI at 3h, 24h, 48h and 72h post injection. Animals received a single IP injection of D-luciferin (150 mg/kg body weight) prepared in PBS. After 20 min, imaging was performed using the Xenogen IVIS® spectrum *in vivo* imaging system with the XGI-8 Gas anaesthesia system. A photographic image of the animal followed by a luminescent image was recorded by the camera. For quantification, a single region of interest (ROI) was manually selected to quantify the luminescent signal in the lung (ROI 1). The ROI size was kept constant between animals and the intensity of the luminescent signal was recorded as total flux (average photons per second, p/sec).[173] All images were analysed using Living Image® 4.3.1 software.

2.2.6 Statistical analysis

Data are expressed as means ± SD. Statistical analyses were carried out using Prism (GraphPad, CA, USA). A Mann-Whitney test was used to assess differences between data means. A *P* value of < 0.05 between data means was considered significant.

2.3   RESULTS

2.3.1 Transduced ASCs maintained their immuno-phenotype

Isolated ASCs were plastic adherent in culture and displayed a typical fibroblast morphology (Figure 2.1 and 2.6E). Evaluation of GFP expression determined that the lowest MOI needed to transduce at least 70% of the ASCs was 10 (Figure 2.6A, B). As the Fluc gene is under the control of a different promotor than the GFP gene, we determined whether our newly transduced cells also expressed Fluc. When D-luciferin, the molecular substrate for Fluc was added to the transduced cells *in vitro*, emitted luminescence was detected. An increase in luminescence, quantified as total flux, was observed with increasing MOIs (Figure 2.6C, D), confirming that the cells were successfully transduced to express not only GFP but also Fluc. Fluorescence for GFP was visible in both the nucleus and the cytoplasm of transduced cells (Figure 2.6E). The percentage of cells expressing GFP was also maintained *in vitro* over different passages showing that greater than 94% of ASCs expressed GFP (Figure 2.6F). Over the three passages evaluated, both non-transduced and transduced ASCs maintained a typical MSC immuno-phenotype, being strongly positive for CD90 and CD29 and negative for CD45 and CD31 (Figure 2.7A-C). However, when the immuno-phenotypic markers were evaluated individually, the transduced ASCs showed slightly higher expression of CD31 (Figure 2.7Cii), but these values were so small (under 0.6% of the cells) that it did not affect the overall immuno-phenotype of the ASCs.

2.3.2 Transduced ASCs maintained their differentiation capacity

When treated with control medium, the non-transduced and transduced ASCs showed no spontaneous differentiation as seen by the absence of intracellular lipid droplets (Figure 2.8Ai-ii) or calcium deposition (Figure 2.8Bi-ii). With induction medium, the non-transduced and transduced ASCs demonstrated comparable formation of intracellular lipid droplets (Figure

2.8Aiii-iv), confirming adipogenesis, and of sparsely distributed cell clumps or nodules that stained positive for ARS (Figure 2.8Biii-iv), confirming osteogenesis. Reverse transcript qPCR analysis was performed for adipogenesis on two samples after 21 days in adipogenic-inducing medium. Adipogenesis genes, *PPARγ* (Figure 2.8C), *C/EBPα* (Figure 2.8D), *Adipor2* (Figure 2.8E) and *FABP4* (Figure 2.8F) were all up-regulated in induced samples compared to non-induced samples. Transduced and non-transduced ASCs showed comparable levels of *Adipor2* and *FABP4* expression. However, transduced, non-induced ASCs had a slightly higher basal level of *PPARγ* and *C/EBPα* expression compared to non-transduced, non-induced ASCs (Figure 2.8C-D).

2.3.3 <u>Systemically administered Fluc expressing ASCs were detectable *in vivo*</u>

Using healthy animals, it was shown that Fluc expressing ASCs could be detected *in vivo* by BLI. Administered ASCs were detected in the lungs as well as in the tail at the site of injection, at all the evaluated timepoints (Figure 2.9A). A decrease in luminescence in the lungs was however observed over time (Figure 2.9B).
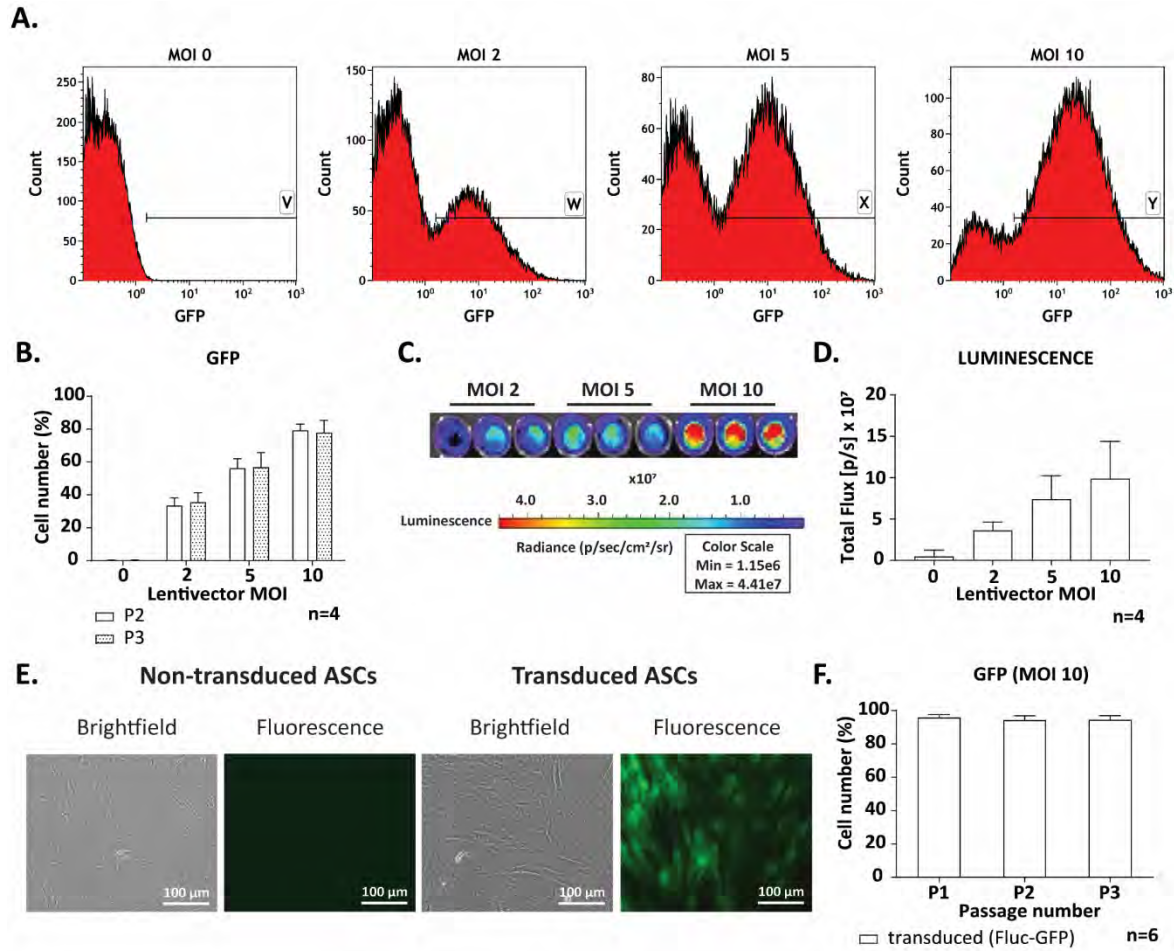
Figure 2.6 Labelling ASCs for *in vivo* tracking.
ASCs were transduced with a dual lentivector expressing GFP and Fluc, pCWX-UBI-Fluc-PGK-GFP at a MOI of 0, 2, 5 and 10. (A) Flow cytometry plots showing the expression of GFP and (B) a graph showing the percentage of ASCs expressing GFP with increasing MOIs. (C) A photographic image of ASCs transduced with different MOIs plated in triplicate for *in vitro* bioluminescence imaging. (D) The quantification of luminescence with increasing MOI. (E) A brightfield image of non-transduced and transduced ASCs in culture and a fluorescent image of non-transduced and transduced ASCs (MOI 10). (F) GFP expression of ASCs transduced with a MOI of 10 in culture from passage 1 to 3 (P1 to P3). Data shown ± SD.
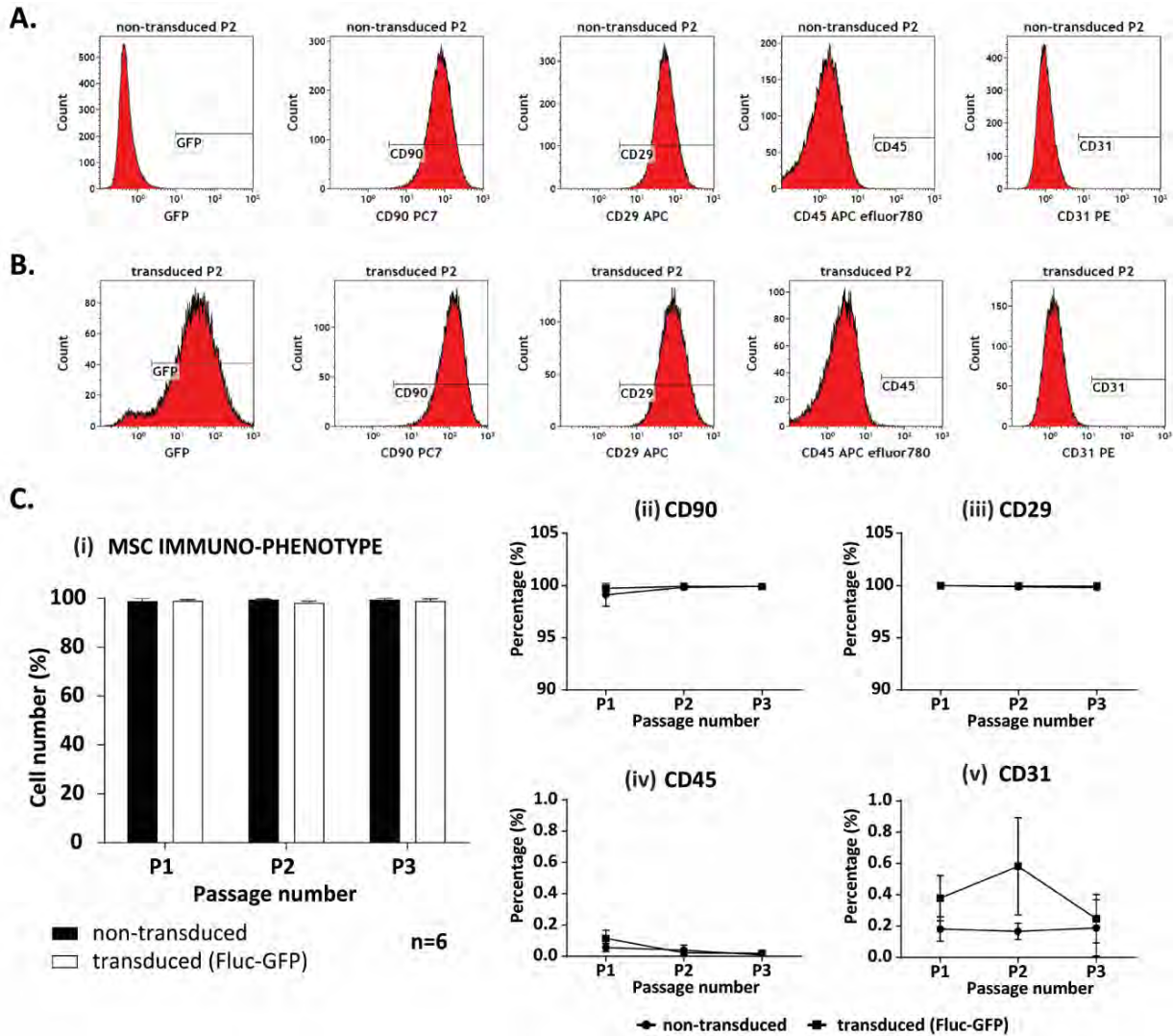
Figure 2.7 Immuno-phenotypic characterisation of non-transduced and transduced ASCs.
Flow cytometry was performed to immuno-phenotype ASCs before and after transduction. ASCs were stained simultaneously with CD90 PC7, CD29 APC, CD45 APC-eFluor 780 and CD31 PE and phenotypically characterised by flow cytometry. One-parameter plots show expression of the different phenotypic markers in (A) non-transduced and (B) transduced ASCs. (C) (i) The transduced cells (positive for GFP) maintained the same immuno-phenotype as the non-transduced cells (positive for CD90 and CD29, and negative for CD45 and CD31) over the passages evaluated; (ii)-(v) shows the phenotypic markers individually. Data shown ± SD.
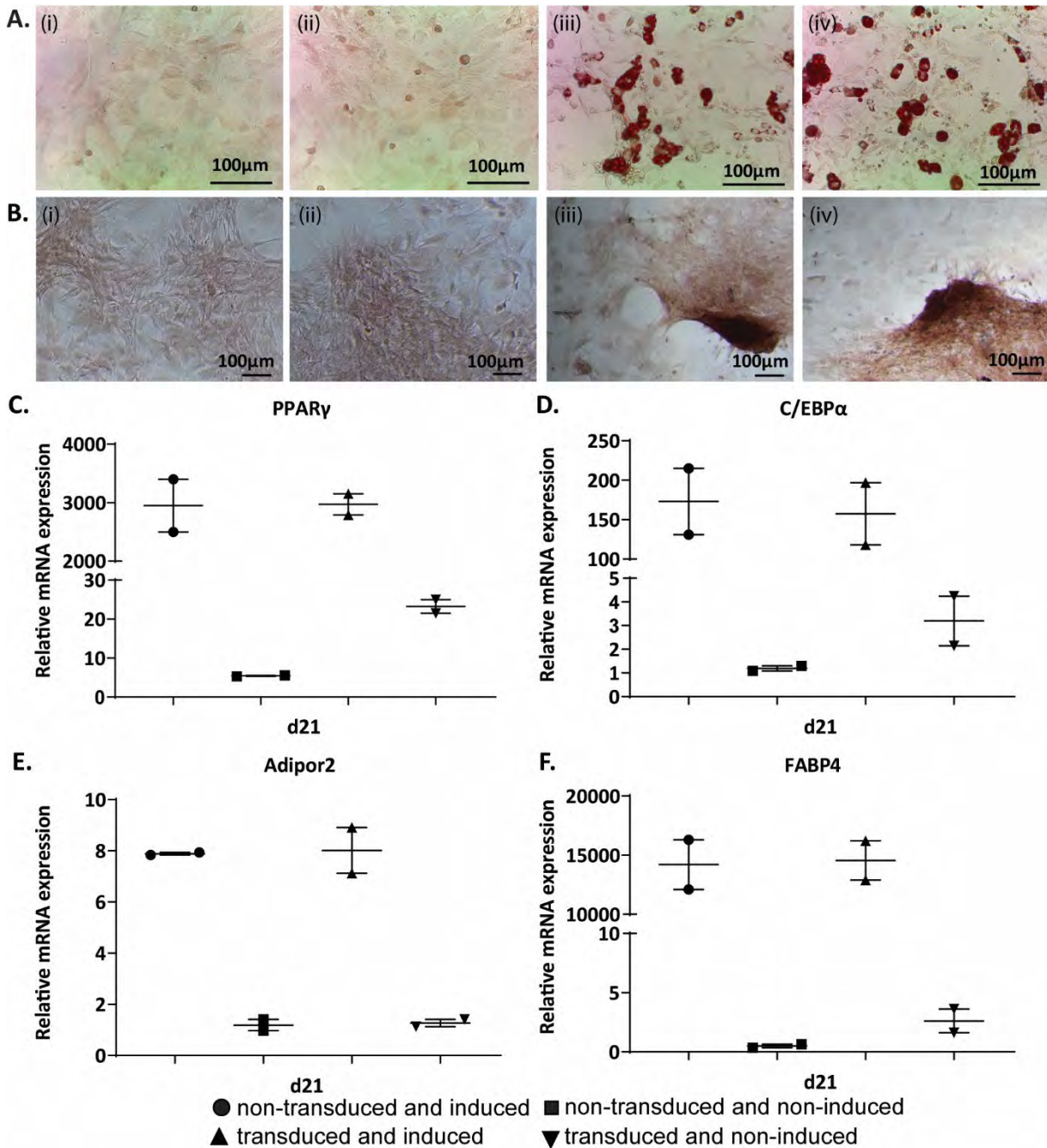
Figure 2.8 Differentiation capacity ASCs.

Qualitative assessment of: (A) adipogenesis for (i, ii) non-induced, (iii, iv) induced, (i, iii) non-transduced and (ii, iv) transduced ASCs all stained for oil red O to identify lipid droplet formation after 14 days in induction medium, and of (B) osteogenesis for (i, ii) non-induced, (iii, iv) induced, (i, iii) non-transduced and (ii, iv) transduced ASCs all stained for alizarin red S to confirm calcium deposition after 21 days in induction medium. (C-F) Relative quantification of the expression of genes expressed during adipogenesis for 2 biological replicates by RT-qPCR after 21 days in induction medium showing relative levels of mRNA expression for (C) *PPARγ*, (D) *C/EBPα*, (E) *Adipor2* and (F) *FABP4*. Data shown ± SD.
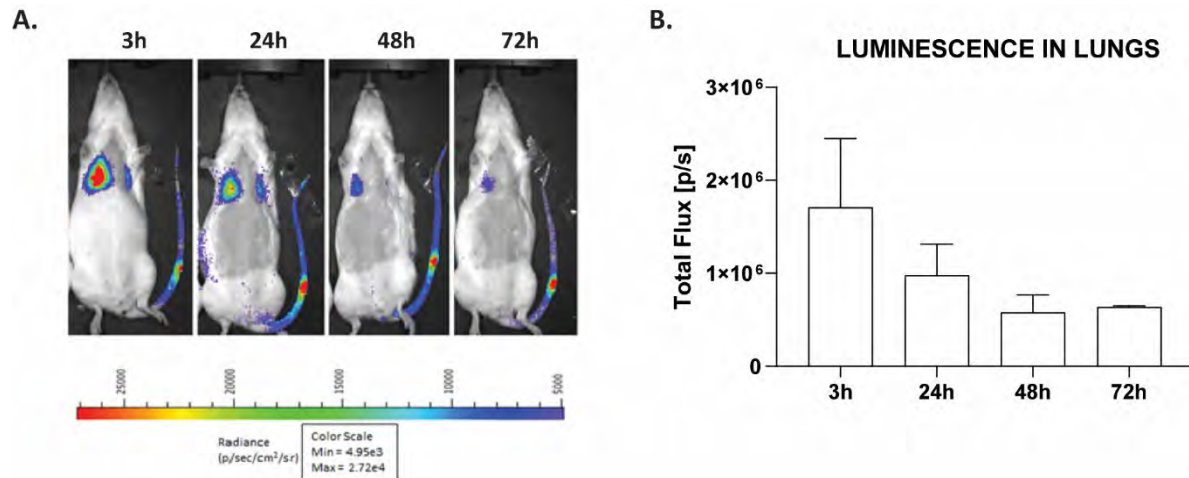
Figure 2.9 *In vivo* imaging to detect systemically administered Fluc+ ASCs.
2 x 10 ^{6} ASCs transduced to express Fluc were injected systemically via the tail vein in rats. Prior to imaging, rats received 150 mg/kg body weight of D-luciferin. (A) A representative image of a single rat imaged at 3h, 24h, 48h, and 72h. (B) The signal in the lungs was quantified and recorded as total flux over time (3h and 24h, n=4; 48h and 72h, n=2, data shown ± SD).

2.4   DISCUSSION

This PhD study will investigate the therapeutic use of exogenously administered ASCs in the treatment of chronic wounds. Before the benefit of ASCs in *in vivo* models of wound repair can be assessed, an appropriate tracking system needs to be established to follow administered cells. This chapter describes a method to label ASCs that enables their tracking by BLI when administered *in vivo*. A reporter construct, such as for Fluc, that leads to the production of the luciferase enzyme, is required for BLI in animal models. Besides the addition of the substrate, D-luciferin, the process of bioluminescence requires magnesium and adenosine triphosphate from metabolically active cells, thus only live cells will be able to emit luminescence.[175] Rat ASCs were genetically modified to express both Fluc and GFP to enable *in vivo* tracking and post mortem identification in animal models of wound repair. Instead of transducing cells to express either Fluc or GFP, a dual lentivector was used, allowing a single cell to express the genes for both markers. Isolated ASCs were successfully labelled to express both Fluc and GFP.

Transduction did not change the immuno-phenotype of ASCs or their ability to differentiate into adipogenic and osteogenic lineages. This confirms previous findings showing that GFP

transduction of ASCs led to no change in either their immuno-phenotype or differentiation capacity.[176, 177] In addition, rat BM-MSCs were previously shown to maintain their characteristics when transduced to express Fluc.[165] Here we report that both GFP and Fluc can be used in combination by using a single lentivector without changing the characteristics of ASCs.

A closer look at gene expression in non-transduced and transduced ASCs when induced into the adipogenic lineage was also undertaken. Four genes known to be involved in the process of adipogenesis were evaluated, namely, *PPARγ*, *FABP4*, *Adipor2* and *C/EBPα*. In mammalian cells, PPARγ and C/EBPα are considered as important early regulators of adipogenesis, while FABP4 and Adipor2 are late regulators responsible for the formation of mature adipocytes.[178] The nuclear receptor PPARγ is described as a master regulator of adipogenesis.[179-181] Pro-adipogenic transcription factors such as C/EBPs promote adipogenesis by either up-regulating the expression of PPARγ or stimulating its transcriptional activity.[182] C/EBPβ is usually induced early on by the adipogenic inducing chemicals IBMX and dexamethasone and hormone treatment (insulin), whereas C/EBPα is expressed later (reviewed in Tontonoz *et al*., 2008). PPARγ and C/EBPα regulate each other's expression positively and work together to promote adipogenesis.[182] In fibroblasts, expression of PPARγ was shown to induce the expression of other adipose-specific genes and the accumulation of lipid droplets.[181] Another regulator, FABP4, is highly expressed in mature adipocytes. FABP4 expression was the highest in the differentiated ASCs followed by PPARγ, whereas C/EBPα and Adipor2 were expressed at the lowest level. This indicates that by day 21 after induction into the adipogenic lineage, ASCs had differentiated into more mature adipocytes. In culture, many loosely attached cells, filled with lipids, were visible.

Prior to having the dual lentivector available, a preliminary experiment was performed to evaluate the detection *in vivo* by BLI in rats of ASCs labelled to express only Fluc. This experiment showed that Fluc expressing ASCs could be successfully detected. This was a very important observation confirming that in this animal model, using rats instead of the usual smaller animals such as the mouse, *in vivo* live cell imaging and tracking could be achieved.

2.5   CONCLUSION

Rat ASCs were successfully labelled to express both Fluc and GFP. The process of transduction did not change the immuno-phenotype or differentiation capacity of the cells. A tracking method had been established and was now ready to be used to follow exogenously administered ASCs in models of wound repair.

CHAPTER 3. THE FATE OF SYSTEMICALLY AND LOCALLY ADMINISTERED ASCs AND THEIR EFFECT ON WOUND REPAIR UNDER PHYSIOLOGICAL CONDITIONS

3.1 INTRODUCTION

In the field of regenerative medicine, cell-based therapies utilising human MSCs have generated a great deal of interest.[183] Although the exact mechanism underlying the therapeutic benefits of MSCs has yet to be fully elucidated, their effectiveness in the treatment of many diseases has been suggested to stem from their specific biological properties.[184, 185] These include their multipotent differentiation capacity, immunomodulatory properties, antimicrobial effect, paracrine signalling and their ability to migrate to sites of injury. Taken together, these observations suggest that MSCs, which naturally have a wide tissue distribution, are therapeutically beneficial because of their role in tissue maintenance, repair and regeneration.[7, 156]

Ongoing clinical trials (www.clinicaltrials.gov) are evaluating the therapeutic potential of MSCs in haematological disease, GvHD, diabetes, diseases of the liver, kidney, lung, bone and cartilage, cardiovascular and neurological disease, as well as inflammatory and autoimmune disorders.[185, 186] Initially, MSC therapy focused on the multilineage differentiation capacity of these cells, especially into bone and cartilage. However, focus is shifting to tissue repair based on MSC immunomodulatory properties as well as their ability to secrete trophic molecules such as cytokines/growth factors and soluble ECM glycoproteins.[73, 185] Although pre-clinical and clinical studies using MSCs to enhance wound repair have suggested positive effects, the benefit of MSC administration for wound healing has yet to be clearly established.[73, 187] The physiological role of MSCs in repair processes might be altered under pathological conditions. Resident MSCs may become dysfunctional or inefficient in their ability to promote tissue repair and regeneration due to diabetes, ischemia and age.[128, 188] In these situations, it has been proposed that administration of exogenous MSCs could promote tissue repair and regeneration by (i) modulation of inflammation, (ii) secretion of growth factors that drive epithelialisation, neo-vascularisation and wound contraction, and (iii) differentiation into cell types required for normal tissue function.[7]

Mesenchymal stromal cells are believed to migrate to damaged tissue in a process called homing.[75] *In vitro*, MSCs are attracted by cytokines and/or chemokines that are known to be up-regulated under conditions of inflammation.[81, 82] More specifically, MSCs respond to the expression of ILs, TNFα and IFNγ.[83] However *in vivo*, homing of MSCs has not been unequivocally shown. Some studies have reported homing of systemically administered MSCs in mouse models of type 2 diabetes,[111] traumatic brain injury,[189] and burn injury,[190] while others reported intrapulmonary cell trapping[135] and minimal evidence for homing[191]. Where re-circulation of MSCs was shown to occur after becoming trapped in the lungs, only a low percentage of MSCs could be found at the injury site or in non-target organs such as the liver and spleen.[163]

The effectiveness of MSCs in regenerative medicine will depend on choosing the most appropriate cell delivery route.[192] Common routes of MSC transplantation include systemic administration (e.g. intravenous (IV), intra-arterial (IA)) and local injection (topical application and regional injection).[193, 194] Unless the administered cells are able to act from a distant site, systemic injection will rely on the trans-endothelial migration (extravasation) of circulating MSCs at the site of injury followed by chemokine guided interstitial migration to the damaged tissue. Local injection will involve the introduction of MSCs close to the target site where directed migration can occur by sensing chemokines released by the injured tissue.[127] Ultimately, delivery routes of MSCs should be tailored to the disease or wound being treated.[135] While local injection of MSCs could be the ideal delivery route to treat small and superficial injuries, systemic injection has been suggested for the treatment of systemic diseases, deep injuries, multiple wounds or for extended wound surfaces.[195] However, whether administered systemically or locally, where the cells go to and whether they can engraft and even survive *in vivo*, is still not well understood. Insights into the basic biology of administered MSCs, their bio-distribution and their engraftment into damaged tissue, needs to be further understood to achieve clinical efficiency.

In this chapter, the distribution and survival of ASCs *in vivo* when administered either systemically or locally was determined using a rat model of wound repair under physiological conditions. As a secondary aim, the effect of different modes of ASC administration was evaluated on wound

closure time. A dual tracking approach was used and included live animal imaging via BLI together with the use of GFP to allow for detection of GFP positive ASCs at the histological level. Information is provided on the bio-distribution of ASCs by identifying the general and tissue-specific location and movement of ASCs post administration as well as their effect on wound closure time. By understanding the fate of administered ASCs in response to injury, this study contributes to determining the mode of administration to be used in the clinical setting.

3.2   MATERIALS AND METHODS

All animal experiments were approved by the local veterinary authority in Geneva (Direction general de la santé de Genève, refer to Appendix 6 for approval letters).

3.2.1 <u>The fate of exogenously administered ASCs</u>

The location and survival of ASCs *in vivo* and their capacity to home or migrate to the wound in a wound repair model under physiological conditions was investigated. Adipose-derived stromal cells were administered either systemically or locally and tracked by using both *in vivo* live cell imaging and histological analysis.

3.2.1.1 *In vivo* rat model and ASC administration

Female Wistar rats (n=57) ≥ 10 weeks old and ≥ 250 g were used. They were fed a standard diet and given water ad libitum. For all procedures, animals were anesthetised by inhalation of 3-5% isoflurane (Baxter AG, Opfikon, Switzerland). Wounds on the dorsal aspect of the hind paws were created bilaterally by removing a full-thickness skin area of 1.2×0.8 cm^2. One day after wounding, animals were treated either with a single injection of 2×10^6 Fluc-GFP positive ASCs systemically into the tail vein (n=27) or locally with 2×10^5 (n=21) Fluc-GFP positive ASCs in total split into two sides of each wound (proximally at the ankle and distally at the toes). For each experiment, ASCs isolated from two rats were cultured and transduced separately before being pooled for either systemic or local injection. Refer to Chapter 2 for the isolation and transduction of ASCs. Control animals received a single injection of sodium chloride (NaCl) systemically into the tail vein (n=9) (Figure 3.1). There was no control group for the local injection site mainly to reduce the number

of animals used unnecessarily for experimentation. All animals received a semi-occlusive wound dressing that was changed weekly.

3.2.1.2 *In vivo* tracking of administered ASCs by BLI

Animals were imaged by BLI at 3h, 24h, 48h, 72h, d7, d15 and at wound closure following systemic and local treatment. Prior to imaging, animals received a single IP injection of firefly D-luciferin potassium salt (150 mg/kg body weight) prepared in PBS. After 20 min, imaging was performed using the Xenogen IVIS® spectrum *in vivo* imaging system with the XGI-8 Gas anaesthesia system. A photographic image of the animal followed by a luminescent image was recorded by the camera. To exclude background luminescence emitted from the ASCs themselves, a single animal that received non-transduced ASCs at the same concentration and mode of administration was included as a control for every BLI experiment. For quantification, three ROIs were manually selected to quantify the luminescent signal in the lung (ROI 1) and the wound area (right foot, ROI 2; left foot ROI 3). The ROI size was kept constant between animals and the intensity of the luminescent signal was recorded as total flux (average photons per second, p/sec).[173] All images were analysed using Living Image® 4.3.1 software.

3.2.1.3 Histological assessment of GFP-positive ASCs

For systemically and locally treated groups, the lungs and the entire foot with the wound and the surrounding uninjured skin were harvested at 3h, 24h, 72h, d7, d15 and at wound closure and fixed in 4% buffered formaldehyde (Merck Millipore, MA, US). Non-target organs (spleen, kidney, heart and liver) from animals systemically treated with ASCs were also harvested, rinsed in PBS and placed in 4% buffered formaldehyde for fixation at all timepoints. After fixation, the wound area along with the uninjured surrounding skin was removed from the foot and processed for paraffin embedding (Figure 3.2A). The lungs were kept whole and processed for paraffin embedding. The spleen and kidney were cut in half transversally, the heart was cut in half longitudinally and the liver separated into the different lobes and processed accordingly for paraffin embedding.

Time after wound creation Day 0   Day 1   Day 2   Day 3   Day 4   Day 8   Day 16   Wound closure
Time after treatment   0h   24h   48h   72h   Day 7   Day 15

Healthy rats
                         3h

Make wounds   Treat wounds*

(a) n=3   n=3   n=3   n=3   n=3   n=3   n=3   n=9
(b) n=3   n=3   n=3   n=3   n=3   n=3   n=3   n=3
(c) n=1   n=1   n=1   n=1   n=1   n=1   n=1   n=3

*Treatment with:
(a) 2x10⁶ Fluc-GFP⁺ ASCs systemically (27 rats)
(b) 2x10⁵ Fluc-GFP⁺ ASCs locally per wound (21 rats)
(c) NaCl systemically (control group) (9 rats)

Note: each rat has 2 feet, so the "n" values should be doubled; for example, if n=3 rats then the final "n" number will be n=6

1. Follow *in vivo* distribution by bioluminescence imaging
2. Follow wound closure by digital photography
3. Collect tissues for immunohistochemistry

Figure 3.1 *In vivo* study design.

For the *in vivo* rat model of wound repair under physiological conditions, full-thickness wounds on the dorsal aspect of the hind paws were created bilaterally in all rats. One day after wounding, animals were either treated with a single injection of 2 x 10⁶ ASCs systemically into the tail vein or locally with 2 x 10⁵ ASCs in total, split into two sides of each wound. Control animals received a single injection of NaCl systemically into the tail vein. Animals were followed by digital photography and bioluminescence imaging and sacrificed for the collection of tissues for histology or immunohistochemistry at 3h, 24h, 48h, 72h, 7 days, and 15 days post treatment and at wound closure.

For IHC analysis, 5 µm thick transverse tissue sections were cut from formaldehyde fixed paraffin embedded (FFPE) samples and analysed using an anti-GFP D5.1 XP® rabbit monoclonal antibody (Cell Signaling Technology Inc., MA, US). A single section of the lungs, spleen, left kidney, heart, liver and feet was analysed for the systemically treated group. For the locally treated group, a single section for the lungs was analysed. However, for the feet, tissue sections were analysed at five different levels into the sample block (Figure 3.2B). Antigen retrieval was performed in a citrate buffer (pH 6) using the DakoCytomation Pascal pressure cooker (125°C, 30 sec) (Hamburg, Germany). After blocking endogenous peroxidases with Dako REAL peroxidase blocking solution (Dako, Hamburg, Germany), sections were incubated with the primary GFP rabbit monoclonal antibody (1/100 dilution; 70 ng/ml) for 1h at RT, and then with a horseradish peroxidase- (HRP) complex secondary antibody (Dako EnVision+System-HRP, Dako, Hamburg, Germany) for 30 min at RT. Sections were developed with aminoethyl carbazole (AEC) for 10 min (BioGenex, CA, USA) and counter stained with haematoxylin for 1-2 min. Sections were scanned using a Zeiss Axio Scan Z1 Brightfield scanner (Carl Zeiss, AG, Germany) at 20x magnification.

In the locally treated group, we determined the precise location of the administered GFP positive ASCs over time. To do so, each section from the five different levels for each FFPE sample was divided into six zones: zone 0 = ASC injection site on the border of wound; zone 00 = ASC injection site on the other border of wound; and the wound itself was divided in four zones: zone 1, 2, 02 and 01 (Figure 3.2C). The location of ASCs in the wound was expressed as a percentage area of GFP staining for a given zone and foot for each timepoint. Using these zones, the percentage area of GFP staining was recorded at 24h, 48h, 72h, and d7 as four sites, summing up all the five levels together as a single value per foot. The injection site was determined as the sum of zone 0 and 00 and the wound site as the sum of zone 1, 2, 02, and 01. More precisely, the outer wound site was defined as the sum of zone 1 and 01, and the inner wound site as the sum of zone 2 and 02 (Figure 3.2C). In total, both feet for each of the three animals were analysed for each timepoint (n=6). All images were processed using Definiens 2.7 software (Munich, Germany). Results were compiled in MATLAB 2018b (MathWorks, MA, US) and the graphs plotted using either MATLAB or Prism (GraphPad, CA, USA).

As a result, there is an elementary region area A per timepoint per foot per tissue per level per zone. The total area A_{foot} of a given foot for every timepoint is defined as:

$$A_{foot} = \sum_{tissue} \sum_{zone} \sum_{level} A_{level,zone,tissue} \quad (1)$$

Similarly, there is an elementary marker area M per timepoint per foot per tissue per level per zone. The total area $M_{zone,\,foot}$ of a given zone and foot for every timepoint is defined as:

$$M_{zone,foot} = \sum_{tissue} \sum_{level} M_{level,tissue} \quad (2)$$

Finally, the normalised area of GFP staining G per timepoint per foot per tissue per level per zone is calculated. The total percentage area $G_{zone,foot}$ of a given zone and foot for every timepoint is defined as:

$$G_{zone,foot} = 100 \frac{M_{zone,foot}}{A_{foot}} \quad (3)$$
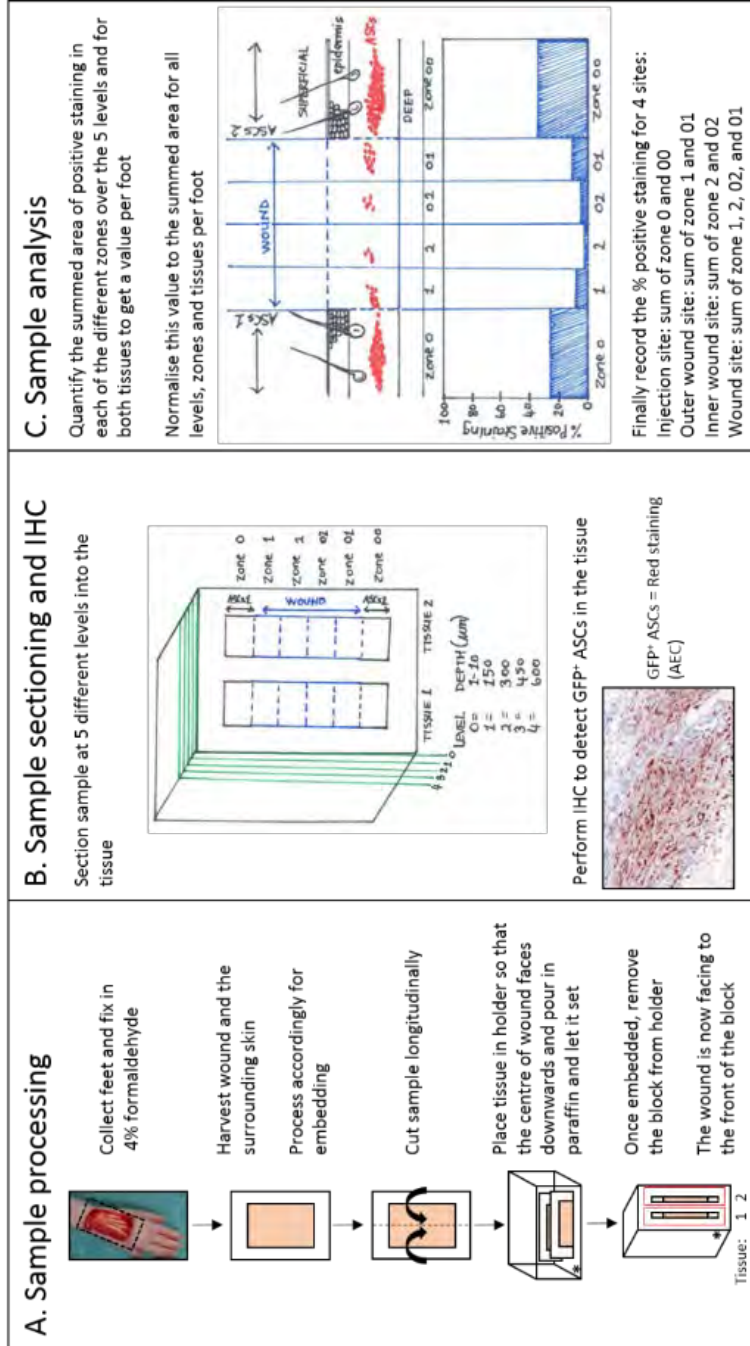
Figure 3.2 Schematic showing how the locally treated feet samples were processed, sectioned, stained for immunohistochemistry (IHC) and analysed.

(A) The feet were collected, fixed, and then processed for embedding in paraffin blocks. (B) Each block consisting of a single sample was sectioned at 5 different levels into the tissue at level 0, 1, 2, 3, and 4. IHC was performed to detect the GFP$^+$ ASCs (Red staining, AEC). (C) The sections were analysed to quantify the area of positive staining using image processing software. Each section was divided into 6 zones, where zone 0 = ASCs 1 (ASC injection site 1), zone 1, 2, 02 and 01 = wound divided into 4 equal regions, and zone 00 = ASCs 2 (ASC injection site 2). The summed area of positive staining in each of the different zones over the 5 levels and for both tissues was quantified to obtain a value per foot. This value was normalised to the summed area for all the levels, zones and tissues per foot. Finally, the percentage of positive staining was recorded as 4 sites: the injection site (sum of zone 0 and 00), the outer wound site (sum of zone 1 and 01), the inner wound site (sum of zone 2 and 02) and the wound site (sum of zone 1, 2, 02, and 01).

3.2.2 The effect of ASCs on wound closure

The time taken to complete wound closure and the contraction/epithelialisation ratio were assessed as previously described.[196] Wound size was documented immediately after wounding and until wound closure by digital photography with the camera placed at a constant distance and a ruler next to the wound for scaling. The photos were analysed using ImageJ 1.48v software[197] to determine the wound area. At complete wound closure (i.e. full epithelialisation), the surface of hairless skin of the scar was measured and considered to correspond to the area of the wound that had healed by epithelialisation. The surface of the wound that healed by contraction was estimated by subtraction of the epithelialised surface from the original wound area measured at day 0 (Figure 3.10C).

3.2.3 Statistical analysis

Data are expressed as means ± SD. Statistical analyses were carried out using Prism (GraphPad, CA, USA). A Mann-Whitney test was used to assess differences between data means. Grouped data was assessed by performing multiple t-tests using the Holm-Sidak method. A *P* value of < 0.05 between data means was considered significant.

3.3 RESULTS

3.3.1 Systemic ASCs were filtered out by in the lung without evidence for homing to the wound site

The luminescent signal was already detectable in the lungs of systemically-treated animals 3h post administration (Figure 3.3A). However, a decrease in signal was observed from 3h to 72h (Figure 3.3B) albeit this decrease in signal was not statistically significant. No signal was detected in the wounds on the feet. When administered locally, the luminescent signal remained strongly detectable for 7 days at the injection site (Figure 3.3C, D) with no signal being detected in the lungs (Figure 3.3C). Also, no signal was detected in other organs when ASCs were injected either systemically or locally (Figure 3.3A, C). At the histological level, systemically administered GFP positive ASCs were strongly detected in the lungs of animals at 3h and 24h, moderately detected at 48h, barely detected at 72h and undetected from day 7 (Figure 3.4A). No GFP staining was

detected in the wounds on the feet (Figure 3.4B) or in other non-target organs such as the spleen (Figure 3.5), kidney (Figure 3.6), heart (Figure 3.7) and liver (Figure 3.8) at any of the timepoints.
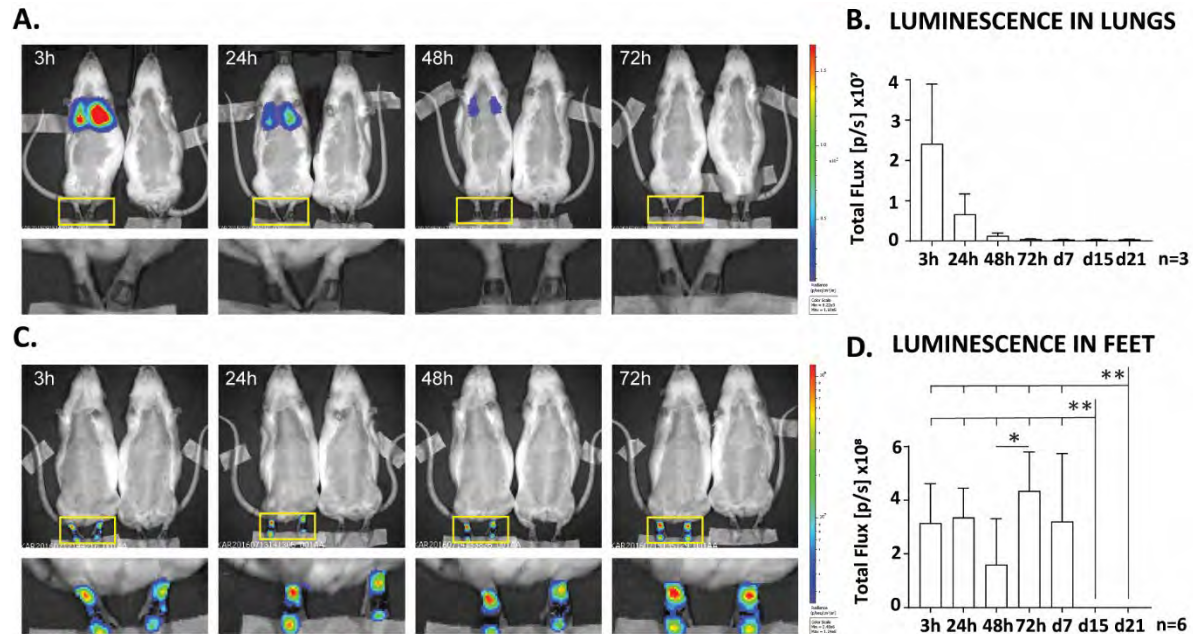
Figure 3.3 *In vivo* tracking of systemically and locally administered Fluc-GFP+ ASCs during wound repair under physiological conditions.

ASCs transduced to express both Fluc and GFP were injected either systemically (2 x 10^6 ASCs) via the tail vein or locally (2 x 10^5 ASCs) into two sides around each wound in rats 24h after bilateral full-thickness wounds were created on the dorsal aspect of the feet. Prior to imaging, animals received 150 mg/kg body weight of D-luciferin. A single representative image of a (A) systemically, (C) locally treated and BLI control animal (rat on the right, received non-transduced cells) imaged at 3h, 24h, 48h, and 72h. An enlarged area of the feet of the treated animals is also shown. The luminescent signal in the (B) lungs of systemically treated and the (D) feet of the locally treated animals was quantified and recorded as total flux over time. Data shown as mean ± SD. Significance is shown where *p<0.05, **p<0.01.

A. 3h. Isotype, LUNG
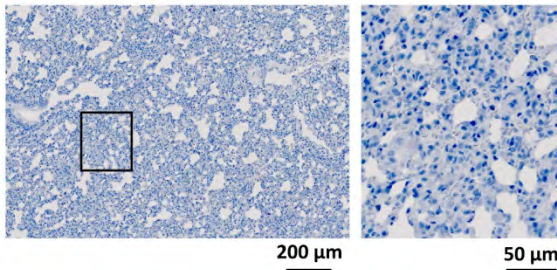
3h. GFP, LUNG
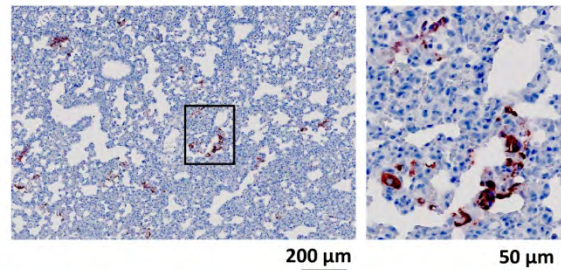
24h. GFP, LUNG
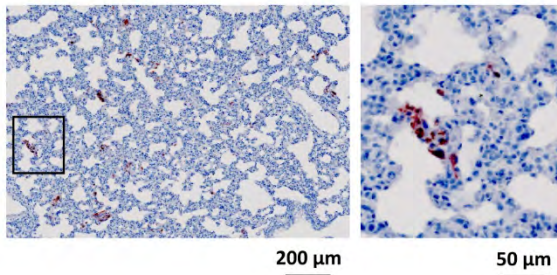
48h. GFP, LUNG
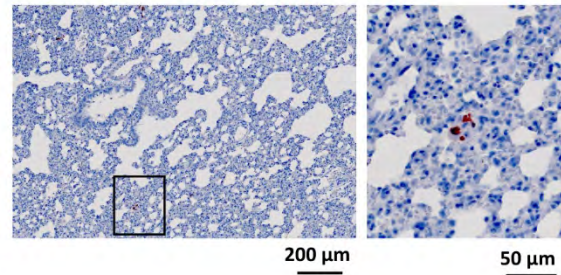
72h. GFP, LUNG
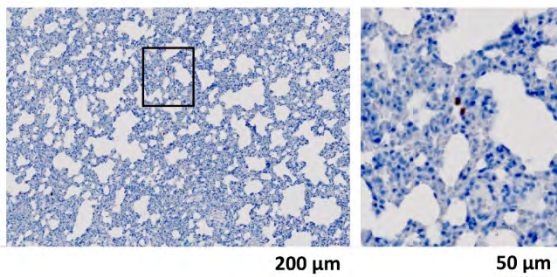
Day 7. GFP, LUNG
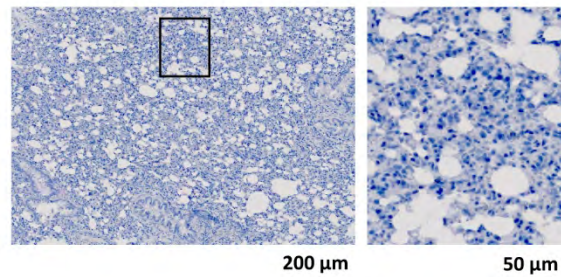
B. 3h. GFP, FEET
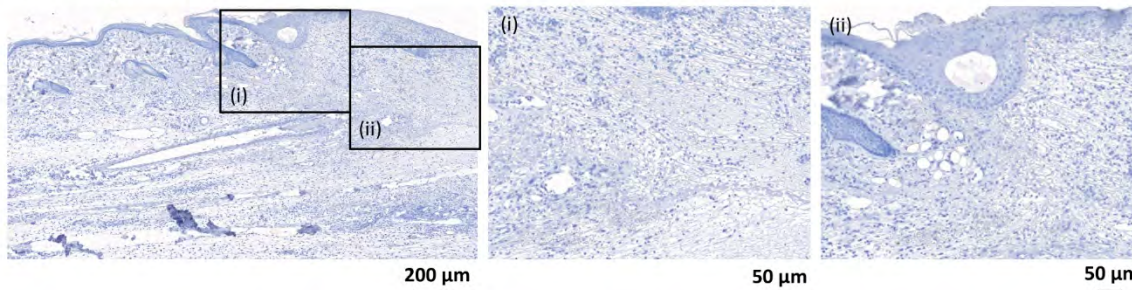
Figure 3.4 Detection of systemically administered ASCs by immunohistochemistry.
ASCs transduced to express both Fluc and GFP were injected systemically (2×10^6 ASCs) into rats via the tail vein 24h after bilateral full-thickness wounds had been created on the dorsal part of the feet. Lungs and feet were processed for immunohistochemistry to detect GFP positive ASCs (red staining, AEC). (A) Images of the lung at 3h, 24h, 48h, 72h, and at day 7 are shown. The right panel is a magnified view of the black rectangle showing positively-stained ASCs. (B) A representative image of the feet at 3h is shown where panel (i) is a magnified view of the epithelium lip and (ii) of the wound bed. Tissue sections were counterstained with haematoxylin (blue staining).

SPLEEN

A. 3h, GFP

50 µm

B. 24h, GFP

50 µm

C. 48h, GFP

50 µm

D. 72h, GFP

50 µm

E. Day 7, GFP

50 µm

F. Day 15, GFP

50 µm

G. 72h, Isotype

50 µm
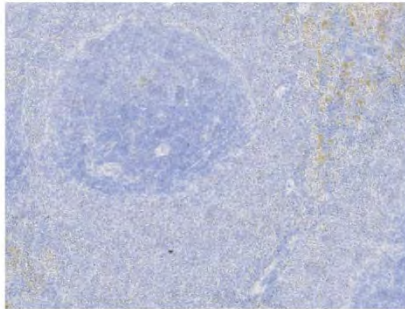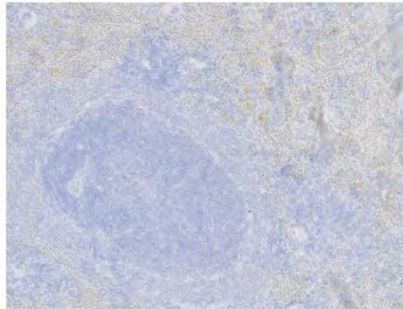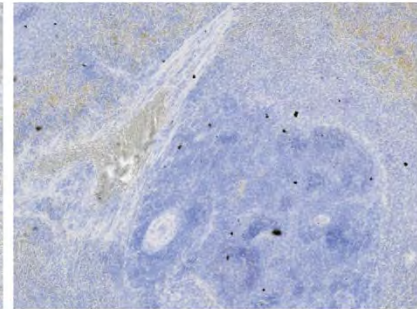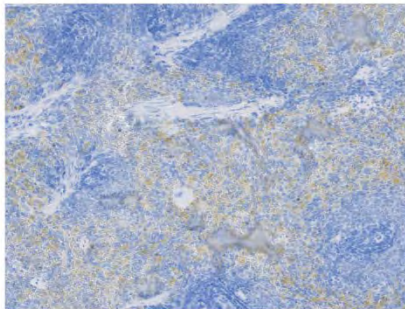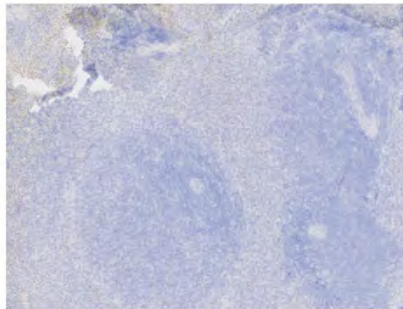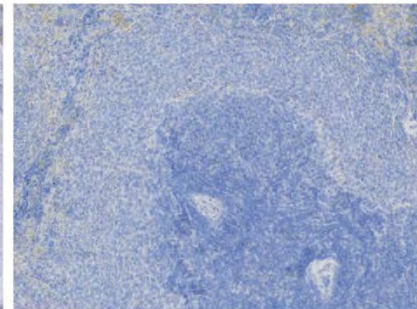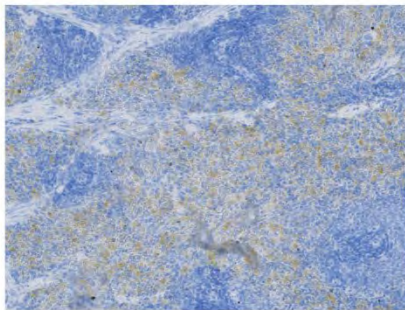
H. Transverse section of the spleen, day 15, GFP

1000 µm
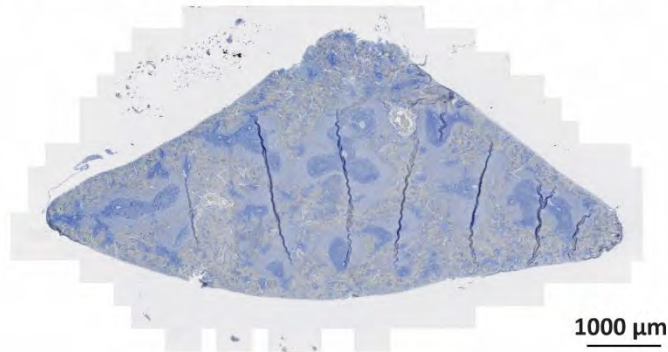
Figure 3.5 Systemically administered ASCs were not detected in the spleen.
The spleen of animals systemically treated with ASCs were collected and processed accordingly for immunohistochemistry to detect whether GFP positive ASCs (red staining, AEC) had migrated to the organ. A representative ROI of the spleen stained for GFP at (A) 3h, (B) 24h, (C) 48h, (D) 72h, (E) day 7 and (F) day 15 post treatment; and stained with an isotypic control at (G) 72h. (H) A day 15 image of a transverse section of the whole spleen. Tissue sections were counterstained with haematoxylin (blue staining). An absence of red staining was found at all timepoints.

LEFT KIDNEY

A. 3h, GFP
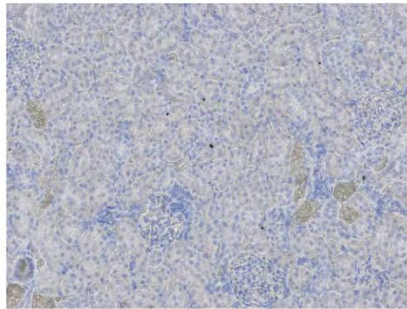
50 µm
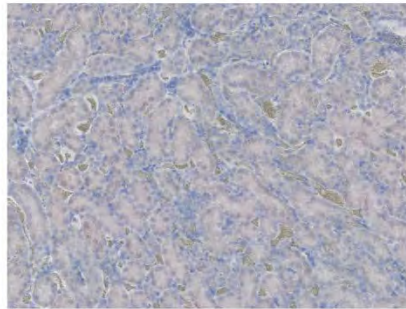
B. 24h, GFP

50 µm

C. 48h, GFP

50 µm

D. 72h, GFP

50 µm

E. Day 7, GFP

50 µm

F. Day 15, GFP

50 µm

G. 72h, Isotype

50 µm
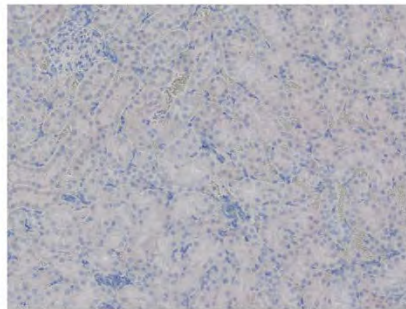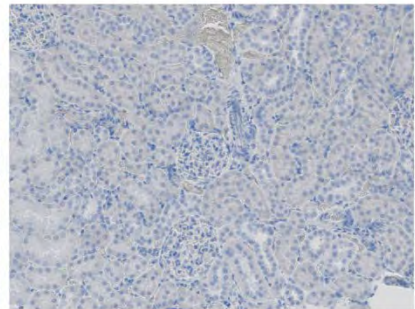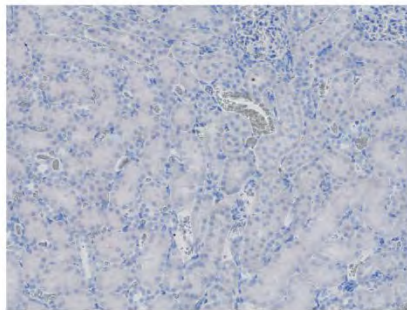
H. Transverse section of the left kidney, day 15, GFP
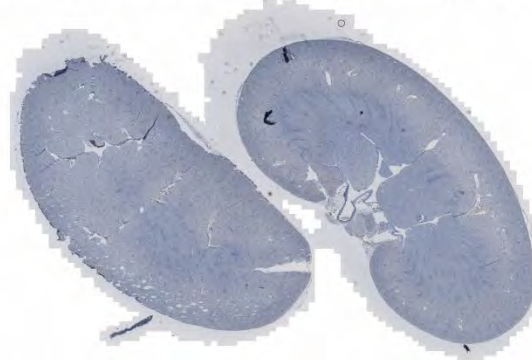
2000 µm

Figure 3.6 Systemically administered ASCs were not detected in the kidney.
The left kidney of animals systemically treated with ASCs were collected and processed accordingly for immunohistochemistry to detect whether GFP positive ASCs (red staining, AEC) had migrated to the organ. A representative ROI of the kidney stained for GFP at (A) 3h, (B) 24h, (C) 48h, (D) 72h, (E) day 7 and (F) day 15 post treatment; and stained with an isotypic control at (G) 72h. (H) A day 15 image of a transverse section of the left kidney. Tissue sections were counterstained with haematoxylin (blue staining). An absence of red staining was found at all timepoints.

HEART

A. 3h, GFP

50 μm

B. 24h, GFP

50 μm

C. 48h, GFP

50 μm

D. 72h, GFP

50 μm

E. Day 7, GFP

50 μm

F. Day 15, GFP

50 μm

G. 72h, Isotype

50 μm
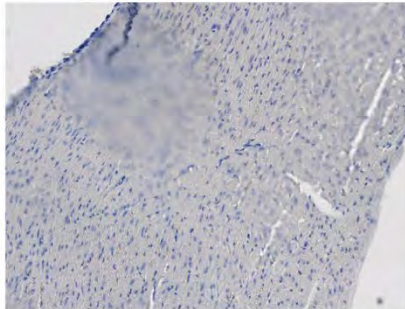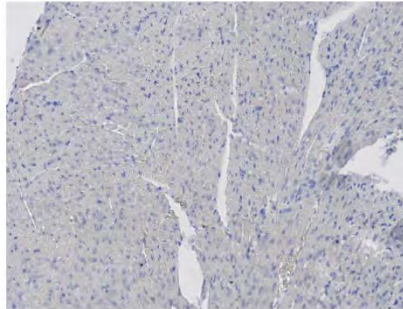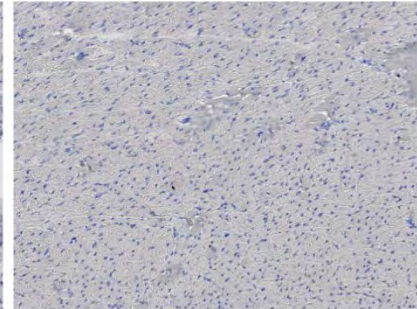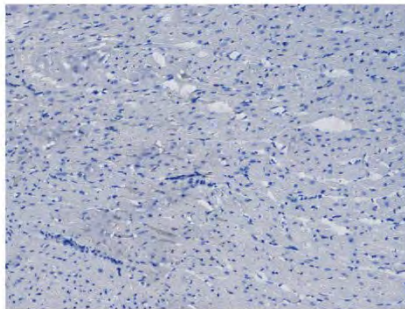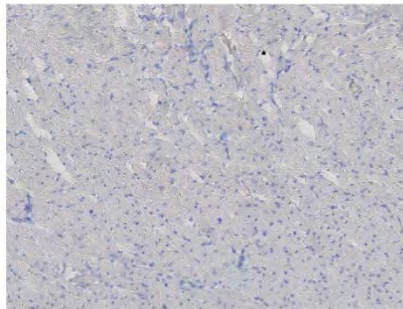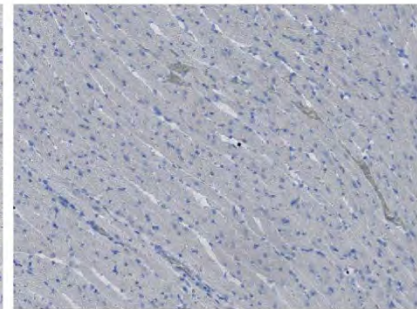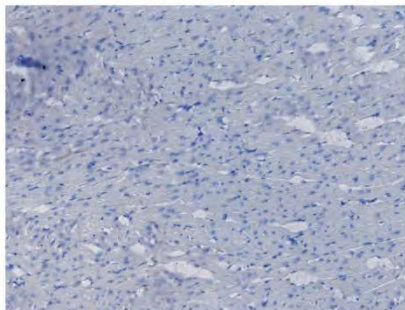
H. Longitudinal section of the heart, day 15, GFP

2000 μm
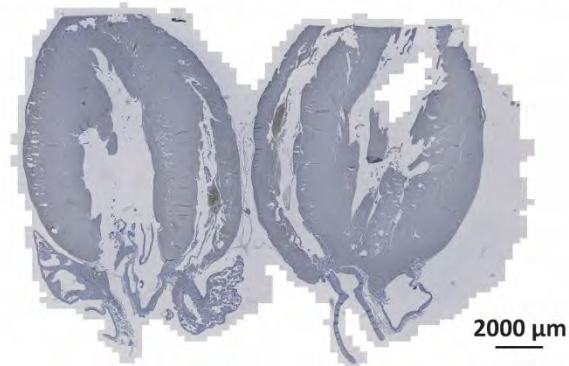
Figure 3.7 Systemically administered ASCs were not detected in the heart.
The heart of animals systemically treated with ASCs were collected and processed accordingly for immunohistochemistry to detect whether GFP positive ASCs (red staining, AEC) had migrated to the organ. A representative ROI of the heart stained for GFP at (A) 3h, (B) 24h, (C) 48h, (D) 72h, (E) day 7 and (F) day 15 post treatment; and stained with an isotypic control at (G) 72h. (H) A day 15 image of a longitudinal section of the heart. Tissue sections were counterstained with haematoxylin (blue staining). An absence of red staining was found at all timepoints.

LIVER

A. 3h, GFP
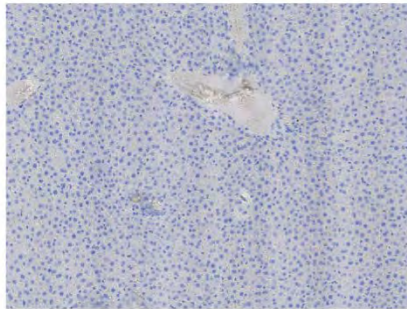
50 µm

B. 24h, GFP

50 µm

C. 48h, GFP

50 µm

D. 72h, GFP

50 µm

E. Day 7, GFP

50 µm

F. Day 15, GFP

50 µm
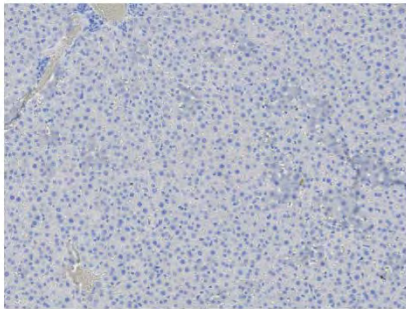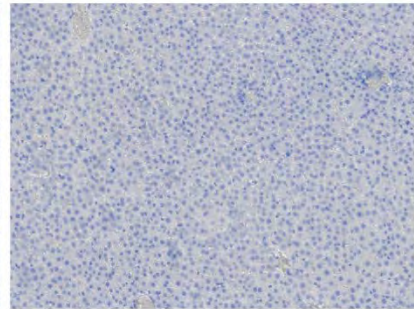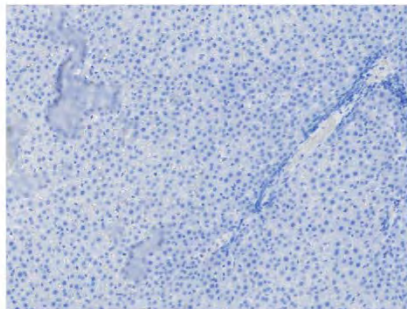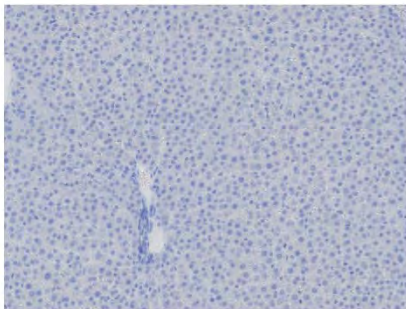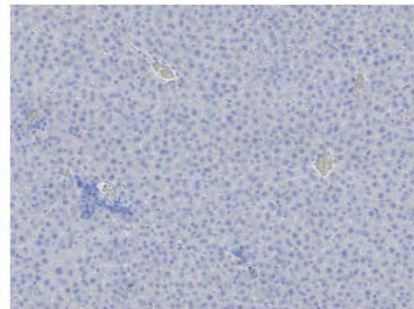
G. 72h, Isotype
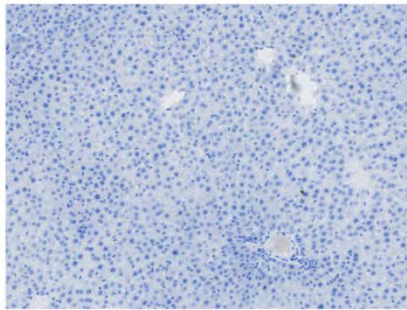
50 µm

H. Section of the liver, right medial lobe, day 15, GFP
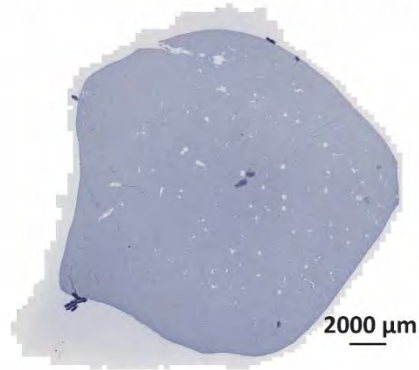
2000 µm

Figure 3.8 Systemically administered ASCs were not detected in the liver.
The liver of animals systemically treated with ASCs were collected and processed accordingly for immunohistochemistry to detect whether GFP positive ASCs (red staining, AEC) had migrated to the organ. A representative ROI of the liver stained for GFP at (A) 3h, (B) 24h, (C) 48h, (D) 72h, (E) day 7 and (F) day 15 post treatment; and stained with an isotypic control at (G) 72h. (H) A day 15 image of a section of the liver (right medial lobe). Tissue sections were counterstained with haematoxylin (blue staining). An absence of red staining was found at all timepoints.

3.3.2 Locally administered ASCs survived and became distributed within the wound bed

Interestingly when the histology slides from animals that received ASCs locally were evaluated, GFP staining was not restricted to the ASC injection sites. When 15% of the wound was analysed as represented by the five levels at which sections were assessed, GFP positive ASCs became distributed within the wound bed as early as 24h after administration and remained there for 7 days (Figure 3.9A-E). At the injection site (zone 0, 00), ASCs remained detectable until day 7 (Figure 3.9B). Within the wound bed (zone 1, 2, 02 and 01), a significant increase in GFP staining was found from 24h to 72h (0.039% vs 0.057%, p=0.0087) with no significant change on day 7 (Figure 3.9C). This significant increase in GFP staining from 24h to 72h was found in both the outer (zone 1 and 01) (0.031% vs 0.047%, p=0.0043) and inner wound sites (zones 2 and 02) (0.010% vs 0.033%, p=0.0173). However, even though the increase was significant in the inner wound site betw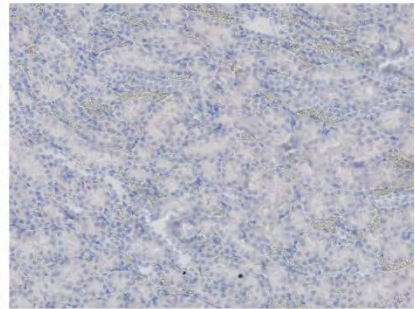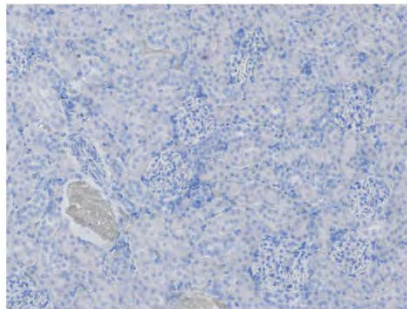een 24h and 72h (0.013% vs 0.043%, p=0.0173), and 48h and 72h (0.014% vs 0.043%, p=0.0152), GFP staining remained lower than in the outer wound site. The outer wound site showed no significant changes in GFP staining from 72h to day 7, whereas in the inner wound site a significant decrease was found from 72h to day 7 (0.043% vs 0.010%, p=0.0152) (Figure 3.9D, E).

3.3.3 Both systemic and local ASC administration led to enhanced wound closure time

As a secondary aim, the effect of ASC administration on wound closure time was determined. In comparison to a total wound closure time of 26 days in the control group, wound closure was more rapid when ASCs were administered locally (19 days, p=0.0108) and systemically (21 days, p=0.0024) (Figure 3.10A). Both ASC treated groups showed an enhancement of wound closure compared to the NaCl control group. After wound creation, the wound size was followed and recorded over time as wound area (percentage, as normalised to the wound on day 0). Both ASC treated groups showed an enhancement in wound size after 3 days before reducing in size. Only at day 7 was wound size significantly smaller in the control group compared to the ASC systemically treated group (p=0.0301). Comparison of ASC treated groups showed significantly smaller wounds with local treatment at 10 days (p=0.0102) (Figure 3.10B). After 7 days, although the values are not significantly different, a change in the trend of wound size reduction can be

noticed with the wounds from the control treated group appearing to close at a slower rate (Figure 3.10B). Further investigation into whether wound closure was favoured more by contraction or epithelialisation showed a significant decrease in contraction and an increase in epithelialisation in both the locally treated group (contraction: 56%, epithelialisation: 44%) and the systemically treated group (contraction: 62%, epithelialisation: 38%) compared to the NaCl control group (contraction: 73%, epithelialisation: 27%) (p=0.0022 and p=0.0002 respectively) (Figure 3.10C, D). A supplementary experiment was performed to investigate whether the local administration of ASCs was dose dependent (refer to Appendix 3). The higher dose of ASCs (2 x 10^5 ASCs) enhanced wound closure significantly faster compared to the lower ASC dose (1 x 10^5 ASCs) (Figure S1). Additionally, no change in the dynamics of how the wound closed, either through contraction or epithelialisation was found with the lower ASC dose. The higher dose of ASCs appeared to be more effective than the lower dose suggesting that ASCs when administered locally may be dose dependant.

3.4   DISCUSSION

Interest in the use of systemically applied MSCs for therapeutic purposes was popularised by the group of Horwitz. Their studies in children with osteogenesis imperfecta showed that allogeneic BM-MSCs injected systemically engrafted in the bone and bone marrow stroma, and led to improvement in growth rates of the children as well as their ability to synthesise intact bone.[198-200] A study in rats showed that BM-MSCs administered either systemically or locally were able to promote fracture healing. Although the proportion of MSCs that migrated into the injury sites following systemic injection was significantly less than those in the local injection group, both groups promoted fracture healing equally well, indicating that systemically injected MSCs may have contributed in an indirect manner. The authors further proposed that systemic administration of MSCs may have advantages over local administration through immune regulation and promoting the function of resident MSCs.[195] The most appropriate mode of administration, along with an understanding of where the cells go to, whether they engraft and survive *in vivo*, is still not well understood in the context of cutaneous wound repair.
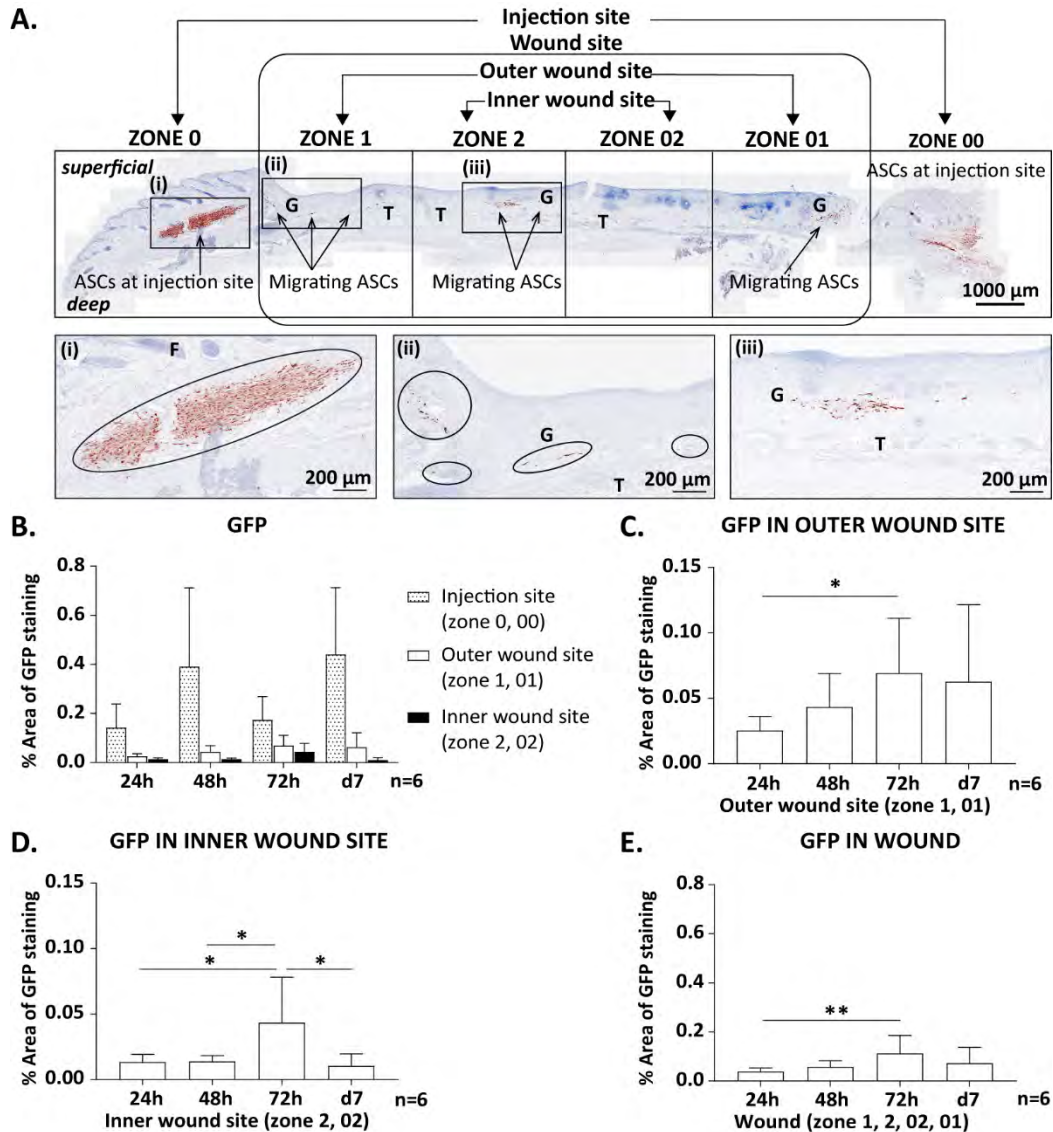
Figure 3.9 Locally administered ASCs were detected within the wound over time.
2 x 10^5 ASCs transduced to express both Fluc and GFP were injected locally into two sides around each wound 24h after bilateral full-thickness wounds had been created on the dorsal part of the feet. (A) A single tissue section from the wound in the feet 24h post injection stained for GFP (red staining, AEC). Magnified images of the (i) injection site, (ii) outer wound site and (iii) inner wound site. The distribution of ASCs in the different sites of the wound was quantified over time showing, (B) the injection site, outer and inner wound site in a single graph (C) the wound site (zone 1, 2, 02, 01), (D) the outer wound site (zone 1, 01) and (E) the inner wound site (zone 2, 02). Data shown as mean ± SD. Significance is shown where *p<0.05, **p<0.01. G= granulation tissue, E= epithelium, T= tendons, and F= hair follicles.
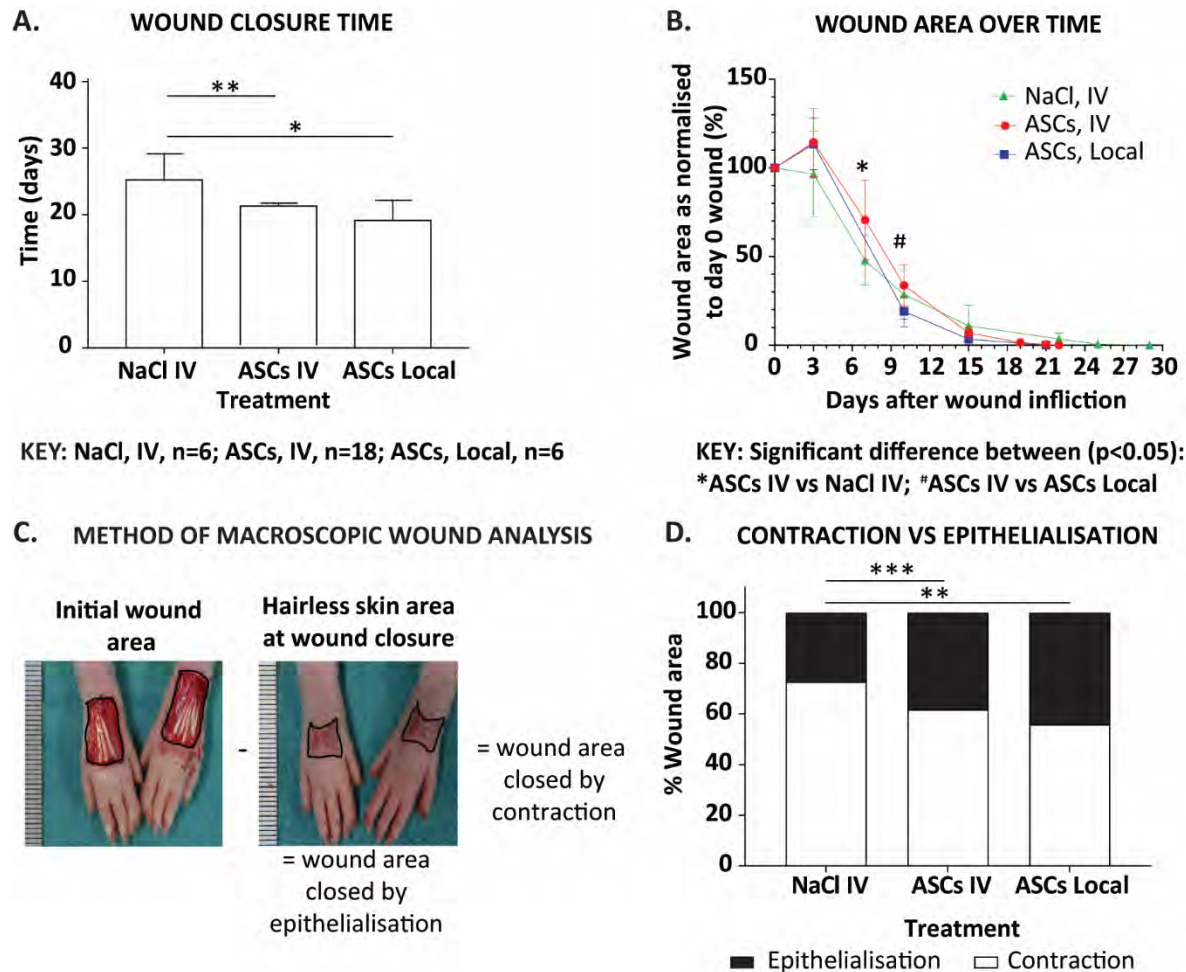
Figure 3.10 Wound closure assessment in animals treated locally and systemically.
Animals were treated with Fluc-GFP+ ASCs, locally into two sides around each wound (2×10^5 ASCs) or systemically (2×10^6 ASCs) into the tail vein. Control animals were treated systemically with NaCl. (A) Time taken for complete wound closure after treatment. (B) Wound area over time after treatment as normalised to the original wound area on day 0. (C) Calculation of the contraction/epithelialisation ratio: the area of the wound is measured directly after surgery. At the day of complete wound closure, the area of hairless skin is measured and considered to correspond to the area of the wound that was closed by epithelialisation. Subtracting the area of epithelialisation from the initial wound area provides the area closed by contraction. (D) Wound area closed by contraction and by epithelialisation. Data shown as mean ± SD. Significance is shown where */#$p<0.05$, **$p<0.01$, ***$p<0.001$.

The main objective of this chapter was to track exogenously administered ASCs in an *in vivo* model of physiological wound repair. The fate and distribution of systemically and locally administered ASCs was determined. Localisation of systemically administered ASCs occurred rapidly in the lung after systemic administration. The luminescent signal intensity in the lungs

declined over time with almost no signal being visible after 3 days. However, at the wound site neither a luminescent signal nor GFP positive ASCs could be detected. These results suggest that systemic administration leads to cell entrapment in the lungs without migration to other tissues/organs. Lung entrapment is likely to have been due to a combination of mechanical and biological phenomena, such as small capillary size, extensive capillary networks in the lungs as well as the large size and strong adhesion properties of MSCs.[200] A study by Fischer *et al*., evaluating the passage of various stromal cells across the pulmonary circulation concluded that the combined effect of cell size and adhesion molecule expression led to lung entrapment.[201] Lung entrapment in the rat model used was not associated with visible signs of distress or deterioration of health. In rodent models of myocardial infarction and ischemia-reperfusion injury in the liver, rodent-derived BM-MSCs became entrapped in the lungs with limited migration to the injured sites.[202, 203] Locally administered ASCs remained strongly detectable at the injection site for 7 days. This is in line with another study reporting that rat BM-MSCs transplanted into traumatised skeletal muscle could be tracked *in vivo* until day 7.[165] In the model used for this study, even though fewer ASCs were administered locally than systemically, the luminescent signal appeared to be stronger at the locally injected sites compared to the signal in the lung of systemically injected animals. This may have been due to the dilution of the signal as the lungs are found deeper than the skin. Even with variability in luminescence in the feet over time, no significant change in overall signal was found between 3h and 7 days post local administration. At the histological level, a significant increase was found in ASCs localised within the wound as opposed to the adjacent injection sites from 24h to 72h post local administration. This could be due to at least three factors: ASC migration, ASC proliferation or ASC displacement due to wound contraction. Over time, more ASCs were found in the outer wound site close to the newly extending epithelium lip at all timepoints evaluated (24h, 48h, 72h, d7), with the most ASCs detected at 72h. In the inner wound site, a similar tendency of increased numbers of ASCs was detected at 72h. This data suggests that locally administered ASCs have the capability to migrate from the injection site into the wound bed.

Another aim was to determine whether locally or systemically administrated ASCs could enhance wound repair under physiological conditions. Of note, an enhancement in wound closure time with ASC treatment independently of the route of administration was observed. Both administration routes resulted in enhanced wound closure by epithelialisation when compared to the NaCl control group. Wounds can close by two mechanisms, contraction and epithelialisation. Contraction occurs predominately as a rapid repair mechanism, whereas epithelialisation takes longer and is closer to regeneration. The enhancement of wound closure by epithelialisation rather than contraction is of clinical relevance as it can have a significant impact on the quality of the scar by decreasing scar retraction. Wound healing of full-thickness wounds occurs via a repair mechanism through the replacement of the damaged tissue with connective tissue, ultimately forming a scar where the tissue used to be. This process is faster than healing through regeneration.[9] A balance in wound contraction is needed as insufficient wound contraction can lead to non-healing wounds and excessive wound contraction can lead to scarring.[35] Furthermore, enhancement of wound closure by epithelialisation may be indicative of wound repair via regeneration rather than scarring. To fully understand how the dynamics of contraction vs epithelialisation influences scarring, more in-depth analysis of the wound, the granulation tissue and the scar is needed. However, this was not part of the scope for this chapter and is an avenue that can be further explored in future studies or analysis. The rate of wound closure was enhanced at day 10 with local ASC administration compared to systemic administration leading to earlier wound closure. The NaCl control group showed an initial trend of smaller wound size than either of the ASC treated groups until day 10 when the dynamics changed, and the wound closure rate slowed down. This could be explained by the observation of wound closure being favoured by contraction, which occurs more rapidly, in the NaCl control group. Around day 10 the wound should be in the proliferative stage of wound repair. During this phase, different cells within the wound such as epithelial cells, start to proliferate and help with epithelialisation of the wound as well as the formation of the ECM.[204] It could thus be inferred that faster wound closure with ASC treatment resulted from enhancement of epithelialisation as compared to the NaCl control group and that this may have resulted from a change during the proliferative phase of wound repair. Changes in the dynamics of the wound over time when

treated with ASCs will be further investigated using a severe model of wound healing in the next chapter.

A recent review eluded to the fact that studies investigating exogenous MSC biodistribution rarely include assessment of their therapeutic efficacy, and vice versa.[205] The animal model used in this study attempted to investigate both the biodistribution and the effect of ASCs exogenously administered. The observed enhancement of wound closure time along with the lack of ASCs at the wound site when systemically administered suggests an indirect effect of ASCs, probably via a secretory mechanism. This confirms findings from a study who found that intravenous human MSCs improved myocardial infarction in mice without significant engraftment. They determined that MSCs had an effect through the secretion of anti-inflammatory protein TSG-6.[206] The mechanism of wound repair by MSCs has been suggested to stem from their paracrine signaling which mobilises the host cells to promote wound repair.[207] Healthy cells are known to release extracellular vesicles that contain different types of molecular cargo, such as RNA, proteins and metabolites. These vesicles are involved in the trafficking of molecules among cells that can regulate physiological functions.[208] The enhanced wound closure time seen with systemic ASC treatment could possibly be explained by the release of exosomes. Exosomes are small extracellular vesicles defined as having a diameter less than 150 nm.[208] Mesenchymal stromal cells are known for their paracrine effect by secreting various factors that can modulate the local environment. Mesenchymal stromal cell-derived extracellular vesicles have been suggested to be partially responsible for this paracrine effect.[209] It has been shown that systemically administered MSC-exosomes attenuated lesion size and improved functional recovery post spinal cord injury.[210] Another study that examined the role of MSC exosomes in wound healing showed that these structures were able to induce proliferation and migration of fibroblasts as well as enhance angiogenesis *in vitro*.[211] In an *in vitro* skin lesion model, the addition of ASC-derived exosomes was found to promote cell proliferation, migration and inhibit cell apoptosis, thereby improving cutaneous wound healing through Wnt/β-catenin signalling.[212]

This study confirms that systemically injected ASCs were able to enhance wound closure despite showing intra-pulmonary trapping and limited homing to the wound site. Evidence of the migration of locally injected ASCs into the wound bed is also provided. Clinical studies using ASCs for cutaneous non-healing/chronic wounds are still limited. Instead, animal models are used. The local administration of ASCs for wound repair is favored and is being evaluated for various injuries with/without scaffolds in animal studies of tendon repair,[213-215] cutaneous non-healing wounds, [216-222] burn injuries,[223] spinal cord injuries,[224, 225] and for bone defects,[226] amongst other indications.

A limitation of this work could be the underestimation of ASC homing and engraftment because of the detection techniques and experimental setup. Although BLI allows for *in vivo* tracking, luminescence in very deep organs cannot be detected. Also, single cell detection is not possible and requires enough cells to emit luminescence to become detectable. To overcome this, we included GFP staining to detect ASCs at a single cell level at the wound site and in non-target organs. However, the lack of GFP positive staining in non-target organs confirmed the absence of luminescence observed by BLI. The animal model used could also have influenced the experimental outcome, as Wistar rats are outbred and thus the ASCs administered were more isogenic in nature than autologous. This could have led to the enhancement of wound closure time we saw as the 'foreign' ASCs might have primed the immune system and enabled a faster response and healing effect. In future studies, the use of alterative systemic routes to overcome the pulmonary first-pass effect, such as IA, or treatment to prevent such filtering e.g. by vasodilation, should be considered.[200] Another avenue to explore is the repeated administration of systemic ASCs. Fischer and colleagues hypothesised that the increase in pulmonary passage seen with their study was due to saturation of receptors during the first treatment, allowing more cells to pass the vasculature with the second treatment.[201] For local administration, the use of scaffolds or dressings could enable longer viability and more directed administration of ASCs into the wound bed.

3.5   CONCLUSION

This study demonstrated that although the survival and homing of systemically administered ASCs was limited, this nonetheless led to enhanced wound repair. Locally administered ASCs survived for 7 days at the transplantation site. They showed the ability to migrate within the wound bed, effectively enhancing wound repair by significantly reducing wound closure time. This data supports the use of ASCs in wound management since physiological wound repair is generally considered to be a naturally effective process with little margin for improvement.

CHAPTER 4. THE EFFECT OF ASCs ON WOUND REPAIR UNDER PATHOLOGICAL CONDITIONS

4.1 INTRODUCTION

Cutaneous wound healing is a physiological process that initiates mechanisms upon injury to limit damage, induce repair and to enable fast wound closure and recovery. It involves the interaction of soluble mediators, signalling molecules (such as cytokines and chemokines), ECM components and a variety of infiltrating and resident cells.[14, 15, 30] Normal wound repair is described as four phases; haemostasis, inflammation, proliferation, and remodelling/ maturation, that are necessary for efficient reconstitution of the cutaneous barrier.[81, 84] Dysregulation of this process will cause prolonged healing, excessive scarring, and can lead to non-healing and chronic wounds. Chronic wounds are identified as wounds that do not proceed to heal within three months, and generally result from complications of other diseases. Major risk factors to the development of chronic wounds are malnutrition, cancer, ischemia (caused by venous or arterial insufficiency), systemic inflammatory disease and diabetes mellitus.[13] In contrast to acute wounds, chronic wounds are characterised by persistent inflammation along with impaired ECM synthesis and neo-vascularisation, preventing the wound from progressing through the normal healing stages.[30]

The treatment of chronic wounds remains a significant clinical challenge. Conventional therapeutic approaches often do not produce satisfying results, leaving patients exposed to a high risk of infection and amputation. Surgical interventions, skin grafts and wound dressings have limited impact as they do not resolve the underlying cause of the chronic state. There is a need to understand why wound healing is impaired and then try to correct it. For example, if hypoxia is the underlying cause, then treatment to improve vascularisation, such as with HBOT, will improve healing. Another underlying cause, a chronic state of inflammation, could be resolved by treatment with anti-inflammatory factors, growth factors and stromal/stem cells. Combinational treatment approaches utilising conventional with newer technology such as wound dressings containing growth factors or stromal/stem cells may be the answer.[56] Due to

the complex aetiology of such wounds, diverse approaches are often needed to improve the healing process, placing a heavy burden on the health care system.[13, 227] There is still a great need for effective therapeutic options for treating chronic wounds. Interest has arisen in the use of cellular therapy to treat chronic wounds.[8, 228-230] The use of MSCs has gained momentum as a potential therapeutic option.[7]

Upon wounding, endogenous MSCs (from the bone marrow, adipose tissue and in the skin) become activated and are recruited to the site of injury where they can help with the repair process.[83] In an *in vivo* model, mice that underwent a femoral osteotomy were implanted with a scaffold containing TGFβ, and enhanced recruitment of endogenous MSCs to the bone defect compared to scaffold alone was reported.[231] However, the microenvironment of chronic wounds can impair MSC proliferation and migration.[232] Oxygen and its reactive species play an important role in the transcription machinery required for MSC differentiation. Chronic inflammation which is associated with high levels of oxidative stress is thought to lead to MSC cell cycle arrest.[134] *In vitro* differentiation capacity of MSCs has been shown to decrease in prolonged hypoxic culture conditions when compared to normoxic conditions.[148] Diabetes *per se* also seems to impair the recruitment of MSCs.[39] Mesenchymal stromal cells derived from diabetic rat adipose tissue and bone marrow show reduced proliferation, differentiation and migration potential.[128] Under such conditions, the exogenous administration of MSCs, which have not yet been affected by the prolonged chronic environment in the wound, could replace or activate these dysfunctional resident MSCs.

Mesenchymal stromal cells are believed to play a role in the wound's ability to progress beyond the inflammatory phase by decreasing pro-inflammatory cytokine secretion and increasing the production of anti-inflammatory cytokines.[85] Systemic administration of MSC-exosomes attenuated cellular apoptosis, decreased levels of pro-inflammatory cytokines (TNFα and IL-1β), increased the level of the anti-inflammatory protein IL-10 and also promoted functional recovery of rats with spinal cord injury.[210] Another study using subcutaneous injection of ASCs in diabetic rats with dorsal full-thickness wounds showed enhancement of wound healing through paracrine

mechanisms.[140] It has been proposed that MSC paracrine signalling is the primary mechanism for the beneficial effects of MSCs in wound healing.[139] In response to inflammatory cues released as a result of an injury, MSCs produce crucial growth factors promoting wound repair by increasing fibroblast, epithelial and endothelial cell division.[83] Mesenchymal stromal cells seem to play a primordial role in wound neo-vascularisation as they promote proliferation and migration, of endothelial cells and show differentiation into vessel forming endothelial cells *in vitro*.[105] Although some pre-clinical and clinical studies using MSCs to enhance wound repair have shown positive outcomes,[187,73] the benefit of MSC administration for wound healing has not yet been clearly established, especially using ASCs. Interestingly, even though subcutaneous adipose tissue is a promising and cost-effective source of autologous MSCs, the majority of studies to date have been performed by using BM-MSCs.

Research into understanding the complex process of wound healing and linking this to the clinical reality is difficult. Variability in wounds such as size, depth, history of wound care and underlying disease, makes it hard to draw comparisons between patients. Instead, animal models provide a platform where the variability between wounds can be eliminated, allowing for research variables to be assessed in a more structured and reproducible manner. Rats are an excellent model to investigate wound healing as they allow for the standardisation of the type, size, shape and depth of the wound.[233] Unfortunately, no single animal model perfectly mimics human wound healing. Rodent models are criticised because they mainly heal by contraction, whereas human wounds heal by re-epithelialisation, contraction and granulation tissue formation. Although the splinted excisional wound model in mice is widely used as the confounding factor of wound healing through contraction is minimised, it does not perfectly mimic ischemic wounds.[234] In this study the previously developed animal model from our research laboratory was used to investigate wound healing under pathological conditions of hyperglycaemia and ischemia.[235-237] Hyperglycaemia was induced by streptozotocin (STZ) as this was an established method in the laboratory. This model was developed to recapitulate delayed healing found in the wounds of diabetic patients with ischemic limbs. It makes use of standardised full-thickness wounds on the dorsal aspect of rodent hind feet in hyperglycaemic animals. Furthermore, this

model has optimised the induction of ischemia in the hind limb to mimic the ischemic conditions of diabetic wounds. This model also allows for the broadest assessment of wound healing mechanisms such as epithelialisation, granulation tissue formation, scar formation, contraction and angiogenesis.

In the previous chapter it was shown that in a normal wound (normoglycaemic rats with non-ischemic wounds) locally administered ASCs survived for at least 7 days at the transplantation site and migrated within the wound bed, effectively enhancing wound repair as shown by a significant reduction in wound closure time. Although systemic administration of ASCs in the physiological model also enhanced wound closure time without showing engraftment at the injury site, we limited the pathological model to local administration. The pathological model requires the femoral artery to be resected, causing a reduction in blood flow to induce ischemia. We thought that the loss of blood flow may have impeded the effect of systemically administered ASCs and thus chose to first investigate the best treatment (local ASC administration) with the most severe condition (hyperglycaemia and ischemia) to evaluate the effect of ASCs on wound healing. If we only investigated systemic administration and found no effect, then we would not know if this is as a result of the ischemia or the ASCs or the mode of administration. If the outcome of local administration proves to have a beneficial effect on wound repair under pathological conditions, then further investigation to determine whether systemic administration has the same effect would be of interest. However, we felt that inclusion of this experiment in this PhD study would not be appropriate, and that this is something to be further investigated in future studies.

This study aimed to elucidate whether local administration of ASCs improve the healing process under pathological conditions in hyperglycaemic rats with ischemic wounds. To further evaluate the effect of ASCs and the mechanisms involved, neo-vascularisation, collagen deposition, macrophage infiltration and myofibroblast differentiation in the wound were assessed. By understanding the effect of ASC administration, the potential use of ASCs in the context of

delayed healing wounds could be proposed as an alternative treatment if the outcome is favourable.

4.2 MATERIALS AND METHODS

All animal experiments were approved by the local veterinary authority (Direction general de la santé de Genève, refer to Appendix 6 for approval letters).

4.2.1 *In vivo* rat model of wound repair under pathological conditions

The effect of locally administered ASCs on wound repair in hyperglycaemic rats with ischemic wounds was investigated. The study design is shown in Figure 4.1.

4.2.1.1 Animals

Female Wistar rats ≥ 10 weeks old and ≥ 250 g were used (experimental animals, n=72; ASC isolation, n=6). Each treatment group consisted of 36 animals: 24 animals = the basal number required; 12 animals were included to compensate for failure to induce hyperglycaemia and unforeseen animal demise during the experiment. The aim was to have three animals per timepoint, and nine at complete wound closure. Table 4.1 specifies the number of animals successfully included at each timepoint during the study. The animals were fed a standard diet and given water ad libitum. For all procedures, animals were anesthetised by inhalation of 3 to 5% isoflurane.

Table 4.1 Number of animals successfully included in the study

Timepoint	Number of animals	
	ASC treated group	NaCl treated group
72h	3	3
Day 7	4	2
Day 10	3	3
Day 15	3	3
Day 21	2 + 2*	3
Wound closure (WC)	6 + 2*	8
TOTAL	**23**	**22**

*At day 21, two animals' wounds reached complete wound closure. These two animals were therefore included as part of both the day 21 and wound closure timepoint.

4.2.1.2 Induction of hyperglycaemia

Hyperglycaemia was induced as previously described[235] by a single IP injection of STZ (Sigma-Aldrich, MO, USA) two weeks before surgery. A 25 mg/ml solution of STZ was prepared in sterile 0.1 M citrate buffer (pH 4.5) and injected IP at 50 mg/kg body weight. Animals were fasted for 4h before STZ injection. Blood glucose levels were measured from tail venous blood (Accu-Chek Aviva, Roche, Manheim, Germany) a week post STZ administration and again before being operated. Only animals with glucose concentrations >11.1 mmol/L were used in the hyperglycaemic group. The citrate buffer was prepared by mixing 2.5 ml of 0.1 M sodium citrate (Sigma-Aldrich, MO, USA), 2.3 ml of 0.1 M citric acid (Merck, Darmstadt, Germany) and 5.2 ml of distilled water.

4.2.1.3 Induction of ischemia and wounds

Ischemia was induced unilaterally in hyperglycaemic rats as described previously.[235] After shaving, a longitudinal incision was made in the inguinal area and the femoral artery followed down to the saphenous artery and the intervening segment between the two was resected (Figure 4.2). This was only performed in the left hind limb, further referred to as the ischemic limb. The right hind limb was conserved (non-ischemic limb) as bilateral ischemia would be too harsh on the animals. The incision was sutured inside and outside with resorbable suturing thread

(Vicryl 4-0, Ethicon, Johnson and Johnson Int., New Jersey, USA). Wounds on the dorsal aspect of the hind paws were created bilaterally in all animals by removing a full-thickness skin area of 1.2 × 0.8 cm. All surgical procedures were performed under an operating microscope (Superflux 300, Carl Zeiss Vanospot, Zeiss, Germany). Animals received 0.05 mg/kg buprenorphine (Temgesic, 0.3 mg/ml, Reckitt Benckiser AG, Zurich, Switzerland) by subcutaneous (SC) injection before the operation and thereafter every 6 to 8h as well as in the drinking water overnight (2 ml Temgesic, 0.3 mg/ml, diluted in 120 ml drinking water). After 3 days, the buprenorphine was replaced with paracetamol (Dafalgan, 1 tablet, 500 mg per 250 ml, UPSA, Rueil-Malmaison, France) in the drinking water until the end of the experiment. To prevent animals from chewing open their sutures, they were housed individually for 48h and wore homemade Elizabethan collars for up to 72h (Figure 4.3). While wearing the collars, food pellets were softened with water to facilitate food consumption. All animals received a semi-occlusive wound dressing that was changed weekly. The dressings were removed prior to BLI imaging and digital photography and replaced with a new dressing afterwards.

4.2.1.4 Treatment groups

One day after wounding, animals were treated either locally with 2×10^5 Fluc-GFP positive ASCs in total split into two sides of each wound (proximally at the ankle and distally at the toes) in the treated group or locally with NaCl in the control group. To better manage the animals, the study was divided into three experiments, each experiment consisted of 24 animals (12 for the NaCl and 12 for the ASC treatment group). For each experiment, ASCs isolated from two rats were cultured and transduced separately before being pooled for local injection. A total of six rats were used for ASC isolation. Isolation and transduction of ASCs was done as previously described in Chapter 2.

4.2.1.5 *In vivo* detection of administered ASCs by BLI

All ASC treated animals were imaged at 3h by BLI to confirm that ASCs were successfully injected and located at the injection sites. Furthermore, only four animals were imaged at 72h, and d7 to allow for *in vivo* detection of the administered ASCs. Prior to imaging, animals received a single IP injection of firefly D-luciferin potassium salt (150 mg/kg body weight) prepared in PBS. After

20 min, imaging was performed using a Xenogen IVIS® spectrum *in vivo* imaging system with an XGI-8 Gas anaesthesia system. A photographic image of the animal followed by a luminescent image was recorded by the camera. For quantification, two ROI were manually selected to quantify the luminescent signal in the wound area for the right foot (ROI 1) and the left foot (ROI 2). The ROI size was kept constant between animals and the intensity of the luminescent signal was recorded as total flux (average photons per second, p/sec).[173] All images were analysed using Living Image® 4.3.1 software.

4.2.2 <u>Assessment of wound repair</u>

Animals were followed by digital photography and sacrificed for histology and IHC at the following timepoints: 72h, d7, d10, d15, d21 and at wound closure.

4.2.2.1 Effect of ASCs on wound closure time

Wound size reduction over time, the time taken to complete wound closure and the contraction/epithelialisation ratio were assessed as previously described.[196] Wound size was documented immediately after wounding and until wound closure by digital photography with the camera placed at a constant distance and a ruler next to the wound for scaling. The photos were analysed using ImageJ 1.48v software[197] to determine the wound area. At complete wound closure (i.e. full epithelialisation), the surface of the scar with hairless skin was measured and considered to correspond to the area of the wound that had healed by epithelialisation. The surface of the wound that healed by contraction was estimated by subtraction of the epithelialised surface from the original wound area measured at day 0 (Refer to Chapter 3, Figure 3.10C).

4.2.2.2 Assessment of the wound: histology and IHC

For the ASC treated and NaCl control groups, the entire foot with the wound and the surrounding uninjured skin were harvested and fixed in 4% formaldehyde. After fixation, the wound area along with the uninjured surrounding skin was removed from the foot and processed for paraffin
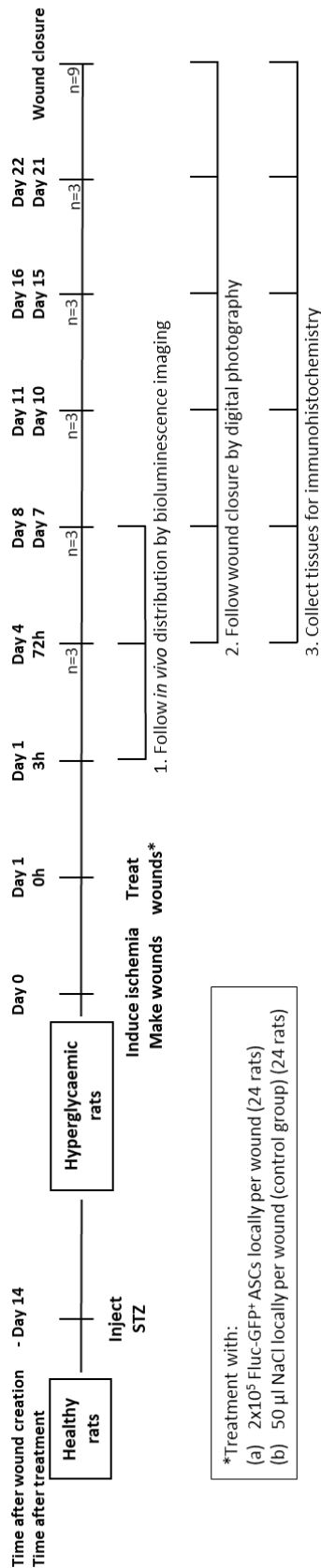
Figure 4.1 Study design.

For the *in vivo* rat model of wound repair under pathological conditions, animals were induced to become hyperglycaemic with a single dose of streptozotocin (50 mg/kg) two weeks before the operation. Ischemia was induced unilaterally (by resection of the femoral artery to the saphenous artery) in hyperglycaemic rats. Wounds on the dorsal aspect of the hind paws were created bilaterally in all animals. One day after wounding, animals were treated with a single injection of 2×10^5 Fluc–GFP positive ASCs in total locally split into two sides of each wound. Control animals received a single injection of NaCl locally. Animals were followed by digital photography and sacrificed for immunohistochemistry at 3h, 72h, d7, d10, d15, d21 and at wound closure (WC). For this model, bioluminescence imaging was only performed at 3h (n=24), 72h (n=4) and d7 (n=4).

embedding (refer to Chapter 3, Figure 3.2A). Haematoxylin/eosin (H/E) staining as well as Masson's trichrome staining and IHC for alpha-smooth muscle actin (αSMA), ionised calcium binding adaptor molecule 1 (Iba1) and GFP were performed on FFPE samples.

For IHC analysis, 5 μm thick transverse tissue sections from FFPE samples were analysed using rabbit anti-GFP, mouse anti-αSMA (monoclonal IgG2a recognising αSMA, clone 1A4,[238] from the research laboratory of Prof Bochaton-Piallat, University of Geneva), and rabbit anti-Iba1 (Wako Chemicals, VA, USA) antibodies. Antigen retrieval was performed for GFP and αSMA in a citrate buffer (pH 6) using the DakoCytomation Pascal pressure cooker (125°C, 30 sec). For Iba1, antigen retrieval was performed in a Tris-EDTA buffer (pH 9) using the BioGenex Microwave EZ-Retriever V-2-2 (Cycle 1: 95°C, 8min; Cycle 2: 100°C, 28 min) (CA, US). After blocking endogenous peroxidases with Dako REAL peroxidase blocking solution, sections were incubated with the primary antibodies diluted at 1/100 (GFP), 1/1000 (αSMA) and 1/750 (Iba1) for 1h at RT, and then with either a rabbit or mouse HRP complex secondary antibody for 30 min at RT. Mouse IgG2 and rabbit IgG isotypic controls were used (Abcam, Cambridge, UK and Dako, Hamburg, Germany). Sections were developed with AEC for 10 min (and counter stained with haematoxylin for 1 to 2 min). Masson's trichrome staining was performed by the Histology platform of the University of Geneva. Sections were scanned using a Zeiss Axio Scan Z1 Brightfield scanner at 20x magnification. All images were processed using Definiens 2.7 software (Munich, Germany). Results were compiled in Microsoft Excel and the graphs plotted using Prism (GraphPad, CA, USA). The ROI was manually defined by drawing around the entire visible granulation tissue. For αSMA staining, blood vessels were manually selected as a second ROI, and excluded when evaluating the presence of myofibroblasts, or selected to analyse vessel formation. The area of positive staining was expressed as a percentage relative to the ROI area. General cellularity was quantified in H/E stained sections by counting the number of nuclei in the manually defined ROI and expressed as cells/mm^2. The expression of collagen was quantified by determining the percentage area staining positive for aniline blue in Masson's trichrome stained sections relative to the ROI area. In the ASC treated group, the location of administered GFP positive ASCs was determined over time as described in Chapter 3, section 3.2.1.3, with some minor modifications.

Briefly, each section from the five different levels for each FFPE sample was divided into two sites, the injection site (the site by the ankle and the toes where the ASCs were injected) and the wound site. The percentage area of GFP staining was recorded at 72h, day 7 and day 10 at the two sites, summing up all the five levels together as a single value per foot.
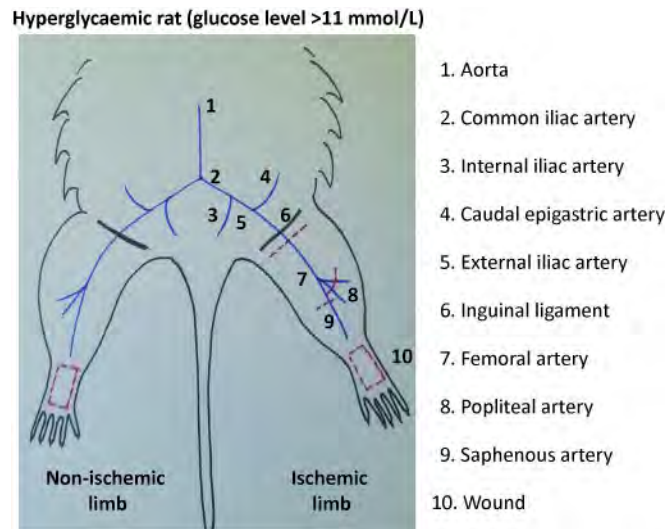
Figure 4.2 Hyperglycaemic and ischemic model.
To create ischemia, the femoral artery, popliteal artery and saphenous artery was resected up to the level of the knee in the left hind limb of hyperglycaemic rats. The right hind limb was conserved and kept as the non-ischemic limb. Full-thickness wounds were created on the dorsal aspect of both hind paws.

Figure 4.3 Elizabethan collar.
A photo of a single experimental animal wearing an Elizabethan collar. The collars were constructed from overhead projector transparency (clear) film and secured with Transpore surgical tape and Velcro.

4.2.3 Statistical analysis

Data are expressed as means ± SD. Statistical analyses were carried out using Prism (GraphPad, CA, USA). A Mann-Whitney test was used to assess differences between data means. Grouped data was assessed by performing multiple t-tests using the Holm-Sidak method. A *P* value of < 0.05 between data means was considered significant.

4.3   RESULTS

4.3.1 Induction of hyperglycaemia and ischemia

Hyperglycaemia was induced by injecting 65 mg/kg STZ three weeks before the operation. This dose was too high, leading to excessive weight loss, very high glucose levels and eventually animal death (these animals were not included in the study). A lower dose of 50 mg/kg two weeks before the operation was therefore used. At this concentration, fewer animal deaths (1 to 2 animals per 12 injected) were observed. However, the success of inducing hyperglycaemia was around 50%. Interventions such as fasting the animals for at least 4h before STZ injection, using animals with a higher initial weight, preparation of smaller volumes of STZ so that it did not lose its activity (stable for 15 min on ice once dissolved in citrate buffer), and being cautious to administer correctly the STZ IP (being careful not to inject into the intestine) led to ≤25% failure to induce hyperglycaemia. Hyperglycaemia was confirmed by having a glucose concentration of >11.1 mmol/L. Before STZ was injected, animals had an average glucose concentration of 7.47 mmol/L. Hyperglycaemic animals had an average glucose concentration of 28.04 mmol/L before being operated on (Table 4.2). Hyperglycaemia was associated with an initial loss in body weight. Comparing the weights of animals before STZ injection and thereafter (prior to being operated on) showed a loss in body weight of 4% in the ASC treated group and 8% in the NaCl treated group. A further loss in body weight was observed after the operation; however, animals started to maintain their body weight 3 to 7 days post treatment and gained a little weight after 15 days (Figure 4.4). No statistically significant differences in weight were observed between the ASC treated and control groups.

None of the operated animals presented with necrosis of the limb after ischemia was induced. Only three animals, from both the control and treated group, presented with a deeper wound on the side of their feet in the ischemic limb next to the full-thickness wound on the dorsal aspect of the feet. This extra wound appeared to have resulted from an infection and failed to heal alongside the main wound on the feet, and thus these animals were excluded from the study. The area where the incision was made to have access to the femoral artery led to some discomfort as animals were inclined to chew open this sutured area. Even with the administration of pain medication, several animals had to be prematurely sacrificed and excluded from the study because they chewed open their entire operated hind limb. Changing the method of suturing as well as the type of suture thread used to close the incision did not prevent this behaviour. Instead animals were given Elizabethan collars to wear for 72h (Figure 4.3). The collars impeded the animals from having unrestricted access to the sutured area. Minor chewing of the lower sutures was still observed, but mostly this did not lead to the incision being chewed open and exposing the whole limb. In cases where this still occurred, if caught early, the incision was re-sutured, and the animals retained in the study, or animals were sacrificed and excluded from the study if this could not be achieved. After ischemia was induced, removal of the full-thickness skin from the dorsal aspect of the ischemic limb resulted in little to no bleeding, whereas bleeding was observed in the non-ischemic limb.

Table 4.2 Average glucose concentration of animals followed until complete wound closure

Treatment group	Average glucose concentration (mmol/L)*	
	Before STZ injection	**After STZ injection (before operation and treatment)**
ASC treated (n=8)	7.44 (± 0.54)	27.10 (± 6.07)
NaCl control (n=8)	7.50 (± 1.22)	28.98 (± 4.43)
Both (n=16)	7.47 (± 0.91)	28.04 (± 5.23)

* The glucose reader could only read values in the range of 1.11 mmol/L to 33.3 mmol/L and readings above this were shown as "HI", thus animals that showed a reading of "HI" were given a value of 34 mmol/L for calculating the average glucose levels.
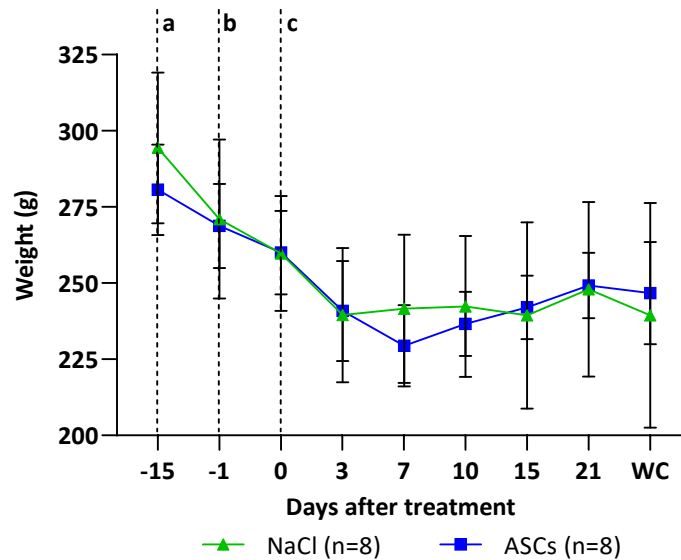
Figure 4.4 Average weight of animals over time.
The weight of animals kept until wound closure (WC) was followed before streptozotocin (STZ) injection, before the operation, and at 3, 7, 10, 15 and 21 days after treatment and at WC. Weights are plotted for the NaCl control (n=8) and ASC treated group (n=8). (a) Two weeks before the operation STZ was injected; (b) During the operation ischemia was induced, and wounds were created; and (c) One day after the operation, wounds were treated with either NaCl or ASCs.

4.3.2 *In vivo* detection of administered ASCs by BLI

All animals from the ASC treated group were imaged by BLI to confirm whether locally administered ASCs were located at the injection sites 3h post injection. A luminescent signal was detectable in all treated animals; however, variability in the signal intensity was observed between injection sites, feet and different animals. Due to the severity of the animal model, only 4 animals were further followed by BLI at 72h and at day 7 (Figure 4.5). The luminescent signal was detectable at the injection sites at all timepoints (Figure 4.5A). Quantification of the luminescent signal showed variability between animals and timepoints as represented by large error bars, and no statistically significant difference in luminescence was found between the non-ischemic and ischemic feet at any of the timepoints (Figure 4.5B). This confirmed that administered ASCs remained viable and present at the injection sites for at least 7 days post administration.
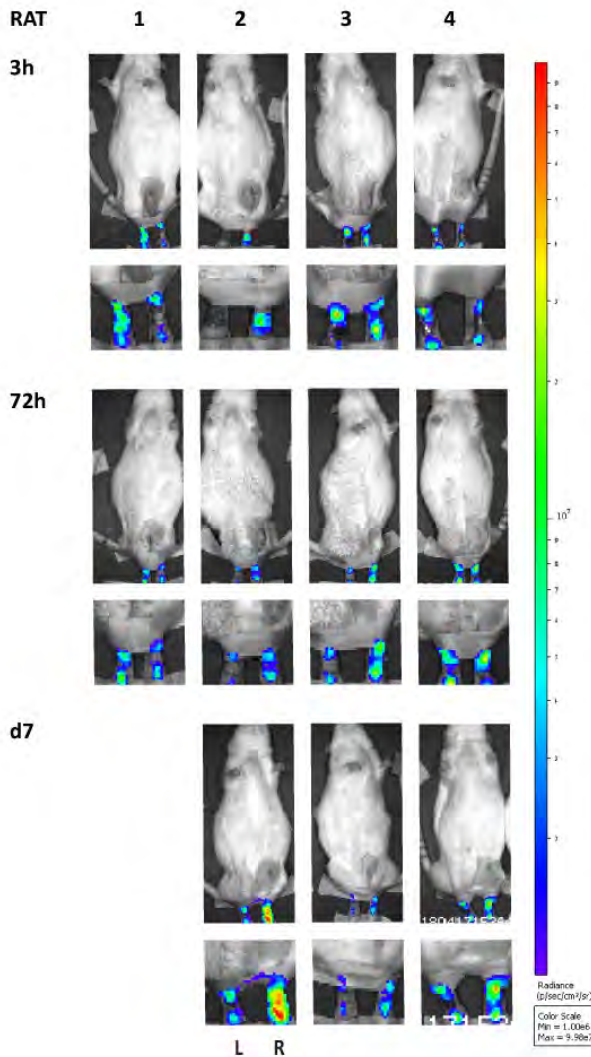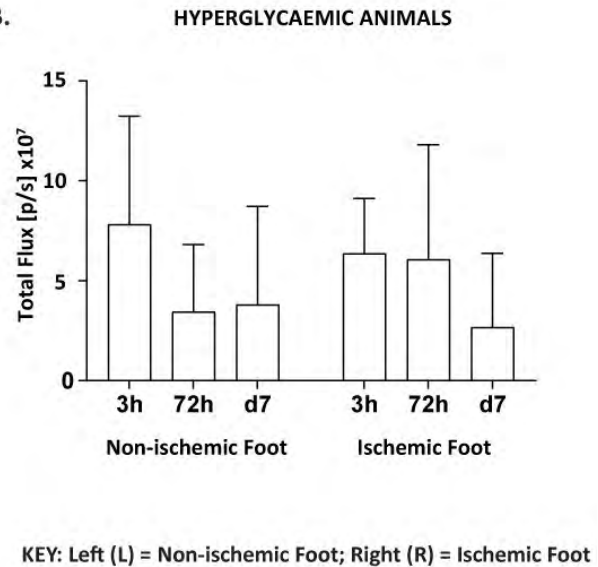
Figure 4.5 *In vivo* tracking of locally administered Fluc-GFP+ ASCs during wound repair under pathological conditions.

ASCs transduced to express both Fluc and GFP were injected locally (2 x 10^5 ASCs) into two sides around each wound in hyperglycaemic rats 24h after ischemia was induced in the left hind limb, and full-thickness wounds were created bilaterally on the dorsal aspect of both feet. Prior to imaging, animals received 150 mg/kg body weight of D-luciferin. (A) ASC treated animals followed by BLI at 3h, 72h and day 7 (d7). (B) The luminescent signal in the non-ischemic and ischemic feet of ASC treated animals was quantified and recorded as total flux over time. Data shown as mean ± SD (n=4 at 3h and 72h and n=3 at d7).

4.3.3 ASC administration led to enhanced wound closure time

The effect of ASC administration on wound closure time was assessed in hyperglycaemic animals with ischemic and non-ischemic wounds. In ischemic wounds, in comparison to a total wound

closure time of 35 days in the NaCl control group, wound closure was more rapid when treated with ASCs (26 days, p=0.0329) (Figure 4.6A). In non-ischemic wounds, in comparison to a total wound closure time of 31 days in the NaCl control group, wound closure was more rapid when treated with ASCs (22 days, p=0.0107) (Figure 4.7A). Both ischemic and non-ischemic wounds when treated with ASCs showed an enhancement of wound closure of 9 days compared to NaCl control wounds. Ischemia delayed wound closure time by 4 days compared to non-ischemic wounds in both treatment groups. After wound creation, the wound size was followed and recorded over time as wound area (percentage, as normalised to the wound on day 0). Wounds treated with ASCs showed a tendency to enlarge after 3 days before reducing in size (Figure 4.6B, 4.7B). In ischemic wounds, wound size was reduced in the ASC treated group compared to NaCl control group from day 10, with a significant difference in wound size observed at day 15 (p=0.0289) (Figure 4.6B). In non-ischemic wounds, no significant difference in wound size between ASC treated and NaCl control group was observed. However, the wounds from the ASC treated group appeared smaller than the NaCl control group from day 15 (Figure 4.7B). Further investigation into whether wound closure was favoured more by contraction or epithelialisation showed no significant difference in the contraction vs epithelialisation ratio between the ASC and NaCl groups in ischemic (p=0.4418) (Figure 4.6C) or non-ischemic (p=0.5737) (Figure 4.7C) wounds. A closer look into the difference in the contraction vs epithelialisation ratio in each treatment group revealed that in ischemic wounds treated with NaCl, epithelialisation (59%) was significantly favoured over contraction (41%, p=0.0011) (Figure 4.6Di). No significant difference (p=0.0830) was observed between contraction and epithelialisation in ischemic wounds treated with ASCs; however, the percentage closed by contraction was lower, 43%, compared to 57% for epithelialisation (Figure 4.6Dii). In non-ischemic wounds treated with NaCl, contraction (55%) was significantly favoured over epithelialisation (45%, p=0.0104) (Figure 4.7Di). Non-ischemic wounds treated with ASCs on the other hand closed 50% by contraction and 50% by epithelialisation (p=0.9591) (Figure 4.7Dii).
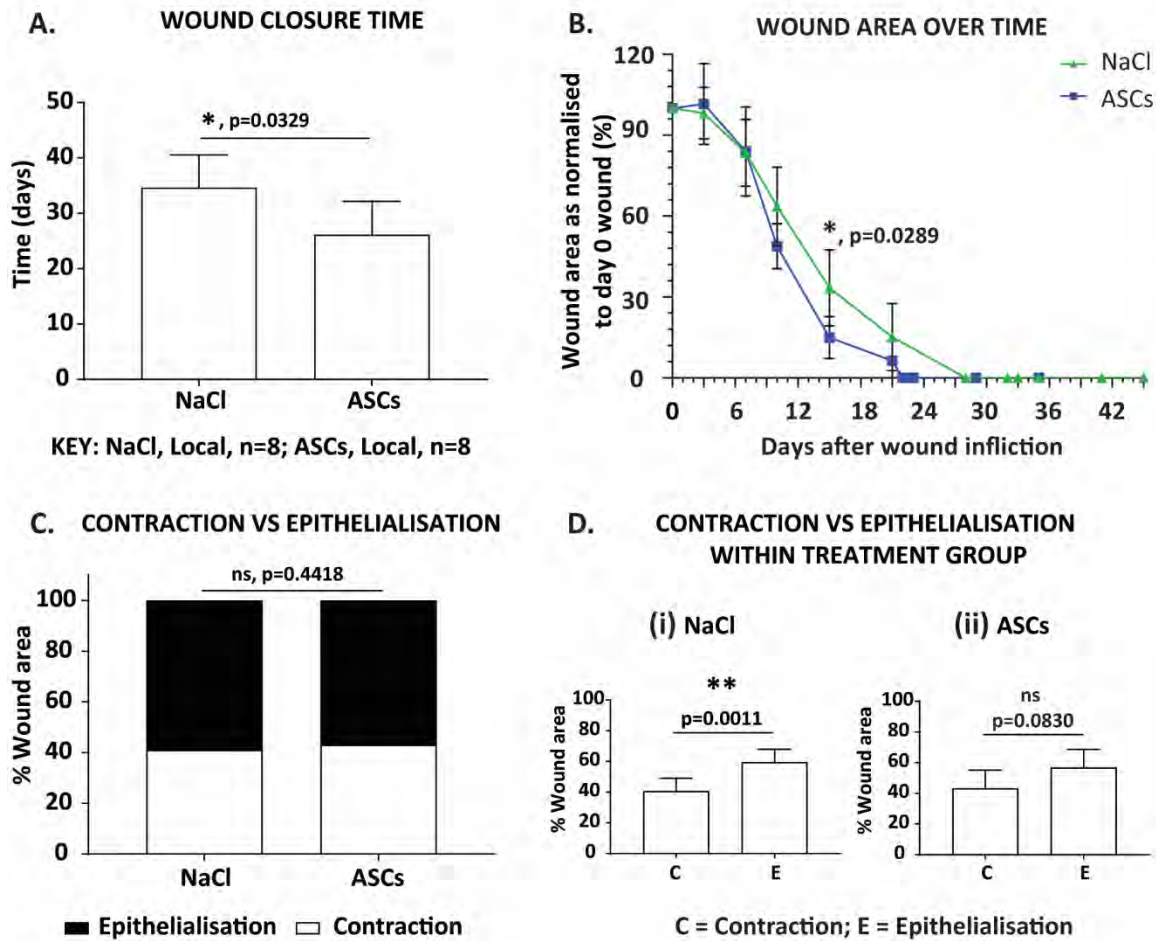
Figure 4.6 Wound closure assessment in ischemic hind limb treated with NaCl and ASCs.
Ischemic limbs of hyperglycaemic animals were treated with NaCl or with Fluc-GFP+ ASCs (2 x 10^5 ASCs) locally into two sides around each wound. (A) Time taken for complete wound closure after treatment. (B) Wound area over time after treatment as normalised to the original wound area on day 0. (C) Wound area closed by contraction and by epithelialisation. (D) Comparing the wound area closed by contraction versus epithelialisation within each treatment group. Data shown as mean ± SD. Significance is shown where *p<0.05, **p<0.01.
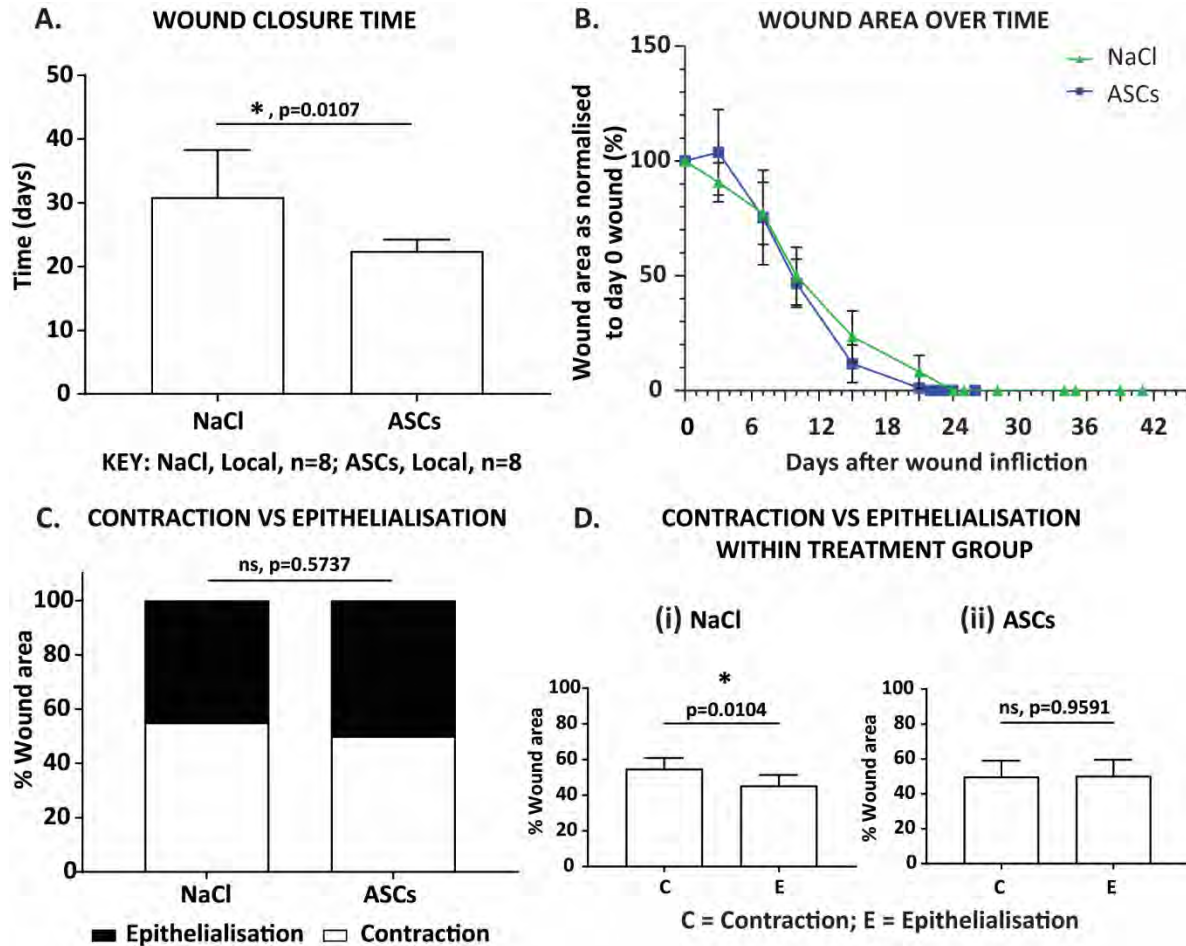
Figure 4.7 Wound closure assessment in non-ischemic hind limb treated with NaCl and ASCs.
Non-ischemic limbs of hyperglycaemic animals were treated with NaCl or with Fluc-GFP+ ASCs (2 x 10^5 ASCs) locally into two sides around each wound. (A) Time taken for complete wound closure after treatment. (B) Wound area over time after treatment as normalised to the original wound area on day 0. (C) Wound area closed by contraction and by epithelialisation. (D) Comparing the wound area closed by contraction versus epithelialisation within each treatment group. Data shown as mean ± SD. Significance is shown where *p<0.05.

4.3.4 Assessment of ischemic wounds

To understand the effect of ASC treatment on the histology of the wound, we decided to evaluate the more severe wound. Thus, only ischemic wounds were further assessed by histological staining for Masson's trichrome and H/E and by IHC to detect αSMA, Iba1, and GFP.

4.3.4.1 ASC administration affects myofibroblast differentiation

Sections from ischemic wounds in hyperglycaemic animals were stained with anti-αSMA to assess whether treatment with ASCs affected myofibroblast phenotypic expression. Computer assisted quantification within the granulation tissue of the wounds revealed that myofibroblasts were already identifiable at 72h in ASC treated animals at a significantly higher percentage (0.24% αSMA, p=0.028) than in the NaCl control animals (0.05% αSMA) where they were barely present (Figure 4.8A). The wounds evaluated at complete wound closure also showed significantly more myofibroblasts at wound closure in ASC treated (2.56% αSMA, p=0.0430) compared to NaCl control treated (1.06% αSMA) wounds. The highest expression of αSMA in the ASC treated wounds was found at day 15 (3.37% αSMA). Both the NaCl control and ASC treated group had more αSMA expression at wound closure than at the earlier timepoints at 72h and day 7. At day 15, myofibroblasts were found throughout the granulation tissue (Figure 4.8C, D and Figure 4.9Ai, Bi) in both treatment groups. However, in the ASC group, myofibroblasts were more evenly distributed throughout the granulation tissue (Figure 4.8Ci-ii, 4.9Ai) whereas in the NaCl group they became concentrated under the newly forming epithelium and in the upper part of the granulation tissue (Figure 4.8Di, ii, Figure 4.9Bi). The granulation tissue appeared thicker in height in the ASC treated group compared to the NaCl control group. At day 21, wound size in the ASC treated group (Figure 4.9Aii) was smaller than in the NaCl control group (Figure 4.9Bii) and fewer myofibroblasts were visible than at day 15 (Figure 4.9Ai, Bi).

4.3.4.2 ASC administration did not improve neo-vascularisation

Blood vessels were also identified by αSMA expression and were distinguished and manually selected by their distinct morphology of having a lumen and the walls of the vessels staining strongly for this marker. No significant difference in the percentage vessels was identified between the NaCl control and ASC treated group (Figure 4.8B). The percentage vessels at the different timepoints was distributed as a Gaussian curve. At 72h and day 7, fewer vessels were seen, with an increase at day 10, 15 and 21, and then decreasing again at wound closure in both the NaCl control and ASC treated group. However, the percentage vessels at wound closure (NaCl: 2.56%; ASC: 1.70%) remained higher than at 72h (NaCl: 0.96%; ASC: 1.48%) and day 7

(NaCl: 1.40%; ASC: 1.01%) (Figure 4.8B). The vessels were distributed not only under the new epithelium but also throughout the granulation tissue (Figure 4.8C and D) in both groups. Many vessels were located under the newly formed epithelium between the folds.

4.3.4.3 ASC administration did not influence macrophage infiltration into the granulation tissue

Macrophages within the granulation tissue were detected by staining with anti-Iba1, a macrophage-specific-calcium binding protein used to label macrophages. Similar patterns in the expression of Iba1 were observed in the ASC treated and NaCl control group. Macrophages were predominately present at day 7 in both groups (Figure 4.10A) in high numbers (25.65% in NaCl and 22.52% in ASC group) and were significantly greater in number than at wound closure (13.08%, p=0.0009) within the NaCl group and at day 21 (16.89%, p=0.0286) and wound closure (10.60%, p=0.0061) in the ASC group. The macrophages were distributed throughout the whole tissue section in both groups (Figure 4.10Bi-ii and Ci-ii, and Figure 4.11Ai-ii and Bi-ii); however, they were more concentrated within the granulation tissue. Fewer macrophages were visible on day 21 than on day 15 (Figure 4.11Aii and Bii).

4.3.5 <u>Collagen deposition increased with time in both the ASC treated and NaCl control group</u>

Masson's trichrome staining was used to identify collagen deposition within the granulation tissue by quantification of the area stained for aniline blue. No significant differences were found in collagen deposition between NaCl control and ASC treated wounds. In both groups, an increase in collagen was detected with time. Significantly more collagen was present at wound closure (NaCl: 37.38%, ASC: 36.05%) compared to 72h, day 7, 10 and 15 in the NaCl and ASC groups (Figure 4.12A). A closer look at the histology images at day 15 (Figure 4.12Bi-ii and Ci-ii, Figure 4.13 Ai and Bi) shows fine collagen strands appearing throughout the granulation tissue. More collagen was observed at day 21 (Figure 4.13Aii and Bii) compared to day 15 (Figure 4.13Ai and Bi). There appeared to be an increase in the percentage of staining for collagen at d15 (NaCl: 8.29%; ASC: 13.55%) and day 21 (NaCl: 19.28%; 30.57%) in the ASC group compared to the NaCl group; however, the differences were not found to be statistically significant.
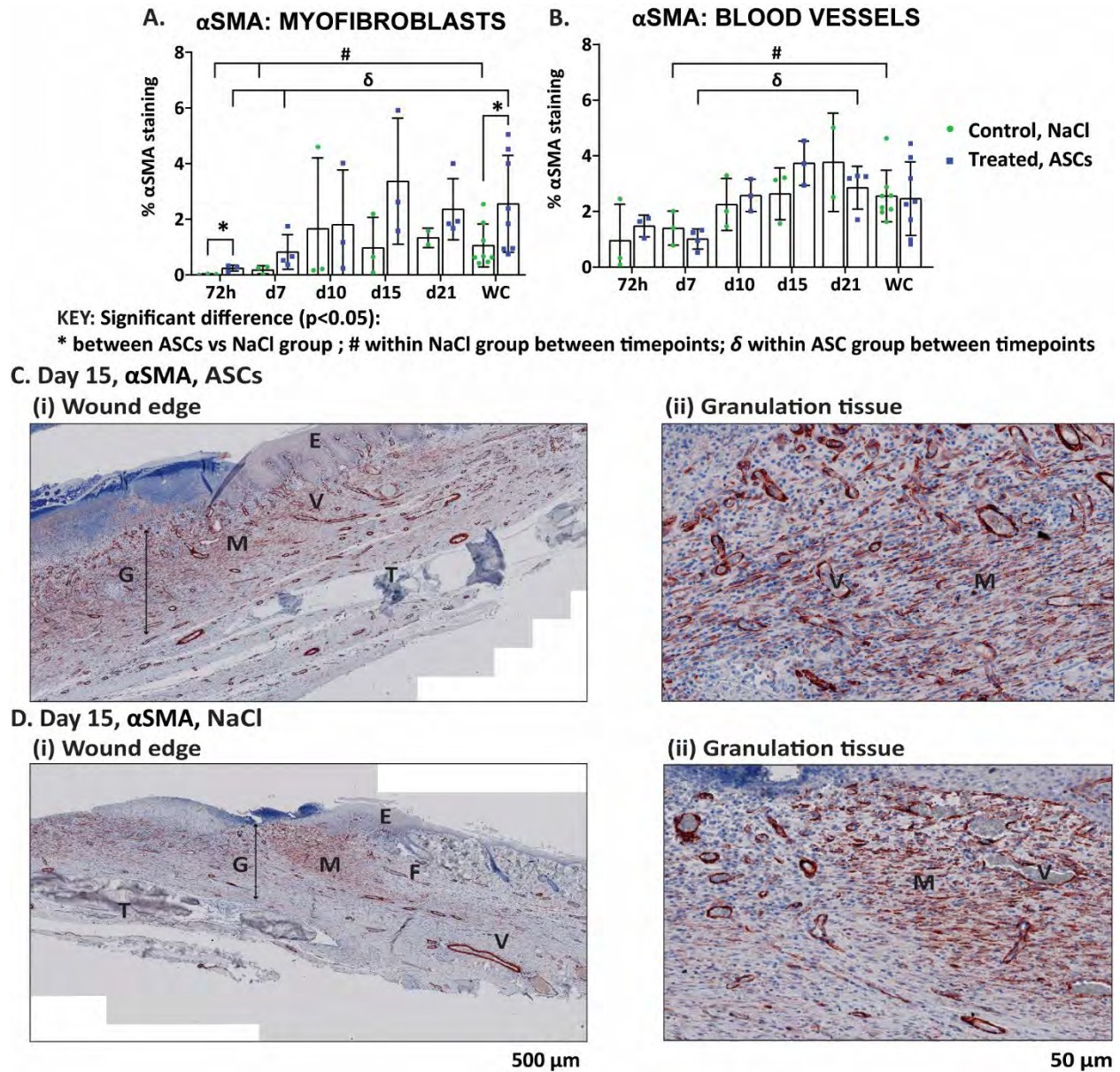
Figure 4.8 Quantification of αSMA expression to detect myofibroblasts and blood vessels.
Results of computer assisted marker quantification within granulation tissue at 72h, day 7 (d7), d10, d15, d21 and at wound closure (WC) in hyperglycaemic animals with ischemic wounds treated with either ASCs or NaCl. Vessels were manually selected as a second ROI and excluded when evaluating the presence of (A) myofibroblasts or selected to analyse (B) blood vessel formation. The area of positive staining (red staining, AEC) was expressed as a percentage relative to the area of the granulation tissue. A representative view of a cross section through the wounds at day 15 in (C) ASC and (D) NaCl treated animals. (i) A magnified view of the wound edge and (ii) granulation tissue. G= granulation tissue, T= tendons, F= hair follicle, V= blood vessel and M= myofibroblasts. Data shown as mean ± SD. Significance is shown where p<0.05: * between ASC and NaCl group, # within NaCl group between timepoints and δ within ASC group between timepoints.

A. αSMA, ASCs
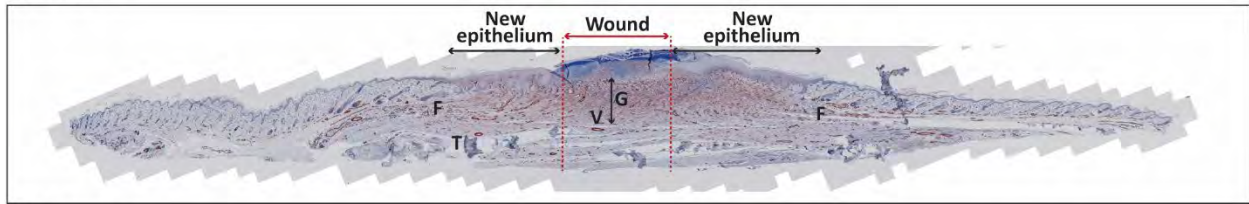
(i) Day 15

(ii) Day 21
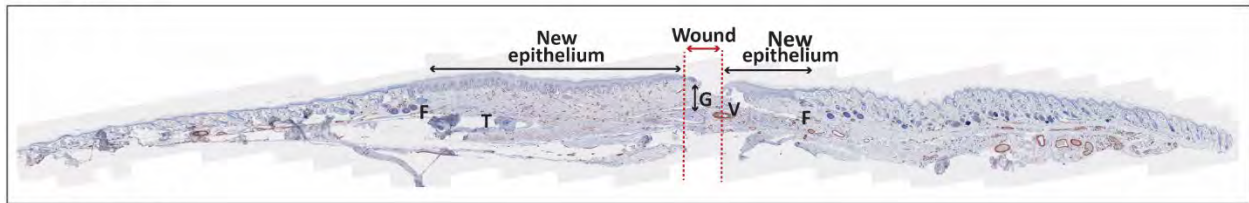
B. αSMA, NaCl

(i) Day 15

(ii) Day 21

2000 μm
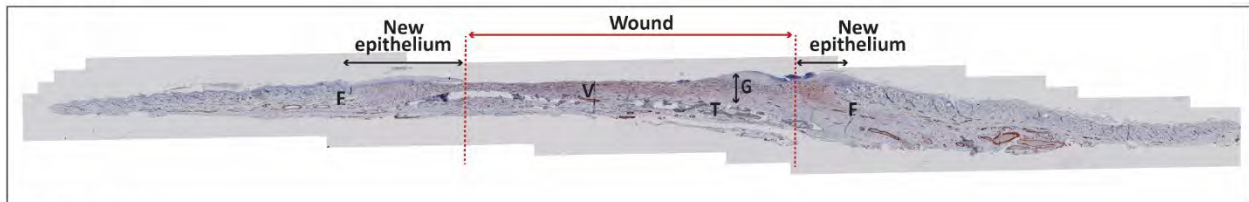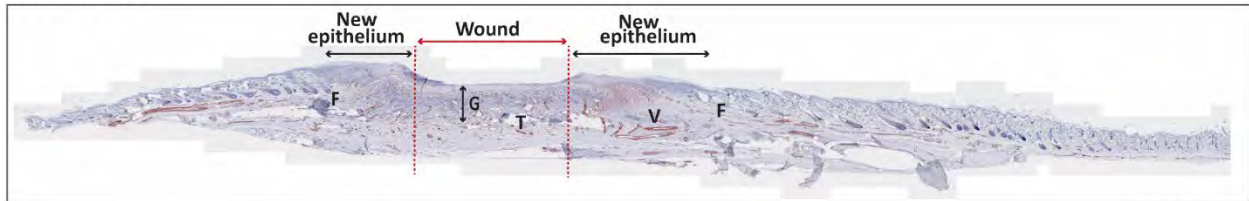
Figure 4.9 αSMA expression at day 15 and 21 to detect myofibroblasts and blood vessels.
View of a cross section through the wounds showing a complete section of animals treated with (A) ASCs and (B) NaCl sacrificed on (i) day 15 and (ii) 21 stained for αSMA (red staining, AEC). The open wound area and the newly formed epithelium is shown. G= granulation tissue, T= tendons, F= hair follicle and V= blood vessel.

4.3.5.1 ASC administration led to enhanced wound cellularity

Overall wound cellularity was evaluated by quantification of cell nucleus counts within the granulation tissue. The administration of ASCs significantly increased wound cellularity compared to the NaCl control group at day 7 (NaCl: 3899 cells per mm^2; ASCs: 10023 cells per mm^2; p=0.0322), day 10 (NaCl: 3596 cells per mm^2; ASCs: 12371 cells per mm^2; p=0.0049), day 15 (NaCl: 3931 cells per mm^2; ASCs: 10982 cells per mm^2; p=0.0002), day 21 (NaCl: 3848 cells per mm^2; ASCs: 6886 cells per mm^2; p=0.0353), and at wound closure (NaCl: 2153 cells per mm^2; ASCs: 7249 cells per mm^2; p=0.0008) (Figure 4.14A). The histology images of the wound edge and granulation tissue (Figure 4.14B and C) show the presence of many cells. However, cells appeared denser in the ASC group compared to the NaCl group (Figure 4.14B(ii) and C(ii), and Figure 4.15). Within the NaCl group a significant reduction in cellularity was observed from day 21 to wound closure (d21: 3848 cells per mm^2; WC: 2152 cells per mm^2; p=0.0485). Within the ASC group, a significant reduction in cellularity was also observed at wound closure compared to day 10 (WC: 7249 cells per mm^2; d10: 12371 cells per mm^2; p=0.0061). A reduction in cell counts in both groups at wound closure was expected due to the wounds already being closed. Once wounds close, they will move into the remodelling phase of the healing process which is known to be associated with cell apoptosis.

4.3.5.2 GFP positive ASCs remained detectable 10 days post administration

Green fluorescent protein positive ASCs remained detectable not only at the injection sites but also within the wound (Figure 4.16A-B). Adipose-derived stromal cells were found migrating into the wound from the injection site at 72h, day 7 and 10. At 72h, the migrating ASCs can be seen at the wound edge as well as in the granulation tissue (Figure 4.16Bi-iii).

A. Iba1: MACROPHAGES

KEY: Significant difference (p<0.05):
* between ASCs vs NaCl group
# within NaCl group between timepoints
δ within ASC group between timepoints

● Control, NaCl ■ Treated, ASCs

B. Day 15, Iba1 ASCs

(i) Wound edge

(ii) Granulation tissue

C. Day 15, Iba1, NaCl

(i) Wound edge

(ii) Granulation tissue

500 µm

100 µm
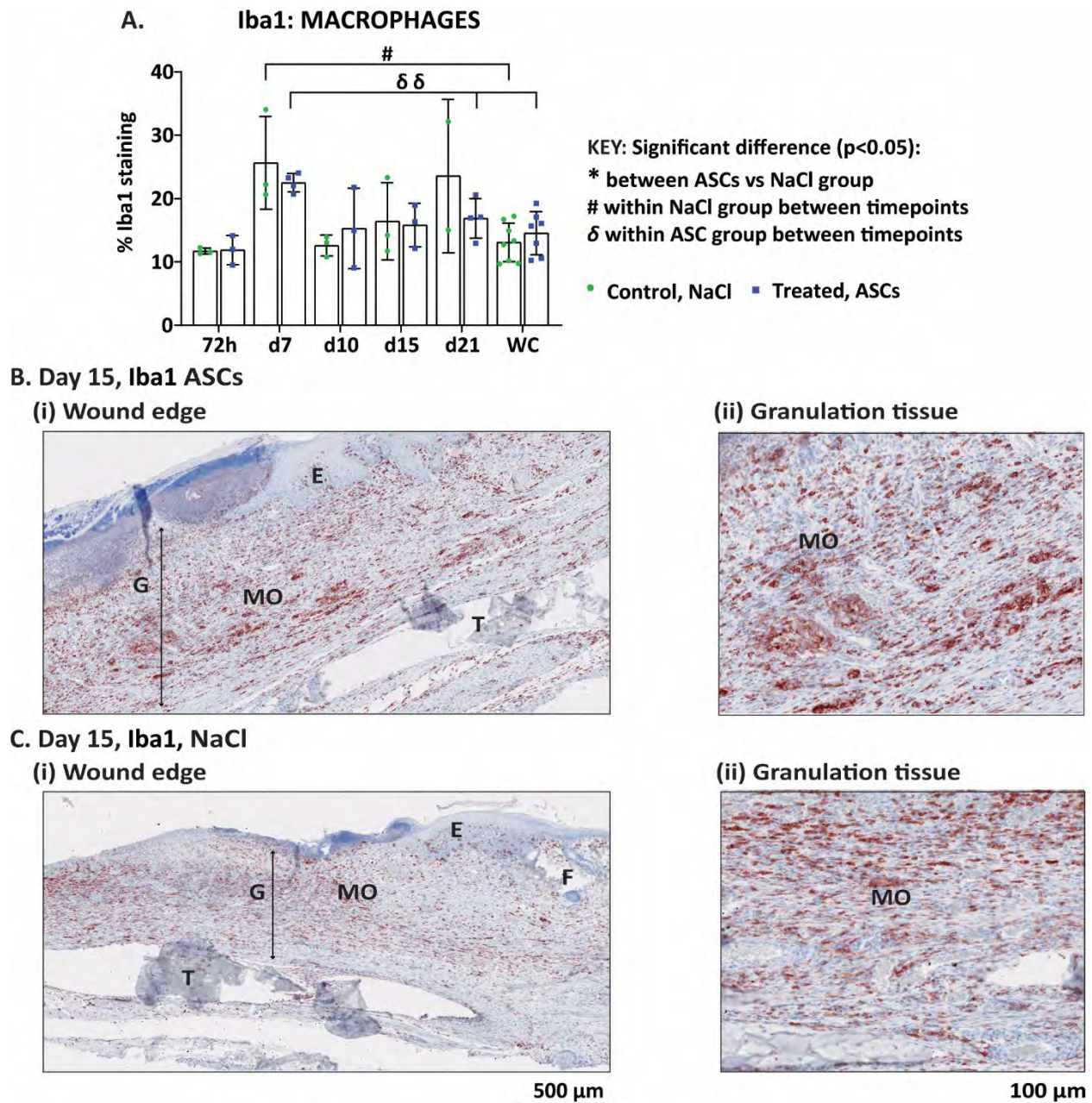
Figure 4.10 Quantification of Iba1 to detect macrophages.

Results of computer assisted marker quantification within the granulation tissue at 72h, day 7 (d7), d10, d15, d21 and at wound closure (WC) in hyperglycaemic animals with ischemic wounds treated with either ASCs or NaCl. (A) The area of positive staining for Iba1 (red staining, AEC) was expressed as a percentage relative to the area of the granulation tissue. A representative view of a cross section through the wounds at day 15 in (B) ASC and (C) NaCl treated animals. (i) A magnified view of the wound edge and (ii) granulation tissue. G= granulation tissue, T= tendons, F= hair follicle, V= blood vessel and MO= macrophages. Data shown as mean ± SD. Significance is shown where p<0.05: * between ASC and NaCl group, # within NaCl group between timepoints and δ within ASC group between timepoints.

A. Iba1, ASCs

(i) Day 15
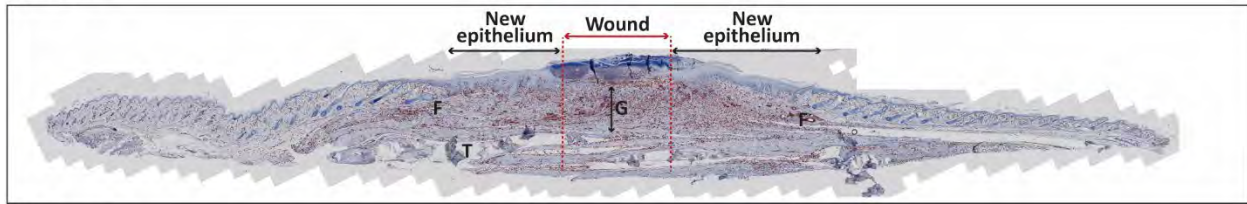
(ii) Day 21
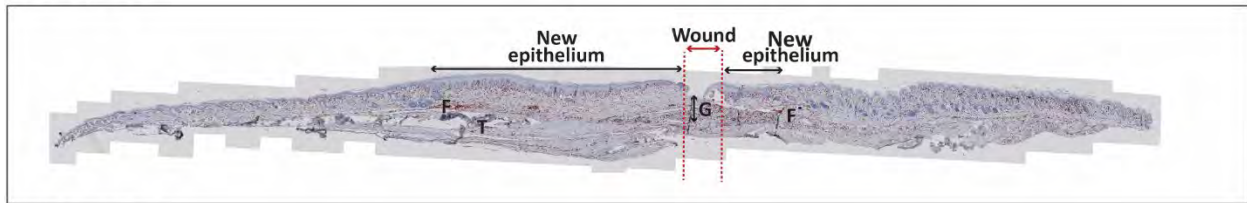
B. Iba1, NaCl

(i) Day 15

(ii) Day 21
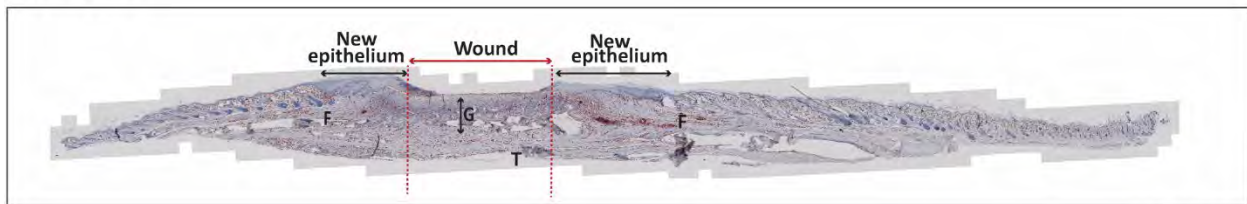
2000 µm

Figure 4.11 Iba1 expression at day 15 and 21 to detect macrophages.
A representative view of a cross section through the wounds showing a complete section of animals treated with (A) ASCs and (B) NaCl sacrificed on (i) day 15 and (ii) 21 stained for Iba1 (red staining, AEC). The open wound area and the newly formed epithelium is shown. G= granulation tissue, T= tendons and F= hair follicle.
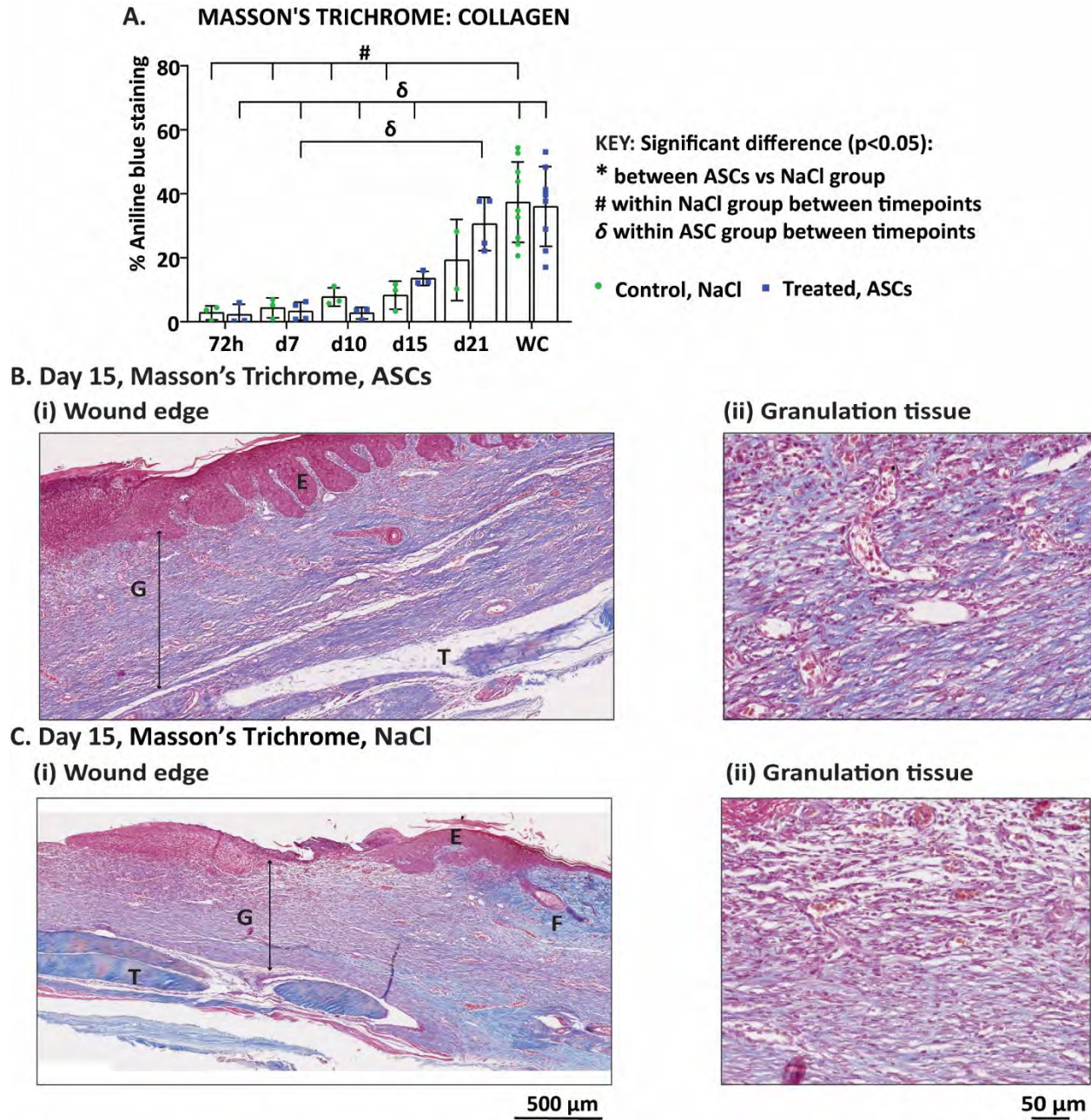
Figure 4.12 Quantification of aniline blue in Masson's trichrome staining to detect collagen.
Results of computer assisted marker quantification within the granulation tissue at 72h, day 7 (d7), d10, d15, d21 and at wound closure (WC) in hyperglycaemic animals with ischemic wounds treated with either ASCs or NaCl. (A) The area of positive staining for aniline blue in Masson's trichrome (blue staining) was expressed as a percentage relative to the area of the granulation tissue. A representative view of a cross section through the wounds at day 15 in (B) ASC and (C) NaCl treated animals. (i) A magnified view of the wound edge and (ii) granulation tissue. G= granulation tissue, T= tendons, F= hair follicle and V= blood vessel. Data shown as mean ± SD. Significance is shown where p<0.05: * between ASC and NaCl group, # within NaCl group between timepoints and δ within ASC group between timepoints.

A. Masson's trichrome, ASCs

(i) Day 15
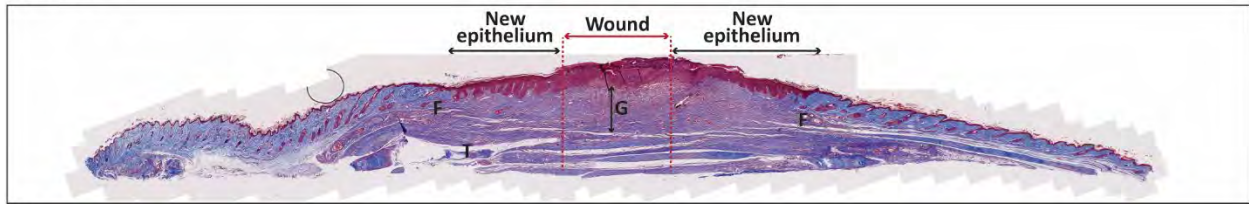
(ii) Day 21
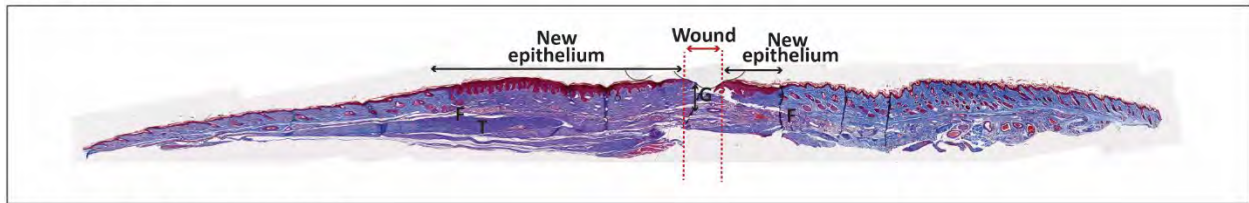
B. Masson's trichrome, NaCl

(i) Day 15
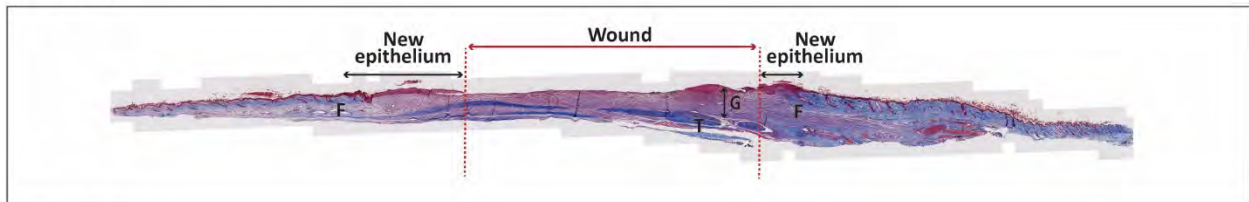
(ii) Day 21
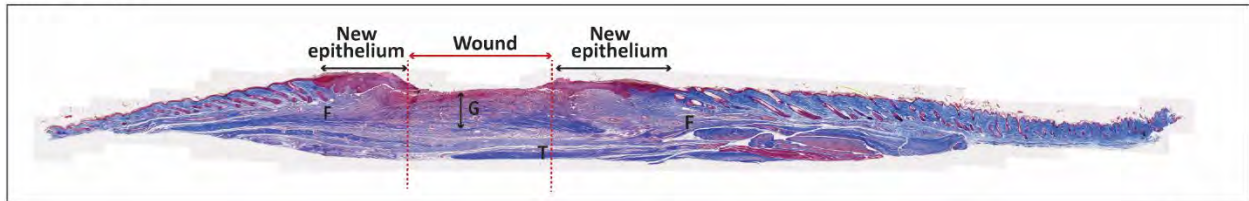
2000 µm

Figure 4.13 Aniline blue expression in Masson's trichrome staining at day 15 and 21 to detect collagen. A representative view of a cross section through the wounds showing a complete section of animals treated with (A) ASCs and (B) NaCl sacrificed on (i) day 15 and (ii) 21 stained for Masson's trichrome. Collagen is detected by aniline blue staining. The open wound area and the newly formed epithelium is shown. G= granulation tissue, T= tendons and F= hair follicle.
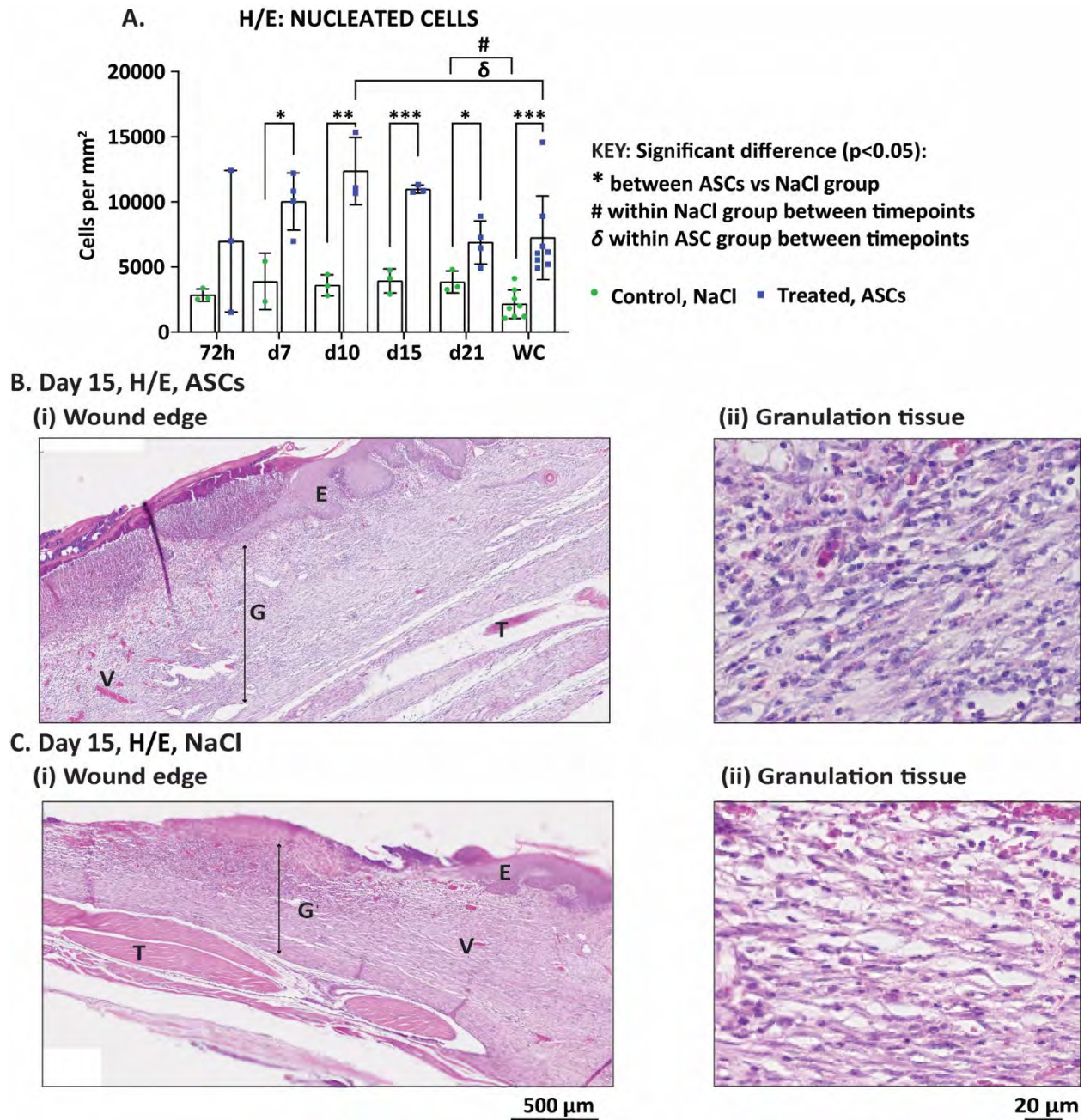
Figure 4.14 H/E staining and nuclei quantification.

Results of computer assisted marker quantification within the granulation tissue at 72h, day 7 (d7), d10, d15, d21 and at wound closure (WC) in hyperglycaemic animals with ischemic wounds treated with either ASCs or NaCl. (A) The number of nuclei in H/E stained sections were counted and expressed as cells per mm^2. A representative view of a cross section through the wounds at day 15 in (B) ASC and (C) NaCl treated animals. (i) A magnified view of the wound edge and (ii) granulation tissue. G= granulation tissue, T= tendons, F= hair follicle and V= blood vessel. Data shown as mean ± SD. Significance is shown where $p < 0.05$: * between ASC and NaCl group, # within NaCl group between timepoints and δ within ASC group between timepoints; **$p < 0.01$ and ***$p < 0.001$.
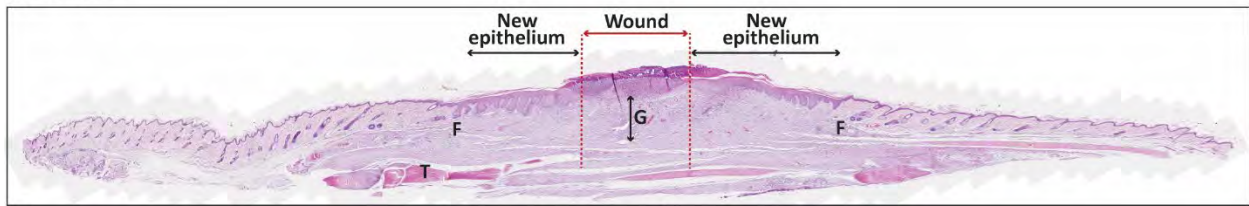
A. H/E, ASCs
(i) Day 15
(ii) Day 21
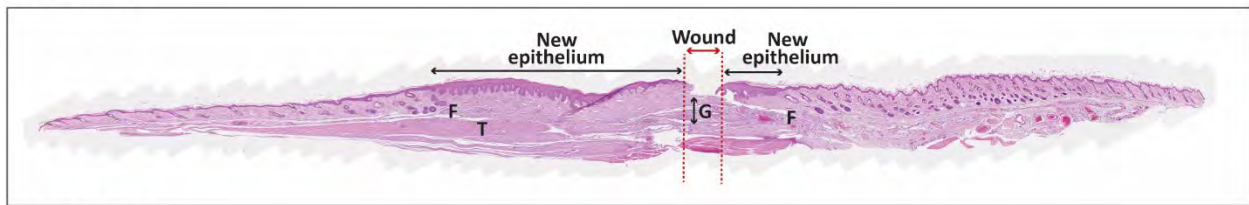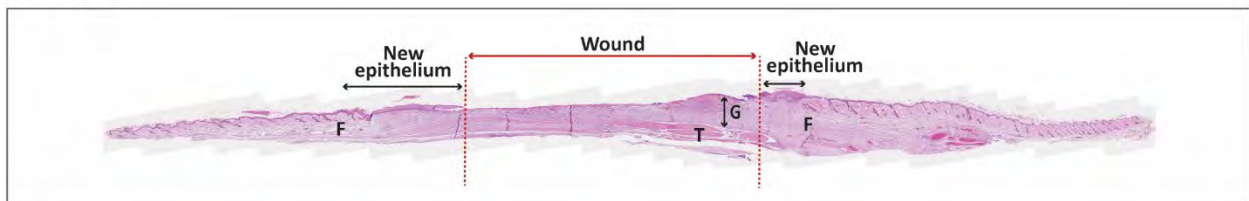
B. H/E, NaCl
(i) Day 15
(ii) Day 21
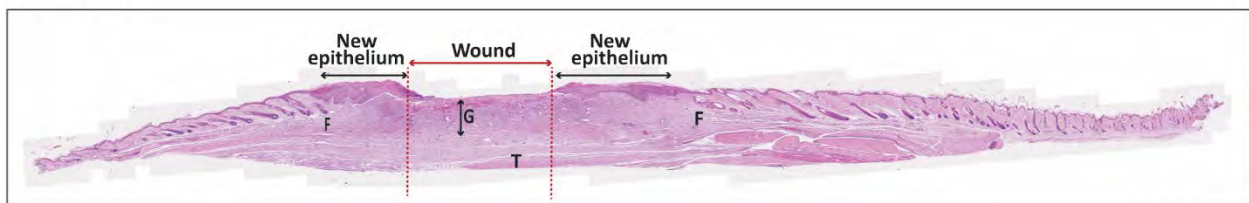
2000 μm

Figure 4.15 H/E staining at day 15 and 21.
A representative view of a cross section through the wounds showing a complete section of animals treated with (A) ASCs and (B) NaCl sacrificed on (i) day 15 and (ii) 21 stained for H/E. The open wound area and the newly formed epithelium is shown. G= granulation tissue, T= tendons, and F= hair follicle.

A.

GFP: ASCs

B. 72h, GFP, ASCs

(i) Cross section through wound

(ii) Injection site

(iii) Wound: migrating ASCs
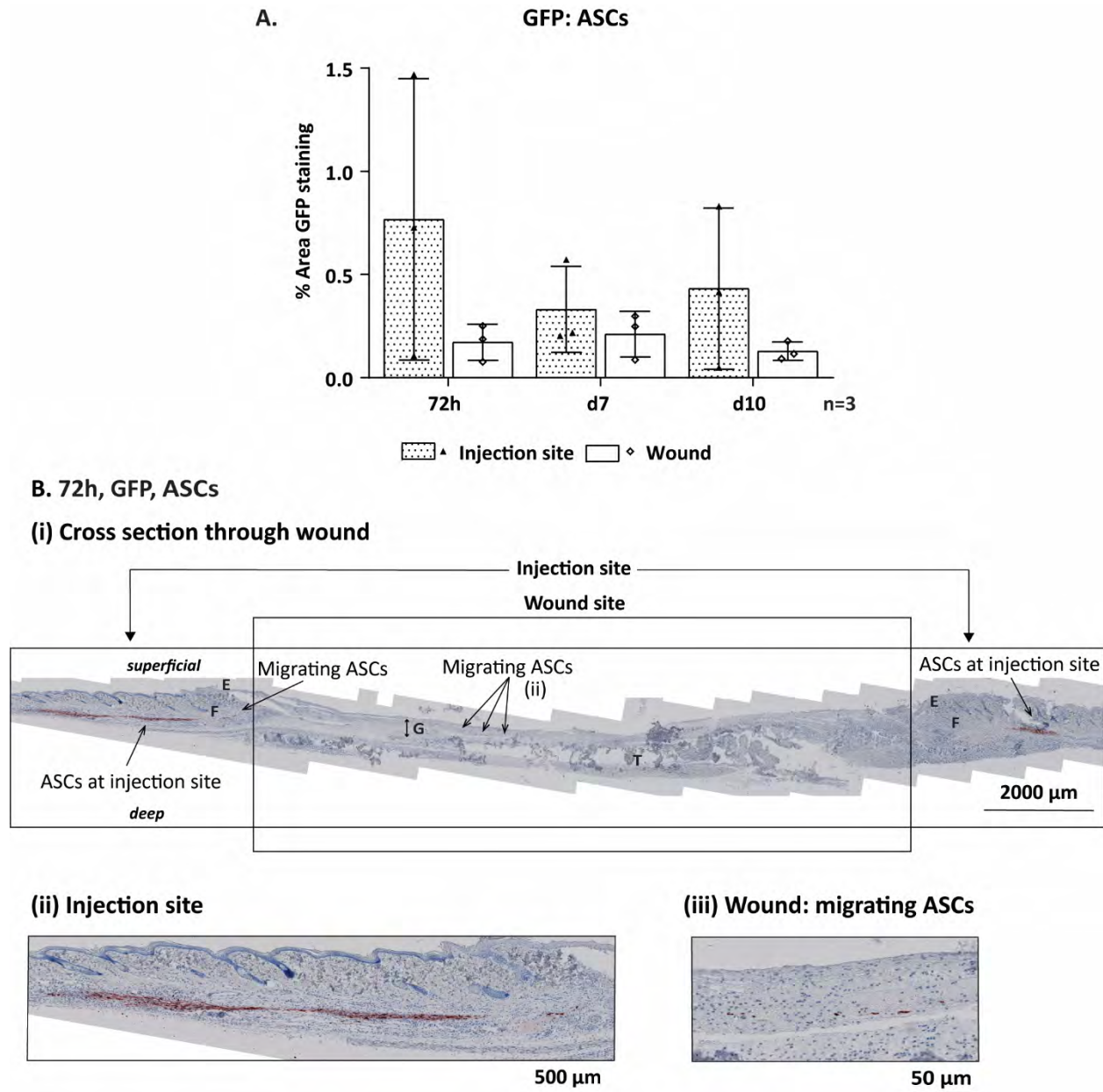
Figure 4.16 GFP staining and quantification.

2×10^5 ASCs transduced to express both Fluc and GFP were injected locally per foot into two sides around each ischemic wound 24h after bilateral full-thickness wounds had been created on the dorsal part of the feet in hyperglycaemic animals. (A) The distribution of GFP positive ASCs (red staining, AEC) was quantified in the injection site and in the wound at 72h, day 7 and day 10. (B)(i) A single tissue section from the wound in the feet 72h post injection stained for GFP. Magnified images of the (ii) injection site and the (iii) wound are shown. Data shown as mean ± SD. Significance is shown where *p<0.05. G= granulation tissue, E= epithelium, T= tendons, F= hair follicles.

4.4 DISCUSSION

Significant enhancement of wound closure was observed with ASC treatment. Both the non-ischemic and ischemic wound closure time was enhanced by 9 days compared to control wounds. This confirms similar findings from published clinical studies. In a small study, injection of BM-MSCs into wound edges of chronic diabetic foot ulcers of patients improved dermal thickness and decreased ulcer size.[150] A study on 20 patients with chronic wounds who were treated with autologous BM-MSCs cultured on a collagen sponge showed that 90% of the wounds closed with this treatment.[152] Two randomised studies on diabetic non-healing ulcers using IM injected autologous BM-MSCs demonstrated improvement in pain-free walking and increased ulcer healing rates.[151, 153] Prochazka *et al.*, in a randomised study including 96 patients with ischemic wound limbs, showed that local injection of autologous BM-MSCs in the wound halved limb amputation frequency (44% vs. 21%).[239] Interestingly, an initial increase in wound size was observed with ASC treatment but not in the control group. Adipose-derived stromal cells affected overall wound closure rate, leading to significantly smaller wounds being observed from day 15. We hypothesised that the enhancement seen in wound closure was due to ASCs promoting myofibroblast differentiation, as impaired myofibroblast differentiation has previously been recorded by colleagues using this model.[236] However, no significant difference in myofibroblast numbers, as detected by the expression of αSMA, was observed between the ASC treated and NaCl control treated groups, except early in the wound repair process and at complete wound closure. Of note, myofibroblasts were detectable in the ASC treated group at 72h post treatment (i.e. 4 days post wound creation), whereas they were barely present in the NaCl group and were present at higher numbers at wound closure. This could imply that even though ASC treatment led to faster wound closure, the remodelling and maturation of the wound was still in progress at wound closure. In the ASC group, the highest expression of αSMA was recorded at day 15, which interestingly coincided with the point where the rate of wound closure became more rapid as noted by the presence of smaller wounds than in the control group.

We further hypothesised that even though the expression of αSMA did not differ significantly between the treatment groups for most part, the enhancement of wound closure resulted from

changes in the contraction and epithelialisation ratio. In full-thickness wounds, both the epidermis and dermis had been destroyed, requiring the wound to heal by epithelialisation as well as the formation of granulation tissue to fill the missing dermis.[2, 15] Granulation tissue provides the substrate for epithelialisation. Fibroblasts start to colonise the provisional ECM to start forming the granulation tissue by producing collagen and a fibronectin-rich matrix. Over time, the ECM composition changes, promoting the maturation of resident fibroblasts into myofibroblasts. Myofibroblasts have contractile activity, which facilitates wound closure by promoting wound contraction. Finally, the marginal epidermis expands as activated epidermal keratinocytes migrate out and advance an epidermal tongue to form the new epithelium across the wound bed.[2, 15] No significant difference in the contraction and epithelialisation ratio was found between the ASC and control groups in either ischemic or non-ischemic wounds. Within the control group, impaired contraction was seen in the ischemic wound, whereas contraction was favoured in the non-ischemic wound. This confirms previous work showing that ischemia and hyperglycaemia together impair wound contraction.[236]

Another proposed mechanism by which ASCs could improve wound healing is by enhanced vascularisation within the granulation tissue. Enhanced vascularisation, as assessed by αSMA expression, was however not detected with ASC treatment. Both the ASC and control group showed similar patterns where the ischemic wound vascularisation increased around day 10 and then reduced from day 21 until wound closure. Wounds treated with BM-MSCs have been shown to accelerate angiogenesis by enhanced CD31 fluorescence staining in a diabetic mouse model.[109] Unfortunately the non-ischemic wounds were not evaluated by IHC, thus we can only postulate that the inability to increase vascularisation with ASC treatment may be due to the ischemia, or that ASCs induce vascularisation less efficiently than BM-MSCs. However, both *in vitro* and *in vivo* studies have reported the angiogenic effect of BM-MSCs and ASCs, through their secretion of soluble factors (such as VEGF, SDF-1, FGF, MMP-9, PDGF and TGF) that regulate the function of endogenous progenitor cells during wound repair.[7, 109, 240, 241] Another possibility is that vascularisation was underestimated by the method of detection used. Both myofibroblasts and vessels were identified by staining for αSMA. Endothelial cells are also known to express CD31

and RECA-1 (specific for rat tissue); however, these antibodies did not work in rat FFPE sections and instead required fresh tissue samples, which we did not have, for performing IHC. The difficulty with removing the wound tissue and the surrounding skin from the feet without compromising its integrity led us to instead fix the feet prior to tissue harvest followed by paraffin embedding. Thus, the vessels were manually selected and αSMA expression quantified, possibly leading to an underestimation, especially as smaller vessels where the lumen could not be seen at a general magnification, were excluded. Also, less mature vessels where αSMA is not yet expressed would have been overlooked. Thus, we cannot make any conclusions regarding the effect of ASCs on vascularisation in our model.

An important player during all phases of wound repair is the macrophage.[7, 22, 23] The specific role of the macrophage has been comprehensively discussed in a recent review.[23] During the inflammatory phase, monocytes infiltrate into the injured site where they differentiate into macrophages with a pro-inflammatory phenotype to phagocytose pathogens and cell debris, and attract other immune cells to the site by the secretion of growth factors, cytokines and chemokines. As the wound moves into the proliferation phase, macrophages move to a pro-wound healing phenotype to play a role in ECM formation, angiogenesis, epithelialisation and wound closure. As the wound enters the remodelling phase, macrophages become pro-resolving as they secrete MMPs for matrix remodelling. In our hyperglycaemic and ischemic wounds, macrophages were abundantly present throughout the wound repair process in a similar pattern in both the ASC and control group. They peaked at day 7, constituting up to 25% of the granulation tissue, and then significantly decreased at wound closure.

Collagen deposition is essential for the formation of the ECM in granulation tissue as well as the remodelling of the repaired wound.[29] Chronic wounds present with impaired ECM production and wound repair with scar formation.[242] We observed no statistically significant difference in collagen deposition with ASC treatment compared to the control group, both showing an increase in collagen deposition with time. Collagen deposition was greatest at wound closure. There appeared to be more collagen in the ASC group at day 15 and day 21 but this was not

statistically significant. Further investigation is required to identify whether ASCs influenced the type of collagen present at wound closure and if this changed the composition of the scar.

A look at the overall cellularity of the granulation tissue confirmed that ASC administration significantly increased cellularity compared to the control group from day 7 and until wound closure. We first hypothesised that the increase in cellularity was from the presence of the ASCs themselves; however, the percentage of ASCs found migrating into the wound bed was too low to have contributed to the increased cellularity. The ASCs remained mostly at the injection sites and were not included in the quantification of cellularity which was restricted to granulation tissue. Another hypothesis was that ASCs recruited more macrophages to the injury site, but this was also disproved as we found similar patterns of macrophage distribution in ASC and control groups. Further investigation into this enhanced cellularity needs to be undertaken. We hypothesise that ASCs recruited more immune regulating and tissue repair cells into the granulation tissue, leading to greater ECM deposition as seen by thicker granulation tissue in the ASC group. A two-fold decrease in cellularity was observed at wound closure compared to day 10 in the ASC group, whereas in the NaCl group cellularity remained constant from day 7 to day 21, after which a decrease was seen from day 21 to wound closure. The decrease in cellularity was expected as the wounds had entered the remodelling phase which is indicative of having fewer cells as a result of apoptosis.[2]

A study looking at the effect of human MSCs on normal and impaired (diabetic) healing in mice, found that wound healing was enhanced through recruiting existing endogenous tissue stem/progenitor cells.[58] They further postulate that the mechanism of action of administered MSCs was through the modulation of host cells. In a mouse excisional wound healing model, full-thickness wounds on the back of the mice were treated systemically with either BM-MSCs or BM-MSC exosomes.[243] Their results showed that wound healing was improved by an increase in M2 macrophages, increased collagen deposition and increased vascularisation at the wound site. In a phase I clinical trial, autologous cultured ASCs were injected intramuscularly to treat patients with non-revascularisable critical limb ischemia.[244] Improvement in trans-cutaneous oxygen

pressure, ulcer evolution and wound healing was reported. A meta-analysis of the treatment of diabetic foot ulcers (DFU) with autologous stem cells reported that stem cell administration significantly favoured healing of diabetic foot ulcers.[245] A total of six randomised controlled trial studies were evaluated using various types of cells: BM-MSCs, BM-MNCs, peripheral blood MNCs, bone marrow enriched repair cells, and human processed lipoaspirate.[151, 187, 246, 247] Although the administration of MSCs showed promise as a therapeutic approach for treating wounds, we still lack data describing the mode of action of administered MSCs. Inconsistencies in dose, source of cells, mode of administration and indication is making it difficult to provide concrete data for the therapeutic use of MSCs.

4.5   CONCLUSION

The administration of ASCs significantly enhanced wound closure time in hyperglycaemic animals with non-ischemic and ischemic wounds. Although no changes in collagen deposition, vascularisation or macrophage infiltration were observed between ASC treated and control groups, αSMA expression was detected earlier and remained higher at wound closure in the former without enhancing wound closure by contraction. The mechanism of action is likely to be related to the general cellularity of the wound being enhanced by ASCs. We provide evidence for the therapeutic use of ASCs as a cellular therapy for treating delayed healing wounds.

Chapter 5. OVERALL DISCUSSION

The management of non-healing/chronic wounds remains a major therapeutic challenge and is worsened with the increased incidence of obesity, diabetes, and vascular disease. Clinical trials to investigate non-healing/chronic wounds are hampered by the heterogeneity of the wounds being treated and the difficulty in managing contributing factors. Patients arrive at clinics at varying times after the onset of their wounds, fall within a wide age range, and have various co-morbidities and different levels of infection.[248] Clinically, MSCs have been identified as an attractive cellular therapy for wound healing.[7, 183, 249] An alternative to the widely used BM-MSCs is ASCs. They can be harvested with ease, producing high yields compared to BM-MSCs.[156, 161, 250] Although both BM-MSCs and ASCs are candidate cell types for treating wounds, laboratory and clinical studies still favour BM-MSCs.[249, 251] To understand the complexity of non-healing/chronic wound healing, animal models are commonly used.[233, 252] Animal models can be created by subjecting an acute wound to pathological conditions that are clinically relevant. The study of wound healing over an accelerated period compared to humans, permits collection of tissue samples at multiple time points and allows researchers to mimic the cause, location and size of wounds reproducibly. Drawing conclusions about the therapeutic effects of MSCs is hampered by the use of non-comparable animal models, lack of uniform MSC isolation and preparation techniques, and variability in dosage and method of delivery used. This study aimed to investigate the homing and healing properties of ASCs. To do so, standardised models of cutaneous wound repair in rats were employed under normal and pathological conditions. The model of normal wound healing allowed for a comparison between local versus systemic delivery of ASCs, and for the homing capacity of administered cells to be investigated. The model of wound healing under pathological conditions allowed for the effect of ASCs to be investigated on delayed wound repair. The same isolation, cell labelling, and wounding techniques were used for both models. In addition, both models enabled wound size, wound closure time as well as mode of wound closure to be followed.

Although the best mode of administration is still under debate, systemic delivery of MSCs has become preferred.[253] Although systemic administration is minimally invasive and allows for multiple infusions, it was originally believed to rely on the homing and migration of MSCs to the target tissue in order to be effective. Interest in systemic administration has been accompanied by establishing tracking methods to follow MSCs and understand their biodistribution and fate post administration. Various labelling methods, such as radioactive labelling, fluorescent vital dyes, contrast agents, transduction with reporter genes and the use of donor-specific DNA markers have been reviewed for the detection of short-term homing.[75, 200] Another technique, optical imaging using BLI, is becoming a favoured imaging method for *in vivo* cell tracking compared to anatomical imaging modalities such as MRI and PET/CT, as it has higher sensitivity and is lower in cost.[164] Additionally, the use of BLI allows only metabolically active, living cells to be detected.[164-166] In our two animal models, we established a combinational tracking system employing BLI as well as GFP detection. Exogenously administered ASCs were followed *in vivo* by BLI to detect Fluc positive cells, and post mortem by IHC to detect GFP positive cells. To enable tracking, ASCs were transduced to express the genes for Fluc and GFP. The first concern with transducing the cells was that this could change their characteristics. Two parameters were assessed to determine a change in characteristics, namely their immuno-phenotype and differentiation capacity. Both characteristics are currently used to identify cells as MSCs.[78, 79] Transduction of ASCs to express Fluc and GFP did not change their immuno-phenotype or differentiation capacity compared to non-transduced ASCs, and the expression of GFP in transduced ASCs was maintained *in vitro* over several passages. This confirmed previous studies showing that transduced MSCs maintain their characteristics *in vitro*.[176, 177]

The mechanism of MSC homing and migration has not been fully described; thus far, these cells have been proposed to home in a similar manner to leukocytes.[254, 255] Intravital microscopy in transgenic zebrafish with GFP expressing vasculature shed some light on this process, showing that systemic MSC extravasation is different from the well described diapedesis of leukocytes.[256] They found that MSCs remained passive during extravasation. Remodelling of the vascular wall allowed the cells to exit. The definition of MSC homing has been defined non-mechanistically as

the active or passive arrest of MSCs within the vasculature of a tissue followed by trans-migration across the endothelium[75] and further redefined[127] to distinguish between non-systemic and systemic homing (Figure 5.1). Non-systemic homing is the recruitment of locally transplanted MSCs near the injury or of resident MSCs to the injured site. Systemic homing is a process whereby MSCs administered into circulation, or endogenous MSC recruitment and ingress into the circulation (from their specific niche, such as from the bone marrow or adipose tissue), exit the blood vessel and migrate towards the target site. Both these mechanisms involve the migration of the MSCs to the injury site by sensing chemokines released by the injured tissue. Where systemic homing of MSCs has previously been described, the process was not very efficient. Systemic BM-MSCs accumulate in the lungs soon after infusion, followed by homing to the liver and spleen and only at low frequency in other tissues.[253, 257 191, 258] In a mouse model of peripheral tissue ischemia, systemic administration of BM-MSCs showed no evidence of ischemia-directed homing.[191] Healthy mice without wounds showed that systemically administered BM-MSCs initially reside in the lung and then home to the liver and spleen at lower frequency, whereas mice with cutaneous wounds additionally showed engraftment, albeit at low frequency, at the injured site.[110] In an inflammatory mouse model of arthritis, systemically administered ASCs were also located in the lungs with minimal homing to the injured tissue.[259]

Adipose-derived stromal cells administered systemically in our rat model of wound repair under physiological conditions showed no detectable homing to the site of injury. An obstacle that impeded homing was the entrapment of ASCs in the lungs. We hypothesise three main reasons for this: first, that ASCs could not bypass entrapment in the lung and re-enter the circulation; second, the inflammatory response from the site of injury was not strong enough to activate ASC homing under physiological conditions of wound repair; and third, culturing and transduction of ASCs influenced their homing capacity. We postulate that the first reason, namely the pulmonary passage, was the major reason for the lack of detectable ASC homing.
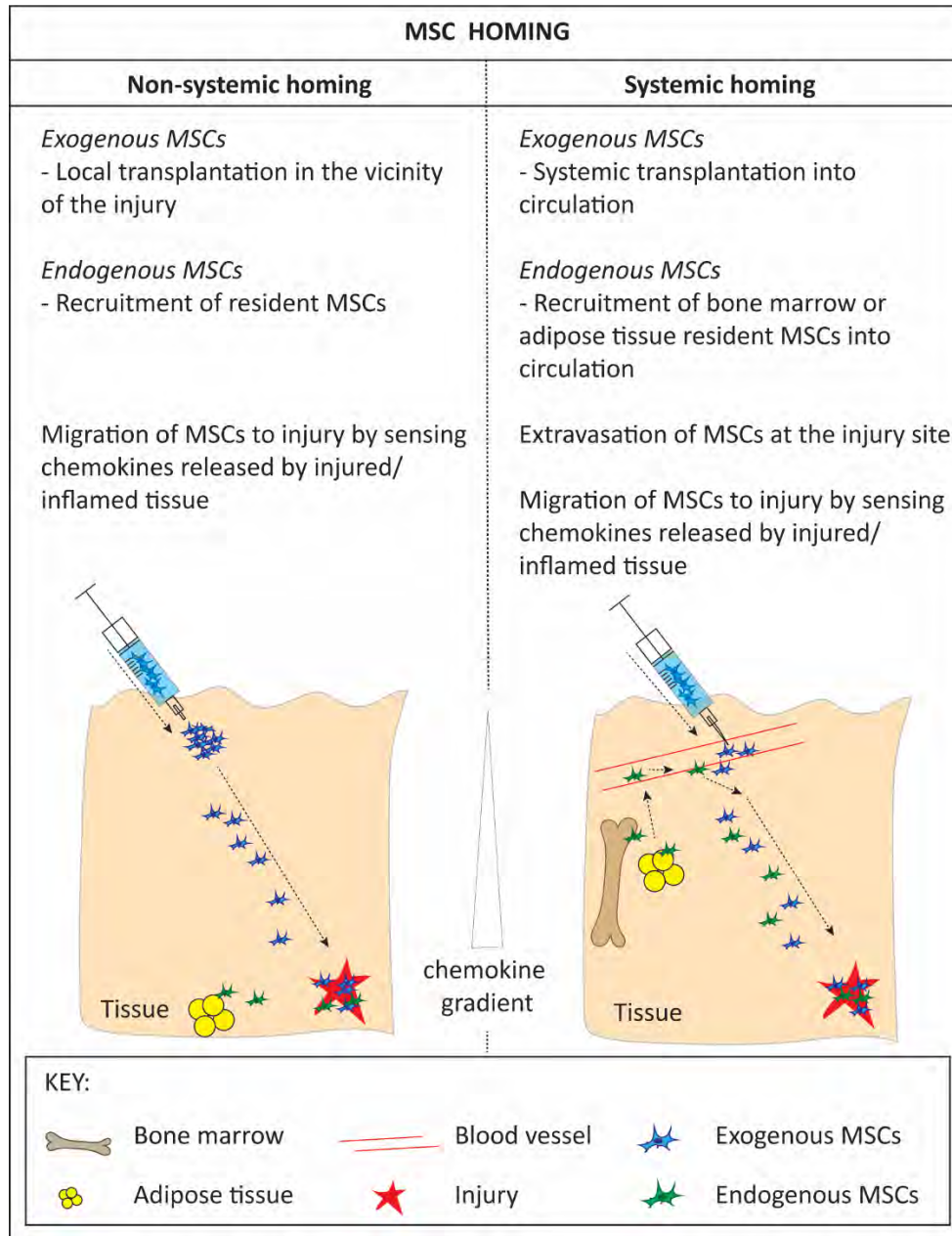
Figure 5.1 Proposed non-systemic and systemic homing mechanisms of mesenchymal stromal/stem cells (MSCs).
Exogenously transplanted or endogenous MSCs are attracted to injured/inflamed tissues based on a chemokine gradient released from the site of injury. Non-systemic homing occurs from the recruitment of transplanted MSCs or local resident MSCs close to the target site which migrate to the site of injury by sensing chemokines released by the injured/inflamed tissue. Systemic homing requires the active or passive extravasation of MSCs administered into the circulation followed by chemokine guided interstitial migration towards the site of injury. Endogenous MSCs from the bone marrow or other niches (such as adipose tissue) can also be recruited to injured/inflamed tissues via the vascular system. Figure adapted from Nitzche, *et al.*, 2017.[127]

Entrapment in the lungs has been a recurring problem with systemic administration of MSCs.[201, 260] To overcome this pulmonary first-pass effect, alternative routes of administration have been suggested.[192, 200] Intra-arterial infusion of MSCs for acute kidney injury showed accumulation of cells in the kidney; however they failed to show long-term engraftment.[166] A comparison of IV and IA infusion of BM-MSCs in a porcine model showed that IA administration reduced lung uptake and increased MSC uptake in other organs.[261] A rat model of transient ischemic stroke also found that IA administration improved the accumulation of MSCs at the target site.[262] However, although IA administration of MSCs improved tissue-specific homing, it has a higher risk of complications as the cells also lead to obstruction of the microcirculation, entrapment in the vessel wall and pulmonary embolism.[262-264] Culturing of MSCs has been shown to influence their migratory capacity.[253, 265] In particular, *in vitro* culturing in a hypoxic environment greatly improved MSC proliferation and the expression of chemokine receptors.[149] Imaging using BLI on the other hand lacks the resolution needed to detect small numbers of Fluc expressing cells, thus homing of a few cells could have been overlooked. Histological sections of the wounds were additionally analysed by IHC to detect GFP positive ASCs; ASCs were still only detectable in the lungs.

To ensure that administered cells reach the wound bed at the injured site in a timely manner and in sufficient numbers, the local administration of MSCs has been suggested as an alternative to systemic administration.[194] This involves the direct application of cells to the wound site in sufficient numbers and at the right time to facilitate the interaction of the administered cells at critical stages of the healing process. Mesenchymal stromal cells can be applied locally if the target site is accessible. Thus, external wounds, rather than internal organ wounds are preferred for this application. We further investigated the non-systemic homing of locally administered ASCs. One day post-wound creation was chosen for administration so that the inflammatory phase would already be initiated with an adequate concentration of chemokines being secreted to attract the ASCs. Locally transplanted ASCs remained viable at the injection sites for at least 7 days post transplantation. Analyses by IHC to detect GFP positive ASCs found that locally administered ASCs became localised at the wound edge as well as in the wound bed. Significant

distribution of ASCs into the wound bed was found at 72h and then reduced until they were no longer detectable after 7 days. It is probable that the ASCs died at the transplantation site after a week. This localisation of ASCs in the wound could be from active ASC migration, ASC proliferation or due to displacement from the injection site into the wound bed as the wound contracts to bring the wound edges closer together. In rabbits, full-thickness incisional wounds were made, sutured and transplanted with fluorescently labelled human MSCs into the wound border at a dose of 1.5 x 10^6 cells.[266] The migration pattern of the transplanted MSCs was followed and they were identified up to day 21 showing specific migration from the epidermal-dermal interface towards the borders of the dermis. In this PhD study, we used seven and a half times less MSCs and the wounds were excisional instead of incisional, which could have led to our shorter detection time.

Our animal model also allowed for measurements of wound size, time to complete healing and ratios of whether the wound closed by contraction or epithelialisation to be recorded. Interestingly, enhancement of wound closure time under physiological conditions was found with ASC treatment, independent of the route of administration. Furthermore, these wounds closed more by epithelialisation than contraction compared to control animals. A review on MSC delivery routes and their fate concluded that MSCs have a "profound clinical effect without trans-differentiation, without homing to target organs in significant numbers and despite the cells disappearance within short periods of time".[192] The disappearance of transplanted cells and low engraftment at the injured site suggests that MSCs play a role as initiators of wound repair rather than effectors.[58] The mechanism of this effect has been suggested to stem from their paracrine signalling[207] which mobilises the host to promote wound repair. The question that still needs to be answered is: How do MSCs filtered out in the lung influence wound repair mechanisms that are located distally? It has been shown that MSCs secrete various molecules that are modulators of cellular growth, replication, differentiation and adherence.[267, 268] The MSC (BM-MSCs and ASCs) secretome consists of soluble factors, such as cytokines, chemokines and growth factors, and proteins, lipids and nucleic acids that are released via extracellular vesicles.[269, 270] A subset of these extracellular vesicles, referred to as exosomes, are believed to be released by trapped

MSCs in the lungs in response to injury cues where they can travel via the circulation to the injured site to exert their therapeutic effects.[200, 271] The addition of ASC-derived exosomes to fibroblasts has recently been shown to improve their proliferation, migration, secretion of growth factors and collagen deposition *in vitro*, and further accelerated wound healing *in vivo* in a mouse model with a full-thickness incisional wound.[272] Furthermore, they have been shown to promote cutaneous repair through ECM remodelling by regulating the ratios of collagen III to collagen I, TGFβ3 to TGFβ1, and MMP3 to TIMP1.[273, 274] The therapeutic potential of exosomes is being investigated for various diseases and has been proposed as a novel cell-free therapy.[275, 276]

Few completed and published clinical trials are listed on clinicaltrials.gov using MSCs for DFU and critical limb ischemia (CLI). One clinical trial evaluated the safety, feasibility and efficacy of BMCs and expanded BM-MSCs for improving microcirculation and lowering amputation rates in patients with DFU.[187] The cells were administered either IM or IA into the ischemic limb. Out of the 22 patients included in the trial, 18 achieved complete wound closure and showed improvements of microcirculation. The safety of IM allogeneic BM-MSCs in patients with CLI was determined in a double blinded randomised placebo controlled multi-centre study of 20 patients. It proved the safety but not the efficacy of BM-MSCs, as few efficacy parameters showed significant improvements.[277] A pilot study treating 15 patients with CLI with multiple IM allogeneic ASCs reported no complications and 66.7% of the patients showed clinical improvement.[278] Clinical studies using MSCs for cutaneous non-healing/chronic wounds is still limited. Instead animal models to investigate the effect of MSCs for cutaneous non-healing/chronic wounds are used. Cellular therapy has the potential to treat non-healing/chronic wounds; however, the ideal cell to use still need to be determined. We report that ASCs show promise for treating wounds under pathological conditions of hyperglycaemia and ischemia.

In this study we used the previously established rat model of wound repair under pathological conditions.[235, 236] This model uses STZ induced hyperglycaemic rats with ischemic wounds to mimic delayed-healing wounds of the extremities e.g. DFUs. Two major causes of chronic wounds, hyperglycaemia and ischemia were studied together using this model. It permitted full-

thickness wounds to be created homogenously in an area with tightly fixed skin where both wound contraction and epithelialisation could be quantified, and the induction of ischemia was inducible in a standardised manner. We investigated the effect of local administration of ASCs using this model. Wound closure was significantly enhanced compared to control animals. Identifying the mechanism that led to this enhancement was difficult to elucidate. Interestingly, the only significant difference that we could detect by histological analysis in response to ASC treatment was an increase in the overall cellularity of the wound throughout the healing time. Figure 5.2 depicts the possible mechanisms involved in enhancing wound repair in our model. We hypothesise that increased cellularity resulted from the enhanced migration of cells into the wound. The migration and proliferation of wound repair cells such as epithelial cells, endogenous stem cells, endothelial cells, fibroblasts and keratinocytes may have been enhanced by the ASCs. Furthermore, ASCs are known to have immunomodulatory effects,[138, 279] thus they may have been responsible for regulating immune cell recruitment into the wound. Studies utilising ASCs have suggested that enhanced wound healing is due to the cells' ability to modulate the immune response, secrete paracrine factors, and promote angiogenesis.[228, 280, 281] Another possibility is that ASCs improved ECM deposition which leads to better cell infiltration and retention.[242] Although no significant change in the ratio of wound closure by contraction and epithelialisation was observed, ASCs may have enhanced both equally well leading to the overall enhancement of wound closure.

The angiogenic effect of MSCs is a common mechanism reported by which wound healing in *in vitro* and *in vivo* studies is enhanced.[240] In a rat model with radiation ulcers, the significant reduction in wound size with ASC treatment compared to control animals was associated with improved neo-vascularisation.[282] Wound healing of excisional wounds on the back of normal and diabetic rats resulted from increased vessel formation, epithelialisation, and granulation tissue deposition, and through the secretion of angiogenic cytokines by ASCs such as VEGF, HGF and FGF-2.[283] Another study reported that the targeted delivery of ASCs within a scaffold accelerated diabetic wound healing. The authors proposed that this resulted from ASC paracrine signalling, enhanced granulation tissue formation and increased epithelialisation and neo-

vascularisation.[284] In our study, neo-vascularisation was evaluated using the same marker as for myofibroblasts, αSMA, as endothelial markers, CD31 and RECA-1 failed to show specificity in our FFPE samples. Unfortunately, newly formed vessels, immature and smaller vessels where the vessels walls are still composed exclusively of endothelial cells, could not be detected and overall no significant change in vessel formation was found.

MECHANISMS OF WOUND REPAIR

With ASC treatment

Increased wound cellularity

Recruitment of cells
Wound repair cells
- Epithelial cells
- Endogenous MSCs/EPCs
- Endothelial cells
- Fibroblasts
- Keratinocytes

This study did not check their individual contribution **?**

Immune cells
- Neutrophils: They normally dominate the first 48 hrs
                There was no incease in cellularity detected so early **X**
- Macrophages: No difference was found between the control and treated group **X**
                This study did not distinguish between M1 and M2 macrophages **?**

ASCs

Other mechanisms

- Improved ECM deposition could have facilitated cell infiltration **?**
- Collagen deposition: No change in overall collagen deposition was found
                This study did not distinguish between type III and type I collagen **?**
- Angiogenesis: No change in overall vessel formation was found by staining
                vessels for αSMA; could have missed smaller, less mature vessels **?**
- Paracrine signalling: This was not investigated **?**

Possible mechanisms that were not proved or disproved by this study are represented by a: **?**
Mechanisms disproved by this study are represented by a: **X**

Figure 5.2 Mechanisms of wound repair.
Using a model of wound repair in hyperglycaemic rats with ischemic full-thickness wounds, the effect on wound repair was investigated when wounds were treated with ASCs locally around the wound. Here graphically represent the mechanisms that could have led to enhanced wound closure. Compared to NaCl control animals, ASC treatment only showed enhanced wound cellularity. Collagen deposition, macrophage infiltration and angiogenesis remained unchanged.

Paracrine signalling and differentiation of ASCs is another mechanism that has been implicated in improving wound healing.[139] However, it is difficult to show that ASC differentiation is a

prominent mechanism due to their poor engraftment at the injured site. Thus, paracrine signalling is likely to be a major mechanism accounting for the beneficial effects of ASCs in response to injury.[228] Paracrine signalling can stimulate various wound repair mechanisms, such as the recruitment, migration and proliferation of endogenous cells around and in the wound, angiogenesis, epithelialisation, granulation tissue formation, modulating inflammation, and regulating ECM remodelling.[285]

In retrospect, we acknowledge that this study had some limitations that could be addressed in future studies. Firefly luciferase generates a relatively low luminescent signal during BLI. This becomes problematic when one wishes to detect low numbers of luciferase expressing cells or when these cells are located in deep tissues. To improve Fluc brightness, companies such as PerkinElmer have developed a new codon-optimised luciferase from *Luciolia Italica*, referred to as RedLuc. It has a red-shifted emission peak wavelength of 617 nm compared to 550 nm for Fluc, and a 100 fold higher signal intensity compared to other firefly luciferases.[286] Culturing and transduction ASCs could have led to changes in their therapeutic effect. We restricted our investigation to the immunophenotype and differentiation capacity of ASCs; however, ASC *in vitro* migration capacity and secretion of paracrine molecules should be evaluated in the future. The pathological model itself could have influenced the results obtained. This model more closely mimicked a model of hyperglycaemia rather than diabetes. Hyperglycaemia was chemically induced by STZ and the animals showed varied responses towards it. Some animals became very hyperglycaemic, had increased loss in body weight, and elevated water consumption, while others displayed this to a lesser extent. Also, glucose levels were not controlled, and several animals died from the inability to tolerate elevated glucose levels. The induction of ischemia was also problematic, surprisingly not the resection, but rather the sutured incision area outside. Animals found the sutures irritating and ended up chewing at their wounds. The animals whose chewed legs could be re-sutured were still included in the study, and this could have led to increased inflammation. We did however try to prevent this with the use of Elizabethan collars. These collars themselves impeded proper animal grooming and due to limited access to the sutures area, some animals instead started to chew at the wounds on their feet. Furthermore, we must acknowledge that this was a model of delayed healing rather than of chronic wounds.

Mimicking chronic wounds in an animal model is difficult and is an avenue to be investigated in future studies before ASC administration can be proposed as a therapy for chronic wounds.

Taken together, this study showed that despite the limited systemic homing capacity of ASCs, they nonetheless improved wound healing. Non-systemic homing distributed ASCs at the wound edge and into the wound bed where they promoted wound repair. Under pathological conditions, ASCs maintained their non-systemic homing capacity and enhancement of wound closure. A significant increase in wound cellularity was observed, possibly through a mechanism of paracrine signalling. The release of various growth factors and anti-inflammatory mediators by MSCs has been identified as a possible mechanism of action for enhancing wound repair.[287, 288] Administration of ASCs for non-healing/chronic wounds shows promise as a cellular treatment by enhancing wound repair on a global scale. Our inability to detect specific changes in the different mechanisms we analysed that are involved in the repair process, while still observing a significant enhancement of wound closure, suggests that ASCs play a role at every level during the process. Thus, we hypothesise that they can globally stimulate the process by regulating angiogenesis, ECM deposition, contraction, epithelialisation, granulation tissue formation and inflammation during the wound healing process.[183, 228, 271] Future directions for cutaneous wounds should focus on combinatorial approaches where ASCs are used in combination with scaffolds, in a matrix or within wound dressings. Another emerging area is utilising the ASC secretome as a cell free treatment by exploiting the use of exosomes. A paradigm shift towards a cell-free therapeutic approach in regenerative medicine has recently been proposed by using MSC-derived exosomes instead of MSCs.[276]

Adipose-derived stromal cells hold great potential as a treatment for various diseases. There is a need for the translation of ASCs from research to the clinic. Routine cell-based therapy using ASCs will require alternate routes of administration, the correct dose (whether to use single or multiple doses) as well as the best time to introduce ASCs, to be investigated further. To ensure the efficacy and safety of ASC therapies there is a need for (1) standardised characterisation to understand ASC heterogeneity, (2) appropriate cell expansion and culturing conditions, (3)

determining the best cell product to use (allogeneic versus autologous ASCs, SVF versus cultured ASCs, and exosomes) and (4) understanding their mechanism of action.[289]

REFERENCES

1. Boer, M., Duchnik, E., Maleszka, R., and Marchlewicz, M. Structural and biophysical characteristics of human skin in maintaining proper epidermal barrier function. Postepy Dermatol Alergol. 2016;33:1-5.
2. Rittie, L. Cellular mechanisms of skin repair in humans and other mammals. J Cell Commun Signal. 2016;10:103-120.
3. Jahoda, C.A., and Reynolds, A.J. Hair follicle dermal sheath cells: Unsung participants in wound healing. Lancet. 2001;358:1445-1448.
4. Rahmani, W., Abbasi, S., Hagner, A., Raharjo, E., Kumar, R., Hotta, A., Magness, S., Metzger, D., and Biernaskie, J. Hair follicle dermal stem cells regenerate the dermal sheath, repopulate the dermal papilla, and modulate hair type. Dev Cell. 2014;31:543-558.
5. Greenwood, J.E. Function of the panniculus carnosus--a hypothesis. Vet Rec. 2010;167:760.
6. Lazarus, G.S., Cooper, D.M., Knighton, D.R., Percoraro, R.E., Rodeheaver, G., and Robson, M.C. Definitions and guidelines for assessment of wounds and evaluation of healing. Wound Repair Regen. 1994;2:165-170.
7. Al-Shaibani, M.B.H., Wang, X.-N., Lovat, P.E., and Dickinson, A.M. Cellular therapy for wounds: Applications of mesenchymal stem cells in wound healing. In: Alexandrescu, V.A., ed. Wound Healing - New insights into Ancient Challenges. Rijeka: InTech; 2016:Ch. 05.
8. Borena, B.M., Martens, A., Broeckx, S.Y., Meyer, E., Chiers, K., Duchateau, L., and Spaas, J.H. Regenerative skin wound healing in mammals: State-of-the-art on growth factor and stem cell based treatments. Cell Physiol Biochem. 2015;36:1-23.
9. Krafts, K.P. Tissue repair: The hidden drama. Organogenesis. 2010;6:225-233.
10. Monaco, J.L., and Lawrence, W.T. Acute wound healing an overview. Clin Plast Surg. 2003;30:1-12.
11. Eming, S.A., Martin, P., and Tomic-Canic, M. Wound repair and regeneration: Mechanisms, signaling, and translation. Sci Transl Med. 2014;6:265sr266.
12. Alonso, L., and Fuchs, E. Stem cells of the skin epithelium. Proc Natl Acad Sci U S A. 2003;100 Suppl 1:11830-11835.
13. Han, G., and Ceilley, R. Chronic wound healing: A review of current management and treatments. Adv Ther. 2017;34:599-610.
14. Martin, P. Wound healing--aiming for perfect skin regeneration. Science. 1997;276:75-81.
15. Reinke, J.M., and Sorg, H. Wound repair and regeneration. Eur Surg Res. 2012;49:35-43.
16. Weisel, J.W., and Litvinov, R.I. Fibrin formation, structure and properties. Subcell Biochem. 2017;82:405-456.
17. Singer, A.J., and Clark, R.A. Cutaneous wound healing. N Engl J Med. 1999;341:738-746.
18. Pierce, G.F., Mustoe, T.A., Altrock, B.W., Deuel, T.F., and Thomason, A. Role of platelet-derived growth factor in wound healing. J Cell Biochem. 1991;45:319-326.
19. Demidova-Rice, T.N., Hamblin, M.R., and Herman, I.M. Acute and impaired wound healing: Pathophysiology and current methods for drug delivery, part 1: Normal and chronic wounds: Biology, causes, and approaches to care. Adv Skin Wound Care. 2012;25:304-314.
20. Yamaguchi, Y., and Yoshikawa, K. Cutaneous wound healing: An update. J Dermatol. 2001;28:521-534.
21. Wilgus, T.A., Roy, S., and Mcdaniel, J.C. Neutrophils and wound repair: Positive actions and negative reactions. Adv Wound Care (New Rochelle). 2013;2:379-388.
22. Koh, T.J., and Dipietro, L.A. Inflammation and wound healing: The role of the macrophage. Expert Rev Mol Med. 2011;13:e23.

23. Krzyszczyk, P., Schloss, R., Palmer, A., and Berthiaume, F. The role of macrophages in acute and chronic wound healing and interventions to promote pro-wound healing phenotypes. Front Physiol. 2018;9:419.

24. Ross, R. The role of T lymphocytes in inflammation. Proc Natl Acad Sci U S A. 1994;91:2879.

25. Schäffer, M., and Barbul, A. Lymphocyte function in wound healing and following injury; 1998: 444-460.

26. Dipietro, L.A. Wound healing: The role of the macrophage and other immune cells. Shock. 1995;4:233-240.

27. Brancato, S.K., and Albina, J.E. Wound macrophages as key regulators of repair: Origin, phenotype, and function. Am J Pathol. 2011;178:19-25.

28. Stein, M., Keshav, S., Harris, N., and Gordon, S. Interleukin 4 potently enhances murine macrophage mannose receptor activity: A marker of alternative immunologic macrophage activation. J Exp Med. 1992;176:287-292.

29. Xue, M., and Jackson, C.J. Extracellular matrix reorganization during wound healing and its impact on abnormal scarring. Adv Wound Care (New Rochelle). 2015;4:119-136.

30. Landen, N.X., Li, D., and Stahle, M. Transition from inflammation to proliferation: A critical step during wound healing. Cell Mol Life Sci. 2016;73:3861-3885.

31. Li, J., Zhang, Y.P., and Kirsner, R.S. Angiogenesis in wound repair: Angiogenic growth factors and the extracellular matrix. Microsc Res Tech. 2003;60:107-114.

32. Velazquez, O.C. Angiogenesis and vasculogenesis: Inducing the growth of new blood vessels and wound healing by stimulation of bone marrow-derived progenitor cell mobilization and homing. J Vasc Surg. 2007;45 Suppl A:A39-47.

33. Bochaton-Piallat, M.L., Gabbiani, G., and Hinz, B. The myofibroblast in wound healing and fibrosis: Answered and unanswered questions. F1000Res. 2016;5:F1000 Faculty Rev-1752.

34. Gabbiani, G. Evolution and clinical implications of the myofibroblast concept. Cardiovasc Res. 1998;38:545-548.

35. Levinson, H. A paradigm of fibroblast activation and dermal wound contraction to guide the development of therapies for chronic wounds and pathologic scars. Adv Wound Care (New Rochelle). 2013;2:149-159.

36. Chatzigeorgiou, A., Harokopos, V., Mylona-Karagianni, C., Tsouvalas, E., Aidinis, V., and Kamper, E.F. The pattern of inflammatory/anti-inflammatory cytokines and chemokines in type 1 diabetic patients over time. Ann Med. 2010;42:426-438.

37. Bekeschus, S., Schmidt, A., Napp, M., Kramer, A., Kerner, W., Von Woedtke, T., Wende, K., Hasse, S., and Masur, K. Distinct cytokine and chemokine patterns in chronic diabetic ulcers and acute wounds. Exp Dermatol. 2017;26:145-147.

38. Wetzler, C., Kampfer, H., Stallmeyer, B., Pfeilschifter, J., and Frank, S. Large and sustained induction of chemokines during impaired wound healing in the genetically diabetic mouse: Prolonged persistence of neutrophils and macrophages during the late phase of repair. J Invest Dermatol. 2000;115:245-253.

39. Xu, F., Zhang, C., and Graves, D.T. Abnormal cell responses and role of TNF-alpha in impaired diabetic wound healing. Biomed Res Int. 2013;2013:754802.

40. Khanna, S., Biswas, S., Shang, Y., Collard, E., Azad, A., Kauh, C., Bhasker, V., Gordillo, G.M., Sen, C.K., and Roy, S. Macrophage dysfunction impairs resolution of inflammation in the wounds of diabetic mice. PLoS ONE. 2010;5:e9539.

41. Loots, M. Fibroblasts derived from chronic diabetic ulcers differ in their response to stimulation with EGF, IGF-I, bFGF and PDGF-AB compared to controls. Eur J Cell Biol. 2002;81:153-160.

42. Lerman, O.Z., Galiano, R.D., Armour, M., Levine, J.P., and Gurtner, G.C. Cellular dysfunction in the diabetic fibroblast: Impairment in migration, vascular endothelial growth factor production, and response to hypoxia. Am J Pathol. 2003;162:303-312.
43. Usui, M.L., Mansbridge, J.N., Carter, W.G., Fujita, M., and Olerud, J.E. Keratinocyte migration, proliferation, and differentiation in chronic ulcers from patients with diabetes and normal wounds. J Histochem Cytochem. 2008;56:687-696.
44. Liao, H., Zakhaleva, J., and Chen, W. Cells and tissue interactions with glycated collagen and their relevance to delayed diabetic wound healing. Biomaterials. 2009;30:1689-1696.
45. Kuo, P.C., Kao, C.H., and Chen, J.K. Glycated type 1 collagen induces endothelial dysfunction in culture. In Vitro Cell Dev Biol Anim. 2007;43:338-343.
46. Reigle, K.L., Di Lullo, G., Turner, K.R., Last, J.A., Chervoneva, I., Birk, D.E., Funderburgh, J.L., Elrod, E., Germann, M.W., Surber, C., Sanderson, R.D., and San Antonio, J.D. Non-enzymatic glycation of type I collagen diminishes collagen-proteoglycan binding and weakens cell adhesion. J Cell Biochem. 2008;104:1684-1698.
47. Castilla, D.M., Liu, Z.J., and Velazquez, O.C. Oxygen: Implications for wound healing. Adv Wound Care (New Rochelle). 2012;1:225-230.
48. Im, M.J., and Hoopes, J.E. Energy metabolism in healing skin wounds. J Surg Res. 1970;10:459-464.
49. Chambers, A., and J Leaper, D. Role of oxygen in wound healing: A review of evidence; 2011: 160-164.
50. Bauer, S.M., Bauer, R.J., and Velazquez, O.C. Angiogenesis, vasculogenesis, and induction of healing in chronic wounds. Vasc Endovascular Surg. 2005;39:293-306.
51. Chan, E.C., Jiang, F., Peshavariya, H.M., and Dusting, G.J. Regulation of cell proliferation by NADPH oxidase-mediated signaling: Potential roles in tissue repair, regenerative medicine and tissue engineering. Pharmacol Ther. 2009;122:97-108.
52. Callaghan, M.J., Ceradini, D.J., and Gurtner, G.C. Hyperglycemia-induced reactive oxygen species and impaired endothelial progenitor cell function. Antioxid Redox Signal. 2005;7:1476-1482.
53. Dowsett, C., and Ayello, E. TIME principles of chronic wound bed preparation and treatment. Br J Nurs. 2004;13:S16-23.
54. Schultz, G.S., Sibbald, R.G., Falanga, V., Ayello, E.A., Dowsett, C., Harding, K., Romanelli, M., Stacey, M.C., Teot, L., and Vanscheidt, W. Wound bed preparation: A systematic approach to wound management. Wound Repair Regen. 2003;11 Suppl 1:S1-28.
55. Falabella, A.F. Debridement and wound bed preparation. Dermatol Ther. 2006;19:317-325.
56. Zeng, R., Lin, C., Lin, Z., Chen, H., Lu, W., Lin, C., and Li, H. Approaches to cutaneous wound healing: Basics and future directions. Cell and Tissue Research. 2018;374:217-232.
57. Chavakis, E., Urbich, C., and Dimmeler, S. Homing and engraftment of progenitor cells: A prerequisite for cell therapy. J Mol Cell Cardiol. 2008;45:514-522.
58. Shin, L., and Peterson, D.A. Human mesenchymal stem cell grafts enhance normal and impaired wound healing by recruiting existing endogenous tissue stem/progenitor cells. Stem Cells Transl Med. 2013;2:33-42.
59. Thomson, J.A., Itskovitz-Eldor, J., Shapiro, S.S., Waknitz, M.A., Swiergiel, J.J., Marshall, V.S., and Jones, J.M. Embryonic stem cell lines derived from human blastocysts. Science. 1998;282:1145-1147.
60. Volarevic, V., Markovic, B.S., Gazdic, M., Volarevic, A., Jovicic, N., Arsenijevic, N., Armstrong, L., Djonov, V., Lako, M., and Stojkovic, M. Ethical and safety issues of stem cell-based therapy. Int J Med Sci. 2018;15:36-45.
61. Marcus, A.J., and Woodbury, D. Fetal stem cells from extra-embryonic tissues: Do not discard. J Cell Mol Med. 2008;12:730-742.

62.   Takahashi, K., and Yamanaka, S. Induction of pluripotent stem cells from mouse embryonic and adult fibroblast cultures by defined factors. Cell. 2006;126:663-676.

63.   Alvarez, C.V., Garcia-Lavandeira, M., Garcia-Rendueles, M.E., Diaz-Rodriguez, E., Garcia-Rendueles, A.R., Perez-Romero, S., Vila, T.V., Rodrigues, J.S., Lear, P.V., and Bravo, S.B. Defining stem cell types: Understanding the therapeutic potential of ESCs, ASCs, and iPS cells. J Mol Endocrinol. 2012;49:R89-111.

64.   Caplan, A.I. Are all adult stem cells the same? Regen Eng Transl Med. 2015;1:4-10.

65.   Jacobson, L.O., Simmons, E.L., Marks, E.K., and Eldredge, J.H. Recovery from radiation injury. Science. 1951;113:510-511.

66.   Gluckman, E., Broxmeyer, H.A., Auerbach, A.D., Friedman, H.S., Douglas, G.W., Devergie, A., Esperou, H., Thierry, D., Socie, G., Lehn, P., and Et Al. Hematopoietic reconstitution in a patient with Fanconi's anemia by means of umbilical-cord blood from an HLA-identical sibling. N Engl J Med. 1989;321:1174-1178.

67.   Kita, K., Lee, J.O., Finnerty, C.C., and Herndon, D.N. Cord blood-derived hematopoietic stem/progenitor cells: Current challenges in engraftment, infection, and ex vivo expansion. Stem Cells Int. 2011;2011:276193.

68.   Munoz, J., Shah, N., Rezvani, K., Hosing, C., Bollard, C.M., Oran, B., Olson, A., Popat, U., Molldrem, J., Mcniece, I.K., and Shpall, E.J. Concise review: Umbilical cord blood transplantation: Past, present, and future. Stem Cells Transl Med. 2014;3:1435-1443.

69.   Rubinstein, P., Rosenfield, R.E., Adamson, J.W., and Stevens, C.E. Stored placental blood for unrelated bone marrow reconstitution. Blood. 1993;81:1679-1690.

70.   Friedenstein, A.J., Petrakova, K.V., Kurolesova, A.I., and Frolova, G.P. Heterotopic of bone marrow. Analysis of precursor cells for osteogenic and hematopoietic tissues. Transplantation. 1968;6:230-247.

71.   Da Silva Meirelles, L., Chagastelles, P.C., and Nardi, N.B. Mesenchymal stem cells reside in virtually all post-natal organs and tissues. J Cell Sci. 2006;119:2204-2213.

72.   Da Silva Meirelles, L., Caplan, A.I., and Nardi, N.B. In search of the in vivo identity of mesenchymal stem cells. Stem Cells. 2008;26:2287-2299.

73.   Ankrum, J., and Karp, J.M. Mesenchymal stem cell therapy: Two steps forward, one step back. Trends Mol Med. 2010;16:203-209.

74.   Taghavi, S., and George, J.C. Homing of stem cells to ischemic myocardium. Am J Transl Res. 2013;5:404-411.

75.   Karp, J.M., and Leng Teo, G.S. Mesenchymal stem cell homing: The devil is in the details. Cell Stem Cell. 2009;4:206-216.

76.   Horwitz, E.M., and Keating, A. Nonhematopoietic mesenchymal stem cells: What are they? Cytotherapy. 2000;2:387-388.

77.   Horwitz, E.M., Le Blanc, K., Dominici, M., Mueller, I., Slaper-Cortenbach, I., Marini, F.C., Deans, R.J., Krause, D.S., and Keating, A. Clarification of the nomenclature for MSC: The International Society for Cellular Therapy position statement. Cytotherapy. 2005;7:393-395.

78.   Bourin, P., Bunnell, B.A., Casteilla, L., Dominici, M., Katz, A.J., March, K.L., Redl, H., Rubin, J.P., Yoshimura, K., and Gimble, J.M. Stromal cells from the adipose tissue-derived stromal vascular fraction and culture expanded adipose tissue-derived stromal/stem cells: A joint statement of the International Federation for Adipose Therapeutics and Science (IFATS) and the International Society for Cellular Therapy (ISCT). Cytotherapy. 2013;15:641-648.

79.   Dominici, M., Le Blanc, K., Mueller, I., Slaper-Cortenbach, I., Marini, F., Krause, D., Deans, R., Keating, A., Prockop, D., and Horwitz, E. Minimal criteria for defining multipotent mesenchymal stromal cells. The International Society for Cellular Therapy position statement. Cytotherapy. 2006;8:315-317.

80. Kallmeyer, K., and Pepper, M.S. Homing properties of mesenchymal stromal cells. Expert Opin Biol Ther. 2015;15:477-479.

81. Liu, L., Yu, Q., Lin, J., Lai, X., Cao, W., Du, K., Wang, Y., Wu, K., Hu, Y., Zhang, L., Xiao, H., Duan, Y., and Huang, H. Hypoxia-inducible factor-1alpha is essential for hypoxia-induced mesenchymal stem cell mobilization into the peripheral blood. Stem Cells Dev. 2011;20:1961-1971.

82. Ponte, A.L., Marais, E., Gallay, N., Langonne, A., Delorme, B., Herault, O., Charbord, P., and Domenech, J. The in vitro migration capacity of human bone marrow mesenchymal stem cells: Comparison of chemokine and growth factor chemotactic activities. Stem Cells. 2007;25:1737-1745.

83. Murphy, M.B., Moncivais, K., and Caplan, A.I. Mesenchymal stem cells: environmentally responsive therapeutics for regenerative medicine. Exp Mol Med. 2013;45:e54.

84. Jackson, W.M., Nesti, L.J., and Tuan, R.S. Mesenchymal stem cell therapy for attenuation of scar formation during wound healing. Stem Cell Res Ther. 2012;3:20.

85. Maxson, S., Lopez, E.A., Yoo, D., Danilkovitch-Miagkova, A., and Leroux, M.A. Concise review: Role of mesenchymal stem cells in wound repair. Stem Cells Transl Med. 2012;1:142-149.

86. Alonso, L., and Fuchs, E. The hair cycle. J Cell Sci. 2006;119:391-393.

87. Brown, J.B., and Mcdowell, F. Epithelial healing and the transplantation of skin. Ann Surg. 1942;115:1166-1181.

88. Martinot, V., Mitchell, V., Fevrier, P., Duhamel, A., and Pellerin, P. Comparative study of split thickness skin grafts taken from the scalp and thigh in children. Burns. 1994;20:146-150.

89. Owczarczyk-Saczonek, A., Krajewska-Wlodarczyk, M., Kruszewska, A., Banasiak, L., Placek, W., Maksymowicz, W., and Wojtkiewicz, J. Therapeutic potential of stem cells in follicle regeneration. Stem Cells Int. 2018;2018:1049641.

90. Morgan, B.A. The dermal papilla: An instructive niche for epithelial stem and progenitor cells in development and regeneration of the hair follicle. Cold Spring Harb Perspect Med. 2014;4:a015180.

91. Claudinot, S., Nicolas, M., Oshima, H., Rochat, A., and Barrandon, Y. Long-term renewal of hair follicles from clonogenic multipotent stem cells. Proc Natl Acad Sci U S A. 2005;102:14677-14682.

92. Ito, M., Liu, Y., Yang, Z., Nguyen, J., Liang, F., Morris, R.J., and Cotsarelis, G. Stem cells in the hair follicle bulge contribute to wound repair but not to homeostasis of the epidermis. Nat Med. 2005;11:1351-1354.

93. Levy, V., Lindon, C., Harfe, B.D., and Morgan, B.A. Distinct stem cell populations regenerate the follicle and interfollicular epidermis. Dev Cell. 2005;9:855-861.

94. Kanji, S., and Das, H. Advances of stem cell therapeutics in cutaneous wound healing and regeneration. Mediators Inflamm. 2017;2017:5217967.

95. Langton, A.K., Herrick, S.E., and Headon, D.J. An extended epidermal response heals cutaneous wounds in the absence of a hair follicle stem cell contribution. J Invest Dermatol. 2008;128:1311-1318.

96. Chamberlain, G., Fox, J., Ashton, B., and Middleton, J. Concise review: Mesenchymal stem cells: Their phenotype, differentiation capacity, immunological features, and potential for homing. Stem Cells. 2007;25:2739-2749.

97. Singer, N.G., and Caplan, A.I. Mesenchymal stem cells: Mechanisms of inflammation. Annu Rev Pathol. 2011;6:457-478.

98. Sato, K., Ozaki, K., Oh, I., Meguro, A., Hatanaka, K., Nagai, T., Muroi, K., and Ozawa, K. Nitric oxide plays a critical role in suppression of T-cell proliferation by mesenchymal stem cells. Blood. 2007;109:228-234.

99. Muriel, P. Nitric oxide protection of rat liver from lipid peroxidation, collagen accumulation, and liver damage induced by carbon tetrachloride. Biochem Pharmacol. 1998;56:773-779.

100. Krasnodembskaya, A., Song, Y., Fang, X., Gupta, N., Serikov, V., Lee, J.W., and Matthay, M.A. Antibacterial effect of human mesenchymal stem cells is mediated in part from secretion of the antimicrobial peptide LL-37. *Stem Cells.* 2010;28:2229-2238.

101. Mei, S.H., Haitsma, J.J., Dos Santos, C.C., Deng, Y., Lai, P.F., Slutsky, A.S., Liles, W.C., and Stewart, D.J. Mesenchymal stem cells reduce inflammation while enhancing bacterial clearance and improving survival in sepsis. *Am J Respir Crit Care Med.* 2010;182:1047-1057.

102. Chen, L., Tredget, E.E., Wu, P.Y., and Wu, Y. Paracrine factors of mesenchymal stem cells recruit macrophages and endothelial lineage cells and enhance wound healing. *PLoS ONE.* 2008;3:e1886.

103. Gruber, R., Kandler, B., Holzmann, P., Vogele-Kadletz, M., Losert, U., Fischer, M.B., and Watzek, G. Bone marrow stromal cells can provide a local environment that favors migration and formation of tubular structures of endothelial cells. *Tissue Eng.* 2005;11:896-903.

104. Kaigler, D., Krebsbach, P.H., Polverini, P.J., and Mooney, D.J. Role of vascular endothelial growth factor in bone marrow stromal cell modulation of endothelial cells. *Tissue Eng.* 2003;9:95-103.

105. Sorrell, J.M., Baber, M.A., and Caplan, A.I. Influence of adult mesenchymal stem cells on in vitro vascular formation. *Tissue Eng Part A.* 2009;15:1751-1761.

106. Wu, Y., Chen, L., Scott, P.G., and Tredget, E.E. Mesenchymal stem cells enhance wound healing through differentiation and angiogenesis. *Stem Cells.* 2007;25:2648-2659.

107. Yamaguchi, Y., Kubo, T., Murakami, T., Takahashi, M., Hakamata, Y., Kobayashi, E., Yoshida, S., Hosokawa, K., Yoshikawa, K., and Itami, S. Bone marrow cells differentiate into wound myofibroblasts and accelerate the healing of wounds with exposed bones when combined with an occlusive dressing. *Br J Dermatol.* 2005;152:616-622.

108. Sasaki, M., Abe, R., Fujita, Y., Ando, S., Inokuma, D., and Shimizu, H. Mesenchymal Stem Cells Are Recruited into Wounded Skin and Contribute to Wound Repair by Transdifferentiation into Multiple Skin Cell Type. *The Journal of Immunology.* 2008;180:2581-2587.

109. Javazon, E.H., Keswani, S.G., Badillo, A.T., Crombleholme, T.M., Zoltick, P.W., Radu, A.P., Kozin, E.D., Beggs, K., Malik, A.A., and Flake, A.W. Enhanced epithelial gap closure and increased angiogenesis in wounds of diabetic mice treated with adult murine bone marrow stromal progenitor cells. *Wound Repair Regen.* 2007;15:350-359.

110. Kidd, S., Spaeth, E., Dembinski, J.L., Dietrich, M., Watson, K., Klopp, A., Battula, V.L., Weil, M., Andreeff, M., and Marini, F.C. Direct evidence of mesenchymal stem cell tropism for tumor and wounding microenvironments using in vivo bioluminescent imaging. *Stem Cells.* 2009;27:2614-2623.

111. Yin, Y., Hao, H., Cheng, Y., Gao, J., Liu, J., Xie, Z., Zhang, Q., Zang, L., Han, W., and Mu, Y. The homing of human umbilical cord-derived mesenchymal stem cells and the subsequent modulation of macrophage polarization in type 2 diabetic mice. *Int Immunopharmacol.* 2018;60:235-245.

112. Ley, K., Laudanna, C., Cybulsky, M.I., and Nourshargh, S. Getting to the site of inflammation: The leukocyte adhesion cascade updated. *Nat Rev Immunol.* 2007;7:678-689.

113. Muller, W.A. Mechanisms of transendothelial migration of leukocytes. *Circ Res.* 2009;105:223-230.

114. Muller, W.A. Mechanisms of leukocyte transendothelial migration. *Annu Rev Pathol.* 2011;6:323-344.

115. Luster, A.D., Alon, R., and Von Andrian, U.H. Immune cell migration in inflammation: Present and future therapeutic targets. *Nat Immunol.* 2005;6:1182-1190.

116. Yago, T., Shao, B., Miner, J.J., Yao, L., Klopocki, A.G., Maeda, K., Coggeshall, K.M., and Mcever, R.P. E-selectin engages PSGL-1 and CD44 through a common signaling pathway to induce integrin $\alpha_L\beta_2$-mediated slow leukocyte rolling. *Blood.* 2010;116:485-494.

117. Delves, P.J., Martin, S.J., Burton, D.R., Roitt, I.M. Roitt's essential immunology. UK: Blackwell Publishing Ltd; 2006.

118. Liu, Z.J., Zhuge, Y., and Velazquez, O.C. Trafficking and differentiation of mesenchymal stem cells. J Cell Biochem. 2009;106:984-991.

119. Honczarenko, M., Le, Y., Swierkowski, M., Ghiran, I., Glodek, A.M., and Silberstein, L.E. Human bone marrow stromal cells express a distinct set of biologically functional chemokine receptors. Stem Cells. 2006;24:1030-1041.

120. Von Luttichau, I., Notohamiprodjo, M., Wechselberger, A., Peters, C., Henger, A., Seliger, C., Djafarzadeh, R., Huss, R., and Nelson, P.J. Human adult CD34- progenitor cells functionally express the chemokine receptors CCR1, CCR4, CCR7, CXCR5, and CCR10 but not CXCR4. Stem Cells Dev. 2005;14:329-336.

121. Levesque, J.P., Hendy, J., Takamatsu, Y., Simmons, P.J., and Bendall, L.J. Disruption of the CXCR4/CXCL12 chemotactic interaction during hematopoietic stem cell mobilization induced by GCSF or cyclophosphamide. J Clin Invest. 2003;111:187-196.

122. Petit, I., Szyper-Kravitz, M., Nagler, A., Lahav, M., Peled, A., Habler, L., Ponomaryov, T., Taichman, R.S., Arenzana-Seisdedos, F., Fujii, N., Sandbank, J., Zipori, D., and Lapidot, T. G-CSF induces stem cell mobilization by decreasing bone marrow SDF-1 and up-regulating CXCR4. Nat Immunol. 2002;3:687-694.

123. Son, B.R., Marquez-Curtis, L.A., Kucia, M., Wysoczynski, M., Turner, A.R., Ratajczak, J., Ratajczak, M.Z., and Janowska-Wieczorek, A. Migration of bone marrow and cord blood mesenchymal stem cells in vitro is regulated by stromal-derived factor-1-CXCR4 and hepatocyte growth factor-c-met axes and involves matrix metalloproteinases. Stem Cells. 2006;24:1254-1264.

124. Jin, W., Liang, X., Brooks, A., Futrega, K., Liu, X., Doran, M.R., Simpson, M.J., Roberts, M.S., and Wang, H. Modelling of the SDF-1/CXCR4 regulated in vivo homing of therapeutic mesenchymal stem/stromal cells in mice. PeerJ. 2018;6:e6072.

125. Ip, J.E., Wu, Y., Huang, J., Zhang, L., Pratt, R.E., and Dzau, V.J. Mesenchymal stem cells use integrin beta1 not CXC chemokine receptor 4 for myocardial migration and engraftment. Mol Biol Cell. 2007;18:2873-2882.

126. Ruster, B., Gottig, S., Ludwig, R.J., Bistrian, R., Muller, S., Seifried, E., Gille, J., and Henschler, R. Mesenchymal stem cells display coordinated rolling and adhesion behavior on endothelial cells. Blood. 2006;108:3938-3944.

127. Nitzsche, F., Muller, C., Lukomska, B., Jolkkonen, J., Deten, A., and Boltze, J. Concise review: MSC adhesion cascade-insights into homing and transendothelial migration. Stem Cells. 2017;35:1446-1460.

128. Cianfarani, F., Toietta, G., Di Rocco, G., Cesareo, E., Zambruno, G., and Odorisio, T. Diabetes impairs adipose tissue-derived stem cell function and efficiency in promoting wound healing. Wound Repair Regen. 2013;21:545-553.

129. Jin, P., Zhang, X., Wu, Y., Li, L., Yin, Q., Zheng, L., Zhang, H., and Sun, C. Streptozotocin-induced diabetic rat-derived bone marrow mesenchymal stem cells have impaired abilities in proliferation, paracrine, antiapoptosis, and myogenic differentiation. Transplant Proc. 2010;42:2745-2752.

130. Eming, S.A., Krieg, T., and Davidson, J.M. Inflammation in wound repair: Molecular and cellular mechanisms. J Invest Dermatol. 2007;127:514-525.

131. Leibovich, S.J., and Ross, R. The role of the macrophage in wound repair. A study with hydrocortisone and antimacrophage serum. Am J Pathol. 1975;78:71-100.

132. Schaffer, M.R., Efron, P.A., Thornton, F.J., Klingel, K., Gross, S.S., and Barbul, A. Nitric oxide, an autocrine regulator of wound fibroblast synthetic function. J Immunol. 1997;158:2375-2381.

133. Werner, S., Krieg, T., and Smola, H. Keratinocyte-fibroblast interactions in wound healing. J Invest Dermatol. 2007;127:998-1008.

134. Atashi, F., Modarressi, A., and Pepper, M.S. The role of reactive oxygen species in mesenchymal stem cell adipogenic and osteogenic differentiation: A review. Stem Cells Dev. 2015;24:1150-1163.

135. Kean, T.J., Lin, P., Caplan, A.I., and Dennis, J.E. MSCs: Delivery routes and engraftment, cell-targeting strategies, and immune modulation. Stem Cells Int. 2013;2013:732742.

136. Le Blanc, K., Tammik, C., Rosendahl, K., Zetterberg, E., and Ringdén, O. HLA expression and immunologic propertiesof differentiated and undifferentiated mesenchymal stem cells. Exp Hematol. 2003;31:890-896.

137. Ma, S., Xie, N., Li, W., Yuan, B., Shi, Y., and Wang, Y. Immunobiology of mesenchymal stem cells. Cell Death Differ. 2014;21:216-225.

138. Leto Barone, A.A., Khalifian, S., Lee, W.P., and Brandacher, G. Immunomodulatory effects of adipose-derived stem cells: Fact or fiction? Biomed Res Int. 2013;2013:383685.

139. Hocking, A.M., and Gibran, N.S. Mesenchymal stem cells: Paracrine signaling and differentiation during cutaneous wound repair. Exp Cell Res. 2010;316:2213-2219.

140. Kuo, Y.R., Wang, C.T., Cheng, J.T., Kao, G.S., Chiang, Y.C., and Wang, C.J. Adipose-derived stem cells accelerate diabetic wound healing through the induction of autocrine and paracrine effects. Cell Transplant. 2016;25:71-81.

141. Krampera, M., Cosmi, L., Angeli, R., Pasini, A., Liotta, F., Andreini, A., Santarlasci, V., Mazzinghi, B., Pizzolo, G., Vinante, F., Romagnani, P., Maggi, E., Romagnani, S., and Annunziato, F. Role for interferon-gamma in the immunomodulatory activity of human bone marrow mesenchymal stem cells. Stem Cells. 2006;24:386-398.

142. Hoogduijn, M.J., and Lombardo, E. Concise review: Mesenchymal stromal cells anno 2019: Dawn of the therapeutic era? Stem Cells Transl Med. 2019.

143. Regateiro, F.S., Cobbold, S.P., and Waldmann, H. CD73 and adenosine generation in the creation of regulatory microenvironments. Clin Exp Immunol. 2013;171:1-7.

144. Kumar, V., and Sharma, A. Adenosine: An endogenous modulator of innate immune system with therapeutic potential. Eur J Pharmacol. 2009;616:7-15.

145. Crop, M.J., Baan, C.C., Korevaar, S.S., Ijzermans, J.N., Pescatori, M., Stubbs, A.P., Van Ijcken, W.F., Dahlke, M.H., Eggenhofer, E., Weimar, W., and Hoogduijn, M.J. Inflammatory conditions affect gene expression and function of human adipose tissue-derived mesenchymal stem cells. Clin Exp Immunol. 2010;162:474-486.

146. De Witte, S.F.H., Luk, F., Sierra Parraga, J.M., Gargesha, M., Merino, A., Korevaar, S.S., Shankar, A.S., O'flynn, L., Elliman, S.J., Roy, D., Betjes, M.G.H., Newsome, P.N., Baan, C.C., and Hoogduijn, M.J. Immunomodulation by therapeutic mesenchymal stromal cells (MSC) is triggered through phagocytosis of MSC by monocytic cells. Stem Cells. 2018;36:602-615.

147. Mohyeldin, A., Garzon-Muvdi, T., and Quinones-Hinojosa, A. Oxygen in stem cell biology: A critical component of the stem cell niche. Cell Stem Cell. 2010;7:150-161.

148. Holzwarth, C., Vaegler, M., Gieseke, F., Pfister, S.M., Handgretinger, R., Kerst, G., and Muller, I. Low physiologic oxygen tensions reduce proliferation and differentiation of human multipotent mesenchymal stromal cells. BMC Cell Biol. 2010;11:11.

149. Haque, N., Rahman, M.T., Abu Kasim, N.H., and Alabsi, A.M. Hypoxic culture conditions as a solution for mesenchymal stem cell based regenerative therapy. Sci World J. 2013;2013:632972.

150. Vojtassak, J., Danisovic, L., Kubes, M., Bakos, D., Jarabek, L., Ulicna, M., and Blasko, M. Autologous biograft and mesenchymal stem cells in treatment of the diabetic foot. Neuro Endocrinol Lett. 2006;27 Suppl 2:134-137.

151. Lu, D., Chen, B., Liang, Z., Deng, W., Jiang, Y., Li, S., Xu, J., Wu, Q., Zhang, Z., Xie, B., and Chen, S. Comparison of bone marrow mesenchymal stem cells with bone marrow-derived mononuclear

cells for treatment of diabetic critical limb ischemia and foot ulcer: A double-blind, randomized, controlled trial. Diabetes Res Clin Pract. 2011;92:26-36.

152. Yoshikawa, T., Mitsuno, H., Nonaka, I., Sen, Y., Kawanishi, K., Inada, Y., Takakura, Y., Okuchi, K., and Nonomura, A. Wound therapy by marrow mesenchymal cell transplantation. Plast Reconstr Surg. 2008;121:860-877.

153. Dash, N.R., Dash, S.N., Routray, P., Mohapatra, S., and Mohapatra, P.C. Targeting nonhealing ulcers of lower extremity in human through autologous bone marrow-derived mesenchymal stem cells. Rejuvenation Res. 2009;12:359-366.

154. Coleman, S.R., and Saboeiro, A.P. Fat grafting to the breast revisited: Safety and efficacy. Plast Reconstr Surg. 2007;119:775-785; discussion 786-777.

155. Galie, M., Pignatti, M., Scambi, I., Sbarbati, A., and Rigotti, G. Comparison of different centrifugation protocols for the best yield of adipose-derived stromal cells from lipoaspirates. Plast Reconstr Surg. 2008;122:233e-234e.

156. Zuk, P.A., Zhu, M., Ashjian, P., De Ugarte, D.A., Huang, J.I., Mizuno, H., Alfonso, Z.C., Fraser, J.K., Benhaim, P., and Hedrick, M.H. Human adipose tissue is a source of multipotent stem cells. Mol Biol Cell. 2002;13:4279-4295.

157. Dominici, M., Paolucci, P., Conte, P., and Horwitz, E.M. Heterogeneity of multipotent mesenchymal stromal cells: From stromal cells to stem cells and vice versa. Transplantation. 2009;87:S36-42.

158. Pittenger, M.F., Mackay, A.M., Beck, S.C., Jaiswal, R.K., Douglas, R., Mosca, J.D., Moorman, M.A., Simonetti, D.W., Craig, S., and Marshak, D.R. Multilineage potential of adult human mesenchymal stem cells. Science. 1999;284:143-147.

159. Zuk, P.A., Zhu, M., Mizuno, H., Huang, J., Futrell, J.W., Katz, A.J., Benhaim, P., Lorenz, H.P., and Hedrick, M.H. Multilineage cells from human adipose tissue: Implications for cell-based therapies. Tissue Eng. 2001;7:211-228.

160. Kern, S., Eichler, H., Stoeve, J., Kluter, H., and Bieback, K. Comparative analysis of mesenchymal stem cells from bone marrow, umbilical cord blood, or adipose tissue. Stem Cells. 2006;24:1294-1301.

161. Strioga, M., Viswanathan, S., Darinskas, A., Slaby, O., and Michalek, J. Same or not the same? Comparison of adipose tissue-derived versus bone marrow-derived mesenchymal stem and stromal cells. Stem Cells Dev. 2012;21:2724-2752.

162. Wagner, W., Wein, F., Seckinger, A., Frankhauser, M., Wirkner, U., Krause, U., Blake, J., Schwager, C., Eckstein, V., Ansorge, W., and Ho, A.D. Comparative characteristics of mesenchymal stem cells from human bone marrow, adipose tissue, and umbilical cord blood. Exp Hematol. 2005;33:1402-1416.

163. Sensebe, L., and Fleury-Cappellesso, S. Biodistribution of mesenchymal stem/stromal cells in a preclinical setting. Stem Cells Int. 2013;2013:678063.

164. Kim, J.E., Kalimuthu, S., and Ahn, B.C. In vivo cell tracking with bioluminescence imaging. Nucl Med Mol Imaging. 2015;49:3-10.

165. Strohschein, K., Radojewski, P., Winkler, T., Duda, G.N., Perka, C., and Von Roth, P. In vivo bioluminescence imaging - a suitable method to track mesenchymal stromal cells in a skeletal muscle trauma. Open Orthop J. 2015;9:262-269.

166. Togel, F., Yang, Y., Zhang, P., Hu, Z., and Westenfelder, C. Bioluminescence imaging to monitor the in vivo distribution of administered mesenchymal stem cells in acute kidney injury. Am J Physiol Renal Physiol. 2008;295:F315-321.

167. Sadie-Van Gijsen, H., Crowther, N.J., Hough, F.S., and Ferris, W.F. Depot-specific differences in the insulin response of adipose-derived stromal cells. Mol Cell Endocrinol. 2010;328:22-27.

168. Van De Vyver, M., Andrag, E., Cockburn, I.L., and Ferris, W.F. Thiazolidinedione-induced lipid droplet formation during osteogenic differentiation. J Endocrinol. 2014;223:119-132.

169. Huang, J.I., Beanes, S.R., Zhu, M., Lorenz, H.P., Hedrick, M.H., and Benhaim, P. Rat extramedullary adipose tissue as a source of osteochondrogenic progenitor cells. Plast Reconstr Surg. 2002;109:1033-1041; discussion 1042-1033.

170. Tennant, J.R. Evaluation of the trypan blue technique for determination of cell viability. Transplantation. 1964;2:685-694.

171. Merten, O.W., Hebben, M., and Bovolenta, C. Production of lentiviral vectors. Molecular therapy. Methods & clinical development. 2016;3:16017.

172. Giry-Laterrière, M., Verhoeyen, E., and Salmon, P. Lentiviral vectors. In: Merten, O.-W., Al-Rubeai, M., eds. Viral vectors for gene therapy: Methods and protocols. Totowa, NJ: Humana Press; 2011:183-209.

173. Bhaumik, S., and Gambhir, S.S. Optical imaging of renilla luciferase reporter gene expression in living mice. Proc Natl Acad Sci U S A. 2002;99:377-382.

174. Vandesompele, J., De Preter, K., Pattyn, F., Poppe, B., Van Roy, N., De Paepe, A., and Speleman, F. Accurate normalization of real-time quantitative RT-PCR data by geometric averaging of multiple internal control genes. Genome Biol. 2002;3:RESEARCH0034.

175. Lembert, N., and Idahl, L.A. Regulatory effects of ATP and luciferin on firefly luciferase activity. Biochem J. 1995;305 (Pt 3):929-933.

176. Van Vollenstee, F.A., Jackson, C., Hoffmann, D., Potgieter, M., Durandt, C., and Pepper, M.S. Human adipose derived mesenchymal stromal cells transduced with GFP lentiviral vectors: Assessment of immunophenotype and differentiation capacity in vitro. Cytotechnology. 2016;68:2049-2060.

177. Wang, Q., Steigelman, M.B., Walker, J.A., Chen, S., Hornsby, P.J., Bohnenblust, M.E., and Wang, H.T. In vitro osteogenic differentiation of adipose stem cells after lentiviral transduction with green fluorescent protein. J Craniofac Surg. 2009;20:2193-2199.

178. Moseti, D., Regassa, A., and Kim, W.K. Molecular regulation of adipogenesis and potential anti-adipogenic bioactive molecules. Int J Mol Sci. 2016;17:124.

179. Lee, J.E., and Ge, K. Transcriptional and epigenetic regulation of PPARgamma expression during adipogenesis. Cell Biosci. 2014;4:29.

180. Garin-Shkolnik, T., Rudich, A., Hotamisligil, G.S., and Rubinstein, M. FABP4 attenuates PPARγ and adipogenesis and is inversely correlated with PPARγ in adipose tissues. Diabetes. 2014;63:900-911.

181. Tontonoz, P., Hu, E., and Spiegelman, B.M. Stimulation of adipogenesis in fibroblasts by PPAR gamma 2, a lipid-activated transcription factor. Cell. 1994;79:1147-1156.

182. Tontonoz, P., and Spiegelman, B.M. Fat and beyond: The diverse biology of PPARgamma. Annu Rev Biochem. 2008;77:289-312.

183. Kim, H.J., and Park, J.S. Usage of human mesenchymal stem cells in cell-based therapy: Advantages and disadvantages. Dev Reprod. 2017;21:1-10.

184. Wei, X., Yang, X., Han, Z.P., Qu, F.F., Shao, L., and Shi, Y.F. Mesenchymal stem cells: A new trend for cell therapy. Acta Pharmacol Sin. 2013;34:747-754.

185. Squillaro, T., Peluso, G., and Galderisi, U. Clinical trials with mesenchymal stem cells: An update. Cell Transplant. 2016;25:829-848.

186. Ghaderi, A., and Abtahi, S. Mesenchymal stem cells: Miraculous healers or dormant killers? Stem Cell Rev. 2018;14:722-733.

187. Kirana, S., Stratmann, B., Prante, C., Prohaska, W., Koerperich, H., Lammers, D., Gastens, M.H., Quast, T., Negrean, M., Stirban, O.A., Nandrean, S.G., Gotting, C., Minartz, P., Kleesiek, K., and

Tschoepe, D. Autologous stem cell therapy in the treatment of limb ischaemia induced chronic tissue ulcers of diabetic foot patients. Int J Clin Pract. 2012;66:384-393.

188. Lafosse, A., Dufeys, C., Beauloye, C., Horman, S., and Dufrane, D. Impact of hyperglycemia and low oxygen tension on adipose-derived stem cells compared with dermal fibroblasts and keratinocytes: Importance for wound healing in type 2 diabetes. PLoS ONE. 2016;11:e0168058.

189. Mishra, S.K., Khushu, S., Singh, A.K., and Gangenahalli, G. Homing and tracking of iron oxide labelled mesenchymal stem cells after infusion in traumatic brain injury mice: A longitudinal in vivo MRI study. Stem Cell Rev. 2018;14:888-900.

190. Oh, E.J., Lee, H.W., Kalimuthu, S., Kim, T.J., Kim, H.M., Baek, S.H., Zhu, L., Oh, J.M., Son, S.H., Chung, H.Y., and Ahn, B.C. In vivo migration of mesenchymal stem cells to burn injury sites and their therapeutic effects in a living mouse model. J Control Release. 2018;279:79-88.

191. Everaert, B.R., Bergwerf, I., De Vocht, N., Ponsaerts, P., Van Der Linden, A., Timmermans, J.P., and Vrints, C.J. Multimodal in vivo imaging reveals limited allograft survival, intrapulmonary cell trapping and minimal evidence for ischemia-directed BMSC homing. BMC Biotechnol. 2012;12:93.

192. Kurtz, A. Mesenchymal stem cell delivery routes and fate. Int J Stem Cells. 2008;1:1-7.

193. Caplan, A.I. Why are MSCs therapeutic? New data: New insight. J Pathol. 2009;217:318-324.

194. Sorrell, J.M., and Caplan, A.I. Topical delivery of mesenchymal stem cells and their function in wounds. Stem Cell Res Ther. 2010;1:30.

195. Huang, S., Xu, L., Zhang, Y., Sun, Y., and Li, G. Systemic and local administration of allogeneic bone marrow-derived mesenchymal stem cells promotes fracture healing in rats. Cell Transplant. 2015;24:2643-2655.

196. Andre-Levigne, D., Modarressi, A., Pignel, R., Bochaton-Piallat, M.L., and Pittet-Cuenod, B. Hyperbaric oxygen therapy promotes wound repair in ischemic and hyperglycemic conditions, increasing tissue perfusion and collagen deposition. Wound Repair Regen. 2016;24:954-965.

197. Rashband, W.S. Image J, U.S. National Institutes of Health, Betheshda, Maryland, USA. Available at: http://imagej.nih.gov/ij.

198. Horwitz, E.M., Gordon, P.L., Koo, W.K., Marx, J.C., Neel, M.D., Mcnall, R.Y., Muul, L., and Hofmann, T. Isolated allogeneic bone marrow-derived mesenchymal cells engraft and stimulate growth in children with osteogenesis imperfecta: Implications for cell therapy of bone. Proc Natl Acad Sci U S A. 2002;99:8932-8937.

199. Horwitz, E.M., Prockop, D.J., Fitzpatrick, L.A., Koo, W.W., Gordon, P.L., Neel, M., Sussman, M., Orchard, P., Marx, J.C., Pyeritz, R.E., and Brenner, M.K. Transplantability and therapeutic effects of bone marrow-derived mesenchymal cells in children with osteogenesis imperfecta. Nat Med. 1999;5:309-313.

200. Leibacher, J., and Henschler, R. Biodistribution, migration and homing of systemically applied mesenchymal stem/stromal cells. Stem Cell Res Ther. 2016;7:7.

201. Fischer, U.M., Harting, M.T., Jimenez, F., Monzon-Posadas, W.O., Xue, H., Savitz, S.I., Laine, G.A., and Cox, C.S., Jr. Pulmonary passage is a major obstacle for intravenous stem cell delivery: The pulmonary first-pass effect. Stem Cells Dev. 2009;18:683-692.

202. Assis, A.C., Carvalho, J.L., Jacoby, B.A., Ferreira, R.L., Castanheira, P., Diniz, S.O., Cardoso, V.N., Goes, A.M., and Ferreira, A.J. Time-dependent migration of systemically delivered bone marrow mesenchymal stem cells to the infarcted heart. Cell Transplant. 2010;19:219-230.

203. Eggenhofer, E., Benseler, V., Kroemer, A., Popp, F.C., Geissler, E.K., Schlitt, H.J., Baan, C.C., Dahlke, M.H., and Hoogduijn, M.J. Mesenchymal stem cells are short-lived and do not migrate beyond the lungs after intravenous infusion. Front Immunol. 2012;3:297-297.

204. Gupta, A., and Kumar, P. Assessment of the histological state of the healing wound. Plast Aesthet Res. 2015;2:239-242.

205. Masterson, C.H., Curley, G.F., and Laffey, J.G. Modulating the distribution and fate of exogenously delivered mscs to enhance therapeutic potential: Knowns and unknowns. Intensive care medicine experimental. 2019;7:41.

206. Lee, R.H., Pulin, A.A., Seo, M.J., Kota, D.J., Ylostalo, J., Larson, B.L., Semprun-Prieto, L., Delafontaine, P., and Prockop, D.J. Intravenous hMSCs improve myocardial infarction in mice because cells embolized in lung are activated to secrete the anti-inflammatory protein TSG-6. Cell Stem Cell. 2009;5:54-63.

207. Epstein, S.E., Luger, D., and Lipinski, M.J. Paracrine-mediated systemic anti-inflammatory activity of intravenously administered mesenchymal stem cells: A transformative strategy for cardiac stem cell therapeutics. Circ Res. 2017;121:1044-1046.

208. Shah, R., Patel, T., and Freedman, J.E. Circulating extracellular vesicles in human disease. N Engl J Med. 2018;379:958-966.

209. Zheng, G., Huang, R., Qiu, G., Ge, M., Wang, J., Shu, Q., and Xu, J. Mesenchymal stromal cell-derived extracellular vesicles: Regenerative and immunomodulatory effects and potential applications in sepsis. Cell and Tissue Research. 2018;374:1-15.

210. Huang, J.H., Yin, X.M., Xu, Y., Xu, C.C., Lin, X., Ye, F.B., Cao, Y., and Lin, F.Y. Systemic administration of exosomes released from mesenchymal stromal cells attenuates apoptosis, inflammation, and promotes angiogenesis after spinal cord injury in rats. J Neurotrauma. 2017;34:3388-3396.

211. Shabbir, A., Cox, A., Rodriguez-Menocal, L., Salgado, M., and Van Badiavas, E. Mesenchymal stem cell exosomes induce proliferation and migration of normal and chronic wound fibroblasts, and enhance angiogenesis in vitro. Stem Cells Dev. 2015;24:1635-1647.

212. Ma, T., Fu, B., Yang, X., Xiao, Y., and Pan, M. Adipose mesenchymal stem cell-derived exosomes promote cell proliferation, migration, and inhibit cell apoptosis via Wnt/beta-catenin signaling in cutaneous wound healing. J Cell Biochem. 2019;120:10847-10854.

213. Gelberman, R.H., Linderman, S.W., Jayaram, R., Dikina, A.D., Sakiyama-Elbert, S., Alsberg, E., Thomopoulos, S., and Shen, H. Combined administration of ASCs and BMP-12 promotes an M2 macrophage phenotype and enhances tendon healing. Clin Orthop Relat Res. 2017;475:2318-2331.

214. Lucke, L.D., Bortolazzo, F.O., Theodoro, V., Fujii, L., Bombeiro, A.L., Felonato, M., Dalia, R.A., Carneiro, G.D., Cartarozzi, L.P., Vicente, C.P., Oliveira, A.L.R., Mendonca, F.a.S., Esquisatto, M.a.M., Pimentel, E.R., and De Aro, A.A. Low-level laser and adipose-derived stem cells altered remodelling genes expression and improved collagen reorganization during tendon repair. Cell Prolif. 2019;52:e12580.

215. De Aro, A.A., Carneiro, G.D., Teodoro, L.F.R., Da Veiga, F.C., Ferrucci, D.L., Simoes, G.F., Simoes, P.W., Alvares, L.E., De Oliveira, A.L.R., Vicente, C.P., Gomes, C.P., Pesquero, J.B., Esquisatto, M.a.M., De Campos Vidal, B., and Pimentel, E.R. Injured achilles tendons treated with adipose-derived stem cells transplantation and GDF-5. Cells. 2018;7:127.

216. Nishiwaki, K., Aoki, S., Kinoshita, M., Kiyosawa, T., Suematsu, Y., Takeoka, S., and Fujie, T. In situ transplantation of adipose tissue-derived stem cells organized on porous polymer nanosheets for murine skin defects. J Biomed Mater Res B Appl Biomater. 2019;107:1363-1371.

217. Irons, R.F., Cahill, K.W., Rattigan, D.A., Marcotte, J.H., Fromer, M.W., Chang, S., Zhang, P., Behling, E.M., Behling, K.C., and Caputo, F.J. Acceleration of diabetic wound healing with adipose-derived stem cells, endothelial-differentiated stem cells, and topical conditioned medium therapy in a swine model. J Vasc Surg. 2018;68:115S-125S.

218. Yu, J., Wang, M.Y., Tai, H.C., and Cheng, N.C. Cell sheet composed of adipose-derived stem cells demonstrates enhanced skin wound healing with reduced scar formation. Acta Biomater. 2018;77:191-200.

219. Chae, D.S., Han, S., Son, M., and Kim, S.W. Stromal vascular fraction shows robust wound healing through high chemotactic and epithelialization property. Cytotherapy. 2017;19:543-554.

220. Kato, Y., Iwata, T., Washio, K., Yoshida, T., Kuroda, H., Morikawa, S., Hamada, M., Ikura, K., Kaibuchi, N., Yamato, M., Okano, T., and Uchigata, Y. Creation and transplantation of an adipose-derived stem cell (ASC) sheet in a diabetic wound-healing model. J Vis Exp. 2017:e54539.

221. Chicharro, D., Carrillo, J.M., Rubio, M., Cugat, R., Cuervo, B., Guil, S., Forteza, J., Moreno, V., Vilar, J.M., and Sopena, J. Combined plasma rich in growth factors and adipose-derived mesenchymal stem cells promotes the cutaneous wound healing in rabbits. BMC Vet Res. 2018;14:288.

222. Rodriguez, J., Boucher, F., Lequeux, C., Josset-Lamaugarny, A., Rouyer, O., Ardisson, O., Rutschi, H., Sigaudo-Roussel, D., Damour, O., and Mojallal, A. Intradermal injection of human adipose-derived stem cells accelerates skin wound healing in nude mice. Stem Cell Res Ther. 2015;6:241.

223. Prasai, A., El Ayadi, A., Mifflin, R.C., Wetzel, M.D., Andersen, C.R., Redl, H., Herndon, D.N., and Finnerty, C.C. Characterization of adipose-derived stem cells following burn injury. Stem Cell Rev Rep. 2017;13:781-792.

224. Yin, H., Jiang, T., Deng, X., Yu, M., Xing, H., and Ren, X. A cellular spinal cord scaffold seeded with rat adiposederived stem cells facilitates functional recovery via enhancing axon regeneration in spinal cord injured rats. Mol Med Rep. 2018;17:2998-3004.

225. Gomes, E.D., Mendes, S.S., Assuncao-Silva, R.C., Teixeira, F.G., Pires, A.O., Anjo, S.I., Manadas, B., Leite-Almeida, H., Gimble, J.M., Sousa, N., Lepore, A.C., Silva, N.A., and Salgado, A.J. Co-transplantation of adipose tissue-derived stromal cells and olfactory ensheathing cells for spinal cord injury repair. Stem Cells. 2018;36:696-708.

226. Corsetti, A., Bahuschewskyj, C., Ponzoni, D., Langie, R., Santos, L.A., Camassola, M., Nardi, N.B., and Puricelli, E. Repair of bone defects using adipose-derived stem cells combined with alpha-tricalcium phosphate and gelatin sponge scaffolds in a rat model. Journal of applied oral science : revista FOB. 2017;25:10-19.

227. Dreifke, M.B., Jayasuriya, A.A., and Jayasuriya, A.C. Current wound healing procedures and potential care. Mater Sci Eng C Mater Biol Appl. 2015;48:651-662.

228. Bertozzi, N., Simonacci, F., Grieco, M.P., Grignaffini, E., and Raposio, E. The biological and clinical basis for the use of adipose-derived stem cells in the field of wound healing. Ann Med Surg (Lond). 2017;20:41-48.

229. Duscher, D., Barrera, J., Wong, V.W., Maan, Z.N., Whittam, A.J., Januszyk, M., and Gurtner, G.C. Stem cells in wound healing: The future of regenerative medicine? A mini-review. Gerontology. 2016;62:216-225.

230. Hu, M.S., Borrelli, M.R., Lorenz, H.P., Longaker, M.T., and Wan, D.C. Mesenchymal stromal cells and cutaneous wound healing: A comprehensive review of the background, role, and therapeutic potential. Stem Cells Int. 2018;2018:6901983.

231. Deng, M., Mei, T., Hou, T., Luo, K., Luo, F., Yang, A., Yu, B., Pang, H., Dong, S., and Xu, J. TGFbeta3 recruits endogenous mesenchymal stem cells to initiate bone regeneration. Stem Cell Res Ther. 2017;8:258.

232. Koenen, P., Spanholtz, T.A., Maegele, M., Sturmer, E., Brockamp, T., Neugebauer, E., and Thamm, O.C. Acute and chronic wound fluids inversely influence adipose-derived stem cell function: Molecular insights into impaired wound healing. Int Wound J. 2015;12:10-16.

233. Dorsett-Martin, W.A., and Wysocki, A.B. Rat models of skin wound healing. In: Conn, P.M., ed. Sourcebook of Models for Biomedical Research. Totowa, NJ: Humana Press; 2008:631-638.

234. Galiano, R.D., Michaels, J.T., Dobryansky, M., Levine, J.P., and Gurtner, G.C. Quantitative and reproducible murine model of excisional wound healing. Wound Repair Regen. 2004;12:485-492.

235. Levigne, D., Tobalem, M., Modarressi, A., and Pittet-Cuenod, B. Hyperglycemia increases susceptibility to ischemic necrosis. Biomed Res Int. 2013;2013:490964.

236. Tobalem, M., Levigne, D., Modarressi, A., Atashi, F., Villard, F., Hinz, B., and Pittet-Cuenod, B. Hyperglycemia interacts with ischemia in a synergistic way on wound repair and myofibroblast differentiation. Plast Reconstr Surg Glob Open. 2015;3:e471.

237. Alizadeh, N., Pepper, M.S., Modarressi, A., Alfo, K., Schlaudraff, K., Montandon, D., Gabbiani, G., Bochaton-Piallat, M.L., and Pittet, B. Persistent ischemia impairs myofibroblast development in wound granulation tissue: a new model of delayed wound healing. Wound Repair Regen. 2007;15:809-816.

238. Skalli, O., Ropraz, P., Trzeciak, A., Benzonana, G., Gillessen, D., and Gabbiani, G. A monoclonal antibody against alpha-smooth muscle actin: A new probe for smooth muscle differentiation. J Cell Biol. 1986;103:2787-2796.

239. Prochazka, V., Gumulec, J., Jaluvka, F., Salounova, D., Jonszta, T., Czerny, D., Krajca, J., Urbanec, R., Klement, P., Martinek, J., and Klement, G.L. Cell therapy, a new standard in management of chronic critical limb ischemia and foot ulcer. Cell Transplant. 2010;19:1413-1424.

240. Gu, C., Huang, S., Gao, D., Wu, Y., Li, J., Ma, K., Wu, X., and Fu, X. Angiogenic effect of mesenchymal stem cells as a therapeutic target for enhancing diabetic wound healing. Int J Low Extrem Wounds. 2014;13:88-93.

241. Kim, Y., Kim, H., Cho, H., Bae, Y., Suh, K., and Jung, J. Direct comparison of human mesenchymal stem cells derived from adipose tissues and bone marrow in mediating neovascularization in response to vascular ischemia. Cell Physiol Biochem. 2007;20:867-876.

242. Hyldig, K., Riis, S., Pennisi, C.P., Zachar, V., and Fink, T. Implications of extracellular matrix production by adipose tissue-derived stem cells for development of wound healing therapies. Int J Mol Sci. 2017;18:1167.

243. He, X., Dong, Z., Cao, Y., Wang, H., Liu, S., Liao, L., Jin, Y., Yuan, L., and Li, B. Msc-derived exosome promotes M2 polarization and enhances cutaneous wound healing. Stem Cells Int. 2019;2019:7132708.

244. Bura, A., Planat-Benard, V., Bourin, P., Silvestre, J.S., Gross, F., Grolleau, J.L., Saint-Lebese, B., Peyrafitte, J.A., Fleury, S., Gadelorge, M., Taurand, M., Dupuis-Coronas, S., Leobon, B., and Casteilla, L. Phase I trial: the use of autologous cultured adipose-derived stroma/stem cells to treat patients with non-revascularizable critical limb ischemia. Cytotherapy. 2014;16:245-257.

245. Guo, J., Dardik, A., Fang, K., Huang, R., and Gu, Y. Meta-analysis on the treatment of diabetic foot ulcers with autologous stem cells. Stem Cell Res Ther. 2017;8:228.

246. Huang, P., Li, S., Han, M., Xiao, Z., Yang, R., and Han, Z.C. Autologous transplantation of granulocyte colony-stimulating factor-mobilized peripheral blood mononuclear cells improves critical limb ischemia in diabetes. Diabetes Care. 2005;28:2155-2160.

247. Han, S.K., Kim, H.R., and Kim, W.K. The treatment of diabetic foot ulcers with uncultured, processed lipoaspirate cells: a pilot study. Wound Repair Regen. 2010;18:342-348.

248. Nunan, R., Harding, K.G., and Martin, P. Clinical challenges of chronic wounds: Searching for an optimal animal model to recapitulate their complexity. Dis Model Mech. 2014;7:1205-1213.

249. Isakson, M., De Blacam, C., Whelan, D., Mcardle, A., and Clover, A.J. Mesenchymal stem cells and cutaneous wound healing: Current evidence and future potential. Stem Cells Int. 2015;2015:831095.

250. Lotfy, A., Salama, M., Zahran, F., Jones, E., Badawy, A., and Sobh, M. Characterization of mesenchymal stem cells derived from rat bone marrow and adipose tissue: A comparative study. Int J Stem Cells. 2014;7:135-142.

251. Nuschke, A. Activity of mesenchymal stem cells in therapies for chronic skin wound healing. Organogenesis. 2014;10:29-37.

252. Dorsett-Martin, W.A. Rat models of skin wound healing: A review. Wound Repair Regen. 2004;12:591-599.

253. De Becker, A., and Riet, I.V. Homing and migration of mesenchymal stromal cells: How to improve the efficacy of cell therapy? World J Stem Cells. 2016;8:73-87.

254. Teo, G.S., Yang, Z., Carman, C.V., Karp, J.M., and Lin, C.P. Intravital imaging of mesenchymal stem cell trafficking and association with platelets and neutrophils. Stem Cells. 2015;33:265-277.

255. Teo, G.S., Ankrum, J.A., Martinelli, R., Boetto, S.E., Simms, K., Sciuto, T.E., Dvorak, A.M., Karp, J.M., and Carman, C.V. Mesenchymal stem cells transmigrate between and directly through tumor necrosis factor-alpha-activated endothelial cells via both leukocyte-like and novel mechanisms. Stem Cells. 2012;30:2472-2486.

256. Allen, T.A., Gracieux, D., Talib, M., Tokarz, D.A., Hensley, M.T., Cores, J., Vandergriff, A., Tang, J., De Andrade, J.B., Dinh, P.U., Yoder, J.A., and Cheng, K. Angiopellosis as an alternative mechanism of cell extravasation. Stem Cells. 2017;35:170-180.

257. Everaert, B.R., Bergwerf, I., De Vocht, N., Ponsaerts, P., Van Der Linden, A., Timmermans, J.P., and Vrints, C.J. Multimodal in vivo imaging reveals limited allograft survival, intrapulmonary cell trapping and minimal evidence for ischemia-directed BMSC homing. BMC Biotechnol. 2012;12:93.

258. Gao, J., Dennis, J.E., Muzic, R.F., Lundberg, M., and Caplan, A.I. The dynamic in vivo distribution of bone marrow-derived mesenchymal stem cells after infusion. Cells Tissues Organs. 2001;169:12-20.

259. Toupet, K., Maumus, M., Luz-Crawford, P., Lombardo, E., Lopez-Belmonte, J., Van Lent, P., Garin, M.I., Van Den Berg, W., Dalemans, W., Jorgensen, C., and Noel, D. Survival and biodistribution of xenogenic adipose mesenchymal stem cells is not affected by the degree of inflammation in arthritis. PLoS ONE. 2015;10:e0114962.

260. Ge, J., Guo, L., Wang, S., Zhang, Y., Cai, T., Zhao, R.C., and Wu, Y. The size of mesenchymal stem cells is a significant cause of vascular obstructions and stroke. Stem Cell Rev. 2014;10:295-303.

261. Makela, T., Takalo, R., Arvola, O., Haapanen, H., Yannopoulos, F., Blanco, R., Ahvenjarvi, L., Kiviluoma, K., Kerkela, E., Nystedt, J., Juvonen, T., and Lehenkari, P. Safety and biodistribution study of bone marrow-derived mesenchymal stromal cells and mononuclear cells and the impact of the administration route in an intact porcine model. Cytotherapy. 2015;17:392-402.

262. Walczak, P., Zhang, J., Gilad, A.A., Kedziorek, D.A., Ruiz-Cabello, J., Young, R.G., Pittenger, M.F., Van Zijl, P.C., Huang, J., and Bulte, J.W. Dual-modality monitoring of targeted intraarterial delivery of mesenchymal stem cells after transient ischemia. Stroke. 2008;39:1569-1574.

263. Furlani, D., Ugurlucan, M., Ong, L., Bieback, K., Pittermann, E., Westien, I., Wang, W., Yerebakan, C., Li, W., Gaebel, R., Li, R.K., Vollmar, B., Steinhoff, G., and Ma, N. Is the intravascular administration of mesenchymal stem cells safe? Mesenchymal stem cells and intravital microscopy. Microvasc Res. 2009;77:370-376.

264. Toma, C., Wagner, W.R., Bowry, S., Schwartz, A., and Villanueva, F. Fate of culture-expanded mesenchymal stem cells in the microvasculature: In vivo observations of cell kinetics. Circ Res. 2009;104:398-402.

265. De Becker, A., Van Hummelen, P., Bakkus, M., Vande Broek, I., De Wever, J., De Waele, M., and Van Riet, I. Migration of culture-expanded human mesenchymal stem cells through bone marrow endothelium is regulated by matrix metalloproteinase-2 and tissue inhibitor of metalloproteinase-3. Haematol. 2007;92:440-449.

266. Stoff, A., Rivera, A.A., Sanjib Banerjee, N., Moore, S.T., Michael Numnum, T., Espinosa-De-Los-Monteros, A., Richter, D.F., Siegal, G.P., Chow, L.T., Feldman, D., Vasconez, L.O., Michael Mathis, J., Stoff-Khalili, M.A., and Curiel, D.T. Promotion of incisional wound repair by human mesenchymal stem cell transplantation. Exp Dermatol. 2009;18:362-369.

267. Di Rocco, G., Baldari, S., and Toietta, G. Towards therapeutic delivery of extracellular vesicles: Strategies for in vivo tracking and biodistribution analysis. Stem Cells Int. 2016;2016:5029619.

268. Tran, C., and Damaser, M.S. Stem cells as drug delivery methods: Application of stem cell secretome for regeneration. Adv Drug Deliv Rev. 2015;82-83:1-11.

269. Kapur, S.K., and Katz, A.J. Review of the adipose derived stem cell secretome. Biochimie. 2013;95:2222-2228.

270. Kupcova Skalnikova, H. Proteomic techniques for characterisation of mesenchymal stem cell secretome. Biochimie. 2013;95:2196-2211.

271. Li, P., and Guo, X. A review: Therapeutic potential of adipose-derived stem cells in cutaneous wound healing and regeneration. Stem Cell Res Ther. 2018;9:302.

272. Zhang, W., Bai, X., Zhao, B., Li, Y., Zhang, Y., Li, Z., Wang, X., Luo, L., Han, F., Zhang, J., Han, S., Cai, W., Su, L., Tao, K., Shi, J., and Hu, D. Cell-free therapy based on adipose tissue stem cell-derived exosomes promotes wound healing via the PI3K/Akt signaling pathway. Exp Cell Res. 2018;370:333-342.

273. Hu, L., Wang, J., Zhou, X., Xiong, Z., Zhao, J., Yu, R., Huang, F., Zhang, H., and Chen, L. Exosomes derived from human adipose mensenchymal stem cells accelerates cutaneous wound healing via optimizing the characteristics of fibroblasts. Sci Rep. 2016;6:32993.

274. Wang, L., Hu, L., Zhou, X., Xiong, Z., Zhang, C., Shehada, H.M.A., Hu, B., Song, J., and Chen, L. Exosomes secreted by human adipose mesenchymal stem cells promote scarless cutaneous repair by regulating extracellular matrix remodelling. Sci Rep. 2017;7:13321.

275. Yaghoubi, Y., Movassaghpour, A., Zamani, M., Talebi, M., Mehdizadeh, A., and Yousefi, M. Human umbilical cord mesenchymal stem cells derived-exosomes in diseases treatment. Life Sci. 2019;233:116733.

276. L, P.K., Kandoi, S., Misra, R., S, V., K, R., and Verma, R.S. The mesenchymal stem cell secretome: A new paradigm towards cell-free therapeutic mode in regenerative medicine. Cytokine Growth Factor Rev. 2019;46:1-9.

277. Gupta, P.K., Chullikana, A., Parakh, R., Desai, S., Das, A., Gottipamula, S., Krishnamurthy, S., Anthony, N., Pherwani, A., and Majumdar, A.S. A double blind randomized placebo controlled phase I/II study assessing the safety and efficacy of allogeneic bone marrow derived mesenchymal stem cell in critical limb ischemia. J Transl Med. 2013;11:143.

278. Lee, H.C., An, S.G., Lee, H.W., Park, J.S., Cha, K.S., Hong, T.J., Park, J.H., Lee, S.Y., Kim, S.P., Kim, Y.D., Chung, S.W., Bae, Y.C., Shin, Y.B., Kim, J.I., and Jung, J.S. Safety and effect of adipose tissue-derived stem cell implantation in patients with critical limb ischemia: A pilot study. Circ J. 2012;76:1750-1760.

279. Barminko, J., Gray, A., Maguire, T., Schloss, R., and Yarmush, M.L. Mesenchymal stromal cell mechanisms of immunomodulation and homing. Mesenchymal Stem Cell Therapy; 2013:15-38.

280. Hassan, W.U., Greiser, U., and Wang, W. Role of adipose-derived stem cells in wound healing. Wound Repair Regen. 2014;22:313-325.

281. Hassanshahi, A., Hassanshahi, M., Khabbazi, S., Hosseini-Khah, Z., Peymanfar, Y., Ghalamkari, S., Su, Y.W., and Xian, C.J. Adipose-derived stem cells for wound healing. J Cell Physiol. 2019;234:7903-7914.

282. Huang, S.-P., Huang, C.-H., Shyu, J.-F., Lee, H.-S., Chen, S.-G., Chan, J.Y.-H., and Huang, S.-M. Promotion of wound healing using adipose-derived stem cells in radiation ulcer of a rat model. J Biomed Sci. 2013;20:51.

283. Nie, C., Yang, D., Xu, J., Si, Z., Jin, X., and Zhang, J. Locally administered adipose-derived stem cells accelerate wound healing through differentiation and vasculogenesis. Cell Transplant. 2011;20:205-216.

284. Nie, C., Zhang, G., Yang, D., Liu, T., Liu, D., Xu, J., and Zhang, J. Targeted delivery of adipose-derived stem cells via acellular dermal matrix enhances wound repair in diabetic rats. J Tissue Eng Regen Med. 2015;9:224-235.

285. Lee, D.E., Ayoub, N., and Agrawal, D.K. Mesenchymal stem cells and cutaneous wound healing: Novel methods to increase cell delivery and therapeutic efficacy. *Stem Cell Res Ther.* 2016;7:37.

286. Mezzanotte, L., Van 'T Root, M., Karatas, H., Goun, E.A., and Lowik, C.W.G.M. In vivo molecular bioluminescence imaging: New tools and applications. *Trends Biotechnol.* 2017;35:640-652.

287. Guillen, M.I., Platas, J., Perez Del Caz, M.D., Mirabet, V., and Alcaraz, M.J. Paracrine anti-inflammatory effects of adipose tissue-derived mesenchymal stem cells in human monocytes. *Front Physiol.* 2018;9:661.

288. Lombardi, F., Palumbo, P., Augello, F.R., Cifone, M.G., Cinque, B., and Giuliani, M. Secretome of adipose tissue-derived stem cells (ASCs) as a novel trend in chronic non-healing wounds: An overview of experimental in vitro and in vivo studies and methodological variables. *Int J Mol Sci.* 2019;20:3721.

289. Patrikoski, M., Mannerstrom, B., and Miettinen, S. Perspectives for clinical translation of adipose stromal/stem cells. *Stem Cells Int.* 2019;2019:5858247.

APPENDIX 1. MIQE GUIDELINES

Experimental design

Definition of experimental and control groups

ASCs harvested from rat subcutaneous inguinal adipose tissue were used. Two groups of ASCs were compared: ASCs that were non-transduced and ASCs transduced to express Fluc and GFP. These ASC cultures were induced by adding induction medium (induced) or control medium (non-induced) for 21 days. After 21 days, RNA was extracted and stored until qPCR experiments were performed (Figure 1).
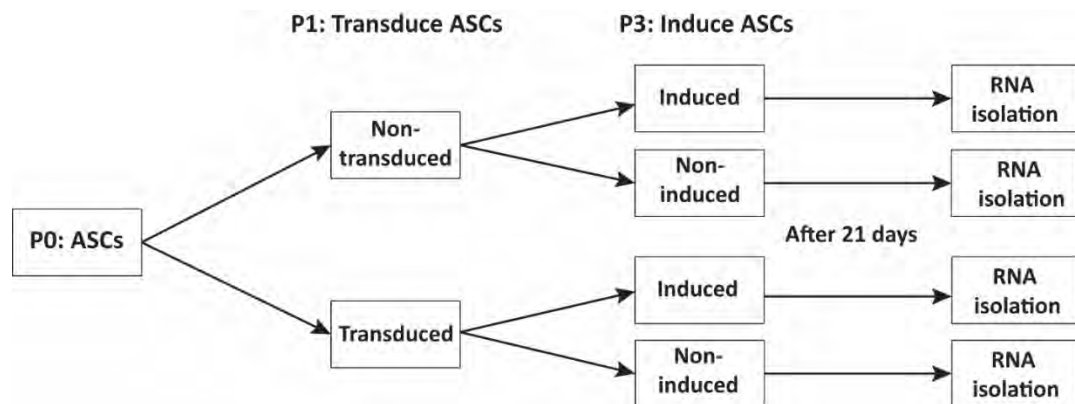

Figure 1. Experimental design of study

Number within each group

Two biological replicates were analysed for each group. For the qPCR run, three technical replicates were analysed for each sample.

Assay carried out by core lab or investigator's lab?

Sample collection, isolation, transduction, induction and RNA isolation were performed at the University of Geneva, and the qPCR was performed at the University of Pretoria.

Samples

Description

Day 21 transduced, induced samples: A single T75 culture flask was used for RNA isolation

Day 21 transduced, non-induced samples: A single T75 culture flask was used for RNA isolation

Day 21 non-transduced, induced samples: A single T75 culture flask was used for RNA isolation

Day 21 non-transduced, non-induced samples: A single T75 culture flask was used for RNA isolation

Microdissection or macrodissection

The samples were not subjected to microdissection or macrodissection

Processing procedure

All samples were processed in the same manner. Each ASC culture was isolated, transduced or kept non-transduced, and then induced with induction or control medium for 21 days. For RNA isolation, cell cultures were trypsinised, resuspended in PBS and the RNA extracted and stored at -80ºC until qPCR was performed. Samples were neither frozen nor fixed prior to RNA extraction.

Nucleic acid extraction

Procedure and/or instrumentation and the kit used

RNA was extracted using the RNeasy Minikit (Qiagen, Hilden, Germany) according to the manufacturer's instructions. The RNA concentration was measured before the RNA was frozen. The extracted RNA was stored at -80˚C until cDNA synthesis, RNA integrity and quality testing were performed.

Details of DNase or RNAse treatment

No DNase or RNase treatment was performed.

Contamination assessment (DNA or RNA)

Contamination was not assessed during RNA isolation.

Nucleic Acid Quantification (instrument, method, purity and yield)

The NanoDrop ND 1000 spectrophotometer (Thermo Scientific, MA, USA) was used to measure RNA concentration as ng/µl. Briefly, the NanoDrop was calibrated and blanked with 2 µl of RNase free water. Thereafter 2 µl of RNA was used to measure RNA concentration and purity (Table 1).

Table 1. RNA concentration, purity and integrity of samples

Sample	Induced/ non-induced	RNA		
		Concentration (ng/µl)	Purity (A260/A280)	Integrity (RIN)
rA060317-01 non-transduced P3	Induced	808	2.16	10
rA060317-01 non-transduced P3	Non-induced	1008	2.16	10
rA060317-01 transduced P3	Induced	682	2.16	10
rA060317-01 transduced P3	Non-induced	1190	2.15	10
rA060317-02 non-transduced P3	Induced	762	2.14	9.9
rA060317-02 non-transduced P3	Non-induced	1798	2.16	10
rA060317-02 transduced P3	Induced	714	2.14	9.9
rA060317-02 transduced P3	Non-induced	1414	2.15	10

RNA integrity method/instrument

RNA integrity and quality were measured using the 2100 Bioanalyzer, Agilent RNA Nano Assay kit and Lab Chip kit (Agilent Technologies, CA, USA). Samples were prepared and analysed according to the manufacturer's instructions using the eukaryote total RNA Nano assay. The RIN values were recorded and are shown in Table 1.

Inhibition testing (Cq dilutions, spike or other)

Inhibition testing was not performed during this study.

Reverse transcription

Complete reaction conditions

This study used the SensiFast cDNA synthesis kit (BIO-65053, Bioline, London, England). Refer to Table 2 for the reaction setup conditions according to the manufacturer's instructions. In total 1 ug of RNA was added to make a final reaction volume of 20 ul. According to the package insert, for reverse transcriptase, one unit catalysed the incorporation of 1 nmol of dTTP into acid-insoluble material in 10 min at 37^0C in 50 mM Tris-HCl (pH 8.6), 40 mM KCl, 1 mM $MnSO_4$, 1 mM DTT, 0.5 mM [3H]TTP and 200 µM oligo(dT)12-18-primed poly(A)n.

The following thermocycling steps were used:

1. Primer annealing: 25 °C for 10 min

2. Reverse transcriptase: 42 °C for 15 min

3. Inactivation: 85 °C for 5 min

4. Hold: 4 °C

After cDNA synthesis, the cDNA was stored at -80^oC until the PCR assays were performed.

Table 2. Reaction setup conditions for the SensiFast cDNA synthesis kit

Reagent	Concentration (µg)	Volume per reaction (µl)
5x TransAmp buffer	n/a	4
Reverse transcriptase	n/a	1
RNA	1	Variable
Nuclease free water	n/a	Variable

qPCR Target information

If multiplex, efficiency and LOD of each assay

No multiplexing was performed during this study.

Sequence accession number

The genes of interest along with their accession numbers used in this study is shown in Table 3. For the reference genes, a 6 gene rat geNORM reference gene selection kit (*18s, MDHI, YWHAZ, UBC, GAPDH, ACTB*, PrimerDesign, Camberley, UK) was used. geNORM analysis using the analysis

software qbase+ version 3.1 was used to select the appropriate number of reference genes for the experiment. The reference genes *18s*, *GAPDH* and *ACTB* were selected.

Table 3. Accession numbers, amplicon location and length for the genes of interest

Genes of interest		Accession Numbers	Amplicon location		Amplicon length
			Start	Stop	
Rattus norvegicus fatty acid binding protein 4	*FABP4*	NM_053365.1	**275**	**379**	**105**
Rattus norvegicus adiponectin receptor 2	*Adipor2*	NM_001037979.1	671	809	139
Rattus norvegicus peroxisome proliferator-activated receptor gamma	*PPARγ*	NM_013124.3	1194	1324	131
Rattus norvegicus CCAAT/enhancer binding protein alpha	*C/EBPα*	NM_001287579.1	2065	2194	130

In silico specificity screen

The specificity of the primers was tested *in silico* using NCBI BLAST. If any of the primer pairs returned matches other than the sequence of interest, they were excluded from the study. However, if no primer sequence was found to be exclusive for the sequence of interest, the sequence with the least matches was used.
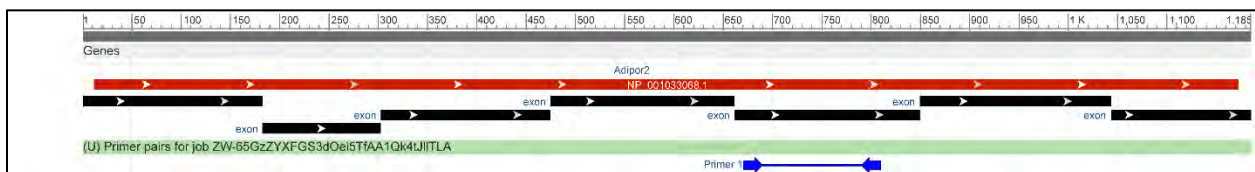
Location of each primer by exon or intron (if applicable)

The location of each primer pair for the genes of interest is shown in Figure 2.
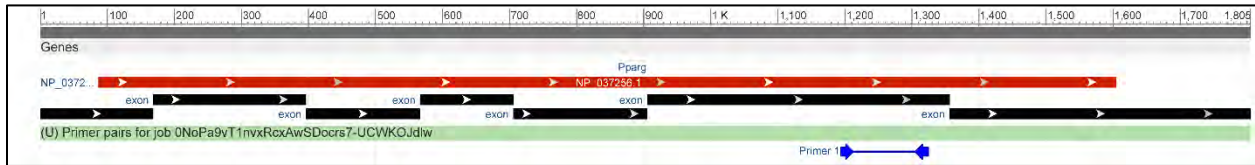
A. FABP4

B. Adipor2
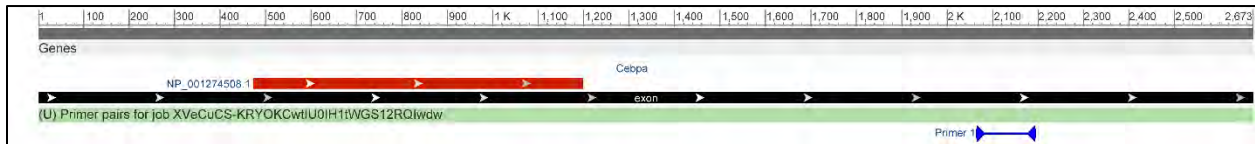
C. PPARγ

D. C/EBPα

Figure 2. The location of each primer is shown for the different genes of interest

qPCR Oligonucleotides

Primer sequences

The primer sequences for the genes of interest are summarised in Table 4. The reference genes were from the geNORM reference gene selection kit (PrimerDesign, Camberley, UK) and the primer sequence information was not supplied. The primer mix batch numbers for the reference genes that were used is: *18s*, GN2360; *ACTB*, GN2345; and *GAPDH*, GN2354.

Table 4. Primer sequences for the genes of interest shown in the 5' to 3' direction

Target Gene		Forward	Reverse
Fatty acid binding protein 4	*FABP4*	CAGGAAAGTGAAGAGCATC	TTGTCACCATCTCGTCTC
Adiponectin receptor 2	*Adipor2*	CTCTGGTATTGCTCTTCTG	CCACTGAGAGACGATAATG
Peroxisome proliferator-activated receptor gamma	*PPARγ*	TCAGAGGGACAAGGATTCA	GCCAAGTCACTGTCATCTAA
CCAAT/enhancer-binding protein alpha	*C/EBPα*	AGAGGGACTGGAGTTATG	GGTGGTTTAGCATAGACG

Location and identity of any modifications

No modifications were made to the primers/sequences.

Manufacturer of oligonucleotides

The oligonucleotides were manufactured by Integrated DNA Technologies (IDT; IA, USA).

Page | 145

Purification method

The method of purification was standard desalting.

qPCR Protocol

Complete reaction conditions

The complete reaction conditions are summarised in Table 5.

Table 5. Complete reaction conditions

Reagent	[Stock]	Quantity	Volume (µl)
---	---	1 x reaction	1 x reaction
dH$_2$O	---	---	2
SYBR green master mix	2 x	1 x	5
F primer	10 µM	0.5 µM	0.5
R primer	10 µM	0.5 µM	0.5
Aliquot	---	---	8
cDNA	---	20 ng/µL	2
Total Volume	---	---	10

Reaction volume and amount of cDNA/DNA

For the qPCR reaction setup, 2 µl of cDNA at a concentration of 20 ng/µl was added to make a final reaction volume of 10 µl.

Primer, (probe), Mg++ and dNTP concentrations

The LightCycler® 480 SYBR Green I Master Mix (Roche, Basel, Switzerland) was used for the RT-qPCR assay. The primers were added at a concentration of 0.5 µM and the master mix was made up to a 1x dilution.

Polymerase identity and concentration

The polymerase in the LightCycler® 480 SYBR Green I Master Mix is FastStart™ Taq DNA polymerase. The concentration was not indicated by the manufacturer.

Buffer/kit identity and manufacturer

The LightCycler® 480 SYBR Green I Master Mix (Catalogue number: 04887352001) was used and supplied by Roche, Basel, Switzerland.

Additives

No additives were used in the master mix.

Manufacturer of plates/tubes and catalogue numbers

The LightCycler 480 Multiwell Plate 96, white plates (Roche, Basel, Switzerland; Catalogue number: 04729692001) were used for the qPCR assays.

Complete thermocycling parameters

The complete thermocycling parameters are defined in Table 6.

Table 6. The complete thermocycling parameters

Step		Duration	Temperature	Number of Cycles
Activation		3 min	94°C	1
Amplification	denaturation	30 sec	94°C	45
	anneal	30 sec	60°C	
	extension	30 sec	72°C	
Melt curve		30 sec	95°C	1
		30 sec	40°C	1
		continuous	40°C to 95°C	1
Cooling		2 min	37°C	NA

Reaction setup (manual/robotic)

The reactions were setup manually.

## Manufacturer of qPCR instrument

The qPCR instrument used was the LightCycler 480 II instrument from Roche (Basel, Switzerland).

qPCR Validation

Specificity

Specificity was measured using a melt curve and a melt peak for every gene as shown in Figure 3. These figures were exported directly from the LightCycler software (version 1.5.1, Roche, Basel, Switzerland). The melt curves and peaks were performed post-PCR during the data analysis step. During optimisation of the qPCR assay, melt curves and peaks were used to detect the presence of primer dimers, secondary products and contamination. Another distinguishable peak would have been visible before or after the T_m peak if secondary products or contamination was present in the NTC. A small shoulder can be seen to the left of the T_m peak in some of the melt peaks and represent primer dimers. However, these shoulders were not detected as peaks by the software.
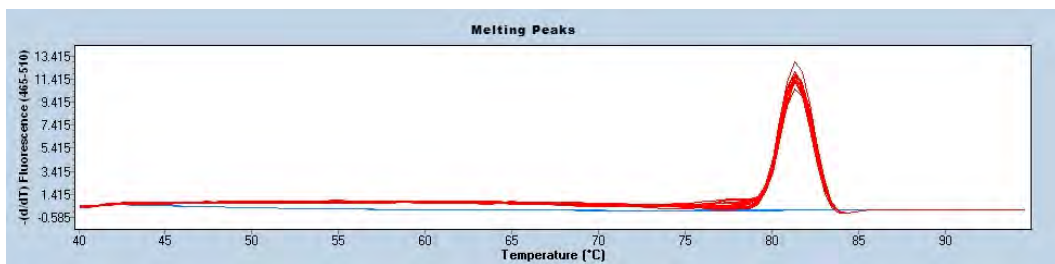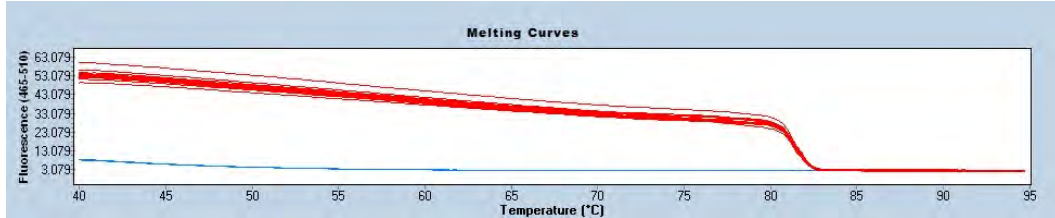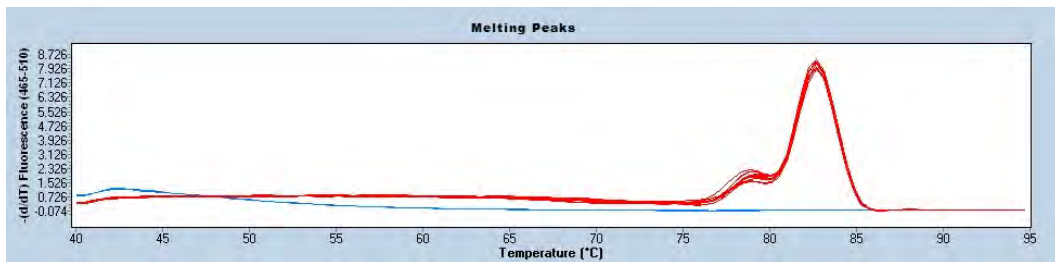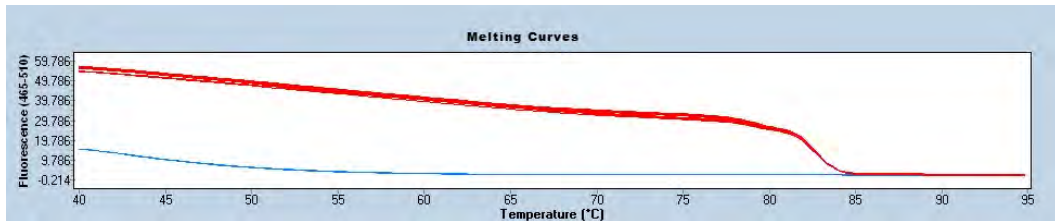
(A) FABP4
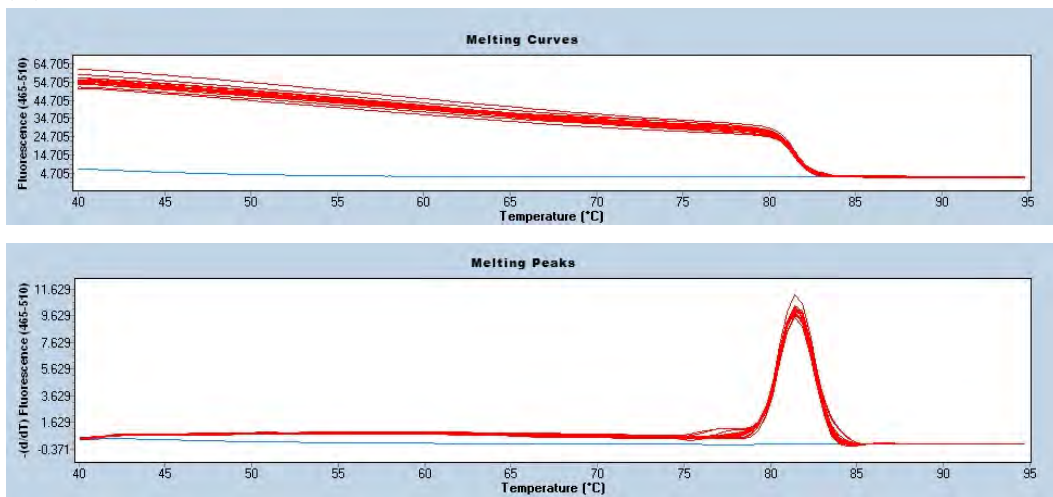
(B) Adipor2
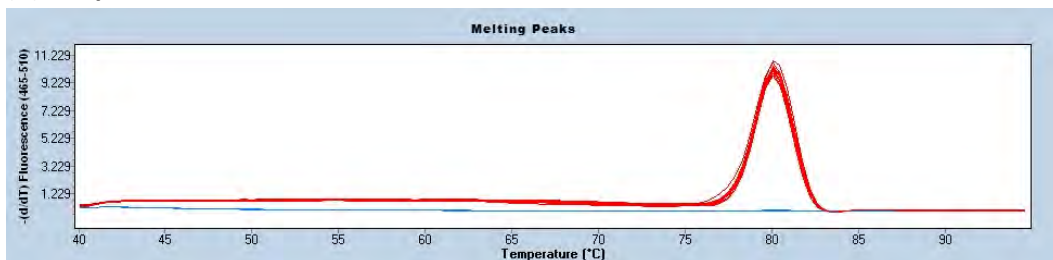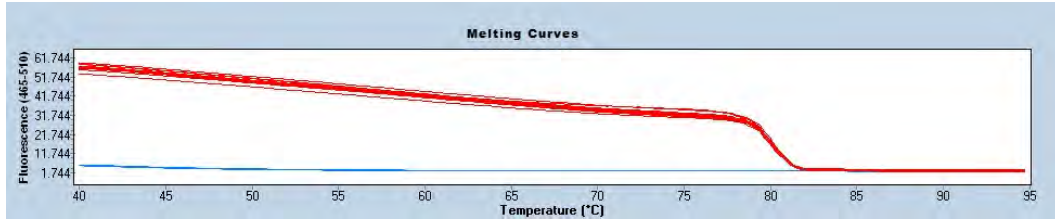
(C) PPARγ

(D) C/EBPα

(E) ACTB
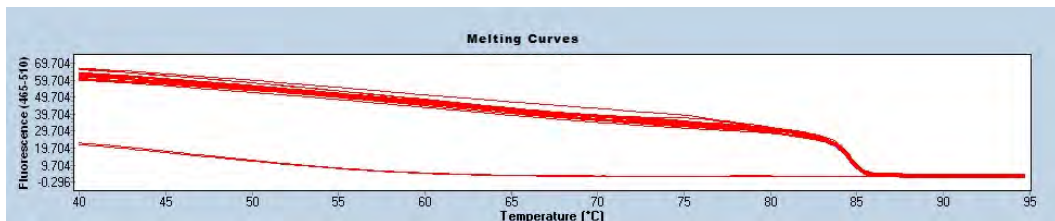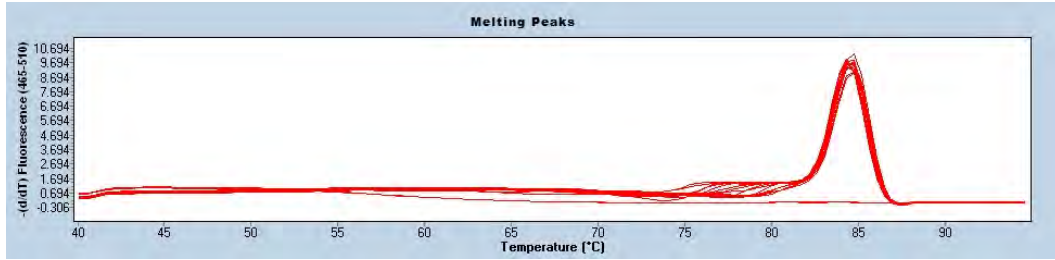
(F) GAPDH
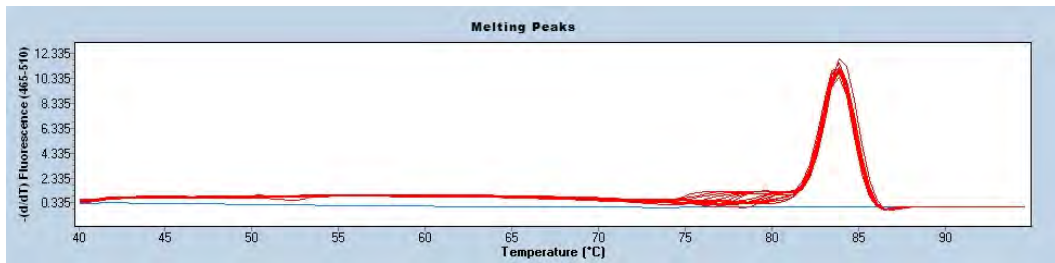
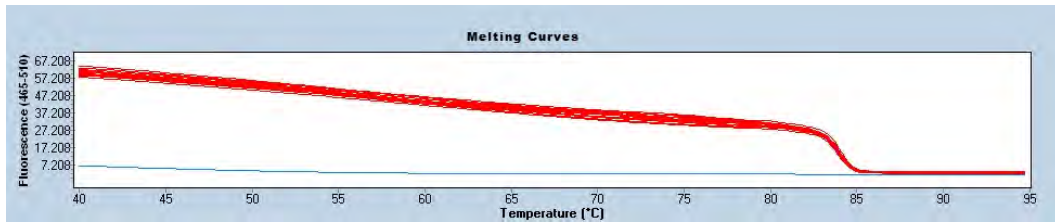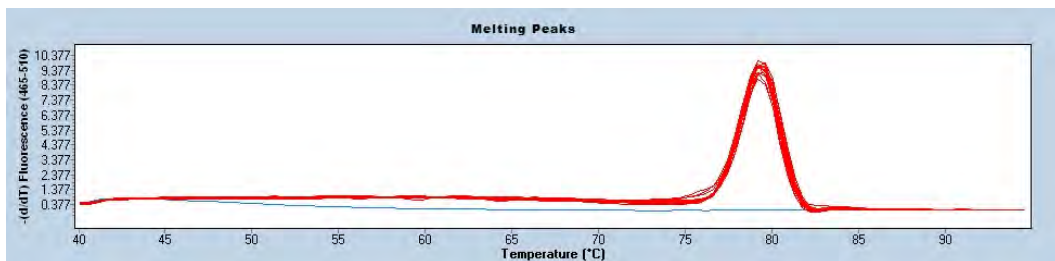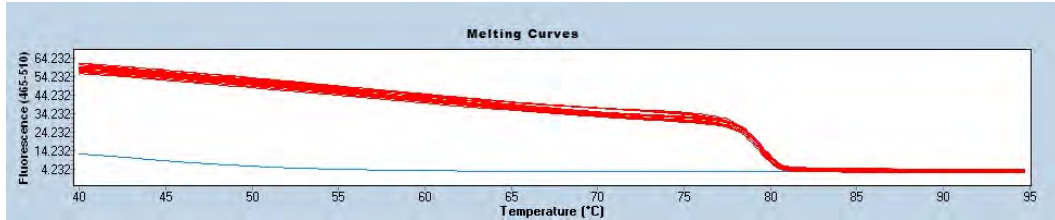**(G) 18s**

Figure 3. Representative melt curves and melt peaks for every gene to show qPCR specificity.

For SYBR Green I, Cq of the NTC

The NTCs had a Cq value of 0. During the analysis, if the NTC was amplified and a Cq value recorded, the plate was assessed for secondary products because of an increase in cycle number and rerun to exclude contamination where necessary.

Standard curves with the slope and y-intercept

The RT-qPCR data was analysed by the relative quantification method; thus, the use of standard curves was not necessary.

If multiplex, efficiency and LOD of each assay

Multiplexing was not performed during this study.

Data Analysis

qPCR analysis program

The LightCycler software (version 1.5.1, Roche, Basel, Switzerland) was used for qPCR analysis.

Cq method determination

The Cq values were determined automatically by the LightCycler software.

Outlier identification and disposition

Outlier tests were not performed due to the small sample size of only 2 biological replicates.

Results of NTCs

The Cq values for all the NTCs were zero. If an NTC was amplified, it was assessed for secondary structure amplification and contamination. If contamination was detected, that assay was rerun.

Justification of number and choice of reference genes

A 6 gene rat geNORM reference gene selection kit (*18s, MDHI, YWHAZ, UBC, GAPDH, ACTB*, PrimerDesign, Camberley, UK) was used. geNORM analysis using the analysis software qbase+ version 3.1 was used to select the appropriate number of reference genes for the experiment. Two to three reference genes were suggested from the analysis. A qPCR using all the samples was also performed to determine the most stable reference genes to use for this study. The reference genes *18s*, *GAPDH* and *ACTB* were selected.

Description of normalisation method

As samples were not always run on a single plate, for each plate, samples were first normalised to a calibrator sample on the plate to obtain a calibrator normalised value. This normalised value was then normalised to the reference genes. Normalisation factors and fold changes were calculated using the geNORM method.[174]

Number and concordance of biological replicates

Due to some experimental constraints only 2 biological replicates were assessed.

Number and stage (RT or qPCR) of technical replicates

For this study, a single replicate was employed for the RT assay and three technical replicates for the qPCR assay. For the qPCR assay, three wells were set up using the same cDNA sample. For the RT reaction, a single reaction per sample was set up.

Repeatability (intra-assay variation)

A measure of the SD between replicates was used to assess repeatability. Replicates were considered repeatable if the SD between Cq values differed by ≤ 0.5.

Power analysis, statistical methods for result significance and software (source, version)

The sample size was too small to enable statistical analysis to be performed. However, trends in gene expression between samples could be identified.

APPENDIX 2. MYCOPLASMA PCR TEST

Mycoplasma PCR preparation		Date	
1	**Collect samples**		

(a)	**Cell medium**
	
	    i. Collect 4 ml culture medium per sample
	    ii. Centrifuge (5 min, 1500 rpm) to remove cells debris
	    iii. Collect supernatant and centrifuge (12 500 g, 15 min)
	    iv. Store pellet at -20ºC dry until processed, usually store 2-4 tubes per sample		

(b)	**Cells**
	
	    i. Collect 50 000 cells
	    ii. Centrifuge (5 min, 1500 rpm)
	    iii. Wash with PBS (centrifuge, 5 min, 1500 rpm)
	    iv. Store pellet at -20ºC dry until processed		

2	**DNA extraction**		

	<u>**Make up Lysis buffer**</u>
	
	 DirectPCR-Tail (ref 31-101-T, Viagen)
	
	 Proteinase K 200 µg/ml final (dilution of 1/50 of PK 10 mg/ml in Viagen buffer)
	
	    i. Add 50µl of lysis buffer (per tube)
	    ii. Incubate at 56ºC for 1 h and then for 85ºC for 45 min (can use PCR machine)
	    iii. Vortex and centrifuge tubes, DNA is ready for PCR
	    iv. Store DNA at -20ºC		

3	**PCR**		
(a)	**Remove the following reagents from the freezer** <u>Taq DNA polymerase kit:</u> 10 x Coral load PCR buffer Taq DNA polymerase Nuclease free water dNTPs <u>Primers: Mycoplasma</u> F: 5' GGC GAA TGG GTG AGT AAC ACG 3' R: 5' CGG ATA ACG CTT GCG ACC TAT 3' <u>Primers: L32 Control</u> F: 5' GTG AAG CCC AAG ATC GTC AA 3' R: 5' TTG GTG ACT CTG ATG GCC AG 3'		
(b)	Two PCR are done in parallel for every sample: L32 PCR and mycoplasma PCR For each PCR, n samples + internal controls (positive and negative control) and NTC (mix control)		
(c)	Mycoplasma PCR program (500bp): 1 - 94°C – 2 min 2 – 94°C – 30 sec	L-32 PCR program (350bp): 1 - 94°C – 2 min 2 – 94°C – 30 sec	

	3 – 55°C – 30 sec 4 – 72 °C – 1 min – from 2 to 4, 30 cycles 5 – 72°C – 10 min 6 – 4°C – ∞			3 – 58°C – 30 sec 4 – 72 °C – 1 min – from 2 to 4, 30 cycles 5 – 72°C – 10 min 6 – 4°C – ∞			

(d) PCR Mycoplasma

500 bp product

mix (quantities in ul)

n=	1	X
10x PCR buffer	2.5	
primer F	1	
primer R	1	
dNTPs 10 mM	0.5	
Taq	0.25	
H2O	17.75	
total	23	

23 ul mix + 2 ul DNA

PCR Mycoplasma - L32 control*

350 bp product

mix (quantities in ul)

n=	1	X
10x PCR buffer	2.5	
primer F	1	
primer R	1	
dNTPs 10 mM	0.5	
Taq	0.25	
H2O	17.75	
total	23	

23 ul mix + 2 ul DNA

(e) **SAMPLES**

1. sample
2. positive control
3. negative control
4. NTC

SAMPLES

1. *sample
2. *positive control
3. *negative control
4. *NTC

4 **Agarose gel**

Make up 1% agarose gel

0.5 g agarose in 50 ml (1x TAE buffer)

1 µl ethidium bromide OR Midori Green 2.5 µl/50 ml

(Midori Green Advance DNA stain, 1 ml, Lot no. 134MG27046, exp. 05/2018, Genetics, Nippon Genetics)

Add 8 µl MWM

Add 12 µl of sample per well

Run gel (100 V, 400 mA) (from negative (black) to positive (red))

Image gel under UV

APPENDIX 3. CHAPTER 3. SUPPLEMENTARY DATA

A lower dose of locally administered ASCs was less effective in enhancing wound repair

Materials and method

To determine whether the effect of locally administered ASCs was dose dependant, a lower dose of ASCs was also investigated. The same animal model was used as described in section 3.2.1.1. Briefly, one day after wounding, animals were treated with a lower dose of ASCs locally: 1×10^5 (n=18) Fluc-GFP positive ASCs in total locally split into two sides of each wound (proximally at the ankle and distally at the toes). Animals were followed by digital photography at 3h, 24h, 48h, 72h, d7, d15 and at wound closure. The wound area over time, time of complete wound closure and the contraction/epithelialisation ratio were assessed as described in section 3.2.2.

Results

Animals who received a lower dose of ASCs locally was compared alongside the locally (higher dose) treated and the NaCl control animals described in the main text from section 3.2.1.1. The lower dose group showed an initial slower wound closure rate. Significantly larger wound size was recorded for the lower dose group compared to the NaCl group (at 3 and 7 days) and the higher ASC dose group (at 3, 10 and 15 days) (Figure S1A). Wound closure assessment showed that the lower dose of ASCs reduced wound closure time compared to the NaCl control group by 3 days (p=0.0222). Whereas the higher ASC dose reduced wound closure time by 7 days (p=0.0108) (Figure S1B). Comparison of the lower with the higher dose showed that the higher dose reduced wound closure time significantly faster than the lower dose (p=0.0009). Further investigation into whether wound closure was favoured more by contraction or epithelialisation of the wound showed no significant difference with the lower ASC dose as compared to the NaCl control group (Figure S1B). The higher dose of ASCs appeared to be more effective than the lower dose of ASCs suggesting that ASCs when administered locally is dose dependant. Taking this into consideration, only the animals who received the higher dose of ASCs were further evaluated to determine the migratory capacity of ASCs into the wound as described in section 3.2.1.3.

A. WOUND AREA OVER TIME
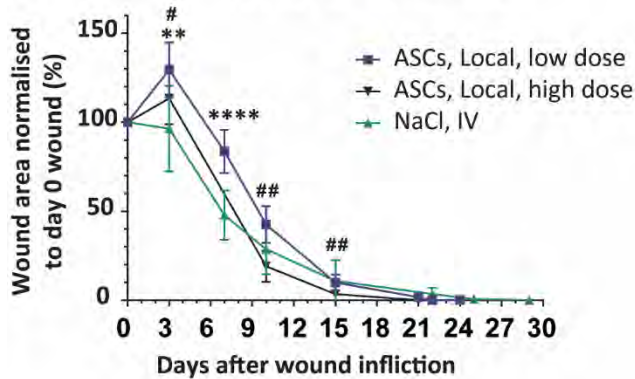
Significant difference between (p<0.05): *ASCs low dose vs NaCl; #ASCs low dose vs high dose

B. WOUND CLOSURE TIME

C. CONTRACTION VS EPITHELIALISATION
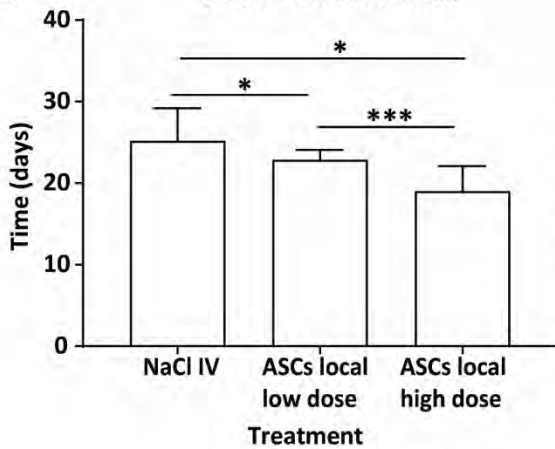
■ Epithelialisation □ Contraction
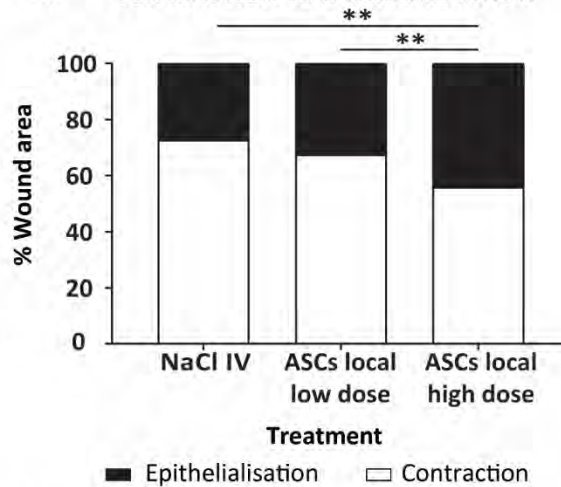
KEY: NaCl, IV, n=6; ASCs, Local, high dose, n=6; ASCs, Local, low dose, n=12

Figure S1. Wound closure assessment in animals treated locally with either a low or high dose of ASCs. Animals were treated with Fluc-GFP+ ASCs, locally into two sides around each wound with 2 different ASC doses: either with a low dose of 1×10^5 ASCs or a high dose of 2×10^5 ASCs. Control animals were treated systemically with NaCl. (A) Wound area over time after treatment as normalised to the original wound area on day 0. (B) Time taken for complete wound closure after treatment. (C) Wound area closed by contraction and by epithelialisation. Data shown as mean ± SD. Significance is shown where */#p<0.05, **/##p<0.01, ***/###p<0.001, ****/####p<0.0001.

APPENDIX 4. PREPARED MANUSCRIPT

Manuscript was prepared for publication combining the data from Chapter 2 and 3

Title: Fate of systemically and locally administered adipose-derived mesenchymal stromal cells and their effect on wound healing

Submitted for publication to: Stem Cells Translational Medicine

Date of submission: 22 March 2019

Outcome: 20 May 2019**,** received feedback from the journal, **"**the manuscript will be reconsidered if major revision is made"-manuscript is being revised for re-submission

Date of acceptance: 10 September 2019

Early view published online: 15 October 2019; https://doi.org/10.1002/sctm.19-0091

IFATS

STEM CELLS
TRANSLATIONAL MEDICINE

Fate of systemically and locally administered adipose-derived mesenchymal stromal cells and their effect on wound healing

Karlien Kallmeyer[1,2] | Dominik André-Lévigne[1] | Mathurin Baquié[5] |
Karl-Heinz Krause[3] | Michael S. Pepper[2,4] | Brigitte Pittet-Cuénod[1] | Ali Modarressi[1]

[1]Department of Plastic, Reconstructive & Aesthetic Surgery, University Hospitals of Geneva, University of Geneva, Geneva, Switzerland

[2]Institute for Cellular and Molecular Medicine (ICMM), Department of Immunology, and SAMRC Extramural Unit for Stem Cell Research and Therapy, University of Pretoria, Pretoria, South Africa

[3]Department of Pathology and Immunology, University of Geneva, Geneva, Switzerland

[4]Department of Human Genetics and Development, University of Geneva, Geneva, Switzerland

[5]Neurix SA, Geneva, Switzerland

Correspondence
Ali Modarressi, MD, Plastic, Reconstructive and Aesthetic Surgery Unit, University Hospitals of Geneva, Case Postal, 1211 Geneva 14, Switzerland.
Email: ali.modarressi@hcuge.ch

Karlien Kallmeyer, MSc Medical Immunology, Room 5-49 (Level 5), Pathology Building, 5 Bophelo Road (Cnr. Steve Biko and Dr. Savage Streets), Prinshof Campus, University of Pretoria, Pretoria, 0002, Republic of South Africa.
Email: karlienkallmeyer@gmail.com

Funding information
SAMRC Extramural Unit for Stem Cell Research and Therapy; South African Medical Research Council University Flagship Program; Swiss National Science Foundation Project, Grant/Award Number: 310030_170132; Institute for Cellular and Molecular Medicine (ICMM); University of Pretoria Postgraduate Bursary Office; Ernst & Ethel Eriksen Trust; National Research Foundation, Grant/Award Number: 88799; Faculty of Medicine of the University of Geneva

Abstract

There is increasing interest in the use of adipose-derived mesenchymal stromal cells (ASCs) for wound repair. As the fate of administered cells is still poorly defined, we aimed to establish the location, survival, and effect of ASCs when administered either systemically or locally during wound repair under physiological conditions. To determine the behavior of ASCs, a rat model with wounds on the dorsal aspect of the hind paws was used and two treatment modes were assessed: ASCs administered systemically into the tail vein or locally around the wound. ASCs were transduced to express both firefly luciferase (Fluc) and green fluorescent protein to enable tracking by bioluminescence imaging and immunohistological analysis. Systemically administered ASCs were detected in the lungs 3 h after injection with a decrease in luminescent signal at 48 h and signal disappearance from 72 h. No ASCs were detected in the wound. Locally administered ASCs remained strongly detectable for 7 days at the injection site and became distributed within the wound bed as early as 24 h post injection with a significant increase observed at 72 h. Systemically administered ASCs were filtered out in the lungs, whereas ASCs administered locally remained and survived not only at the injection site but were also detected within the wound bed. Both treatments led to enhanced wound closure. It appears that systemically administered ASCs have the potential to enhance wound repair distally from their site of entrapment in the lungs whereas locally administered ASCs enhanced wound repair as they became redistributed within the wound bed.

KEYWORDS

adipose-derived mesenchymal stromal cells, bioluminescence imaging, firefly luciferase, green fluorescent protein, *in vivo* imaging, wound healing, wound repair

Page | 158

1 | INTRODUCTION

In the field of regenerative medicine, cell-based therapies utilizing human mesenchymal stromal cells (MSCs) have generated a great deal of interest for wound healing.[1-3] The exact mechanism underlying the therapeutic benefits of MSCs has yet to be fully elucidated. Their role in tissue maintenance, repair, and regeneration is suggested to stem from their multipotent differentiation capacity, immunomodulatory properties, antimicrobial effect, paracrine signaling, and their ability to migrate to sites of injury.[2,4-6] Although MSCs were originally isolated from bone marrow (BM),[7] a source used with increasing frequency is subcutaneous adipose tissue.[4] Both BM-MSCs and adipose-derived MSCs (ASCs) are candidate cell types for treating wounds; laboratory and clinical studies, however, favor BM-MSCs.[3,8] ASCs are considered to be a potentially useful cell population because of their availability, ease of harvest, high cell yield, and ability to be expanded in culture for clinical use.[4,9-11]

MSCs are believed to migrate to damaged tissue in a process called homing.[12] *In vitro*, MSCs are attracted by cytokines and chemokines that are known to be upregulated under conditions of inflammation.[13-15] However, *in vivo*, homing of MSCs has not been unequivocally shown. Some studies have reported homing of systemically administered MSCs in mouse models of type 2 diabetes,[16] traumatic brain injury,[17] and burn injury,[18] whereas others reported intrapulmonary cell trapping[19] and minimal evidence for homing.[20] Where recirculation of MSCs was shown to occur after becoming trapped in the lungs, only a low percentage of MSCs could be found at the injury site or in non-target organs.[20-23] Most of these studies evaluated the homing of BM-MSCs. Although BM-MSCs and ASCs share biological characteristics, differences in their phenotype, differentiation potential, gene expression profile, and immunomodulatory activity have been noted.[11,24,25] Thus, differences in their homing capacity may also exist, establishing a need to investigate the homing of ASCs and compare this to available BM-MSCs homing data.

Commonly suggested routes of MSC transplantation include systemic and local injection.[19,26-29] Local injection relies on the activity of locally transplanted MSCs at the target site. Systemic injection requires circulating MSC to exit the blood vessels and to migrate to the target site. However, whether administered systemically or locally, where the cells go to and whether they can bind, engraft and even survive *in vivo*, is still not well understood, particularly for ASCs. Insights into the basic biology of administered ASCs, their biodistribution and their engraftment into damaged tissue, need to be understood to achieve clinical efficiency.

In this study, we evaluate the distribution and survival of ASCs *in vivo* when administered either systemically or locally using a standardized rat model of cutaneous wound repair under physiological conditions. Defining the location of administered ASCs *in vivo* is complicated by the lack of a single identifying marker. *In vitro*, ASCs are characterized by their co-expression of a panel of surface markers; however, this is not possible to achieve *in vivo*.[30] Molecular imaging offers the opportunity to track cells in intact organisms. Fluorescent

Significance statement

The exogenous administration of adipose-derived mesenchymal stromal cells (ASCs) holds promise as a treatment strategy for wound healing by promoting tissue repair and regeneration. However, the best route of administration is still not well defined. Herein, this study describes the biodistribution and survival of systemically vs locally administered ASCs. Interestingly, both routes of administration led to enhanced wound repair as seen by earlier wound closure. Systemically administered ASCs have the potential to enhance wound repair distally from their site of entrapment in the lungs, whereas locally administered ASCs migrate into the wound bed.

reporters, such as green fluorescent protein (GFP), do not give a sufficiently strong signal to allow for efficient detection *in vivo*.[31] A useful method for *in vivo* cell tracking in small animal models is bioluminescence imaging (BLI).[32-34] BLI allows for non-invasive imaging over a longer period and provides information on the viability[35] of cells after transplantation. In this study, we used both BLI and GFP to enable *in vivo* tracking and post-mortem identification, respectively.

The therapeutic potential of MSCs for cutaneous wound repair is being investigated in clinical trials for burn wounds,[36,37] diabetic foot ulcers,[37-39] and critical limb ischemia.[40,41] Although preclinical and clinical studies using MSCs to enhance wound repair have shown positive outcomes, the benefit of MSC administration for wound healing has not yet been clearly established.[39,42-45] As a secondary aim, we evaluated the effect of different modes of ASC administration on wound closure (WC) time. Information is provided on the biodistribution of ASCs and their tissue-specific location post administration, as well as their effect on WC time. By understanding the fate of administered ASCs in response to injury, this study contributes to establishing the optimal mode of administration required in the clinical setting.

2 | MATERIALS AND METHODS

All animal experiments were approved by the local veterinary authority (authorization number GE/70/18).

2.1 | Isolation and culture of primary rat ASCs

Female Wistar rats (≥10 weeks old, ≥250 g, *n* = 14, Janvier labs, Le Genest-Saint-Isle, France) were sacrificed by intraperitoneal (IP) injection of 150 mg/kg sodium pentobarbital (Esconarkon AD US. VET., Streuli Pharma, Uznach, Switzerland) followed by excision of the inguinal subcutaneous adipose tissue. The stromal vascular fraction (SVF) was isolated as previously described and plated into a flask (NUNC, Kamstrupvej, Denmark) overnight at 37°C, 5% CO_2 in high glucose Dulbecco's Modified Eagle's Medium (DMEM 1× +

159

GlutaMAX, 4.5 g/L glucose) supplemented with 20% fetal bovine serum (FBS) and 1% penicillin (10 000 units/mL)-streptomycin (10 000 μg/mL; pen/strep; Gibco, Life Technologies, NY).[46–48] After 24 h, non-adherent cells were removed and the medium changed to complete growth medium (CGM, high glucose DMEM supplemented with 10% FBS and 1% pen/strep). Isolated cells were maintained in CGM (37°C, 5% CO_2) until 80% confluent before being trypsinized. Cells were counted using the trypan blue dye exclusion assay[49] and replated as passage 1 (P1) at a density of 5×10^3 cells/cm^2.

2.2 | Transduction of ASCs

ASCs were transduced with a dual lentivector expressing GFP and firefly luciferase (Fluc), pCWX-UBI-Fluc-PGK-GFP. To determine the amount of lentivector needed to transduce greater than 70% of the cells, a multiplicity of infection (MOI) of 0, 2, 5, and 10 was tested ($n = 4$). A MOI of 10 was used for all further experiments. ASCs at P1/P2 were plated at 5×10^3 cells/cm^2 and allowed to adhere for 24 h. Lentivectors were added and the cultures left for 72 h before replacing the medium with fresh CGM. At 80% confluence, ASCs were trypsinized and an aliquot prepared for flow cytometric analysis ($n = 6$) as described below to determine their immunophenotype and the percentage of ASCs expressing GFP. To determine whether ASCs also expressed Fluc, 1×10^5 cells ($n = 4$) were plated in opaque flat bottom 96 well plates (Thermo Fisher Scientific, MA) in triplicate for 24 h before being imaged. Prior to imaging on the Xenogen IVIS spectrum *in vivo* imaging system, XenoLight D-luciferin potassium salt (PerkinElmer, MA) in CGM was added at 150 μg/mL. A photographic image of the plate followed by a luminescent image was recorded. For quantification, the intensity of the luminescent signal in each well was recorded as total flux (average photons per second, p/s).[50] Images were analyzed using the Living Image 4.3.1 software (PerkinElmer).

2.3 | Immunophenotypic assessment by flow cytometry

Immunophenotyping was done on batches of isolated ASCs ($n = 6$) before and after transduction. The following monoclonal antibodies were used: Armenian hamster anti-mouse/rat CD29 APC and IgG isotype control APC (1.25 μL), mouse anti-rat CD45 APC-eFluor780 and IgG1 K isotype control APC-eFluor780 (2 μL), mouse anti-mouse/rat CD90.1 PE-Cyanine 7 and IgG2a K isotype control PE-Cyanine 7 (1 μL; eBioscience, ThermoFisher Scientific, MA), and mouse anti-rat CD31 PE and IgG1, κ isotype control PE (3 μL; BD Biosciences, CA). A 100 μL cell aliquot containing at least 1×10^5 viable cells was incubated in the dark (15 min, 37°C) after adding the four monoclonal antibodies (CD29, CD45, CD90, and CD31). Following incubation, cells were washed thrice with phosphate-buffered saline (PBS, Gibco, Life Technologies) supplemented with 2% FBS, resuspended in PBS and then analyzed for antigen expression. A single tube containing unstained cells and a tube stained with the isotype controls were prepared for every sample to verify protocol settings and to serve as a negative control. Data were acquired on a Gallios flow cytometer (Beckman Coulter, CA).

To determine the percentage transduced cells, GFP expression was measured together with the surface markers. The viability stain 4′,6-diamidino-2-phenylindole (DAPI, Beckman Coulter) was included to allow analysis only of living cells. Data analysis was performed using Kaluza Flow Cytometry analysis software 1.3 (Beckman Coulter).

2.4 | *In vitro* differentiation capacity of ASCs

To confirm the differentiation capacity of non-transduced and transduced ASCs, they were induced to differentiate along adipogenic and osteogenic lineages using specific induction media. Cell cultures were trypsinized, counted, phenotypically characterized, and replated into 24-well microplates (iBidi, Martinsried, Germany) at 5×10^3 cells/cm^2. Adipogenic induction medium consisted of CGM supplemented with 0.1 μM dexamethasone, 0.5 mM 3-isobutyl-methylxanthine (IBMX), 56 μM indomethacin, and 10 μM insulin (human recombinant zinc, Gibco, Life Technologies). Osteogenic induction medium consisted of CGM supplemented with 10 nM dexamethasone, 50 μM ascorbate-2-phosphate, and 10 mM β-glycerophosphate. Stock solutions of dexamethasone and indomethacin were prepared in ethanol, whereas IBMX stock solutions were prepared in dimethyl sulfoxide (DMSO). Non-induced control cells were maintained in CGM. After 14 or 21 days in either induction medium or CGM, cultures were fixed (60 min) using 4% (vol/vol) formaldehyde solution. The accumulation of lipid droplets was detected by staining the cultures with a 0.3% oil red O (ORO, 10 min, RT) after 14 days of induction. Mineralization was detected by staining the cultures with 2% alizarin red S (ARS, pH 4.1, 30 min, RT) 21 days after induction. Both the differentiated and control cells were stained. Images were acquired using an Eclipse Ts2-FL inverted microscope fitted with a DS-Fi3 camera and DS-L4 control unit (Nikon corporation, Tokyo, Japan). Dexamethasone, IBMX, indomethacin, ascorbate-2-phosphate, β-glycerophosphate, DMSO, formaldehyde solution, ORO, and ARS were all from Sigma–Aldrich Chemie, Steinheim, Germany.

2.5 | *In vivo* rat model and ASC administration

Female Wistar rats (≥10 weeks old, ≥250 g) were fed a standard diet and given water ad libitum. For all procedures, animals were anesthetized by inhalation of 3%–5% isoflurane (Baxter AG, Opfikon, Switzerland). Wounds on the dorsal aspect of the hind paws were created bilaterally by removing a full-thickness skin area of 1.2 cm × 0.8 cm. One day after wounding, 27 animals received a single injection of 2×10^6 Fluc-GFP positive ASCs systemically into the tail vein and 21 animals locally with 2×10^5 Fluc-GFP positive ASCs in total, split between two sides of each wound (proximally at the ankle and distally at the toes). One day post wound creation was chosen for administration so that the inflammatory phase would already be initiated to attract the ASCs. Moreover, by postponing the injection of the ASCs, we avoided the probability of the cells being washed away due to bleeding immediately after wound creation. For each experiment, ASCs isolated from two rats were cultured and transduced separately before being pooled for either systemic or local administration. Nine control animals received a single injection of sodium chloride (NaCl)
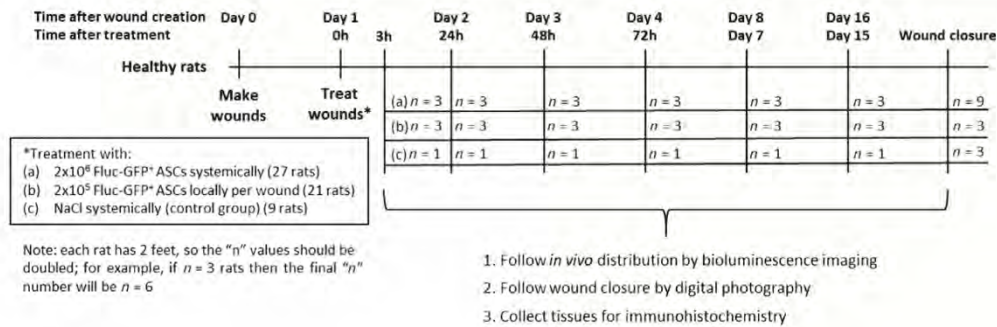
Time after wound creation	Day 0	Day 1		Day 2	Day 3	Day 4	Day 8	Day 16	
Time after treatment		0h	3h	24h	48h	72h	Day 7	Day 15	Wound closure
Healthy rats									
	Make wounds	Treat wounds*							
			(a) $n = 3$	$n = 3$	$n = 3$	$n = 3$	$n = 3$	$n = 3$	$n = 9$
			(b) $n = 3$	$n = 3$	$n = 3$	$n = 3$	$n = 3$	$n = 3$	$n = 3$
			(c) $n = 1$	$n = 1$	$n = 1$	$n = 1$	$n = 1$	$n = 1$	$n = 3$

*Treatment with:
(a) 2×10^6 Fluc-GFP+ ASCs systemically (27 rats)
(b) 2×10^5 Fluc-GFP+ ASCs locally per wound (21 rats)
(c) NaCl systemically (control group) (9 rats)

Note: each rat has 2 feet, so the "n" values should be doubled; for example, if $n = 3$ rats then the final "n" number will be $n = 6$

1. Follow *in vivo* distribution by bioluminescence imaging
2. Follow wound closure by digital photography
3. Collect tissues for immunohistochemistry

FIGURE 1 Study design. For the rat model of wound repair under physiological conditions, full-thickness wounds were created bilaterally on the dorsal aspect of the hind paws. One day after wounding, animals were treated either with a single injection of 2×10^6 ASCs systemically into the tail vein or locally with 2×10^5 ASCs in total, split into two sides of each wound. Control animals received a single injection of NaCl systemically into the tail vein. Animals were followed by digital photography and bioluminescence imaging and sacrificed for the collection of tissues for histology at 3 h, 24 h, 48 h, 72 h, 7 days, and 15 days post-treatment and at wound closure. Abbreviations: ASCs, adipose-derived mesenchymal stromal cells; Fluc, firefly luciferase; GFP, green fluorescent protein

systemically into the tail vein. Both feet were evaluated separately for each animal. All animals received a semi-occlusive wound dressing that was changed at every evaluated time-point (Figure 1).

2.6 | *In vivo* tracking of administered ASCs by BLI

Animals treated systemically and locally were imaged by BLI at 3 h, 24 h, 48 h, 72 h, d7, d15 and at WC. Prior to imaging, animals received a single IP injection of firefly D-luciferin potassium salt (150 mg/kg body weight) prepared in PBS. After 20 min, imaging was performed using the Xenogen IVIS spectrum *in vivo* imaging system with an XGI-8 Gas anesthesia system. A photographic image of the animal followed by a luminescent image was recorded by the camera. To exclude background luminescence emitted from the ASCs themselves, a single animal that received non-transduced ASCs at the same concentration and mode of administration was included as a control for every BLI experiment. For quantification, three regions of interest (ROI) were manually selected to quantify the luminescent signal in the lung (ROI 1) and the wound area (right foot, ROI 2; left foot ROI 3). The ROI size was kept constant between animals and the intensity of the luminescent signal was recorded as total flux (average photons per second, p/s).[50] All images were analyzed using the Living Image 4.3.1 software.

2.7 | Histological assessment of GFP-positive ASCs

For systemically and locally treated groups, the lungs and the entire foot with the wound and the surrounding uninjured skin were harvested at 3 h, 24 h, 72 h, day 7 (d7), d15, and at WC and fixed in 4% formalin (Merck Millipore, MA). After fixation, the wound area along with the uninjured surrounding skin was removed from the foot and processed for paraffin embedding (Figure 2A). The lungs were kept whole and processed for paraffin embedding.

For immunohistochemistry (IHC), 5 µm thick transverse tissue sections were cut from formaldehyde fixed paraffin embedded (FFPE)

samples and analyzed using an anti-GFP D5.1 XP rabbit monoclonal antibody (Cell Signaling Technology Inc., MA). A single section of the lungs and feet was analyzed for the systemically treated group. For the locally treated group, a single section of the lungs was analyzed. However, for the feet, tissue sections were analyzed at five different levels into the sample block (Figure 2B). Antigen retrieval was performed using the Pascal Citrate system (DakoCytomation, Hamburg, Germany). After blocking endogenous peroxidases with Dako REAL peroxidase blocking solution (Dako, Hamburg, Germany), sections were incubated with the primary GFP rabbit monoclonal antibody (1/100 dilution; 70 ng/mL) for 1 h at RT, and then with a horseradish peroxidase-(HRP) complex secondary antibody (Dako EnVision+System-HRP, Dako, Hamburg, Germany) for 30 min at RT. Sections were developed with aminoethyl carbazole (AEC) for 10 min (BioGenex, CA) and counterstained with hematoxylin for 1–2 min. Sections were scanned using a Zeiss Axio Scan Z1 Brightfield scanner (Carl Zeiss, AG, Germany) at ×20 magnification.

In the locally treated group, we determined the precise location of the administered GFP positive ASCs over time. To do so, each section from the five different levels for each FFPE sample was divided into six zones: zone 0 = ASCs injection site on the border of wound; zone 00 = ASCs injection site on the other border of wound; and the wound itself divided in four zones: zone 1, 2, 02, and 01 (Figure 2C). The location of ASCs in the wound was expressed as a percentage area of GFP staining for a given zone and foot for each time-point. Using these zones, the percentage area of GFP staining was recorded at 24 h, 48 h, 72 h, and d7 as four sites, summing up all the five levels together as a single value per foot. The injection site was determined as the sum of zone 0 and 00 and the wound site as the sum of zone 1, 2, 02, and 01. More precisely, the outer wound site was defined as the sum of zone 1 and 01, and the inner wound site as the sum of zone 2 and 02 (Figure 2C). In total, three animals each with two feet per animal per timepoint were analyzed ($n = 6$). All images were processed using Definiens 2.7 software (Munich, Germany).
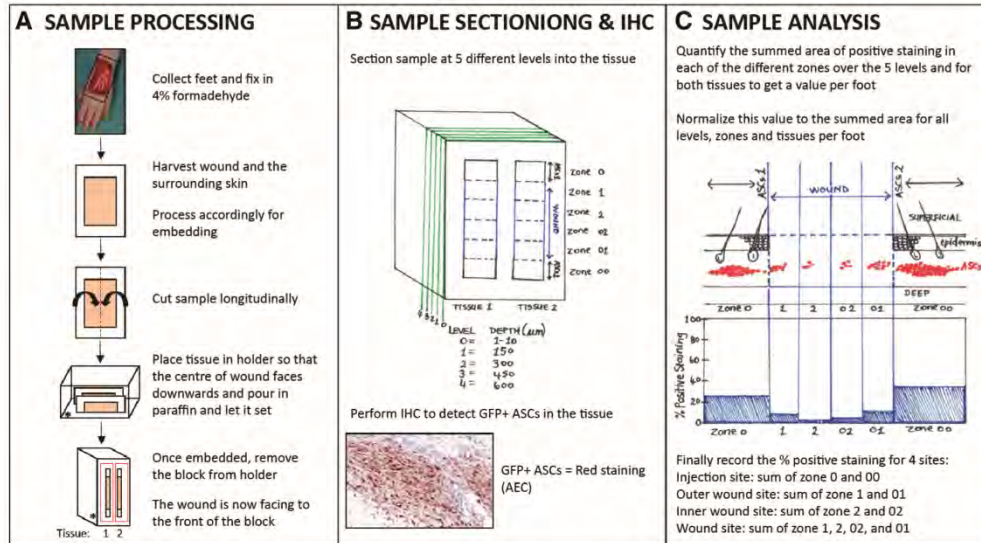
161

FIGURE 2 Schematic showing how the locally treated feet samples were processed, sectioned, stained for IHC, and analyzed. A, The feet were collected, fixed, and then processed for embedding in paraffin blocks. B, Each block, consisting of a single sample, was sectioned at five different levels into the FFPE tissue at levels 0, 1, 2, 3, and 4. IHC was performed to detect GFP+ ASCs (red staining, AEC). C, The sections were analyzed to quantify the area of positive staining using image processing software. Each section was divided into six zones, where zone 0 = ASCs 1 (ASC injection site 1), zone 1, 2, 02, and 01 = wound divided into four equal regions, and zone 00 = ASCs 2 (ASC injection site 2). The summed area of positive staining in each of the different zones over the five levels and for both tissues was quantified to obtain a value per foot. This value was normalized to the summed area for all the levels, zones, and tissues per foot. Finally, the percentage of positive staining was recorded as four sites: the injection site (sum of zone 0 and 00), the outer wound site (sum of zone 1 and 01), the inner wound site (sum of zone 2 and 02), and the wound site (sum of zone 1, 2, 02, and 01). Abbreviations: IHC, immunohistochemistry; FFPE, formaldehyde fixed paraffin embedded; ASCs, adipose-derived mesenchymal stromal cells; AEC, aminoethyl carbazole; GFP, green fluorescent protein

Results were compiled in the MATLAB 2018b (MathWorks, MA) and the graphs plotted using either MATLAB or Prism (GraphPad, CA).

performing multiple t tests using the Holm–Sidak method. A p value of <0.05 between data means was considered significant.

2.8 | Assessment of wound repair

The time taken to complete WC and the contraction/re-epithelialization ratio were assessed as previously described.[51] Wound size was documented immediately after wounding and until WC by digital photography at a constant distance with a ruler next to the wound for scaling. The photos were analyzed using ImageJ 1.48v software[52] to determine the wound area. At complete WC (ie, full epithelialization), the surface of the scar with hairless skin was measured and considered to correspond to the area of the wound that had healed by re-epithelialization. The surface of the wound that healed by contraction was estimated by subtraction of the epithelialized surface from the original wound area measured at day 0 (Figure 7C).

2.9 | Statistical analysis

Data are expressed as means ± SD. Statistical analyses were carried out using Prism (GraphPad, CA). A Mann–Whitney test was used to assess differences between data means. Grouped data were assessed by

3 | RESULTS

3.1 | Transduced ASCs maintained their immunophenotype and differentiation capacity

Isolated ASCs were plastic adherent in culture and displayed a typical fibroblast morphology (Figure 3A). Evaluation of GFP expression established that the lowest MOI needed to transduce at least 70% of the ASCs was 10 (Figure 3B). As the Fluc gene is under the control of a different promoter than the GFP gene, we determined whether our newly transduced cells also expressed Fluc. When D-luciferin, the molecular substrate for firefly luciferase, was added to the transduced cells *in vitro*, emitted luminescence was detected. An increase in luminescence, quantified as total flux, was observed with increasing MOIs (Figure 3C), confirming that the cells were successfully transduced to express not only GFP but also Fluc. GFP fluorescence was visible in both the nucleus and the cytoplasm of the transduced cells (Figure 3D). The percentage cells expressing GFP was also maintained *in vitro* over different passages showing that greater than 94% of ASCs expressed
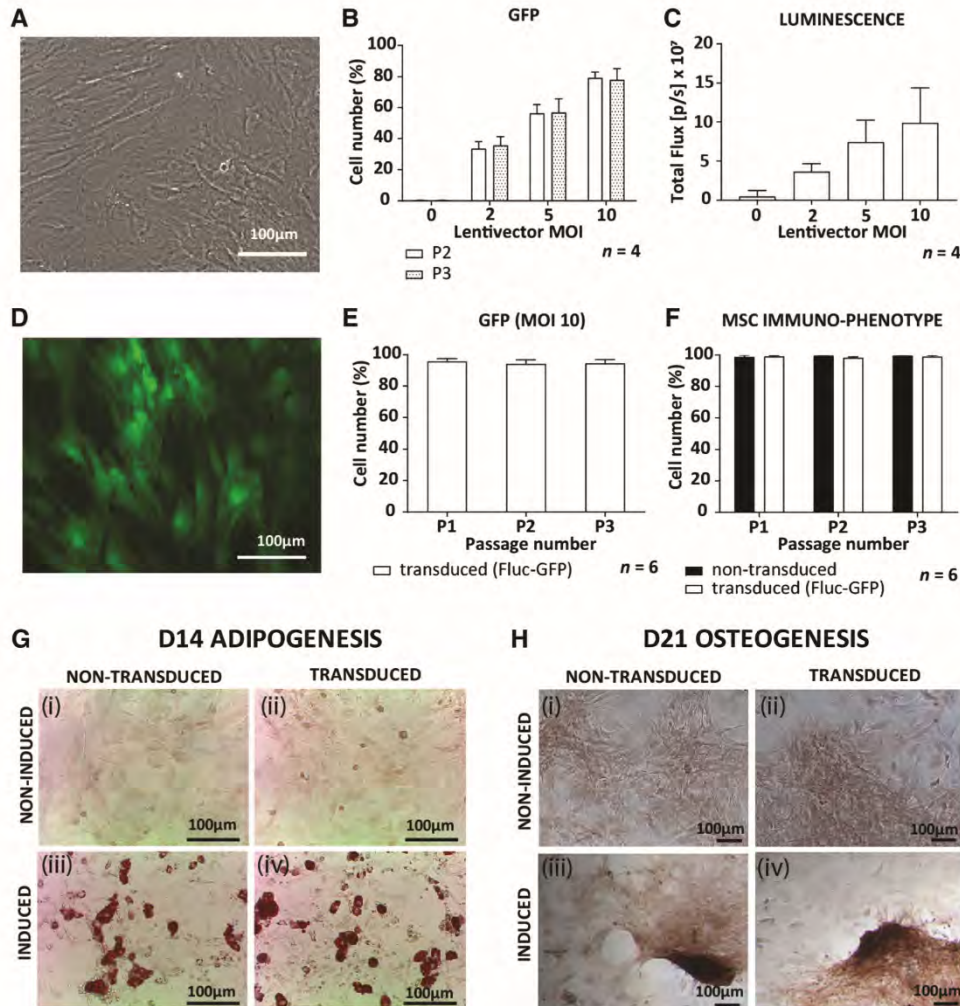
FIGURE 3 Characterization of non-transduced and transduced rat ASCs. A, Brightfield image of non-transduced ASCs in culture. B, GFP expression of transduced ASCs measured by flow cytometry with increasing MOIs as well as, C, luminescence measured by *in vitro* bioluminescence imaging. D, A fluorescent image of transduced ASCs (MOI 10) expressing GFP. E, GFP expression by ASCs transduced with an MOI of 10 in culture from passage 1 to 3 (P1 to P3). F, MSC immunophenotype (CD90+, CD29+, CD45−, CD31−) for transduced and non-transduced ASCs. G, Qualitative assessment of adipogenesis for (i, ii) non-induced control ASCs, (iii, iv) induced ASCs, (i, iii) non-transduced ASCs, and (ii, iv) transduced ASCs all stained for oil red O to identify lipid droplet formation after 14 days in induction medium. H, Qualitative assessment of osteogenesis for (i, ii) non-induced control ASCs, (iii, iv) induced ASCs, (i, iii) non-transduced ASCs, and (ii, iv) transduced ASCs all stained for alizarin red S to confirm calcium deposition after 21 days in induction medium. Abbreviations: ASCs, adipose-derived mesenchymal stromal cells; GFP, green fluorescent protein; MOI, mode of infection

GFP (Figure 3E). Over the three passages evaluated, both transduced and non-transduced ASCs maintained a typical MSC immunophenotype, being strongly positive for CD90 and CD29 and negative for CD45 and CD31 (Figure 3F). When treated with control medium, the non-transduced and transduced ASCs showed no spontaneous differentiation as seen by the absence of intracellular lipid droplets or calcium deposition. With induction media, the non-transduced and transduced ASCs showed comparable levels of intracellular lipid droplet formation, confirming that adipogenesis had occurred. In addition, sparsely distributed cell clumps or nodules that stained
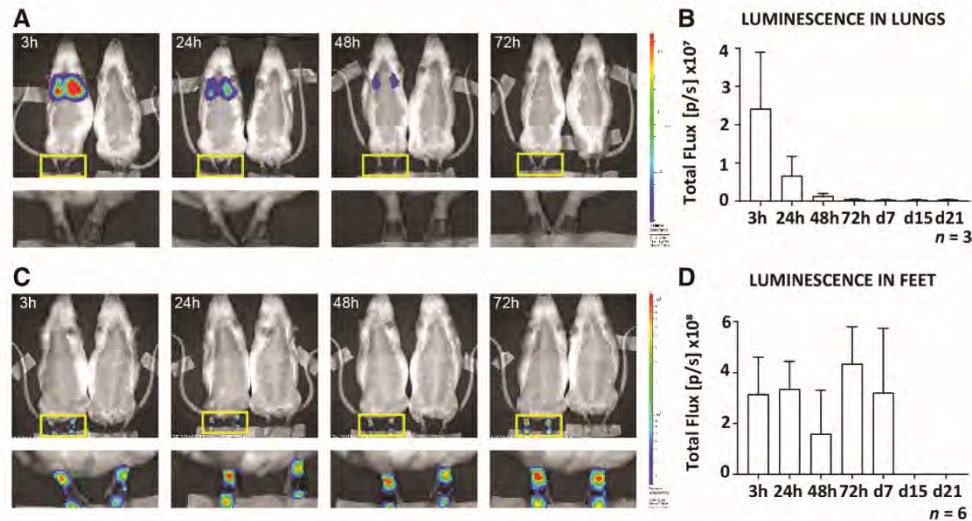
163

FIGURE 4 *In vivo* tracking of systemically and locally administered Fluc-GFP$^+$ ASCs during wound repair under physiological conditions. ASCs transduced to express both Fluc and GFP were injected either systemically (2×10^6 ASCs) via the tail vein or locally (2×10^5 ASCs) into two sides around each wound in rats 24 h after bilateral full-thickness wounds had been created on the dorsal aspect of the feet. Prior to imaging, rats received 150 mg/kg body weight of D-luciferin. A single representative image of a, A, systemically and, C, locally treated rat and BLI control rat (received non-transduced cells) imaged at 3 h, 24 h, 48 h, and 72 h. An enlarged area of the feet of the treated animals is also shown. The luminescence signal in the, B, lungs of systemically treated and the, D, feet of locally treated rats was quantified and recorded as total flux over time (gray bars). Data shown as mean ± SD. Abbreviations: ASCs, adipose-derived mesenchymal stromal cells; BLI, bioluminescence imaging; Fluc, firefly luciferase; GFP, green fluorescent protein

positive for ARS were observed, confirming that osteogenesis had occurred (Figure 3G,H).

3.2 | Systemically administered ASCs were filtered out in the lungs without homing to the wound site

Following systemic administration, the luminescent signal was detectable in the lungs 3 h post administration (Figure 4A), and a decrease in signal was observed from 3 h to 72 h (Figure 4B). No signal was detected in the wound on the feet. No signal was detectable in other organs when ASCs were injected either systemically or locally. At the histological level, systemically administered GFP positive ASCs were easily detected in the lungs of injected animals at 3 h and 24 h, moderately detectable at 48 h, barely detectable at 72 h, and undetectable from day 7 (Figure 5A). No GFP staining was detected in the wounds on the feet (Figure 5B) or in other non-target organs such as the spleen, heart, kidney, and liver at any of the time-points (data not shown).

3.3 | Locally administered ASCs survived and became distributed within the wound bed

When administered locally, the luminescent signal remained strongly detectable for 7 days at the injection site (Figure 4C,D) with no signal being detectable in the lungs (Figure 4C). Interestingly, histological

analysis of animals that received ASCs locally revealed that GFP staining was not restricted to the ASC injection sites. When 15% of the wound was analyzed as represented by the five levels at which sections were assessed, GFP positive ASCs became distributed within the wound bed as early as 24 h after administration (Figure 6A–E). At the injection site (zone 0, 00), ASCs remained detectable until d7 (Figure 6B). Within the wound bed (zone 1, 2, 02, and 01), a significant increase in GFP staining was found from 24 h to 72 h (0.039% vs 0.057%, $p = 0.0087$) with no significant change on d7 (Figure 6C). This significant increase in GFP staining from 24 h to 72 h was found in both the outer (zone 1 and 01; 0.031% vs 0.047%, $p = 0.0043$) and inner wound sites (zones 2 and 02; 0.010% vs 0.033%, $p = 0.0173$). However, even though the increase was significant in the inner wound site between 24 h and 72 h (0.013% vs 0.043%, $p = 0.0173$), and 48 h and 72 h (0.014% vs 0.043%, $p = 0.0152$), GFP staining remained lower than in the outer wound site. The outer wound site showed no significant changes in GFP staining from 72 h to d7, whereas in the inner wound site a significant decrease was found from 72 h to d7 (0.043% vs 0.010%, $p = 0.0152$; Figure 6D,E).

3.4 | Both systemic and local administration lead to enhanced WC time

As a secondary aim, we determined whether ASC administration might lead to a change in WC time. In comparison to a total WC time of
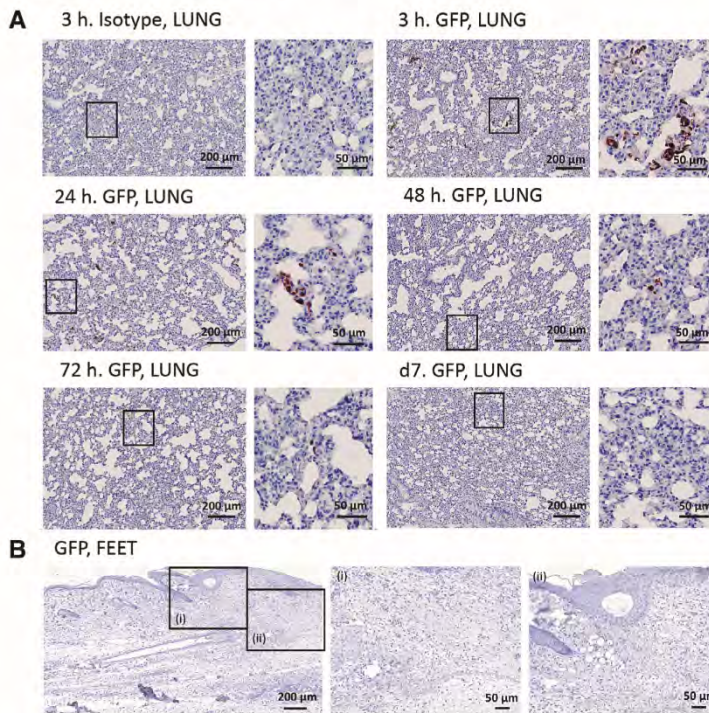
164

A

FIGURE 5 Detection of systemically administered ASCs during physiological wound repair by IHC. ASCs transduced to express both Fluc and GFP were injected systemically (2×10^6 ASCs) via the tail vein in rats 24 h after bilateral full-thickness wounds had been created on the dorsal part of the feet. Lungs and feet were processed for IHC to detect GFP positive ASCs (red staining, AEC). A, Images of the lung at 3 h, 24 h, 48 h, 72 h, and at d7 are shown. The right panel is a magnified view of the black rectangle showing positively stained ASCs. B, A representative image of the feet is shown where panel (i) is a magnified view of the epithelium lip and (ii) of the wound bed. Tissue sections were counterstained with hematoxylin (blue staining). Abbreviations: AEC, aminoethyl carbazole; ASCs, adipose-derived mesenchymal stromal cells; Fluc, firefly luciferase; GFP, green fluorescent protein; IHC, immunohistochemistry

26 days in the NaCl treated group, WC was significantly faster when ASCs were administered locally (19 days, $p = 0.0108$) and systemically (21 days, $p < 0.0024$; Figure 7A). Both ASC treated groups showed an increase in wound size after 3 days before reducing in size. At 7 days, wound size was significantly smaller in the control group compared with the ASC systemically treated group ($p = 0.03013$); however, this was not maintained. Comparison of ASC treated groups showed significantly smaller wounds with local treatment at 10 days ($p = 0.0102$; Figure 7B). Further investigation into whether WC was favored more by contraction (C) or epithelialization (E) showed a significant decrease in C and an increase in E in both the locally (C: 56%, E: 44%) and systemically treated groups (C: 62%, E: 38%) compared with the NaCl treated group (C: 73%, E: 27%; $p = 0.0022$ and $p = 0.0002$, respectively; Figure 7C,D).

4 | DISCUSSION

Interest in the use of systemically applied MSCs for therapeutic purposes was popularized by the group of Horwitz. Their studies in children with osteogenesis imperfecta demonstrated that allogeneic BM-MSCs injected systemically engrafted in the bone and BM stroma, and led to improvement in growth rates of the children as well as their ability to synthesize intact bone.[53-55] A study in rats showed that

BM-MSCs administered either systemically or locally were able to promote fracture healing.[56] Although the proportion of BM-MSCs that migrated into the injury sites following systemic injection was significantly less compared with locally injected BM-MSCs, both groups promoted fracture healing equally well, indicating that systemically injected BM-MSCs may have contributed in an indirect manner.[56]

We set out to compare the fate and distribution of systemically and locally administered ASCs in an *in vivo* model of physiological wound repair. The first concern with using transduced ASCs was that this could change their characteristics. Two parameters currently used to identify MSCs were assessed, namely their immunophenotype and differentiation capacity.[30,57] Transduction of ASCs did not change their immunophenotype or differentiation capacity compared with non-transduced ASCs and transduced ASCs maintained GFP expression *in vitro* over several passages. This confirmed previous studies showing that MSCs transduced to express GFP[58,59] or Fluc[33] maintain their characteristics *in vitro*. Here, we report that by using a single lentivector, both GFP and Fluc can be used in combination without changing the characteristics of ASCs.

Systemically administered ASCs showed no detectable homing to the site of injury. We suggest two reasons for this: first, ASCs could not bypass entrapment in the lung and re-enter the circulation; and second, the inflammatory response from the site of injury was not strong enough to activate ASC homing during physiological wound
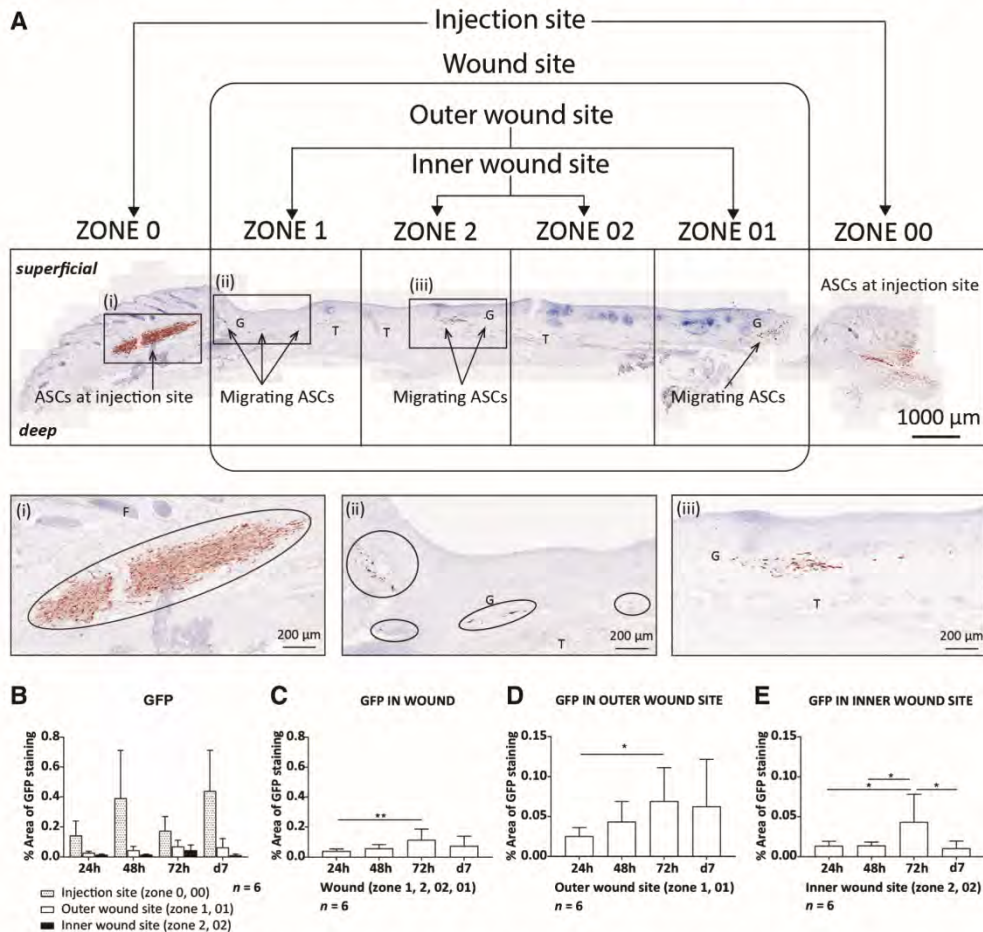
165

FIGURE 6 Locally administered ASCs were detected within the wound over time. A total of 2×10^5 ASCs transduced to express both Fluc and GFP were injected locally into two sides around each wound 24 h after bilateral full-thickness wounds had been created on the dorsal part of the feet. A, a single tissue section from the wound in the feet 24 h post injection stained for GFP (red staining, AEC). Magnified images of the (i) injection site, (ii) outer wound site, and (iii) inner wound site. The distribution of ASCs at the different sites of the wound was quantified over time showing, B, The injection site, outer, and inner wound site in a single graph, C, the wound site (zone 1, 2, 02, 01), D, the outer wound site (zone 1, 01), and, E, the inner wound site (zone 2, 02). Data shown as mean ± SD. Significance is shown where *, $p < 0.05$; **, $p < 0.01$. Abbreviations: AEC, aminoethyl carbazole; ASCs, adipose-derived mesenchymal stromal cells; E, epithelium; F, hair follicles; Fluc, firefly luciferase; G, granulation tissue; GFP, green fluorescent protein; T, tendons

repair. We postulate that pulmonary passage was the major reason for the lack of detectable ASC homing. Entrapment in the lungs has been a recurring problem with systemic administration of MSCs.[60,61] Of note, lung entrapment in our rat model was not associated with any visible signs of distress or deterioration of health.

To overcome this pulmonary first-pass effect and to ensure that administered cells reach the wound bed at the injured site in a timely manner and in sufficient numbers, alternative routes of administration have been suggested such as regional or local injection.[27,29,55] We investigated the fate of locally administered ASCs and found that they remained viable at the injection sites for 7 days. This is in line with another study reporting that rat BM-MSCs transplanted into traumatized skeletal muscle could be tracked in vivo until day 7.[33] At the histological level, we found a significant increase in ASCs localized within the wound as opposed to the adjacent injection sites from 24 h to 72 h. This localization of ASCs could be explained by active ASC migration, ASC proliferation, or the passive displacement from the injection site into the wound bed as the wound contracts to bring the

166
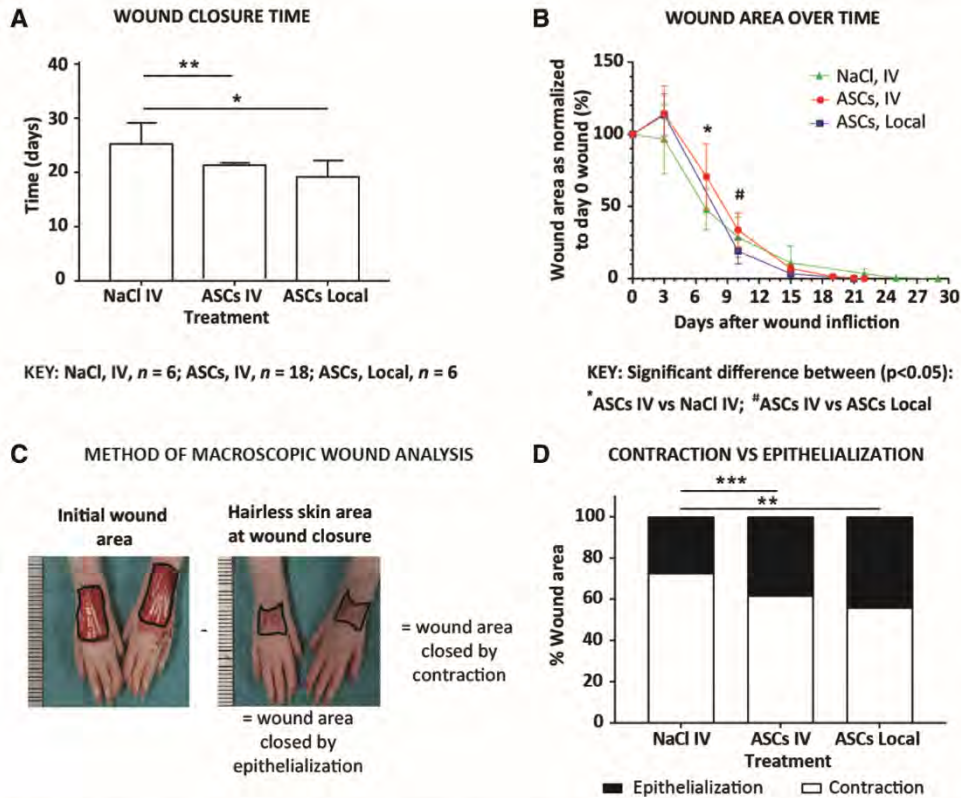
FIGURE 7 Wound closure assessment in animals treated locally and systemically. Animals were treated with Fluc-GFP$^+$ ASCs, injected locally into two sides around each wound (2×10^5 ASCs) or systemically (2×10^6 ASCs) into the tail vein. Control animals were treated systemically with NaCl. A, Time taken for complete wound closure after treatment. B, Wound area over time after treatment normalized to the original wound area on day 0. C, Calculation of the contraction/epithelialization ratio: the area of the wound is measured directly after surgery. At the day of complete wound closure, the area of hairless skin is measured and considered to correspond to the area of the wound closed by epithelialization. Subtracting the area of epithelialization from the initial wound area provides the area closed by contraction. D, Wound area closed by contraction and by epithelialization. Data shown as mean ± SD. Significance is shown where *, $p < 0.05$; **, $p < 0.01$; ***, $p < 0.001$. Abbreviations: ASCs, adipose-derived mesenchymal stromal cells; Fluc, firefly luciferase; GFP, green fluorescent protein

wound edges closer together. Over time, more ASCs were found in the outer wound site close to the newly extending epithelium lip at all time-points evaluated, with the greatest number of ASCs being detected at 72 h. In the inner wound site, increased numbers of ASCs were detected at 72 h. Our data suggest that locally administered ASC have the capability to migrate within the wound bed.

Wounds can close by two mechanisms, contraction, or re-epithelialization. Contraction occurs predominately as a rapid repair mechanism, whereas re-epithelialization takes longer and is closer to regeneration. Our animal model allowed for measurements of wound size, time to complete healing, and ratios of WC by contraction and epithelialization. Interestingly, an enhancement in WC time was found with ASC treatment independently of the route of administration. Both administration routes resulted in more rapid WC by re-epithelialization rather than contraction as compared with the control

group. The enhancement of WC by re-epithelialization rather than contraction is of clinical relevance, as it can have a significant impact on the quality of the scar by decreasing scar retraction.

The disappearance of transplanted cells and low engraftment at the injured site while still enhancing WC time suggests that ASCs play a role as initiators of wound repair rather than effectors.[62] This confirms findings from a study using a mouse model of acute acid-burn injury.[63] The authors also found that despite short-lived survival of locally transplanted ASCs, WC was enhanced. Another study found that intravenous human MSCs improved myocardial infarction in mice without significant engraftment through the secretion of anti-inflammatory protein TSG-6.[64] The mechanism of wound repair by MSCs has been suggested to stem from their paracrine signaling,[65] which mobilizes the host cells to promote wound repair. This leads us to ask; how do MSCs filtered out in the lung influence wound repair

167

mechanisms that are located distally? It has been shown that MSCs secrete various molecules that are modulators of cellular growth, replication, differentiation, and adherence.[66,67] The MSC (BM-MSCs and ASCs) secretome consists of soluble factors, such as cytokines, chemokines and growth factors, and proteins, lipids, and nucleic acids that are released via extracellular vesicles.[68,69] A subset of these extracellular vesicles, referred to as exosomes, are believed to be released by MSCs trapped in the lungs in response to injury cues where they can travel via the circulation to the injured site to exert their therapeutic effects.[55,70] MSC-derived extracellular vesicles have been suggested to be partially responsible for this paracrine effect.[71] It has been shown that systemically administered MSC exosomes attenuated lesion size and improved functional recovery post spinal cord injury.[72] A study that examined the role of MSC exosomes in wound healing showed that these structures were able to induce proliferation and migration of fibroblasts as well as enhance angiogenesis *in vitro*.[73]

This study confirms that systemically injected ASCs behave in a manner similar to BM-MSCs, being able to enhance WC despite showing intrapulmonary trapping and limited homing to the wound area. We provide evidence of migration of locally injected ASCs into the wound bed. We suggest that the therapeutic effect of ASCs is due to their paracrine signaling. Clinical studies using ASCs for cutaneous non-healing/chronic wounds are still limited. Instead, animal models are used. The local administration of ASCs for wound repair is favored and is being evaluated for various injuries with/without scaffolds in animal studies of tendon repair,[74-76] cutaneous non-healing wounds,[77-83] burn injuries,[84] spinal cord injuries,[85,86] and for bone defects,[87] among other indications. In the field of plastic and reconstructive surgery, since the discovery of ASCs within adipose tissue,[4,88] the addition of both the SVF and ASCs have been investigated in order to overcome the re-absorption of fat grafts.[89-91]

A limitation of our work could be the underestimation of ASC homing and engraftment because of our detection techniques and experimental setup. Although BLI allows for *in vivo* tracking, single cells and luminescence in deep organs cannot be detected. To overcome this, we included GFP staining to detect ASCs at a single cell level and in non-target organs. The animal model may have influenced the experimental outcome since Wistar rats are outbred and thus ASCs were isogenic rather than autologous. The "foreign" or isogenic ASCs might have primed the immune system and enabled a faster response and healing effect. In future studies, the use of alterative systemic routes such as intra-arterial to overcome the pulmonary first-pass effect, or treatment to prevent such filtering for example, by vasodilation, should be considered.[55] Another avenue to explore is the repeated administration of systemic ASCs. Fischer and colleagues hypothesized that the increase in pulmonary passage seen with their study was due to saturation of receptors during the first treatment, allowing more cells to pass the vasculature with the second treatment.[61] For local administration, the use of scaffolds or dressings could enable longer viability and more directed administration of ASCs into the wound bed. The lentiviral transduction of ASCs could alter properties that we were unable to detect. This could be a limitation

for acceptance by regulatory authorities as proof of principle for advancing to phase I clinical trials. More in depth characterization of ASCs is needed to confirm that transduction does not affect their characteristics *in vivo*.

In this study, we provide data showing an accelerating effect of ASCs on cutaneous wound repair under physiological conditions. These data support the use of ASCs in wound management since physiological wound repair is generally considered a naturally effective process with little margin for improvement. In order to determine the clinical usefulness of ASC injection in the management of chronic wounds, we plan to perform further investigations studying their effect in a model of wound repair under pathological conditions.

5 | CONCLUSION

This study demonstrates that although the survival and homing of systemically administered ASCs was limited, they nonetheless led to enhanced wound repair. Locally administered ASCs survived for 7 days at the transplantation site. They showed the ability to migrate within the wound bed, effectively enhancing wound repair by significantly reducing WC time. Taken together, ASCs have the potential to enhance wound repair without the need for homing to the injured site, possibly by paracrine signaling through the release of exosomes.

CONFLICT OF INTEREST

M.S.P. declared leadership position with Anion Biosciences, researcher funding from South African Medical Research Council, Wellcome

168

Trust and stock ownership with Transcure Bioservices. The other authors indicated no potential conflicts of interest.

ORCID

Karlien Kallmeyer https://orcid.org/0000-0002-9181-694X
Michael S. Pepper https://orcid.org/0000-0001-6406-2380

REFERENCES

1. Kim HJ, Park JS. Usage of human mesenchymal stem cells in cell-based therapy: advantages and disadvantages. Dev Reprod 2017; 21:1–10.
2. Al-Shaibani MBH, Wang X-N, Lovat PE et al. Cellular therapy for wounds: applications of mesenchymal stem cells in wound healing. In: Alexandrescu VA, ed. *Wound Healing—New insights into Ancient Challenges*. Rijeka, Croatia: InTech, 2016.
3. Isakson M, De Blacam C, Whelan D et al. Mesenchymal stem cells and cutaneous wound healing: current evidence and future potential. Stem Cells Int 2015;2015:1–12.
4. Zuk PA, Zhu M, Ashjian P et al. Human adipose tissue is a source of multipotent stem cells. Mol Biol Cell 2002;13:4279–4295.
5. Wei X, Yang X, Han ZP et al. Mesenchymal stem cells: a new trend for cell therapy. Acta Pharmacol Sin 2013;34:747–754.
6. Squillaro T, Peluso G, Galderisi U. Clinical trials with mesenchymal stem cells: an update. Cell Transplant 2016;25:829–848.
7. Friedenstein AJ, Petrakova KV, Kurolesova AI et al. Heterotopic of bone marrow. Analysis of precursor cells for osteogenic and hematopoietic tissues. Transplantation 1968;6:230–247.
8. Nuschke A. Activity of mesenchymal stem cells in therapies for chronic skin wound healing. Organogenesis 2014;10:29–37.
9. Fraser JK, Wulur I, Alfonso Z et al. Fat tissue: an underappreciated source of stem cells for biotechnology. Trends Biotechnol 2006;24: 150–154.
10. Lotfy A, Salama M, Zahran F et al. Characterization of mesenchymal stem cells derived from rat bone marrow and adipose tissue: a comparative study. Int J Stem Cells 2014;7:135–142.
11. Strioga M, Viswanathan S, Darinskas A et al. Same or not the same? Comparison of adipose tissue-derived versus bone marrow-derived mesenchymal stem and stromal cells. Stem Cells Dev 2012;21: 2724–2752.
12. Karp JM, Leng Teo GS. Mesenchymal stem cell homing: the devil is in the details. Cell Stem Cell 2009;4:206–216.
13. Liu L, Yu Q, Lin J et al. Hypoxia-inducible factor-1alpha is essential for hypoxia-induced mesenchymal stem cell mobilization into the peripheral blood. Stem Cells Dev 2011;20:1961–1971.
14. Ponte AL, Marais E, Gallay N et al. The in vitro migration capacity of human bone marrow mesenchymal stem cells: comparison of chemokine and growth factor chemotactic activities. Stem Cells 2007;25: 1737–1745.
15. Murphy MB, Moncivais K, Caplan AI. Mesenchymal stem cells: environmentally responsive therapeutics for regenerative medicine. Exp Mol Med 2013;45:e54.
16. Yin Y, Hao H, Cheng Y et al. The homing of human umbilical cord-derived mesenchymal stem cells and the subsequent modulation of macrophage polarization in type 2 diabetic mice. Int Immunopharmacol 2018;60:235–245.
17. Mishra SK, Khushu S, Singh AK et al. Homing and tracking of iron oxide labelled mesenchymal stem cells after infusion in traumatic brain injury mice: a longitudinal in vivo MRI study. Stem Cell Rev 2018;14:888–900.
18. Oh EJ, Lee HW, Kalimuthu S et al. In vivo migration of mesenchymal stem cells to burn injury sites and their therapeutic effects in a living mouse model. J Control Release 2018;279:79–88.
19. Kean TJ, Lin P, Caplan AI et al. MSCs: delivery routes and engraftment, cell-targeting strategies, and immune modulation. Stem Cells Int 2013;2013:732742.
20. Everaert BR, Bergwerf I, De Vocht N et al. Multimodal in vivo imaging reveals limited allograft survival, intrapulmonary cell trapping and minimal evidence for ischemia-directed BMSC homing. BMC Biotechnol 2012;12:93.
21. Sensebe L, Fleury-Cappellesso S. Biodistribution of mesenchymal stem/stromal cells in a preclinical setting. Stem Cells Int 2013;2013: 678063.
22. De Becker A, Riet IV. Homing and migration of mesenchymal stromal cells: how to improve the efficacy of cell therapy? World J Stem Cells 2016;8:73–87.
23. Gao J, Dennis JE, Muzic RF et al. The dynamic in vivo distribution of bone marrow-derived mesenchymal stem cells after infusion. Cells Tissues Organs 2001;169:12–20.
24. Kern S, Eichler H, Stoeve J et al. Comparative analysis of mesenchymal stem cells from bone marrow, umbilical cord blood, or adipose tissue. Stem Cells 2006;24:1294–1301.
25. Wagner W, Feldmann RE Jr, Seckinger A et al. The heterogeneity of human mesenchymal stem cell preparations—evidence from simultaneous analysis of proteomes and transcriptomes. Exp Hematol 2006; 34:536–548.
26. Caplan AI. Why are MSCs therapeutic? new data: new insight. J Pathol 2009;217:318–324.
27. Sorrell JM, Caplan AI. Topical delivery of mesenchymal stem cells and their function in wounds. Stem Cell Res Ther 2010;1:30.
28. Nitzsche F, Muller C, Lukomska B et al. Concise review: MSC adhesion cascade-insights into homing and transendothelial migration. Stem Cells 2017;35:1446–1460.
29. Kurtz A. Mesenchymal stem cell delivery routes and fate. Int J Stem Cells 2008;1:1–7.
30. Bourin P, Bunnell BA, Casteilla L et al. Stromal cells from the adipose tissue-derived stromal vascular fraction and culture expanded adipose tissue-derived stromal/stem cells: a joint statement of the International Federation for Adipose Therapeutics and Science (IFATS) and the International Society for Cellular Therapy (ISCT). Cytotherapy 2013;15:641–648.

31. Progatzky F, Dallman MJ, Lo Celso C. From seeing to believing: labelling strategies for in vivo cell-tracking experiments. Interface Focus 2013;3:20130001.

32. Kim JE, Kalimuthu S, Ahn BC. In vivo cell tracking with bioluminescence imaging. Nucl Med Mol Imaging 2015;49:3–10.

33. Strohschein K, Radojewski P, Winkler T et al. In vivo bioluminescence imaging—a suitable method to track mesenchymal stromal cells in a skeletal muscle trauma. Open Orthop J 2015;9:262–269.

34. Togel F, Yang Y, Zhang P et al. Bioluminescence imaging to monitor the in vivo distribution of administered mesenchymal stem cells in acute kidney injury. Am J Physiol Renal Physiol 2008;295:F315–F321.

35. Lembert, N., and Idahl, L.A. Regulatory effects of ATP and luciferin on firefly luciferase activity. Biochem J 1995;305 (Pt:929–933.

36. Francis E, Kearney L, Clover J. The effects of stem cells on burn wounds: a review. Int J Burns Trauma 2019;9:1–12.

37. Maranda EL, Rodriguez-Menocal L, Badiavas EV. Role of mesenchymal stem cells in dermal repair in burns and diabetic wounds. Curr Stem Cell Res Ther 2017;12:61–70.

38. Chen Y, Ma Y, Li N et al. Efficacy and long-term longitudinal follow-up of bone marrow mesenchymal cell transplantation therapy in a diabetic patient with recurrent lower limb bullosis diabeticorum. Stem Cell Res Therapy 2018;9:99–99.

39. Kirana S, Stratmann B, Prante C et al. Autologous stem cell therapy in the treatment of limb ischaemia induced chronic tissue ulcers of diabetic foot patients. Int J Clin Pract 2012;66:384–393.

40. Gupta PK, Chullikana A, Parakh R et al. A double blind randomized placebo controlled phase I/II study assessing the safety and efficacy of allogeneic bone marrow derived mesenchymal stem cell in critical limb ischemia. J Transl Med 2013;11:143.

41. Lee HC, An SG, Lee HW et al. Safety and effect of adipose tissue-derived stem cell implantation in patients with critical limb ischemia: a pilot study. Circ J 2012;76:1750–1760.

42. Ankrum J, Karp JM. Mesenchymal stem cell therapy: two steps forward, one step back. Trends Mol Med 2010;16:203–209.

43. Iijima H, Isho T, Kuroki H et al. Effectiveness of mesenchymal stem cells for treating patients with knee osteoarthritis: a meta-analysis toward the establishment of effective regenerative rehabilitation. NPJ Regen Med 2018;3:15–15.

44. Lukomska B, Stanaszek L, Zuba-Surma E et al. Challenges and controversies in human mesenchymal stem cell therapy. Stem Cells Int 2019;2019:10.

45. Galipeau J, Sensébé L. Mesenchymal stromal cells: clinical challenges and therapeutic opportunities. Cell Stem Cell 2018;22:824–833.

46. Sadie-Van Gijsen H, Crowther NJ, Hough FS et al. Depot-specific differences in the insulin response of adipose-derived stromal cells. Mol Cell Endocrinol 2010;328:22–27.

47. Van De Vyver M, Andrag E, Cockburn IL et al. Thiazolidinedione-induced lipid droplet formation during osteogenic differentiation. J Endocrinol 2014;223:119–132.

48. Huang JI, Beanes SR, Zhu M et al. Rat extramedullary adipose tissue as a source of osteochondrogenic progenitor cells. Plast Reconstr Surg 2002;109:1033–1041.

49. Tennant JR. Evaluation of the trypan blue technique for determination of cell viability. Transplantation 1964;2:685–694.

50. Bhaumik S, Gambhir SS. Optical imaging of renilla luciferase reporter gene expression in living mice. Proc Natl Acad Sci USA 2002;99:377–382.

51. Andre-Levigne D, Modarressi A, Pignel R et al. Hyperbaric oxygen therapy promotes wound repair in ischemic and hyperglycemic conditions, increasing tissue perfusion and collagen deposition. Wound Repair Regen 2016;24:954–965.

52. Rashband, W.S. Image J, U.S. National Institutes of Health, Betheshda, MD, USA. http://imagej.nih.gov/ij.

53. Horwitz EM, Gordon PL, Koo WK et al. Isolated allogeneic bone marrow-derived mesenchymal cells engraft and stimulate growth in children with osteogenesis imperfecta: implications for cell therapy of bone. Proc Natl Acad Sci USA 2002;99:8932–8937.

54. Horwitz EM, Prockop DJ, Fitzpatrick LA et al. Transplantability and therapeutic effects of bone marrow-derived mesenchymal cells in children with osteogenesis imperfecta. Nat Med 1999;5:309–313.

55. Leibacher J, Henschler R. Biodistribution, migration and homing of systemically applied mesenchymal stem/stromal cells. Stem Cell Res Ther 2016;7:7.

56. Huang S, Xu L, Zhang Y et al. Systemic and local administration of allogeneic bone marrow-derived mesenchymal stem cells promotes fracture healing in rats. Cell Transplant 2015;24:2643–2655.

57. Dominici M, Le Blanc K, Mueller I et al. Minimal criteria for defining multipotent mesenchymal stromal cells. The International Society for Cellular Therapy position statement. Cytotherapy 2006;8:315–317.

58. Van Vollenstee FA, Jackson C, Hoffmann D et al. Human adipose derived mesenchymal stromal cells transduced with GFP lentiviral vectors: assessment of immunophenotype and differentiation capacity in vitro. Cytotechnology 2016;68:2049–2060.

59. Wang Q, Steigelman MB, Walker JA et al. In vitro osteogenic differentiation of adipose stem cells after lentiviral transduction with green fluorescent protein. J Craniofac Surg 2009;20:2193–2199.

60. Ge J, Guo L, Wang S et al. The size of mesenchymal stem cells is a significant cause of vascular obstructions and stroke. Stem Cell Rev 2014;10:295–303.

61. Fischer UM, Harting MT, Jimenez F et al. Pulmonary passage is a major obstacle for intravenous stem cell delivery: the pulmonary first-pass effect. Stem Cells Dev 2009;18:683–692.

62. Shin L, Peterson DA. Human mesenchymal stem cell grafts enhance normal and impaired wound healing by recruiting existing endogenous tissue stem/progenitor cells. Stem Cells Transl Med 2013;2:33–42.

63. Muhammad G, Xu J, Bulte JWM et al. Transplanted adipose-derived stem cells can be short-lived yet accelerate healing of acid-burn skin wounds: a multimodal imaging study. Sci Rep 2017;7:4644–4644.

64. Lee RH, Pulin AA, Seo MJ et al. Intravenous hMSCs improve myocardial infarction in mice because cells embolized in lung are activated to secrete the anti-inflammatory protein TSG-6. Cell Stem Cell 2009;5:54–63.

65. Epstein SE, Luger D, Lipinski MJ. Paracrine-mediated systemic anti-inflammatory activity of intravenously administered mesenchymal stem cells: a transformative strategy for cardiac stem cell therapeutics. Circ Res 2017;121:1044–1046.

66. Di Rocco G, Baldari S, Toietta G. Towards therapeutic delivery of extracellular vesicles: strategies for in vivo tracking and biodistribution analysis. Stem Cells Int 2016;2016:1–12.

67. Tran C, Damaser MS. Stem cells as drug delivery methods: application of stem cell secretome for regeneration. Adv Drug Deliv Rev 2015;82-83:1–11.

68. Kapur SK, Katz AJ. Review of the adipose derived stem cell secretome. Biochimie 2013;95:2222–2228.

69. Kupcova Skalnikova H. Proteomic techniques for characterisation of mesenchymal stem cell secretome. Biochimie 2013;95:2196–2211.

70. Li P, Guo X. A review: therapeutic potential of adipose-derived stem cells in cutaneous wound healing and regeneration. Stem Cell Res Ther 2018;9:302.

71. Zheng G, Huang R, Qiu G et al. Mesenchymal stromal cell-derived extracellular vesicles: regenerative and immunomodulatory effects and potential applications in sepsis. Cell Tissue Res 2018;374:1–15.

72. Huang JH, Yin XM, Xu Y et al. Systemic administration of exosomes released from mesenchymal stromal cells attenuates apoptosis, inflammation, and promotes angiogenesis after spinal cord injury in rats. J Neurotrauma 2017;34:3388–3396.

73. Shabbir, A., Cox, A., Rodriguez-Menocal, L., Salgado, M., and Van Badiavas, E. Mesenchymal stem cell exosomes induce proliferation

170

and migration of normal and chronic wound fibroblasts, and enhance angiogenesis in vitro. Stem Cells Dev 2015;24:1635–1647.

74. Gelberman RH, Linderman SW, Jayaram R et al. Combined administration of ASCs and BMP-12 promotes an M2 macrophage phenotype and enhances tendon healing. Clin Orthop Relat Res 2017;475: 2318–2331.

75. Lucke LD, Bortolazzo FO, Theodoro V et al. Low-level laser and adipose-derived stem cells altered remodelling genes expression and improved collagen reorganization during tendon repair. Cell Prolif 2019;52:e12580.

76. De Aro AA, Carneiro GD, Teodoro LFR et al. Injured achilles tendons treated with adipose-derived stem cells transplantation and GDF-5. Cell 2018;7:127.

77. Nishiwaki K, Aoki S, Kinoshita M et al. In situ transplantation of adipose tissue-derived stem cells organized on porous polymer nanosheets for murine skin defects. J Biomed Mater Res B Appl Biomater 2019;107:1363–1371.

78. Irons RF, Cahill KW, Rattigan DA et al. Acceleration of diabetic wound healing with adipose-derived stem cells, endothelial-differentiated stem cells, and topical conditioned medium therapy in a swine model. J Vasc Surg 2018;68:115S–125S.

79. Yu J, Wang M-Y, Tai H-C et al. Cell sheet composed of adipose-derived stem cells demonstrates enhanced skin wound healing with reduced scar formation. Acta Biomater 2018;77:191–200.

80. Chae D-S, Han S, Son M et al. Stromal vascular fraction shows robust wound healing through high chemotactic and epithelialization property. Cytotherapy 2017;19:543–554.

81. Kato Y, Iwata T, Washio K et al. Creation and transplantation of an adipose-derived stem cell (ASC) sheet in a diabetic wound-healing model. JoVE 2017;126:e54539.

82. Chicharro D, Carrillo JM, Rubio M et al. Combined plasma rich in growth factors and adipose-derived mesenchymal stem cells promotes the cutaneous wound healing in rabbits. BMC Vet Res 2018; 14:288–288.

83. Rodriguez J, Boucher F, Lequeux C et al. Intradermal injection of human adipose-derived stem cells accelerates skin wound healing in nude mice. Stem Cell Res Therapy 2015;6:241–241.

84. Prasai A, El Ayadi A, Mifflin RC et al. Characterization of Adipose-Derived Stem Cells Following Burn Injury. Stem Cell Rev 2017;13:781–792.

85. Yin H, Jiang T, Deng X et al. A cellular spinal cord scaffold seeded with rat adipose-derived stem cells facilitates functional recovery via enhancing axon regeneration in spinal cord injured rats. Mol Med Rep 2018;17:2998–3004.

86. Gomes ED, Mendes SS, Assunção-Silva RC et al. Co-transplantation of adipose tissue-derived stromal cells and olfactory ensheathing cells for spinal cord injury repair. Stem Cells 2018;36:696–708.

87. Corsetti A, Bahuschewskyj C, Ponzoni D et al. Repair of bone defects using adipose-derived stem cells combined with alpha-tricalcium phosphate and gelatin sponge scaffolds in a rat model. J Appl Oral Sci 2017;25:10–19.

88. Zuk PA, Zhu M, Mizuno H et al. Multilineage cells from human adipose tissue: implications for cell-based therapies. Tissue Eng 2001;7: 211–228.

89. Simonacci F, Bertozzi N, Grieco MP et al. From liposuction to adipose-derived stem cells: indications and technique. Acta Biomed 2019;90:197–208.

90. Paik KJ, Zielins ER, Atashroo DA et al. Studies in fat grafting: part V. Cell-assisted lipotransfer to enhance fat graft retention is dose dependent. Plast Reconstr Surg 2015;136:67–75.

91. Domenis R, Lazzaro L, Calabrese S et al. Adipose tissue derived stem cells: in vitro and in vivo analysis of a standard and three commercially available cell-assisted lipotransfer techniques. Stem Cell Res Therapy 2015;6:2.

171

APPENDIX 5. UNIVERSITY OF PRETORIA ETHICAL APPROVAL LETTERS

Ethical approval letter for change of title

UNIVERSITEIT VAN PRETORIA
UNIVERSITY OF PRETORIA
YUNIBESITHI YA PRETORIA

Faculty of Health Sciences

14 March 2019

Approval Certificate
Amendment

Ethics Reference No.: 305/2014
Title: OLD: Investigating the homing properties of adipose-derived mesenchymal stromal cells.
NEW: Investigating the homing and healing properties of adipose-derived mesenchymal stromal cells using a model of wound repair

Dear Ms K Kallmeyer

The Amendment   as supported by documents received between 2019-02-07 and 2019-03-14 for your research, was approved by the Faculty of Health Sciences Research Ethics Committee on its quorate meeting of 2019-03-13.

Please note the following about your ethics approval:
- Please remember to use your protocol number (305/2014) on any documents or correspondence with the Research Ethics Committee regarding your research.
- Please note that the Research Ethics Committee may ask further questions, seek additional information, require further modification, monitor the conduct of your research, or suspend or withdraw ethics approval.

Ethics approval is subject to the following:
- The ethics approval is conditional on the research being conducted as stipulated by the details of all documents submitted to the Committee. In the event that a further need arises to change who the investigators are, the methods or any other aspect, such changes must be submitted as an Amendment for approval by the Committee.

We wish you the best with your research.

Yours sincerely

Dr R Sommers
MBChB MMed (Int) MPharmMed PhD
Deputy Chairperson   of the Faculty of Health Sciences Research Ethics Committee, University of Pretoria

The Faculty of Health Sciences Research Ethics Committee complies with the SA National Act 61 of 2003 as it pertains to health research and the United States Code of Federal Regulations Title 45 and 46. This committee abides by the ethical norms and principles for research, established by the Declaration of Helsinki, the South African Medical Research Council Guidelines as well as the Guidelines for Ethical Research: Principles Structures and Processes, Second Edition 2015 (Department of Health).

Research Ethics Committee
Room 4-60, Level 4, Tswelopele Building
University of Pretoria, Private Bag X323
Arcadia 0007, South Africa
Tel +27 (0)12 356 3084
Email deepeka.behari@up.ac.za
www.up.ac.za

Fakulteit Gesondheidswetenskappe
Lefapha la Disaense tša Maphelo

172

Ethical approval letter for PhD studies

UNIVERSITEIT VAN PRETORIA
UNIVERSITY OF PRETORIA
YUNIBESITHI YA PRETORIA

Faculty of Health Sciences Research Ethics Committee

2/10/2014

Approval Certificate
New Application

Ethics Reference No.: 305/2014

Title: Investigating the homing properties of adipose-derived mesenchymal stromal cells

Dear Ms Karlien Kallmeyer

The **New Application** as supported by documents specified in your cover letter dated 24/08/2014 for your research received on the 31/07/2014, was approved by the Faculty of Health Sciences Research Ethics Committee on the 1/10/2014.

Please note the following about your ethics approval:
- Ethics Approval is valid for 4 years.
- Please remember to use your protocol number (**305/2014**) on any documents or correspondence with the Research Ethics Committee regarding your research.
- Please note that the Research Ethics Committee may ask further questions, seek additional information, require further modification, or monitor the conduct of your research.

Ethics approval is subject to the following:
- The ethics approval is conditional on the receipt of 6 monthly written Progress Reports, and
- The ethics approval is conditional on the research being conducted as stipulated by the details of all documents submitted to the Committee. In the event that a further need arises to change who the investigators are, the methods or any other aspect, such changes must be submitted as an Amendment for approval by the Committee.

We wish you the best with your research.

Yours sincerely

Dr R Sommers; MBChB; MMed (Int); MPharMed.
Deputy Chairperson of the Faculty of Health Sciences Research Ethics Committee, University of Pretoria

The Faculty of Health Sciences Research Ethics Committee complies with the SA National Act 61 of 2003 as it pertains to health research and the United States Code of Federal Regulations Title 45 and 46. This committee abides by the ethical norms and principles for research, established by the Declaration of Helsinki, the South African Medical Research Council Guidelines as well as the Guidelines for Ethical Research: Principles Structures and Processes 2004 (Department of Health).

☎ 012 354 1677   ☒ 0866516047   ✉ deepeka.behari@up.ac.za   🖰 http://www.healthethics-up.co.za
✉ Private Bag X323, Arcadia, 0007 - 31 Bophelo Road, HW Snyman South Building, Level 2, Room 2.33, Gezina, Pretoria

173

APPENDIX 6. UNIVERSITY OF GENEVA VETERINARY ETHICAL APPROVAL LETTERS

	REPUBLIQUE ET CANTON DE GENEVE Département de l'emploi, des affaires sociales et de la santé Direction générale de la santé Domaine de l'expérimentation animale	GE/34/15
	Direction générale de la santé, Avenue de Beau-Séjour 24, 1206 Genève Astrid Rod, personne responsable	26345

Autorisation pour expériences sur animaux (Formulaire B)

Art. 18 al. 1 Loi fédérale sur la protection des animaux (LPA, RS455)

Directeur/trice de l'expérimentation animale Marjolaine Philit	Institut UNI DUFOUR rue du Général Dufour 24 1211 Genève 4 022 000 000

Directeur/trice de l'expérience

Ali Modarressi

Titre de l'expérience

L'effet des cellules souches mésenchymateuses d'origine graisseuse administrées par voie systémique sur la cicatrisation cutanée.

Type de la demande

[]   [N] nouvelle demande

Décision   La demande fait partie intégrante de l'autorisation.

Autorisée

Date de l'autorisation

13.04.2015

Valid From_fr

13.04.2015

Autorisation valable jusqu'à

13.05.2018

Page 1.

174

Charges et conditions

- Il n'y aura pas de détention individuelle des rats de manière générale. En effet, la détention se fera par 2 avec une surveillance accrue les 2 premiers jours p.o. Les rats seront détenus avec plus d'enrichissement, plus de nourriture à disposition. Si malgré ces conditions des blessures survenaient, alors la détention serait individuelle.

Dérogations relatives au personnel, à la formation continue, à la détention d'animaux, etc.

Animaux autorisés

Espèce	Nombre d'animaux demandés	Nombre d'animaux autorisés
Rats	140	**140**

Degré de gravité prospectif maximal: **2**

Emoluments

Description	Nombre	Unité	Prix
étude du dossier	3	h	480.0
frais administratifs	1	h	80.0
Total			560.0

Charges relatives aux rapports et à des modifications de la demande

Il y a lieu de nous annoncer par courriel (dgs.experimentation-animale@etat.ge.ch), au moins 48 heures ouvrables d'avance :

- n° complet de l'autorisation ;

- date ;

- heure ;

- lieu (étage, n° de laboratoire) ;

- les manipulations sur l'animal durant **6 mois** dès le début effectif de l'expérience.

Les manipulations se font pendant les jours ouvrables (8h-17h). Les dérogations à cette règle doivent être dûment justifiées.

Toute annulation ou modification d'horaire et/ou de lieu - qui n'aura pas été notifiée par écrit - ½ journée ouvrable à l'avance, sera facturée.

- En cas de souffrances manifestes qui ne pourraient être soulagées par l'administration d'analgésiques, les animaux doivent être immédiatement euthanasiés.

- Si un taux de mortalité élevé devait être constaté, la Direction générale de la santé, (Dr A. Rod) doit en être immédiatement informée.

Attention à l'identification des cages : elle doit porter l'intégralité du n° de l'autorisation !

Formation continue:

Nous vous rappelons que suite à l'obtention du module 1 et/ou 2, il est obligatoire d'effectuer **4 jours de formation continue par tranche de 4 années**.

Exemple : pour un module obtenu en janvier 2004, il sera nécessaire d'effectuer 4 jours de formation entre janvier 2004 et janvier 2008.

RAPPORTS ET MODIFICATIONS DE L'EXPERIENCE (art. 63a OPAn)

Le/la responsable de l'institut ou du laboratoire doit annoncer dans les 2 mois sur formule C la clôture de l'expérience soumise à autorisation et de celle non soumise à autorisation. Dans le cas d'expériences s'étendant sur plusieurs années, l'annonce avec les indications correspondantes pour l'année civile écoulée doit se faire au plus tard jusqu'à fin mars.

Avant de modifier l'expérience selon l'indication sous ch. 4-10 de la demande et ch. 2 de cette autorisation/décision officielle (telles que modification de la méthode et durée de l'expérience, utilisation d'autres espèces animales, augmentation du nombre des animaux, changement du responsable de l'intitut ou du laboratoire, changement des expérimentateurs, etc.), il faut impérativement demander une autorisation complémentaire ou autre accord à l'Office vétérinaire cantonal.

Moyens légaux

La présente autorisation est susceptible de recours par l'office fédéral de la sécurité alimentaire et des affaires vétérinaires OSAV (LPA, art.26, al.1).

Il ne peut en être fait usage qu'au moment où il est établi, **soit en attendant l'expiration du délai de recours de 30 jours (depuis la date de l'autorisation), soit en s'informant directement auprès de l'OSAV qu'aucune voie de droit n'a été utilisée.**

GE   13.04.2015   Astrid Rod

Fichiers annexés

Titre du document	Nom du fichier	Taille du fichier
Figures 1 à 6	Figures 1-6.pdf	229 KB
Tableaux 1 à 4	Tablaux 1-4.pdf	13 KB

176

![blason]	REPUBLIQUE ET CANTON DE GENEVE Département de l'emploi, des affaires sociales et de la santé Direction générale de la santé Domaine de l'expérimentation animale	**GE/72/17**
	Direction générale de la santé, Rue Adrien-Lachenal 8, 1207 Genève Astrid Rod, personne responsable	**26345**

Autorisation pour expériences sur animaux (Formulaire B)

Art. 18 al. 1 Loi fédérale sur la protection des animaux (LPA, RS455)

Directeur/trice de l'expérimentation animale Marjolaine Philit	Institut UNI DUFOUR rue du Général Dufour 24 1211 Genève 4 022 000 000

Directeur/trice de l'expérience

Ali Modarressi

Titre de l'expérience

L'effet des cellules souches mésenchymateuses d'origine graisseuse administrées par voie systémique sur la cicatrisation cutanée.

Type de la demande

[C] demande complémentaire

Demande précédente:

GE/34/15

Décision   La demande fait partie intégrante de l'autorisation.

Autorisée

Date de l'autorisation

25.04.2017

Valid From_fr

25.04.2017

Autorisation valable jusqu'à

177

13.05.2018

Charges et conditions

- Il n'y aura pas de détention individuelle des rats de manière générale. En effet, la détention se fera par 2 avec une surveillance accrue les 2 premiers jours p.o. Les rats seront détenus avec plus d'enrichissement, plus de nourriture à disposition. Si malgré ces conditions des blessures survenaient, alors la détention serait individuelle.

Dérogations relatives au personnel, à la formation continue, à la détention d'animaux, etc.

Animaux autorisés

Espèce	Autrefois autorisé	Nombre d'animaux demandés	Nombre d'animaux autorisés
Rats	140	40	**180**

Degré de gravité prospectif maximal: **2**

Emoluments

Description	Nombre	Unité	Prix
étude du dossier	1	h	160.0
frais administratifs	1	h	80.0
Total			240.0

Charges relatives aux rapports et à des modifications de la demande

Il y a lieu de nous annoncer par courriel (dgs.experimentation-animale@etat.ge.ch), au moins 48 heures ouvrables d'avance :

- n° complet de l'autorisation ;

- date ;

- heure ;

- lieu (étage, n° de laboratoire) ;

- les manipulations sur l'animal durant **6 mois** dès le début effectif de l'expérience.

Les manipulations se font pendant les jours ouvrables (8h-17h). Les dérogations à cette règle doivent être dûment justifiées.

Toute annulation ou modification d'horaire et/ou de lieu - qui n'aura pas été notifiée par écrit - ½ journée ouvrable à l'avance, sera facturée.

- En cas de souffrances manifestes qui ne pourraient être soulagées par l'administration d'analgésiques, les animaux doivent être immédiatement

euthanasiés.

- Si un taux de mortalité élevé devait être constaté, la Direction générale de la santé, (Dr A. Rod) doit en être immédiatement informée.

Attention à l'identification des cages : elle doit porter l'intégralité du n° de l'autorisation !

Formation continue:

Nous vous rappelons que suite à l'obtention du module 1 et/ou 2, il est obligatoire d'effectuer **4 jours de formation continue par tranche de 4 années**.

Exemple : pour un module obtenu en janvier 2004, il sera nécessaire d'effectuer 4 jours de formation entre janvier 2004 et janvier 2008.

RAPPORTS ET MODIFICATIONS DE L'EXPERIENCE (art. 63a OPAn)

Le/la responsable de l'institut ou du laboratoire doit annoncer dans les 2 mois sur formule C la clôture de l'expérience soumise à autorisation et de celle non soumise à autorisation. Dans le cas d'expériences s'étendant sur plusieurs années, l'annonce avec les indications correspondantes pour l'année civile écoulée doit se faire au plus tard jusqu'à fin mars.

Avant de modifier l'expérience selon l'indication sous ch. 4-10 de la demande et ch. 2 de cette autorisation/décision officielle (telles que modification de la méthode et durée de l'expérience, utilisation d'autres espèces animales, augmentation du nombre des animaux, changement du responsable de l'intitut ou du laboratoire, changement des expérimentateurs, etc.), il faut impérativement demander une autorisation complémentaire ou autre accord à l'Office vétérinaire cantonal.

Moyens légaux

La présente autorisation est susceptible de recours par l'office fédéral de la sécurité alimentaire et des affaires vétérinaires OSAV (LPA, art.26, al.1).

Il ne peut en être fait usage qu'au moment où il est établi, **soit en attendant l'expiration du délai de recours de 30 jours (depuis la date de l'autorisation), soit en s'informant directement auprès de l'OSAV qu'aucune voie de droit n'a été utilisée.**

GE   25.04.2017   Astrid Rod

Fichiers annexés

Titre du document	Nom du fichier	Taille du fichier
Figures 1 à 6	Figures 1-6.pdf	229 KB
Tableaux 1 à 4	Tablaux 1-4.pdf	13 KB
Abtract pour congrès scientifique résumant phase 1 et 2	Abstract faith of ADSC.docx	16 KB

	REPUBLIQUE ET CANTON DE GENEVE Département de l'emploi, des affaires sociales et de la santé Direction générale de la santé **Domaine de l'expérimentation animale**	**GE/15/18**
Direction générale de la santé, Rue Adrien-Lachenal 8, 1207 Genève Astrid Rod, personne responsable		26345

Autorisation pour expériences sur animaux (Formulaire B)

Art. 18 al. 1 Loi fédérale sur la protection des animaux (LPA, RS455)

Directeur/trice de l'expérimentation animale	Institut
Marjolaine Philit	UNI DUFOUR rue du Général Dufour 24 1211 Genève 4 022 000 000

Directeur/trice de l'expérience
Ali Modarressi

Titre de l'expérience

L'effet des cellules souches mésenchymateuses d'origine graisseuse administrées par voie systémique sur la cicatrisation cutanée.

Type de la demande
[C] demande complémentaire

Demande précédente:
GE/72/17

Décision La demande fait partie intégrante de l'autorisation.

Autorisée

Date de l'autorisation
29.01.2018

Valid From_fr
29.01.2018

180

Autorisation valable jusqu'à

13.05.2018

Charges et conditions

- Il n'y aura pas de détention individuelle des rats de manière générale. En effet, la détention se fera par 2 avec une surveillance accrue les 2 premiers jours p.o. Les rats seront détenus avec plus d'enrichissement, plus de nourriture à disposition. Si malgré ces conditions des blessures survenaient, alors la détention serait individuelle.

Dérogations relatives au personnel, à la formation continue, à la détention d'animaux, etc.

Animaux autorisés

Espèce	Autrefois autorisé	Nombre d'animaux demandés	Nombre d'animaux autorisés
Rats	180	80	**260**

Degré de gravité prospectif maximal: **3**

Emoluments

Description	Nombre	Unité	Prix
étude du dossier	1	h	160.0
frais administratifs	1	h	80.0
Total			240.0

Charges relatives aux rapports et à des modifications de la demande

Il y a lieu de nous annoncer par courriel (dgs.experimentation-animale@etat.ge.ch), au moins 48 heures ouvrables d'avance :

- n° complet de l'autorisation ;

- date ;

- heure ;

- lieu (étage, n° de laboratoire) ;

- les manipulations sur l'animal durant **6 mois** dès le début effectif de l'expérience.

Les manipulations se font pendant les jours ouvrables (8h-17h). Les dérogations à cette règle doivent être dûment justifiées.

Toute annulation ou modification d'horaire et/ou de lieu - qui n'aura pas été notifiée par écrit - ½ journée ouvrable à l'avance, sera facturée.

- En cas de souffrances manifestes qui ne pourraient être soulagées par l'administration d'analgésiques, les animaux doivent être immédiatement euthanasiés.

- Si un taux de mortalité élevé devait être constaté, la Direction générale de la santé, (Dr A. Rod) doit en être immédiatement informée.

Attention à l'identification des cages : elle doit porter l'intégralité du n° de l'autorisation !

Formation continue:

Nous vous rappelons que suite à l'obtention du module 1 et/ou 2, il est obligatoire d'effectuer **4 jours de formation continue par tranche de 4 années**.

Exemple : pour un module obtenu en janvier 2004, il sera nécessaire d'effectuer 4 jours de formation entre janvier 2004 et janvier 2008.

RAPPORTS ET MODIFICATIONS DE L'EXPERIENCE (art. 63a OPAn)

Le/la responsable de l'institut ou du laboratoire doit annoncer dans les 2 mois sur formule C la clôture de l'expérience soumise à autorisation et de celle non soumise à autorisation. Dans le cas d'expériences s'étendant sur plusieurs années, l'annonce avec les indications correspondantes pour l'année civile écoulée doit se faire au plus tard jusqu'à fin mars.

Avant de modifier l'expérience selon l'indication sous ch. 4-10 de la demande et ch. 2 de cette autorisation/décision officielle (telles que modification de la méthode et durée de l'expérience, utilisation d'autres espèces animales, augmentation du nombre des animaux, changement du responsable de l'intitut ou du laboratoire, changement des expérimentateurs, etc.), il faut impérativement demander une autorisation complémentaire ou autre accord à l'Office vétérinaire cantonal.

Moyens légaux

La présente autorisation est susceptible de recours par l'office fédéral de la sécurité alimentaire et des affaires vétérinaires OSAV (LPA, art.26, al.1).

Il ne peut en être fait usage qu'au moment où il est établi, **soit en attendant l'expiration du délai de recours de 30 jours (depuis la date de l'autorisation), soit en s'informant directement auprès de l'OSAV qu'aucune voie de droit n'a été utilisée.**

GE   29.01.2018   Astrid Rod

Fichiers annexés

Titre du document	Nom du fichier	Taille du fichier
Argumentation pour animaux supplémentaire	Argumentation pour animaux supplémentaires 18012018.docx	32 KB

Autorisation pour expériences sur animaux (Formulaire B)

Art. 18 al. 1 Loi fédérale sur la protection des animaux (LPA, RS455)

Directeur/trice de l'expérimentation animale Marjolaine Philit	Institut UNI DUFOUR rue du Général Dufour 24 1211 Genève 4 022 000 000

Directeur/trice de l'expérience
Ali Modarressi

Titre de l'expérience

L'effet des cellules souches mésenchymateuses d'origine graisseuse administrées par voie systémique sur la cicatrisation cutanée.

Type de la demande
[C] demande complémentaire

Demande précédente:
GE/15/18

Décision   La demande fait partie intégrante de l'autorisation.

Autorisée

Date de l'autorisation

19.03.2018

Valid From_fr

19.03.2018

13.05.2018

Charges et conditions

- Cette modification méthodologique consistant en l'augmentation du port de la collerette jusqu' à 7 jours maximum est aussi valable pour l'autorisation GE/20/18 (29718).
Cette complémentaire est la 3ème complémentaires d'une autorisation de base. La Dgs n'acceptera plus d'autre complémentaire. Une nouvelle demande devra être introduite .

- Il n'y aura pas de détention individuelle des rats de manière générale. En effet, la détention se fera par 2 avec une surveillance accrue les 2 premiers jours p.o. Les rats seront détenus avec plus d'enrichissement, plus de nourriture à disposition. Si malgré ces conditions des blessures survenaient, alors la détention serait individuelle.

Dérogations relatives au personnel, à la formation continue, à la détention d'animaux, etc.

Animaux autorisés

Espèce	Autrefois autorisé	Nombre d'animaux demandés	Nombre d'animaux autorisés
Rats	260	0	**260**

Degré de gravité prospectif maximal: **3**

Emoluments

Description	Nombre	Unité	Prix
étude du dossier	1	h	160.0
frais administratifs	1	h	80.0
Total			240.0

Charges relatives aux rapports et à des modifications de la demande

Il y a lieu de nous annoncer par courriel (dgs.experimentation-animale@etat.ge.ch), au moins 48 heures ouvrables d'avance :

- n° complet de l'autorisation ;

- date ;

- heure ;

- lieu (étage, n° de laboratoire) ;

- les manipulations sur l'animal durant **6 mois** dès le début effectif de l'expérience.

Les manipulations se font pendant les jours ouvrables (8h-17h). Les dérogations à cette règle doivent être dûment justifiées.

Toute annulation ou modification d'horaire et/ou de lieu - qui n'aura pas été notifiée par écrit - ½ journée ouvrable à l'avance, sera facturée.

- En cas de souffrances manifestes qui ne pourraient être soulagées par l'administration d'analgésiques, les animaux doivent être immédiatement euthanasiés.

- Si un taux de mortalité élevé devait être constaté, la Direction générale de la santé, (Dr A. Rod) doit en être immédiatement informée.

Attention à l'identification des cages : elle doit porter l'intégralité du n° de l'autorisation !

Formation continue:

Nous vous rappelons que suite à l'obtention du module 1 et/ou 2, il est obligatoire d'effectuer **4 jours de formation continue par tranche de 4 années**.

Exemple : pour un module obtenu en janvier 2004, il sera nécessaire d'effectuer 4 jours de formation entre janvier 2004 et janvier 2008.

RAPPORTS ET MODIFICATIONS DE L'EXPERIENCE (art. 63a OPAn)

Le/la responsable de l'institut ou du laboratoire doit annoncer dans les 2 mois sur formule C la clôture de l'expérience soumise à autorisation et de celle non soumise à autorisation. Dans le cas d'expériences s'étendant sur plusieurs années, l'annonce avec les indications correspondantes pour l'année civile écoulée doit se faire au plus tard jusqu'à fin mars.

Avant de modifier l'expérience selon l'indication sous ch. 4-10 de la demande et ch. 2 de cette autorisation/décision officielle (telles que modification de la méthode et durée de l'expérience, utilisation d'autres espèces animales, augmentation du nombre des animaux, changement du responsable de l'intitut ou du laboratoire, changement des expérimentateurs, etc.), il faut impérativement demander une autorisation complémentaire ou autre accord à l'Office vétérinaire cantonal.

Moyens légaux

La présente autorisation est susceptible de recours par l'office fédéral de la sécurité alimentaire et des affaires vétérinaires OSAV (LPA, art.26, al.1).

Il ne peut en être fait usage qu'au moment où il est établi, **soit en attendant l'expiration du délai de recours de 30 jours (depuis la date de l'autorisation), soit en s'informant directement auprès de l'OSAV qu'aucune voie de droit n'a été utilisée.**

GE   19.03.2018   Astrid Rod

Fichiers annexés

Titre du document	Nom du fichier	Taille du fichier
Argumentation pour animaux supplémentaire	Argumentation pour animaux supplémentaires 18012018.docx	32 KB
Argumentation pour collerette d'une durée de 7j	Demande complémentaire colerette.docx	53 KB

	REPUBLIQUE ET CANTON DE GENEVE Département de l'emploi, des affaires sociales et de la santé Direction générale de la santé **Domaine de l'expérimentation animale**	**GE/70/18**
	Direction générale de la santé, Rue Adrien-Lachenal 8, 1207 Genève Lucia Henchoz, personne responsable	**26345**

Autorisation pour expériences sur animaux (Formulaire B)

Art. 18 al. 1 Loi fédérale sur la protection des animaux (LPA, RS455)

Directeur/trice de l'expérimentation animale Marjolaine Philit	Institut UNI DUFOUR rue du Général Dufour 24 1211 Genève 4 022 000 000

Directeur/trice de l'expérience

Ali Modarressi

Titre de l'expérience

L'effet des cellules souches mésenchymateuses d'origine graisseuse administrées par voie systémique sur la cicatrisation cutanée.

Type de la demande

[C] demande complémentaire

Demande précédente:

GE/70/18

Décision   La demande fait partie intégrante de l'autorisation.

Autorisée

Date de l'autorisation

03.05.2018

Valid From_fr

03.05.2018

186

Autorisation valable jusqu'à

13.09.2018

Charges et conditions

- Cette modification méthodologique consistant en l'augmentation du port de la collerette jusqu' à 7 jours maximum est aussi valable pour l'autorisation GE/20/18 (29718).
Cette complémentaire est la 3ème complémentaires d'une autorisation de base. La Dgs n'acceptera plus d'autre complémentaire. Une nouvelle demande devra être introduite .

- Il n'y aura pas de détention individuelle des rats de manière générale. En effet, la détention se fera par 2 avec une surveillance accrue les 2 premiers jours p.o. Les rats seront détenus avec plus d'enrichissement, plus de nourriture à disposition. Si malgré ces conditions des blessures survenaient, alors la détention serait individuelle.

Dérogations relatives au personnel, à la formation continue, à la détention d'animaux, etc.

Animaux autorisés

Espèce	Autrefois autorisé	Nombre d'animaux demandés	Nombre d'animaux autorisés
Rats	260	0	**260**

Degré de gravité prospectif maximal: **3**

Emoluments

Charges relatives aux rapports et à des modifications de la demande

Il y a lieu de nous annoncer par courriel (dgs.experimentation-animale@etat.ge.ch), au moins 48 heures ouvrables d'avance :

- n° complet de l'autorisation ;

- date ;

- heure ;

- lieu (étage, n° de laboratoire) ;

- les manipulations sur l'animal durant **6 mois** dès le début effectif de l'expérience.

Les manipulations se font pendant les jours ouvrables (8h-17h). Les dérogations à cette règle doivent être dûment justifiées.

Toute annulation ou modification d'horaire et/ou de lieu - qui n'aura pas été notifiée par écrit - ½ journée ouvrable à l'avance, sera facturée.

- En cas de souffrances manifestes qui ne pourraient être soulagées par l'administration d'analgésiques, les animaux doivent être immédiatement

euthanasiés.

- Si un taux de mortalité élevé devait être constaté, la Direction générale de la santé, (Dr A. Rod) doit en être immédiatement informée.

Attention à l'identification des cages : elle doit porter l'intégralité du n° de l'autorisation !

Formation continue:

Nous vous rappelons que suite à l'obtention du module 1 et/ou 2, il est obligatoire d'effectuer **4 jours de formation continue par tranche de 4 années**.

Exemple : pour un module obtenu en janvier 2004, il sera nécessaire d'effectuer 4 jours de formation entre janvier 2004 et janvier 2008.

RAPPORTS ET MODIFICATIONS DE L'EXPERIENCE (art. 63a OPAn)

Le/la responsable de l'institut ou du laboratoire doit annoncer dans les 2 mois sur formule C la clôture de l'expérience soumise à autorisation et de celle non soumise à autorisation. Dans le cas d'expériences s'étendant sur plusieurs années, l'annonce avec les indications correspondantes pour l'année civile écoulée doit se faire au plus tard jusqu'à fin mars.

Avant de modifier l'expérience selon l'indication sous ch. 4-10 de la demande et ch. 2 de cette autorisation/décision officielle (telles que modification de la méthode et durée de l'expérience, utilisation d'autres espèces animales, augmentation du nombre des animaux, changement du responsable de l'intitut ou du laboratoire, changement des expérimentateurs, etc.), il faut impérativement demander une autorisation complémentaire ou autre accord à l'Office vétérinaire cantonal.

Moyens légaux

La présente autorisation est susceptible de recours par l'office fédéral de la sécurité alimentaire et des affaires vétérinaires OSAV (LPA, art.26, al.1).

Il ne peut en être fait usage qu'au moment où il est établi, **soit en attendant l'expiration du délai de recours de 30 jours (depuis la date de l'autorisation), soit en s'informant directement auprès de l'OSAV qu'aucune voie de droit n'a été utilisée.**

GE   03.05.2018   Lucia Henchoz

Fichiers annexés

Titre du document	Nom du fichier	Taille du fichier
Argumentation pour animaux supplémentaire	Argumentation pour animaux supplémentaires 18012018.docx	32 KB
nouveau planning des expériences	schedule for in vivo phase 2 grp 2 and 3 animal experiments.pptx	31 KB
Argumentation pour collerette d'une durée de 7j	Demande complémentaire colerette.docx	53 KB

188